

THE UNIVERSITY *of* EDINBURGH

This thesis has been submitted in fulfilment of the requirements for a postgraduate degree (e.g. PhD, MPhil, DClinPsychol) at the University of Edinburgh. Please note the following terms and conditions of use:

This work is protected by copyright and other intellectual property rights, which are retained by the thesis author, unless otherwise stated.
A copy can be downloaded for personal non-commercial research or study, without prior permission or charge.
This thesis cannot be reproduced or quoted extensively from without first obtaining permission in writing from the author.
The content must not be changed in any way or sold commercially in any format or medium without the formal permission of the author.
When referring to this work, full bibliographic details including the author, title, awarding institution and date of the thesis must be given.

Dissecting the function and targets of FOXG1 in glioblastoma

Harry JCJ Bulstrode

Supervisor: Dr Steven M Pollard

MRC Centre for Regenerative Medicine

University of Edinburgh

2015

A thesis submitted to the University of Edinburgh for the degree of Doctor of Philosophy



Abstract

Glioblastoma (GBM) is the most common intrinsic primary brain tumour. It is uniformly fatal, with median survival approximately 14 months. These tumours comprise a mixture of neural stem cell-like cells and more differentiated astrocytic cells. The former are thought to be responsible for tumour development and recurrence, and display self-renewal and differentiation capacity *in vitro*. Glioma stem cells (GSCs) are defined operationally by their capacity to initiate tumours on orthotopic transplant into immunocompromised mice.

The Pollard lab has identified the neural developmental transcription factor Forkhead Box G1 (*FOXG1*) as the most consistently overexpressed gene in GBM-derived neural stem (GNS) cells compared to their genetically normal neural stem (NS) cell counterparts. Here we explore the function and critical downstream effectors of FOXG1 in NS and GNS cells.

We find that, although FOXG1 is not essential for sustaining proliferation of NS or GNS cells (in vitro), high FOXG1 restricts astrocyte differentiation in response to BMP and can drive dedifferentiation of postmitotic astrocytes. We identify a potential cooperation with SOX2. ChIP-Seq and RNA-Seq were used to define transcriptional targets. FOXG1 directly controls critical cell cycle regulators *FOXO3* and *FOXO6* (two forkhead family proteins), as well as the proto-oncogene *MYCN* and key regulators of both DNA and chromatin methylation, including *TET3* and *CHD3*. Pharmacological inhibitors of MYC block FOXG1-driven de-differentiation, whereas Vitamin C and 5-azacytidine – agents that disrupt DNA and chromatin methylation – can facilitate de-differentiation. CRISPR/Cas genome editing was used to genetically ablate the cell cycle inhibitor *FOXO3*, or remove the FOXG1-bound cis-regulatory region. These data suggest direct transcriptional repression of *FOXO3* by FOXG1 may drive cells into cycle. We conclude that high levels of FOXG1 in GBM limit astrocyte differentiation commitment by direct transcriptional control of core cell cycle regulators and DNA/histone methylation.

Lay Summary

Brain tumours are now the leading cause of cancer death in children and young adults. Glioblastoma (GBM) is the most common and the most lethal: the majority of patients survive little more than one year from diagnosis.

It seems that the cells which form the GBM in the first place, and which cause it to recur after surgery, have switched on genes used by stem cells to grow and divide when our brains are still developing in the womb. These genes should be switched off in the adult brain, and when that fails to happen they can drive the uncontrolled growth which makes brain tumours. One such gene is called FOXG1.

FOXG1 is switched on in all the GBM tumours we have examined, and I have shown that it can on its own force brain support cells (astrocytes) to start growing and dividing like cancer cells. On the other hand, removing this gene from GBM cells means they lose the ability to form tumours. I have begun the process of working out which other genes FOXG1 controls: once we know the details of how FOXG1 is working and why the tumours need it, we can look for drugs which will target GBM cells with few side effects in the rest of the body, where FOXG1 is not needed.

Table of Contents

Abstract i

Lay Summary ii

Table of Contents iii

Acknowledgements xi

Declaration of Originality xi

Copyright declaration xi

List of Abbreviations xii

List of Figures xiv

1 Introduction 1

1.1 Overview 1

1.2 The biology of glioma 1

1.2.1 Gliomas are the most common primary brain tumours 1

1.2.2 Gliomas are classified and graded on histopathological features 4

1.2.3 Glioblastoma is rapidly and uniformly fatal with few treatment options 6

1.2.4 RTK/PI3K, CDK4/RB and P53 pathways are typically mutated in GBM 6

1.2.5 Stem Cells and Glioma 10

1.2.6 Glioma is a disease of cancer stem cells 10

1.2.7 Transcription factors control self-renewal and differentiation 15

1.2.8 FoxG1 and Sox2 demonstrate reprogramming potential to an NS state 15

1.2.9 Glioma stem cells have neural stem cell transcriptional identity 16

1.3 Insights from neural stem cell biology 21

1.3.1 Neural stem cells comprise one lineage from gastrulation to adulthood 21

1.3.2 Astrocytes are a candidate cell of origin for many glioma subtypes 24

1.3.3 Astrocytes exhibit diverse molecular and phenotypic characteristics 25

1.3.4 Astrocyte Differentiation can be modelled in vitro 26

1.3.5 Reactive astrocytes express NS cell markers and exhibit latent multipotency ..28

1.3.6 Astrocytes can undergo experiementally imposed lineage conversions 30

1.4 The Role of FOXG1 and SOX2 in NS cell and GNS cell function 31

1.4.1 Forkhead Box G1 (FOXG1) is a forebrain-specific Forkhead Box TF 31

1.4.2 The Forkhead domain confers pioneer factor potential 31

1.4.3 The Forkhead family includes members that are deregulated in human cancer and control stem cell fate 35

1.4.4 Forkhead factors interact with protein cofactors to regulate transcription 36

1.4.5 FOXG1 is critical to brain development and post-natal neurogenesis 39

1.4.6 High FoxG1 Levels may drive glioma stem cell self-renewal 42

1.4.7 Sox2 is a neural stem cell master regulator and is amplified in glioma 46

1.5 Aims and Hypotheses 47

1.5.1 A Hypothesis for FoxG1 Activity in NS cells and GNS cells 47

2 Materials and Methods 48

2.1 Cell culture 48

2.1.1 Self-renewal media 48

2.1.2 NS cell astrocyte differentiation media 48

2.1.3 Primary astrocyte culture media 48

2.1.4 Freezing media 48

2.2 Immunocytochemistry 49

2.2.1 Quantitation of Ki67 immunoreactive cells 49

2.2.2 EdU incorporation assays 49

2.2.3 Primary Antibodies used in this study 50

2.2.4 Secondary Antibodies 50

2.3 Western immunoblotting 51
2.4 Taqman qRT-PCR and Taqman Low Density Arrays 51
2.5 Plasmid construction 52
2.5.1 Gibson Assembly 52
2.5.2 Cloning of full length V5 tagged FOXG1 52
2.5.3 Cloning of additional lentiviral FOXG1 constructs 52
2.5.4 Bacterial transformation 53
2.5.5 Gateway cloning of FOXG1, FOXG1V5 and SOX2 expression casettes 55
2.5.6 Polycistronic expression cassettes 57
2.6 Genome editing using the CRISPR/Cas9 system 57
2.6.1 Guide RNA Design and Cloning 58
2.6.2 Targeting Vector Design and Cloning 58
2.7 Derivation of stable transgenic cell lines 58
2.7.1 shRNA Knockdown 59
2.7.2 Lentiviral transduction (pHIV-tomato-FOXG1 overexpression constructs) 59
2.7.3 Lipofection of Mouse NS Cells for PiggyBac Stable Integration 59
2.7.4 Neon/Amaxa Transfection of Human Cell NS Cells for PiggyBac Stable Integration 60
2.8 Next generation sequencing: ChIP-Seq, RNA-Seq, and ATAC-Seq 60
2.8.1 Isolation and Preparation of FOXG1 cross-linked Chromatin 61
2.8.2 Chromatin immunoprecipitation 61
2.8.3 Library preparation for ChIP-Seq 62
2.8.4 ChIP-PCR Primers 63
2.8.5 RNA Seq Library preparation 63
2.8.6 ATAC Library preparation 63
2.8.7 Library Quality Control 63

2.8.8 Library Sequencing *64*

2.8.9 Analysis of NGS Data *64*

3 Results 1 – FOXG1 loss-of-function in NS cells and GNS cells 65

3.1 Introduction 65

3.2 Exploring FoxG1 expression in mouse and human 66

3.2.1 FoxG1 expression in developing forebrain, brain tumours and NS/GNS cell lines suggests a potential role in glioma *66*

3.2.2 FOXG1 expression correlates to an extent with malignant grade *70*

3.3 Acute FoxG1 genetic deletion using a new conditional mouse NS cell line 73

3.3.1 Generation of FoxG1$^{fl/fl}$ mouse NS cell lines *73*

3.3.2 foxg1 null NS cells proliferate normally and retain NS cell marker expression 73

3.3.3 FoxG1 null Mouse NS cells exit cycle readily in response to inductive differentiation cues. *74*

3.3.4 Summary 1 ..... *75*

3.4 *FOXG1* knockdown in human GNS cells using shRNA 77

3.4.1 GNS cells remain proliferative following FOXG1 knockdown *77*

3.5 FOXG1 knockout in human GNS using CRISPR/Cas-assisted gene targeting 80

3.5.1 Generation of FOXG1 null clonal GNS cells using CRISPR/Cas gene targetting.80

3.5.2 FOXG1 deletion in GNS line G7 has no discernible impact on proliferation in vitro 82

3.5.3 Preliminary results suggest that FOXG1 deletion impairs tumour formation ...82

3.6 Conclusions 84

4 Results 2 – Overexpression of FOXG1 and SOX2 in NS cells and astrocytes 85

4.1 Introduction 85

4.2 BMP4 treatment of mouse NS cells plated at low density drives stable cell cycle exit and astrocyte differentiation commitment 86

4.3 Effects of FOXG1 overexpression on mouse NS cell proliferation and differentiation 90

4.3.1 Constitutive FOXG1-V5 expression in mouse NS cells does not influence cell proliferation, but attenuates BMP4-induced cell cycle exit 90

4.3.2 FOXG1 and SOX2 were overexpressed in isolation or in combination using PiggyBac Doxycycline-inducible Transgenes 92

4.3.3 Forced expression of FOXG1 and SOX2 prevents cell cycle exit in response to differentiation cues. 94

4.4 Astrocyte de-differentiation is triggered in response to FOXG1 and SOX2 overexpression 96

4.4.1 Combined overexpression of FOXG1 and SOX2 drives differentiated astrocytes to re-enter cell cycle and acquire an NS cell-like morphology 96

4.4.2 Establishment of a colony-forming assay to explore astrocyte cell cycle re-entry and de-differentiation 99

4.4.3 Combined overexpression of FOXG1 and SOX2 is sufficient to drive re-entry into cell cycle by postmitotic astrocytes 99

4.4.4 Primary cortical astrocytes are driven to a proliferative NS cell-like state upon overexpression of FOXG1 and SOX2 102

4.5 FOXG1/SOX2 derived cell cycle re-entry is accompanied by reacquisition of the radial glia-like NS cell state 104

4.5.1 Cycling cells re-express NS cell markers 104

4.5.2 High levels of FOXG1 overexpression are sufficient to drive astrocyte dedifferentiation with high efficiency 106

4.5.3 Conclusions 110

5 Results 3 – Targets of FOXG1 and SOX2 in mouse. 111

5.1 Introduction 111

5.2 Defining FoxG1 transcriptional targets in mouse NS cells 112

5.2.1 Exploring the feasibility of FoxG1 Native ChIP in mouse NS cells 112

5.2.2 Defining binding sites of FOXG1-V5 in mouse NS cells using ChIP-Seq 112

5.2.3 FOXG1 binds to multiple key NS cell regulators 113

5.2.4 FOXG1 and Sox2 bind together to regions enriched for the respective canonical motifs, at loci encoding cell cycle and epigenetic regulators. 114

5.3 Expression profiling to establish regulated targets of FOXG1 and SOX2. 114

5.3.1 ChIP-Seq alone fails to reliably identify regulated targets 114

5.3.2 RNA-Seq identifies transcriptional correlates of dedifferentiation 118

5.3.3 Direct targets identified using ChIP-Seq and RNA-Seq 120

5.4 MycN is an early direct target of FOXG1/SOX2 122

5.4.1 MycN protein is rapidly induced following induction of FOXG1/SOX2 122

5.4.2 Pharmacological inhibition points to a key role for Myc in cell cycle re-entry 124

5.5 *foxo3* and *foxo6* are transcriptional targets of FOXG1 126

5.5.1 foxo3 is a direct target downregulated in response to FOXG1/SOX2 126

5.5.2 Genetic ablation of the FOXG1/SOX2 bound foxo3 cis-regulatory element was achieved using Crispr/Cas. 129

5.5.3 Deletion of the FOXG1/SOX2 cis-regulatory region derepresses FOXO3, and abolishes NS cell colony forming ability. 129

5.5.4 foxo3 genetic deletion using CRISPR/Cas assisted gene targeting 132

5.5.5 foxo3 deleted populations re-enter cell cycle spontaneously after BMP treatment 135

5.5.6 foxo6 is a strongly upregulated in response to FOXG1 138

5.6 Epigenetic remodelling factors are candidate FOXG1/SOX2 direct targets 141

5.6.1 Induction of DNA methylation remodelling combines with foxo3 deletion to drive dedifferentiation. 141

6 Results 4 – FOXG1 Targets in Human NS and GNS 144

6.1 Introduction 144

6.2 ChIP-Seq to define FOXG1 binding in human GNS cells 144

6.2.1 Chromatin preparation and immunoprecipitation 144

6.2.2 ChIP-Seq for native FOXG1 in human NS and GNS cells identifies binding at key NS regulatory targets 144

6.3 Expression of FOXG1 bound genes in GNS cells was assessed in NS cell lines overexpression of FOXG1 148

6.4 ATAC Seq reveals that differentially open chromatin regions in GNS cells versus NS cells are enriched for the forkhead box factor binding 151

7 Discussion 158

7.1 Function and Targets of FOXG1 in GBM 158

7.1.1 FoxG1 is dispensable for NS cell and GNS cell proliferation in vitro 158

7.1.2 FoxG1 deletion predisposes to cell cycle exit and differentiation, whereas FOXG1 and SOX2 overexpression prevent these responses 159

7.1.3 FOXG1 overexpression drives astrocyte dedifferentiation 160

7.1.4 FOXG1 drives dedifferentiation through key pathways and candidate drug targets 160

7.2 Further application of BMP-treated NS colony forming assays 161

7.2.1 BMP Assay Development 161

7.2.2 Assay Application to Human NS cells 162

7.2.3 Investigation of Density Effects 162

7.3 Implications for our understanding of NS and GNS cell identity 163

7.3.1 Roles of FOXG1 163

7.3.2 A model for FOXG1 function in GBM 164

7.3.3 Validating the role of FOXG1 in gliomagenesis in vivo 167

7.3.4 A unifying model for FOXG1 function in health and disease *167*

7.3.5 Translational implications *168*

8 References **170**

9 Appendices **181**

9.1 Taqman assays (qRT-PCR and Taqman Low Density Array Cards) 181

9.1.1 Taqman Assays – Mouse *181*

9.1.2 Taqman Assays - Human *182*

9.2 Plasmids 184

9.2.1 Destination Vectors *184*

9.2.2 Entry Vectors and Expression Vectors *184*

9.2.3 Plasmid Maps *185*

9.3 Guide RNA and Targeting Vector Homology Arm oligos 187

9.3.1 AAVS1 Targeting *187*

9.3.2 FOXG1 Targeting *187*

9.3.3 FoxO3 Targeting *187*

9.3.4 FoxO3 Cis Regulatory Region Deletion *187*

9.4 Mouse NS Cells Derivatives 188

9.4.1 Constitutive/inducible transgene overexpressing lines *188*

9.4.2 Conditional and knockout lines *188*

9.5 Human GNS Derivatives 188

Acknowledgements

First and foremost, I am in debt to my supervisor Steve Pollard, for the extraordinary enthusiasm, knowledge and insight which made this project so exciting to pursue. Likewise I am forever grateful to Sabine Gogolok, who helped me to grasp the science which underpinned my lab work, and to Stefan Stricker who always had wise advice for me. The staff and students working with Steve Pollard, and more widely in the UCL Cancer Institute in London and in the Scottish Centre for Regenerative Medicine in Edinburgh, made the project possible in countless ways. In particular, I must thank Raul Bressan, Mantas Matjusaitis and Claudia Garcia Diaz for advice and bench work related to CRISPR technologies. Paul Brennan, Maria Angeles Marques and Vivien Grant helped me to establish and maintain cell lines. Ewan Johnstone and Paul Bertone are responsible for much of the bioinformatic analysis presented here. I will always consider my years in the Pollard lab the best of times, and I aspire to build on the work I've started here in my future career.

Declaration of Originality

I hereby declare that this thesis and the work presented in it was composed by and originated entirely from me and has not been submitted in any form for another degree or diploma at any other institution. Any information derived from the published or unpublished work of others has been acknowledged in the text and references are listed in the bibliography.

Copyright declaration

The copyright of this thesis rests with the author and is made available under a Creative Commons Attribution Non-Commercial No Derivations license. Researchers are free to copy, distribute or transmit the thesis on the condition that the attribute it, that they do not use it for commercial purposes and that they do not alter, transform or build upon it. For any reuse or redistribution, researchers must make clear to others the license terms of this work.

List of Abbreviations

ATAC	Assay of Transposase Accessible Chromatin
Aza	5-Azacytidine (DNA methyltransferase inhibitor)
BMP	Bone morphogenic protein
BSA	Bovine serum albumin
BSD	Blasticidin
Cas9	CRISPR associated protein 9
cDNA	Copy DNA
ChIP	Chromatin immunoprecipitation
CRISPR	Clustered regularly interspaced short palindromic repeats
DMEM	Dulbecco's modified Eagle's medium
DMSO	Dimethyl sulfoxide
Dox	Doxycycline hyclate (1ug/ml unless otherwise specified)
EdU	5-ethynyl-2-deoxyuridine
EGF	Epidermal Growth Factor
EMT	Epithelial mesenchymal transition
FACS	Fluorescence activated cell sorting
FGF	Fibroblast growth factor
GAPDH	Glyceraldehyde-3-phosphate dehydrogenase
GBM	Glioblastoma
GFAP	Glial fibrillary acidic protein
GFP	Green fluorescent protein
GNS	Glioma Neural Stem
HRP	Horseradish peroxidase
ICC	Immunocytochemistry
Ig	Immunoglobulin

IRES	Internal Ribosomal Entry Site
KD	Knockdown
KO	Knockout
mRNA	Messenger RNA
NS	Neural stem
PCR	Polymerase chain reaction
PI3K	Phosphatidyl-3-kinase
qPCR	Quantitative PCR
rpm	Revolutions per minute
Rb	Retinoblastoma
RT-PCR	Reverse transcriptase PCR
RTK	Receptor tyrosine kinase
rtTA	Reverse tetracycline transactivator
SDS PAGE	Sodium dodecylsulfate polyacrylamide gel electrophoresis
SGZ	Subgranular zone
Shh	Sonic hedgehog
shRNA	Short hairpin RNA
siRNA	Silencing RNA
TCGA	The cancer genome atlas
TLDA	Taqman Low Density Array
TRE-3G	Tetracycline Response Element (Third Generation)
WHO	World Health Organization
wt	Wild type

List of Figures

Figure 1-1 - Typical histopathological features of glioblastoma 5

Figure 1-2 - Summary of key cell fate pathways dysregulated in primary GBM. 8

Figure 1-3 - Contrasting models of tumour heterogeneity 13

Figure 1-4 - Gliomas contain a glioma neural stem cell (GNS) fraction. 14

Figure 1-5 - A model of GBM cell epigenetic heterogeneity 19

Figure 1-6 - Neural stem cells through development 23

Figure 1-7 – Cell identity relations in astrocytes and NS cells, quiescent and activated 29

Figure 1-8 - Simplified forkhead family phylogenetic tree 33

Figure 1-9 – The FOXG1 locus and gene product 34

Figure 1-10 - A model of FoxO and FoxG1 activity in GBM 38

Figure 1-11 - Patterns of FOXG1 expression in development 40

Figure 1-12 - Roles of FoxG1 in cell fate and patterning during development. 41

Figure 1-13 - Tissue-specific FOXG1 expression patterns in health and disease 44

Figure 1-14 - FOXG1 expression in GBM and GNS cells 45

Figure 2-1 - FOXG1 lentiviral expression vector cloning 53

Figure 2-2 - Gateway cloning of FOXG1 inducible constructs 56

Figure 3-1 - FOXG1 expression in NS and GNS cells 68

Figure 3-2 - FOXG1 expression in newly-derived WHO Grade III and Grade IV cell lines 71

Figure 3-3 - FoxG1 knockout in a newly generated foxg1$^{fl/fl}$ mouse NS cell line. 75

Figure 3-4 - FOXG1 shRNA knockdown in G7 GNS cells 78

Figure 3-5 - FOXG1 Crispr Targeting Strategy 80

Figure 3-6 – Functional consequences of FOXG1 knockout in G7 GNS cells 84

Figure 4-1 - Assays of astrocyte commitment by NS cells in response to BMP treatment. 88

Figure 4-2 - Functional effects of FOXG1 overexpression 91

Figure 4-3 - Clonal NS cell lines with doxycycline-inducible expression cassettes. 93

Figure 4-4 - Effects of transgene overexpression on proliferation 94

Figure 4-5 – Driving astrocyte cell cycle re-entry by FOXG1-SOX2 forced expression 97

Figure 4-6 - Induction of cell cycle re-entry by astrocytes at low plating density *100*

Figure 4-7 - Induction of cell cycle re-entry by primary astrocytes..... *103*

Figure 4-8 – Operetta-based image cytometry analysis of the dedifferentiation process..... *105*

Figure 4-9 - Dedifferentiation in response to FOXG1 induction alone..... *109*

Figure 5-1 - FOXG1V5 ChIP-Seq in mouse and intersection with Sox2 ChIP-Seq..... *115*

Figure 5-2 – Dedifferentiation Day 1 TLDA Card data for FS3 lines (TLDA 96 card) *117*

Figure 5-3 - RNA-Seq in FS3 cells on differentiation and dedifferentiation..... *119*

Figure 5-4 – TLDA 48 Card data for the F6 line- day 1 dedifferentiation..... *120*

Figure 5-5 - MycN is a regulated direct target of FoxG1 both with and without Sox2 ..... *122*

Figure 5-6 - Myc inhibition impairs dedifferentiation, but not NS cell proliferation..... *125*

Figure 5-7 – foxo3 is a regulated target of FoxG1 and Sox2..... *127*

Figure 5-8 - Crispr deletion of the FoxO3 intron cis-regulatory region..... *131*

Figure 5-9 - Crispr targeting of foxo3 exon 1 ..... *134*

Figure 5-10 – foxo3 genetic deletion prevents stable BMP-induced cell cycle exit..... *137*

Figure 5-11 – FoxO6 is a regulated direct target of FoxG1 +/- Sox2 ..... *140*

Figure 5-12- Epigenetic modifier direct targets drive reacquisition of NS cell identity..... *142*

Figure 6-1 - Human Native antibody FOXG1 ChIP-Seq *147*

Figure 6-2 – Transcription responses to FOXG1 overexpression - Human U5 ..... *149*

Figure 6-3 - ATAC-Seq profiles chromatin accessibility in NS and GNS cell lines..... *155*

Figure 6-4 - Example chromatin accessibility profiles for loci of interest in NS and GNS..... *157*

Figure 7-1- A model for gliomagenesis and high grade transformation..... *166*

1 Introduction

1.1 Overview

Gliomas are the most common and most malignant primary brain tumours. A population of tumour initiating cells within these tumours exhibits transcriptional and epigenetic hallmarks of neural stem cells (1,2). Comparisons of the molecular and cellular processes controlling the fate decisions involved in self-renewal and differentiation in NS cells and GNS cells may reveal important therapeutic targets to block the unconstrained self-renewal that underpins glioma.

In this introductory chapter I discuss three key topics. First, the biology of glioma and relevance of cancer stem cell models. Second, the currently known mechanisms controlling neural stem cell self-renewal and differentiation in the developing and adult mammalian central nervous stem. Third, the specific roles for neural developmental transcription factors in GBM, with a focus on FOX and SOX families. I then outline the major aims and working hypothesis of this thesis.

1.2 The biology of glioma

1.2.1 Gliomas are the most common primary brain tumours

Glioma represents the most common and the most lethal intrinsic primary brain tumour. They most often arise in the forebrain, but can more rarely be seen in midbrain, hindbrain and spinal cord. Glioma incidence is estimated at ~5 per 100,000 per year (3), and reported incidence has been increasing steadily worldwide since the 1970s, probably as a result of better imaging and access to neurosurgical services: the trend is less apparent or absent in developed countries (4).

Incidence is higher in Caucasian populations, in men, and increases with age. However the significant incidence in younger age groups, and generally poor prognosis, means that these tumours now represent the most common cause of cancer death in children

and young adults. Ionising radiation exposure and certain key heritable heterozygous germline mutations detailed below are recognised risk factors, but the vast majority of these tumours occur sporadically (Table 1).

The presentation of gliomas, as for any expanding intracranial mass lesion, typically includes focal neurological deficit, seizures, and symptoms of mass effect (headaches, nausea and vomiting, visual disturbance). CT and MRI imaging have high sensitivity and specificity for identifying high grade glioma, but definitive diagnosis is made on histopathological grounds.

Syndrome	Gene Mutation	Brain Tumour Types
BRCA	**BRCA-1/2**	Glioma
Li Fraumeni	**TP53**	Glioma; medulloblastoma choroid plexus carcinoma;
Melanoma-astrocytoma	**P14(ARF)**	Astrocytoma
NF1	**NF1**	Optic glioma; pilocytic astrocytoma
NF2	**NF2**	glioma; ependymoma; meningioma; schwannoma
Turcot (Type 1)	**MMR** (MLH1,MSH2, MSH6, PMS2)	Astrocytoma; GBM; medulloblastoma; PNET
Turcot (Type 2)	**APC**	Glioma

Table 1 Germline gene mutations associated with glioma

A number of germline mutations conferring heritable cancer syndromes have been associated with increased glioma risk.

1.2.2 Gliomas are classified and graded on histopathological features

Gliomas are classified according to the guidelines of the World Health Organisation (WHO) Classification of Tumours of the Central Nervous System (5). Hemispheric glioma generally comprises cell populations with predominantly astrocytic, oligodendroglial or mixed appearances, and on this basis will usually be designated astrocytoma, oligodendroglioma or oligoastrocytoma.

Each subtype of glioma is also graded on a scale of I to IV; benign/ low grade (Grade I or II), or malignant/ high grade (Grade III or IV). Low grade tumours exhibit a homogeneous well-differentiated appearance, while the grade IV astrocytomas termed glioblastomas (GBMs), represent about half of all glioma cases, and are defined based on the specific histopathological criteria (Figure 1-1).

GBMs can be further subcategorised into variants exhibiting distinct histopathology. These include gliosarcoma, giant-cell GBM, and 'classic' GBM variants with oligodendroglial, fibrillary, primitive neuroectodermal or other features. In children, glioblastoma histology is encountered in the hemispheres (paediatric high grade glioma) and brainstem (diffuse intrinsic pontine glioma).

GBMs can be further subcategorised into primary GBM, describing de novo clinical presentation with high grade pathology, and secondary GBM, the malignant transformation of a previously diagnosed low grade glioma. Secondary GBM accounts for about 10% of cases. This distinction seems to have a biological basis, with most secondary GBMs and very few primary GBMs exhibiting IDH1 mutation (6), and these entities display distinct gene expression profiles (7). It now seems likely that some clinically-defined 'primary GBM' cases actually represent malignant transformation of clinically silent low grade lesions, on the basis of 'secondary GBM' features in the underlying biology.

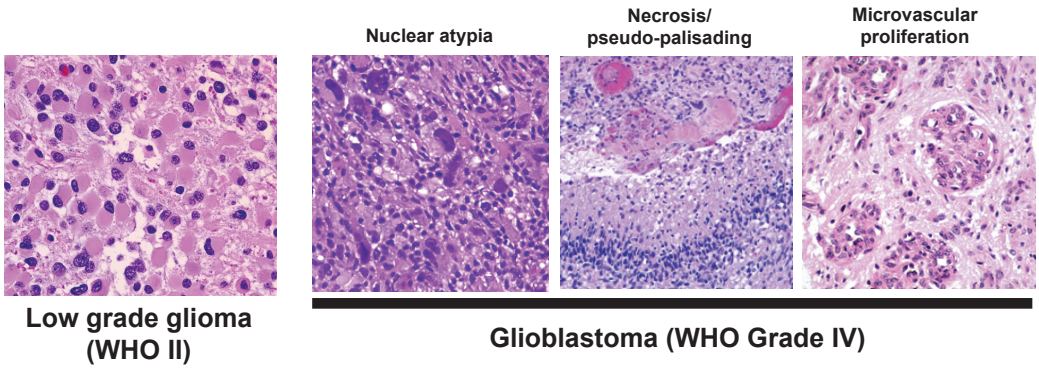


Figure 1-1 - Typical histopathological features of glioblastoma

Hallmarks of glioblastoma include nuclear atypia, high cell density, necrosis with pseudo-palisading and microvascular proliferation (Images from neuropathologyweb.org).

1.2.3 Glioblastoma is rapidly and uniformly fatal with few treatment options

Clinically, intrinsic brain tumours may be difficult to access or to resect fully because of their proximity to eloquent brain structures. In any case the tumours are highly invasive so that even radical resection cannot prevent early recurrence: early attempts to cure the disease by resection of the entire affected hemisphere also failed, with recurrence due to established transcallosal spread in the remaining hemisphere. The blood-brain barrier, although disrupted in advanced malignant lesions, complicates drug delivery, and intrinsic genetic heterogeneity means that subclones resistant to conventional chemotherapeutics are thought to be present in the primary tumour. These features of the disease explain the dismal prognosis for patients diagnosed with GBM.

The current standard of care for GBM involves total surgical resection of the bulk tumour, followed by concurrent radiotherapy and chemotherapy using the DNA methylating agent temozolomide (TMZ). This regime, referred to as the Stupp protocol achieved a median survival of 14.6 months from diagnosis, compared to 12.1 months for post-operative radiotherapy alone (8). The DNA methylation resulting from TMZ chemotherapy is repaired by O-6-methylguanine-DNA methyltransferase (MGMT). Tumours exhibiting epigenetic silencing of this gene through methylation of its promoter region demonstrate a better response to chemotherapy (9).

Carmustine, another alkylating agent, can be implanted locally in the form of wafers at the time of surgery, in cases where gross total resection without breach of the CSF spaces has been achieved (10). This confers a modest increase in survival but is associated with a risk of wound breakdown.

1.2.4 RTK/PI3K, CDK4/RB and P53 pathways are typically mutated in GBM

Oncogenic driver mutations associated with gliomagenesis have been catalogued most extensively by The Cancer Genome Atlas across large groups of patient samples (11). Individual tumours may comprise many subclones with distinct driver mutation patterns, and

abundant passenger mutations. Extensive whole chromosome gains and losses (chromosome instability) are common. Moreover the GBM genome is highly unstable and emergence of new driver mutations at recurrence is typical (12). Nonetheless, primary GBMs share genetic disruptions to three key signalling pathways controlling cell cycle and survival: these are the receptor tyrosine kinase/PI3-Kinase signalling pathway, Cyclin dependent kinase/retinoblastoma, and *TP53* (13) (Figure 1-2). Typical 'hits' include activating mutations of the receptor tyrosine kinases, *EGFR, PDGFR* and *MET*, and downstream effectors *PI3K, AKT, MTOR* and *RAS*. Tumour suppressors responsible for regulating these cascades include *PTEN, NF-1, RB1* and *TP53*, and these are subject to loss of function mutations in GBM. Deep sequencing of a large set of GBMs has formed the basis of a biological classification system proposed by The Cancer Genome Atlas project (11). This classification is not used as a basis for deciding clinical management currently, although proneural subtype seems to predict relatively poor response to chemotherapy. The choice to classify inter-tumour genetic and epigenetic heterogeneity into four subgroups is essentially arbitrary, and the subtypes are not particularly robust: recurrences after treatment tend to converge on the mesenchymal subtype (13). The finding of extensive subclonal heterogeneity, likely imposed through Darwinian branched evolution, calls into question the validity and potential value of any classification applied to the tumour as a whole (14).

Original exon sequencing studies in 21 tumour samples, with targeted evaluation of selected mutations in a further 83 samples, identified unexpected key driver mutations in the isocitrate dehydrogenase (*IDH1*) (15). As discussed above, clinically *IDH1* mutations are found in secondary GBMs, that subgroup which arise in the context of a previously diagnosed lower grade glioma. More recent analysis of paediatric GBM identified replication independent histone H3 gene mutations in paediatric tumours (primarily *H3F3A*) (16). Both *IDH1* and *H3F3A* mutations are believed to drive gliomagenesis through disruption of normal mechanisms of epigenetic maintenance(17).

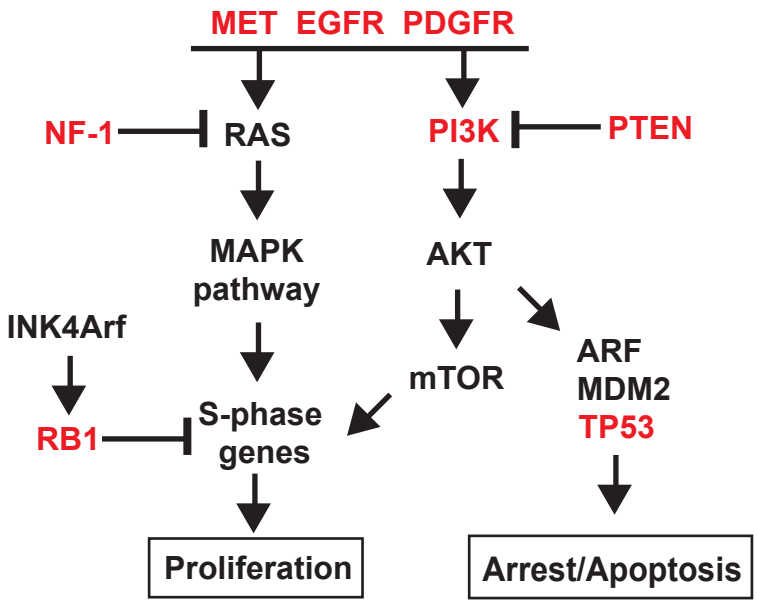


Figure 1-2 - Summary of key cell fate pathways dysregulated in primary GBM.

Recurrent mutations in GBM are highlighted in red. After (18)

Subtype	Expression Signature	Mutations
Proneural	OLIG2, NKX2-2	TP53, PDGFRA,PI3K, IDH1
Neural	MBP, SYT1	
Classical	EGFR, AKT2	EGFR gain, Chr10 loss, PDGFRA
Mesenchymal	CD44, YKL40	NFkB, NF1

Table 2 - TCGA classification of GBM subtype

Summary of the Cancer Genome Atlas classification of GBM subtype (11)

1.2.5 Stem Cells and Glioma

The lack of progress to date in developing effective novel GBM therapies reflects a lack of understanding of the disease biology. The tumours display both intra-tumoral and inter-tumoral genetic and epigenetic heterogeneity (19). One aspect of the epigenetic heterogeneity that has attracted much attention is whether tumours undergo hierarchical programs of differentiation that mirror normal tissue stem cells. There is experimental evidence to support the idea that tumour initiation and propagation depends on a glioma stem cell fraction capable of supporting self-renewal and generation of quiescent or differentiated derivatives (1-5,20). Putative glioma stem cells (GSCs) exhibit markers and transcription factor expression reminiscent of normal neural stem cells, in parent primary tumours and *in vitro* (7,8,20,21).

1.2.6 Glioma is a disease of cancer stem cells

Parallels between embryogenesis and cancer development were first observed in the late 19th century from Virchow and others, and these seeded the embryonal rest theory. This proposes that tumours might arise from 'left over' stem cells that persist in adult tissues – explaining why tumours often resemble foetal tissues. It was also noted in the very first classification systems for brain tumours devised by Bailey and Cushing in 1926, that there were clear histological similarities between tumour cells and developing CNS progenitors. Studies of teratacarcinoma stem cells in the 1960's also raised the idea that solid tumours might be driven by cells with stem cell characteristics. Tumours might therefore be viewed as caricatures of normal developmental processes (22).

The traditional model of glioma cell type identity, based on histopathology of primary tumours and analysis of serum-derived cell lines, viewed these lesions as comprising a functionally homogeneous population of transformed glia, usually astrocytes. However, within the bulk population, primary gliomas incorporate a diversity of distinct cells

expressing markers of the various differentiated neural lineages represented. Serum-derived glioma cell lines demonstrate very marked genetic and epigenetic drift from the parental tumours, and on xenotransplant form tumours with poor resemblance to primary gliomas. This is due to the selective pressure exerted by culture conditions over many passages in non-permissive media. These 'classic' cell lines therefore prevent severe limitiations, especially for the study of stem cell based models in glioma.

By contrast, in cultures derived in serum-free neural stem cell culture conditions, it has become clear that glioma stem cell fractions within the tumour can be isolated, and are tumour intiating (1). GSCs are defined functionally in much the same terms as their normal tissue counterparts. These cells are capable of self-renewal, tumour propagation in vivo, and can generate postmitotic progeny with recognisable glial and neuronal phenotypes (2,11,13). Homogeneous populations of GSCs can be grown in monolayer on laminin in serum free conditions supplemented with the mitogens EGF and FGF2 identical to those applied to derivation of NS cell cultures (15,16,23,24), and the resulting glioma neural stem cell (GNS) cultures are capable of generating invasive gliomas on xenotransplant (2). These primary patient-derived cultures represent a tractable and disease-relevant cellular model for studies of GBM. Glioma stem cells can be prospectively isolated using surface markers such as CD133, CD15 or CD44 (25) and expanded continuously in culture (2,9-12,20,26). For instance the lineage hierarchy which exists within primary tumours can be recreated following xenotransplantion into NOD-SCID mice of a small number of glioma stem cells prospectively isolated using CD133 (27). The value of individual surface markers has been debated and may vary from tumour to tumour (28); it is unequivocal, however, that glioma cells contain subsets of cells with many of the core transcriptional regulators associated with immature stem and progenitor cells (21). This finding challenges the traditional view of glioma cells as aberrantly proliferating astrocytes.

In general cancer stem cells may be selectively treatment-resistant as a result of slow cell cycle parameters, high expression of drug export proteins and lack of dependence on

signalling pathways targeted by novel therapeutics (29). It has been proposed that glioma stem cells exhibit more effective DNA damage responses compared to the bulk population following chemoradiotherapy (30). Elegant studies using a genetically engineered mouse model in which *p53, NF1* and *Pten* could be conditionally deleted using a Nestin driven TK-GFP construct have shown that it is the Nestin-positive glioma cells that regenerate tumours after temozolamide chemotherapy (31). Thus, the validity of the hierarchical/stem cell model has important consequences for how we design rational treatment strategies.

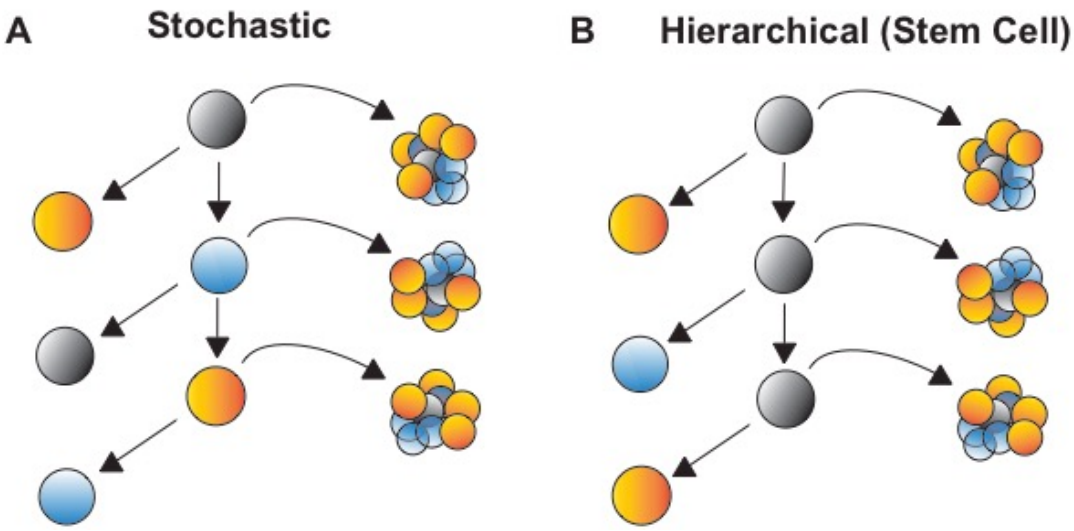


Figure 1-3 - Contrasting models of tumour heterogeneity

A Stochastic models hold that a variety of cell types within a tumour have the potential to proliferate extensively and generate new tumours **B** A cancer stem cell model posits a lineage hierarchy within the tumour, with only the cancer stem cell fraction capable of regenerating tumours with high efficiency. After Weissman (32).

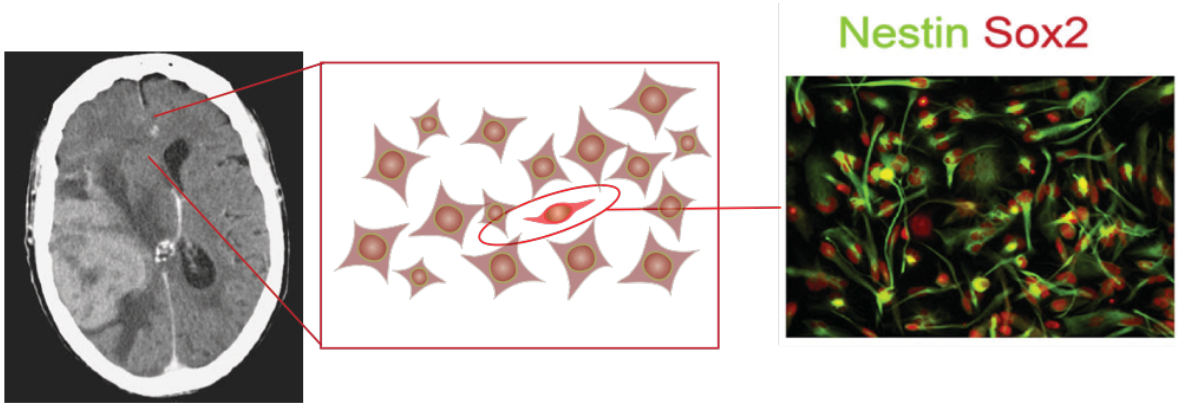


Figure 1-4 - Gliomas contain a glioma neural stem cell (GNS) fraction.

A simplified model of the cellular composition of glioma. The majority of cells in primary tumours resemble differentiated astrocytes morphologically and by marker expression. The Glioma Neural Stem Cell fraction can be selectively expanded in serum free culture conditions, expresses neural stem cell markers Nestin and Sox2, and generates tumours on xenotransplant into mice.

1.2.7 Transcription factors control self-renewal and differentiation

Cell identity is determined by the specific transcriptional state, imposed by sequence-specific transcription factors and gene regulatory networks operating in that cell. There are around 2000 transcription factors in the mammalian genome, and subsets of these bind to DNA in a sequence-specific fashion, 'programming' gene expression and epigenetic configuration (11,17).

Whether a gene is active or repressed, is a function of interactions between the basal transcription machinery and cell type specific transcription factors, often binding in combination to cis regulatory regions to determine expression levels. Repressed loci in a closed chromatin environment can be activated *de novo* through the activity of pioneer transcription factors, or recruitment of chromatin modifying cofactors (33).

In seminal studies over the past 10-20 years it has been shown that reprogramming of cell identity can be achieved by forced expression of a limited set of 'master regulator' transcription factors, such as MyoD (fibroblast to muscle), or the Yamanaka factors Oct4, Sox2, Klf4 and cMyc (fibroblast to iPS cell). Such reprogramming factors often drive their own expression through autoregulatory loops, and trigger target gene expression, as well as repression of lineage commitment genes – for example by recruitment of polycomb group complexes. The mechanisms through which TFs can demonstrate such potent activity in resetting the transcriptional and epigenetic state are being actively explored in many laboratories.

1.2.8 FoxG1 and Sox2 demonstrate reprogramming potential to an NS state

Several groups have recently reported reprogramming of fibroblasts to a neural stem cell state. It was first demonstrated that induction of the Yamanaka factors in NS-permissive culture conditions could result in bipotent neural precursors (34), capable of generating astrocytes and neurons. Early extinction of Oct4 expression, or replacement of Oct4 with neural lineage specific factors, allowed derivation of tripotent NS cells with oligodendrocyte

differentiation potential, from fibroblasts and from Sertoli cells (35-37). These studies likely involved a transient resetting to a pluripotent-like state. Tumorigenesis in response to induction of the Yamanaka factor combination, and cMyc in particular, in vivo represents a significant barrier for its application in reprograming cocktails for future cell based therapies (38). Therefore work from the Wernig laboratory was important in demonstrating derivation of tripotent NS cells using a combination of 11 neural lineage specific TFs. Factors were then excluded from the list to arrive at minimal combinations of FoxG1 and Sox2, or Foxg1 and Brn2, capable of generating bipotent precursors. Tripotent NS cells were produced upon induction of all three (39). The Huang group in San Francisco reported the derivation of multipotent neural stem cell colonies using overexpression of Sox2 alone (40), albeit at low efficiency. However, a recent report suggests that viral transduction of SOX2 expression in the mouse striatum drives transdifferentiation of glia to neurons, without evidence of an intermediate neural stem cell state (41). SOX2 forced expression may not be a universal requirement: the Mallamaci group in Italy have achieved NS reprogramming using the combination of FoxG1 and Pax6 (42). From these studies, FoxG1 and Sox2 are identified as transcription master regulators capable of driving reproducible reprogramming of fibroblasts to a neural stem cell state.

1.2.9 Glioma stem cells have neural stem cell transcriptional identity

Comparison of gene expression patterns of NS and GNS cells, which are expanded under identical conditions in vitro, enables identification of transcriptional and epigenetic characteristics shared between these cell types, and also those associated with malignancy (either decreased or increased in GNS versus NS) (43). As well as the surface markers and Nestin (discussed above) GNS cells express well established neural stem cell lineage-affiliated transcription factors such as SOX2, OLIG2, ASCL1, and FOXG1 (44) (45) (46) (47) (2). Importantly, the expression of these TFs is not an adaptation or response to in vitro culture conditions, as single cell RNA-Seq has recently demonstrated that individual cells in

primary tumour samples exhibit expression profiles incorporating a broad set of core neural stem cell transcription factors (21).

Similarly to genetically normal NS cells, treatment of certain GNS cell lines with BMP4 or serum can drive cell cycle exit, adoption of astrocytic morphology and corresponding changes in marker expression (25). This is accompanied by a loss of the core transcriptional regulators driving self-renewal. It has been suggested that BMP4 treatment is sufficient to ablate tumour-initiating capacity in glioma stem cell populations, but the Pollard lab has found extensive variation between GNS cell lines in the cytostatic and differentiation response. Additionally these cells to undergo differentiation commitment, and remain able to readily revert back into cycle, likely perhaps reflecting increased levels of the core TFs such as SOX2 (Caren et al., Stem Cell Reports, in press).

The increased stability of the core self-renewal gene regulatory network is likely to have functional importance in sustaining GSC self-renewal. Using an elegant model system for analysis of the neural stem program in glioma, Bradley Bernstein's laboratory has identified part of the core gene regulatory network that operates in glioma stem cells . In this study glioma cultures were grown in parallel in either serum free conditions as tumour propagating cells (TPCs, or in our terminology GNS cells), or as 'differentiated glioma cells' (DGCs) in serum based adherent conditions. Comparison of differentially expressed genes identified the expected downregulation of neural stem markers including *SOX2, ASCL1, OLIG2, POU3F2* and *NESTIN* in the DGC population. Forced expression of a subset of these neural stem cell associated TFs (SOX2, OLIG2, POU3F2 and SALL2) in DGCs was sufficient to reinstate tumor propagating potential in vivo, along with sphere formation in serum free conditions (Figure 1-5).

Further evidence for the critical role of the transcriptional and epigenetic state in driving glioma has been provided by previous work from the Pollard lab, involving reprogramming of GNS cells to glioma-iPS cells (with KLF4 and OCT4), and subsequent in vitro 'redifferentiation' to an alternative mesodermal lineage. This prevented formation of

invasive malignancies on xenotransplant. Such experimentally induced lineage reprogramming confirms the efficacy of developmental and differentiation mechanisms in suppressing the glioma phenotype despite a full complement of genetic mutations. Disruption of the core gene regulatory network that sustains GBM is therefore a important avenue to explore in the development of new therapies. Examples of transcription factors with putative functional roles in the regulation of GNS cell identity are provided below (Table 3).

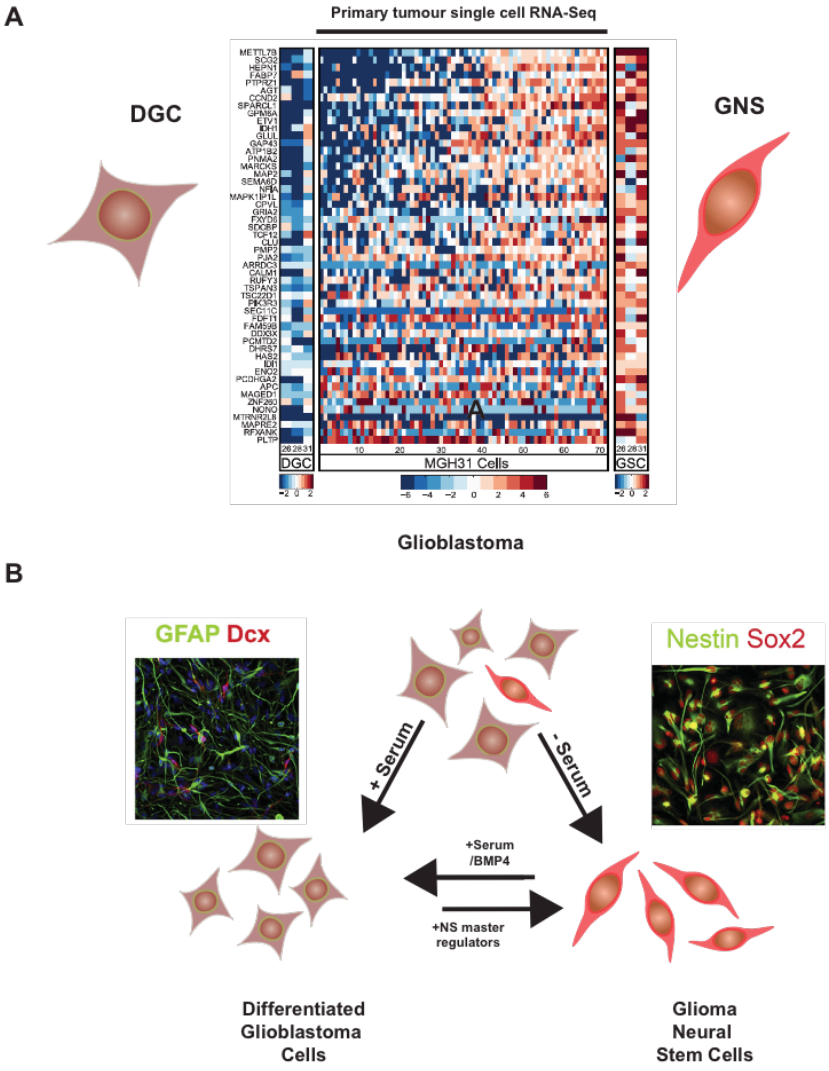


Figure 1-5 - A model of GBM cell epigenetic heterogeneity

Work from the Bernstein laboratory confirms that GBMs comprise a mixed population at single cell level with distinct populations resembling serum derived DGCs and serum-free derived tumour-propagating GNS cells (21). Inductive cues including BMP4 or serum treatment can drive transition from GNS to DGC state, while forced expression of lineage specific neural developmental transcription factors can drive the reverse process (51).

Family	Gene	Role identified in glioma stem cells
CEBP	*CEBPB*	Mesenchymal transformation
Forkhead	*FoxO3*	TGF-beta induced cytostasis (48)
	FoxG1	FoxO3 antagonist; proliferation (45)
	FoxM1	Self-renewal, invasion, angiogenesis (49)
GATA	*Gata6*	Tumour suppressor (50)
bHLH	*Ascl1*	Wnt signalling; self-renewal (47)
	Olig2	Glioma stem program (51)
	Id1	Invasion/EMT ((52))
HMG	*Sox2*	Proliferation (53);Invasion (54)
		TGF-beta response (46);
		Glioma stem program (55)
HOX	*NKX2-2*	Suppression of self-renewal (56)
	HOXA10	Downstream homeobox network driving tumorigenesis (57)
NFI	*NFIA*	Proliferation, migration (58)
POU	*Pou3f2*	Glioma stem program (8) (51)
RING	*Bmi-1*	Upstream of FoxG1 (59);
		Gliomagenesis (60)
STAT	*STAT3*	Mesenchymal transformation (61)

Table 3 Neural lineage-affiliated transcription factor families with reported roles in human GBM

1.3 Insights from neural stem cell biology

In the following sections I introduce relevant aspects of our current understanding of neural stem cell self-renewal, fate specification and commitment during normal development and in adult CNS. I then focus on discussion of glial differentiation and its relevance to GBM, as well as the specific roles of two key candidate neural stem cell master regulators which are the focus of this thesis, FOXG1 and SOX2.

1.3.1 Neural stem cells comprise one lineage from gastrulation to adulthood

Neural stem (NS) cells are defined by the ability to self-renew and to generate neurons and macroglia (primarily oligodendrocytes and astrocytes), and they have been proposed to form a continuous lineage through development, postnatally and into adulthood (62). The earliest cells fulfilling these criteria are the neuroepithelial cells present at the early neural plate stages of development in gastrula stage embryos. Neuroepithelial cells express Nestin, Sox2, and epithelial markers including the tight junction protein occludin, but not astroglial markers. They maintain apical-basal extensions and their nuclei move relative to the ventricle wall through cell cycle by the process of interkinetic nuclear migration (IKNM), forming a pseudostratified epithelium.

Asymmetric divisions by neuroepithelial cells give rise to early born neurons, and to radial glia which form an achitectural scaffold that traverses the developing layers of neurons. Radial glia express astroglial markers including BLBP, RC2 and GLAST, but also express Nestin and remain tripotent in vitro and in vivo. This neural stem cell population retains ventricular contact and IKNM neurogenesis, and corresponds closely in expression profile to the *in vitro* cultured adult mouse neural stem cell lines described here .

Around midgestation a switch from neurogenesis to gliogenesis occurs and continues postnatally. In the cortex, the astrocyte progenitors descendent from radial glia divide to generate the majority of mature astrocytes. Likewise, in the subventricular zone (SVZ) neurogenic niche, radial glia give rise to progeny expressing mature astrocyte markers

including GFAP, and have a typical astrocyte morphology. However these SVZ astrocytes, also known as Type B cells, retain self-renewal and neurogenic capacity into adulthood- they are the adult neural stem cells (63).

Thus, our current understanding comprises a continuum of neural stem cells from neuroepithelial cells through radial glia to adult neural stem cells (Figure 1-6). These populations generally share expression of surface markers CD133 and SSEA-1, the intermediate filament nestin, and the neural stem cell master regulator Sox2.

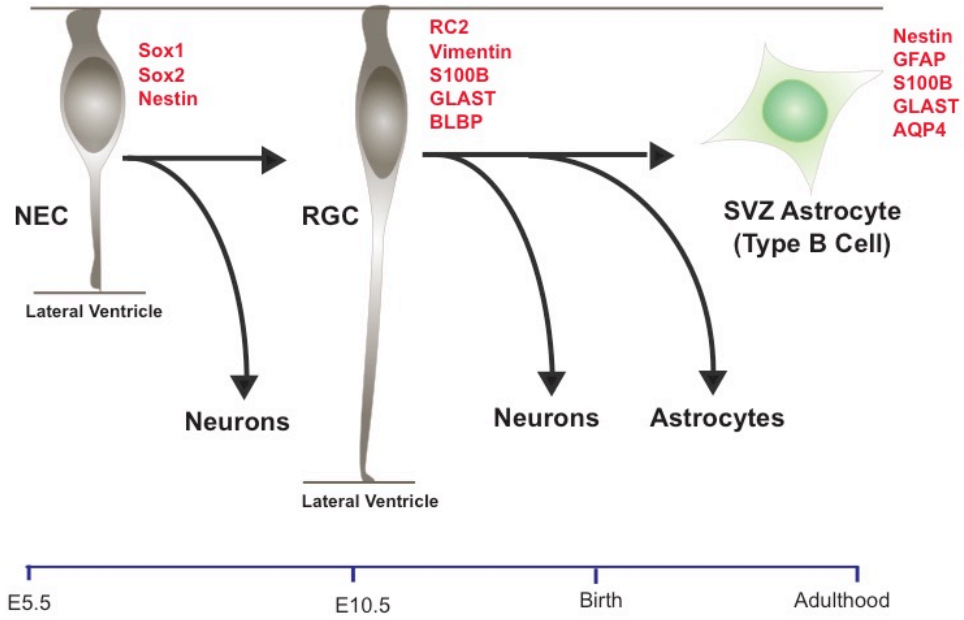


Figure 1-6 - Neural stem cells through development

A continuous lineage of neural stem cells is maintained throughout life. Terminology varies by developmental stage, reflecting distinct morphologies and marker expression, but these cells retain key elements of a common transcriptional and functional identity. Adapted from (62).

1.3.2 Astrocytes are a candidate cell of origin for many glioma subtypes

What is the cell of origin of glioma? This has been an area of intense investigation as it relates to cancer stem cells models. Persistence of aspects of the cell of origin identity in the resulting tumour will likely explain some of the diversity of glioma subtypes. The identification of endogenous neural stem cells within the adult CNS in the late 1990's raised the possibility that these could be a cell of origin. Evidence subsequently emerged from mouse models in support of this. However, the absolute number of neural stem cells in the adult brain is extremely small relative to other types of progenitors and glial cells. The diversity of primary glial tumour types observed and the broad anatomical distribution of these tumours, often outwith germinal centres, suggests a possible additional or alternative cell of origin for gliomas. These might include alternative gliogenic progenitors, such as the oligodendrocyte progenitor cells (OPCs), or mature postmitotic cells undergoing dedifferentiation to reacquire the neural stem cell identity. There is experimental evidence from mouse studies for each of these possibilities.

In the mouse, the adult germinal centres are located within the SVZ of the lateral walls of the forebrain ventricles and also within the dentate gyrus of the hippocampus. These regions contain actively cycling stem cell populations and introduction of glioma driver mutations or carcinogens can result in gliomas (21,64). However, in the cerebral cortex, where most adult gliomas arise, glia are the predominant cell type by number (65), and oncogenic transformation of mouse astrocyte populations has been observed repeatedly across a variety of models to generate realistic invasive gliomas. Defined human disease relevant mutations, for example Ink4a/Arf deletion with EGFRvIII overexpression, were sufficient to drive gliomagenesis in astrocytes in mouse (66). Lineage-specific conditional knockout of *tp53* and *nf1* is also sufficient to generate tumours from all lineages, including neurons and astrocytes, within and outside the neurogenic niches (67). GFAP expression is

common to astrocytes and adult mouse neural stem cells, but conditional mutations of *tp53*, *pten* and *rb1,* targeted to the GFAP-expressing population in adult mice, result in formation of tumours both within and remote from the neurogenic niche, implying successful transformation of astrocytes in at least some cases (68). Thus, it is likely that there are distinct cell of origins for the each subtype of the disease; however, we have only poor understanding of the specific details of this for the human disease as cell of origin is difficult to determine retrospectively: it is equally likely that during tumour progression and evolution genetic and epigenetic insults can establish a distinct cell type identity.

1.3.3 Astrocytes exhibit diverse molecular and phenotypic characteristics

Astrocytes arise from a population of radial glial progenitors. Fate mapping techniques have suggested that while a few multipotent radial glia first generate neurons and then switch to gliogenesis, a distinct population generate astrocytes in the post-natal period following the neuronal-glial switch (69). Regional difference in positional identity of astrocyte progenitors has also been noted and still remains largely unexplored (69,70). Rodent astrocytes are predominantly generated in the post-natal period by ongoing slow division of immature astrocytes. GFAP is the best established marker of mature astrocytes, and stellate GFAP-high fibrous astrocytes are the archetypal population in white matter (71). However protoplasmic astrocytes, irregular in shape and GFAP-negative or only weakly positive, are predominant in the gray matter (72). How these distinct popuations relate to earlier positional identity in the radial glia remains ill-defined. Other markers commonly used as astrocyte markers include S100beta (73), GLAST (74), Aquaporin-4 (75) and NFIA (70). Co-labelling studies indicate that each of these markers in isolation fails to uniquely identify astroglial lineage cells e.g (76). Likewise A2B5 has been used as a marker of astrocyte progenitors (APC), but also labels oligodendrocyte precursors. Fgfr3 is specific to astrocytes and astrocyte progenitors, but is not expressed universally across brain regions (77). The cerebellum, spinal cord and other regions contain their own distinct astrocyte

populations, and astrocyte identity seems to be further complicated by patterning in specification in the spinal cord at least, mediated through a bHLH transcription factor code (78). Recent studies have begun to better define differences between astrocyte like stem cells and parenchymal astrocytes. Use of single cell RNA-Seq is also providing a wealth of new candidate markers to explore to better understand astrocyte cell type identity and diversity.

Although mature astrocytes expressing markers including AQP-4, S100B and GFAP are generally considered to be post-mitotic, they retain the ability to become re-activated and re-enter cycle in response to injury (Section 1.3.5). This latent capacity for cell cycle re-entry may underpin the susceptibility to become neoplastic.

1.3.4 Astrocyte Differentiation can be modelled *in vitro*

In vitro models of astrocyte differentiation date from studies of O2-A progenitors in the early 1980's, and latterly the use of primary neural stem cell cultures. In neurosphere or adherent NS cell cultures, astrocyte differentiation can be efficiently induced by exposing cells to serum. Differentiation can be steered to alternative lineages by replacement of the growth factors EGF/FGF with instructive drivers of astrocyte differentiation, including Ciliary Neurotrophic Factor (CNTF), Leukaemia Inhibitory Factor (LIF) and Bone Morphogenic protein 4 (BMP-4) (2). CNTF appears to exert its effects through the JAK-STAT and MAPK pathways (79). Bone morphogenetic proteins (BMPs) are part of the TGF-beta superfamily and act through serine threonine kinase receptors on the cell surface. Ligand binding results in formation of a tetrameric BMP receptor complex, which phosphorylates R-Smads, enabling Smad complex formation, nuclear translocation and modulation of target gene transcription (Figure 1-10) (80). The astrocyte differentiation inductive signals BMP, LIF, CNTF, and Cardiotrophin-1 (CT1) also converge on JAK/STAT downstream signalling pathways (81). Additionally, BMPs act to inhibit oligodendroglial and neuronal specification through SMAD mediated induction of transcription of Id proteins (inhibitors of DNA binding and differentiation) that in turn block

the proneural activity of factors such as Mash1 (Ascl1) by sequestering the essential partner E proteins (82).

Previous work suggests that, whereas LIF treatment of SVZ-derived NS cells drives the generation of GFAP+ cycling progenitors – possibly with neural stem cell character – BMP4 treatment is necessary and sufficient to drive mature astrocyte differentiation, has potent cytostatic effects and triggers downregulation of NS cell markers, and upregulation of GFAP expression, and adoption of a differentiated morphology (81). In keeping with this, as presented in Results 2, we find that mouse NS cells exposed to BMP4 alone (no FGF2), at low plating densities for 24 hours or more, are unable to re-enter cycle on re-exposure to growth factors. Although these populations may upregulate components of the neural stem transcriptional program in response to EGF/FGF stimulus, for example Olig2 expression, they retain astrocyte marker expression and morphology. Therefore we propose that BMP4 exposure in the absence of paracrine FGF signalling or cell contact (likely Notch mediated), can enforce astrocyte specification, commitment and terminal differentiation.

The Guillemot laboratory has demonstrated a distinct phenotype upon exposure of NS cells to BMP4 together with FGF at high plating densities (350-650 cells/ mm2) (83). In this case, NS cells were seen to exit cycle, to downregulate EGFR, upregulate GFAP but not S100B, and to sustain some expression of Nestin and Sox2. On return to EGF/FGF, these cells re-entered cycle and readopted an NS cell transcriptional profile. This phenotype resembles endogenous type B stem cell-like quiescent astrocytes. We observed a similar response on exposure to BMP alone in our NS cell lines at high plating densities, and these findings are in keeping with the behaviour of rat NS cells, which spontaneously enter a quiescent/dormant state after a small number of divisions in culture. This state is shown to depend on the interaction of autocrine BMP and FGF signalling, respectively driving and suppressing cycle arrest (84). Thus, the balance between BMP alone or BMP plus FGF or other signals (e.g Notch, Eph/Ephrins) might determine whether astrocytes commit to a

terminal differentiation fate, or instead remain immature and retain neuronal differentiation capacity (Figure 1-7).

1.3.5 Reactive astrocytes express NS cell markers and exhibit latent multipotency

Mature protoplasmic astrocytes have been traditionally considered permanently post-mitotic, so that injury results in polyploidy/ death. However both cortical and spinal astrocytes have demonstrated the ability to upregulate Nestin and proliferate in response to a range of insults, including trauma and stroke (87,88). Fate mapping studies in injured cortex using GLAST-Cre-ERT2 or GFAP-CreERT (which will also label endogenous NSCs in SEZ) indicate that reactive protoplasmic astrocytes re-enter cycle and upregulate nestin in response to injury, but remain within their lineage (86). However uniform astrocyte lineage commitment is also observed in NSCs transplanted into injured cortex, suggesting that this identity may be adopted in response to the prevailing microenvironment rather than as an intrinsic cell autonomous property. In keeping with this, reactive astrocytes harvested after injury could be propagated as spheres in standard serum free conditions with mitogens, and are tripotent (86). Likewise mature spinal cord astrocytes can generate neural precursors on injury or indeed on exposure to injured astrocyte conditioned media (89).

The overlap in function and marker expression between radial glia in development and the type B neural stem cells of the subventricular zone extends to reactivated astrocytes. Therefore a stable mature postmitotic astrocyte phenotype may be conditional on environment, and the molecular and phenotypic similarities between an astrocyte-like neural stem cell and a terminally differentiated astrocyte may be closer than many would have anticipated.

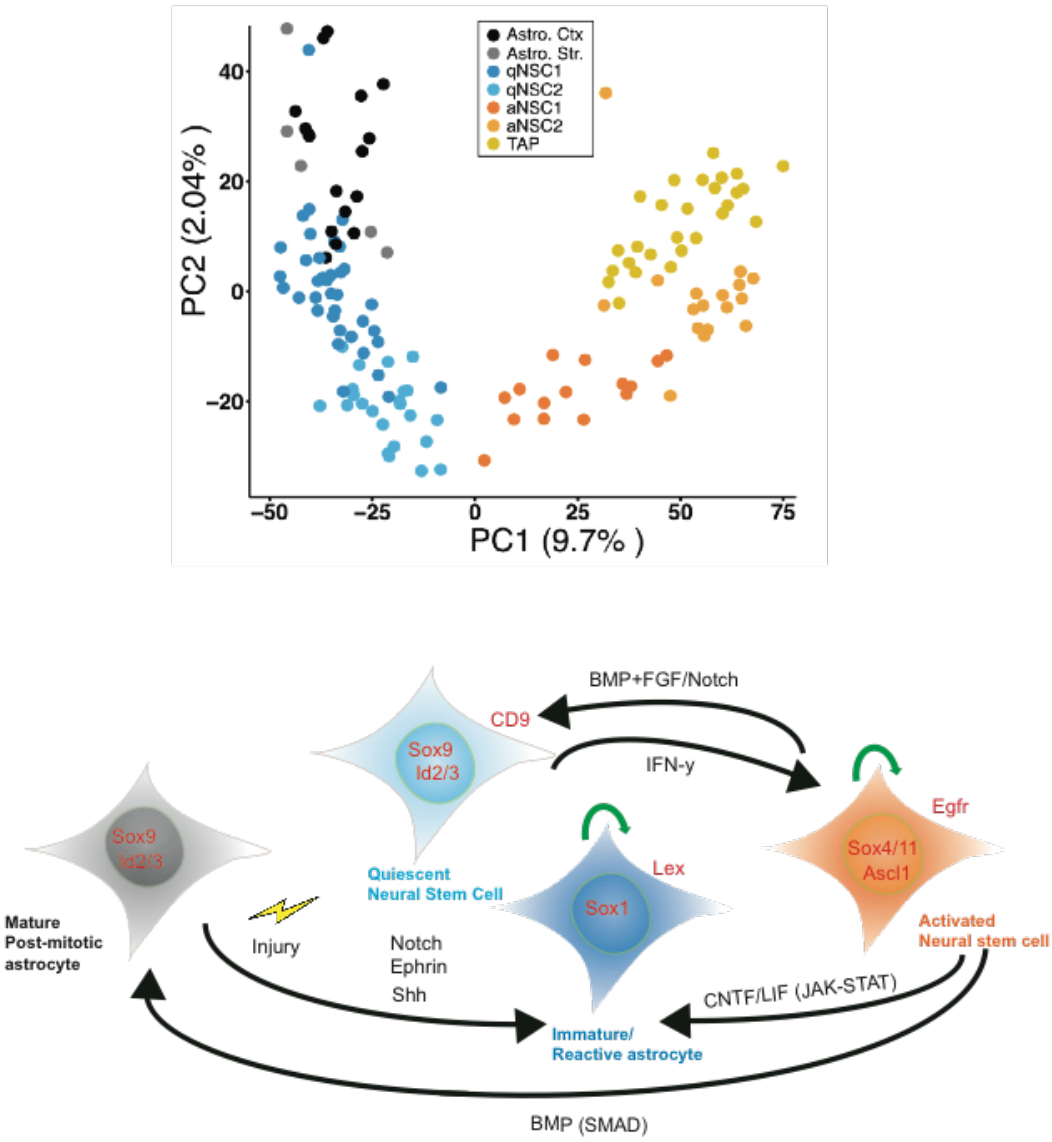


Figure 1-7 – Cell identity relations in astrocytes and NS cells, quiescent and activated

Single cell RNA-Seq data points to a continuum of cell identity incorporating the cell types shown, with transcriptomes clustering as shown in the upper panel (85). Expression of the nuclear TFs and cell surface markers indicated in the lower panel is characteristic but not exclusive for specific states. Inductive signals drive the identity transitions shown, including astrocyte differentiation (81), NS cell quiescence (83), and astrocyte reactivation (86).

1.3.6 Astrocytes can undergo experiementally imposed lineage conversions

Direct lineage conversion of astrocytes into neurons has been reported using forced expression of individual transcription factors including PAX6, ASCL1, NGN2 and DLX2, by the Gotz lab and others (41,90-92). Importantly lineage tracing of this process in SOX2-induced astrocytes indicates that the cells involved do not transition through a Nestin positive neural stem cell state (41).

The principle of induced astrocyte dedifferentiation in gliomagenesis has been established by lineage specific conditional knockdown experiments mimicking glioma-relevant mutations. Targeting astrocytes *in vitro* and *in vivo* with shRNA against *p53* and *nf1* drives convincing expression of NS cell markers, sphere formation *in vitro* and tumour formation *in vivo* (67).

Transcription-factor induced astrocyte dedifferentiation outside the context of oncogenic manipulation is less well established. A report exists of human astrocyte dedifferentiation to an NS cell state in response to lentiviral expression of OCT4, SOX2 or Nanog (93). The evidence presented is compromised by the failure to present control negative lentiviral infections using unrelated transcription factors: given that astrocytes are able to dedifferentiate in response to injury, lentiviral transduction in isolation may well induce this process. Equally any dedifferentation elicited by these factors may proceed via a process incorporating induction of pluripotency by these established drivers of the iPS state (94). Finally the mixed starting population inherent in the use of primary astrocytes introduces ambiguity as to the nature of any fate transitions achieved. Indeed in our hands, primary serum-derived mouse astrocyte cultures exposed to neural stem cell growth conditions are able to generate NS-like colonies at low efficiency, presumably as a result of a contaminating NS fraction, or a transcriptional resetting of other progenitors (e.g. OPCs) in response to the culture conditions. *In vivo* studies also suffer from heterogeneity of starting populations: even for approaches involving genetic lineage mapping the conditional markers are often overlapping between astrocytes and NS populations. New molecular markers that

can distinguish distinct subset of astrocytes and astrocyte-like stem cells are emerging, and will be assessed against classifications based on single cell whole transcriptome sequencing (95). Initial analysis of single cell neural stem cell datasets indicates that quiescent NS cells are characterised by expression of astrocyte-associated TFs including *Sox9, Id2, Id3* and *Id4,* raising the question of whether there is in fact a genuine cell-intrinsic distinction between these populations, or whether in fact differentiated astrocytes might generally represent competent neural stem cells on exposure to the appropriate niche.

1.4 The Role of FOXG1 and SOX2 in NS cell and GNS cell function

1.4.1 Forkhead Box G1 (FOXG1) is a forebrain-specific Forkhead Box TF

The Forkhead Box (Fox) superfamily comprises 50 human transcription factors, conserved through vertebrate evolution and sharing a winged helix DNA-binding domain (96). The term forkhead derives from a phenotype associated with knockout of the founding member in drosophila (97). These factors are subdivided into 19 subfamilies, characterised by distinct domain architecture including a range of cofactor binding sites mediating transcriptional activation, repression and interactions with epigenetic regulatory apparatus. A range of post-translational modifications confers a further level of functional complexity in forkhead function. For example phosphorylation of FoxO factors can lead to their cytoplasmic relocation or degradation (98). Many forkhead factors have established roles in control of cell cycle and fate, and several are strongly implicated in cancer (99). Human *FOXG1* is a single exon gene encoding a peptide of 489 amino acids. FOXG1 is a key regulator of forebrain-specific neural stem cells and is a member of the forkhead box family of transcription factors.

1.4.2 The Forkhead domain confers pioneer factor potential

Biochemically, the forkhead domain is distinctive for binding one side of the DNA helix irrespective of nucleosome occupancy on the opposite side. In this context, FoxA1 at

least has a demonstrated role as a pioneer factor (100), and the defining structural homology of other forkhead proteins is likely to confer similar activity in some at least. Binding may directly displace repressive chromatin features and recruit chromatin modifying factors. For example, the FoxG1 sequence incorporates a predicted Jarid binding domain, raising the possibility of interactions with the Polycomb repressive complex component Jarid2 (101). The unusual ability of pioneer factors to bind and derepress closed chromatin seems key to reassigning identity in differentiated cells, as exemplified by SOX2 in the early reprogramming of fibroblasts to iPS cells (102). The ability of pioneer factors to drive new transcriptional patterns may well have importance during tumorigenesis.

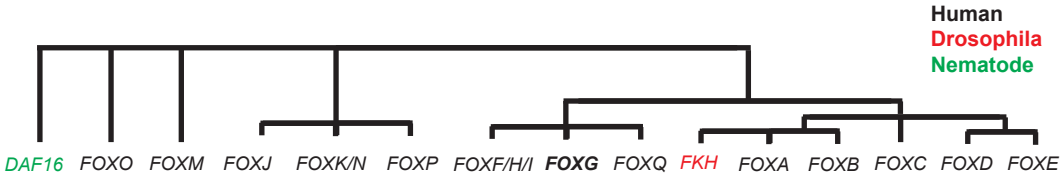


Figure 1-8 - Simplified forkhead family phylogenetic tree

This classification is based on sequence homology with reference to common ancestors in *C.elegans* and *D.melanogaster*; redrawn from (103), not to scale.

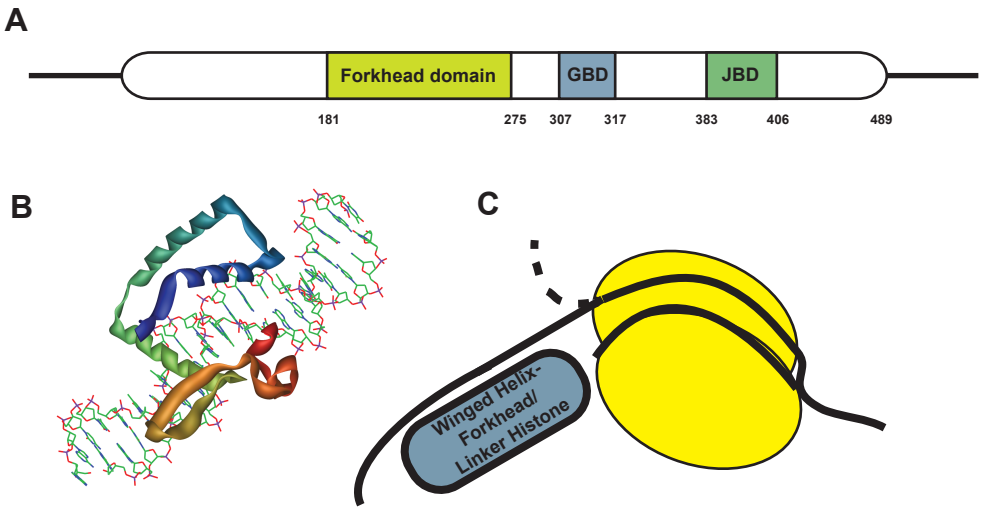


Figure 1-9 – The FOXG1 locus and gene product

A *FOXG1* is a single exon gene encoding a 489aa peptide with Forkhead DNA binding domain, and predicted Groucho binding and Jarid binding domains. **B** The forkhead DNA binding domain resembles the H1 linker histone structurally (PDB structural prediction model from cisreg.ca) **C** The forkhead domain has been shown to be capable of binding to nucleosome-bound heterochromatin, conferring pioneer factor activity{Zaret:2011dl}.

1.4.3 The Forkhead family includes members that are deregulated in human cancer and control stem cell fate

Many Forkhead family members have been shown to be deregulated in diverse human cancers (Table 4). The most extensively studied forkhead proteins include the FoxO family of tumour suppressors and FoxM1, an oncogene overexpressed in many carcinomas. In both neural stem cell and glioma contexts, FoxM1 maintains self-renewal through Wnt/B-catenin signalling (49). Canonical roles of FoxO factors include transcriptional repression of Cyclin D1 and activation of cell cycle inhibitors p21Cip1/Waf1 and p27Kip1(104), mechanisms believed to account for their involvement in the activity of a number of novel chemotherapeutic agents in vitro (105-107). FoxO3 also competes for occupancy at the VEGF promoter with FoxM1 (108), and these factors respectively repress and activate VEGF transcription (109).

A number of Fox factors are established regulators of stem cell identity. In the neural lineages, deletion of FoxO3 in mice leads to premature depletion of the NS pool, and it seems likely that FoxO3 regulates the quiescent neural stem cell population: ChIP-Seq demonstrates a large pool of genomic targets shared with Ascl1, and FoxO3 expression is shown to impede both Ascl1-induced terminal neuronal differentiation and transdifferentiation of fibroblasts to neurons (110). Other investigators have suggested that FoxO3a expression reduces tumorgenicity by promoting differentiation of glioma cells(104).

Simple functional subcategorisation of Fox family members into either oncogene or tumour suppressor roles is difficult as cellular context profoundly influences their function. For example individual FoxP and FoxA factors reported to be of prognostic significance in glioma (111,112), may have opposing effects on tumour progression in different cancers, and even in the same cancer histology depending on hormonal factors (113). Thus, a complicated picture emerges in cancer biology where the same transcriptional and epigenetic regulators could have different roles at different stages of tumour development and within the differentiation hierarchy.

The Massague laboratory implicated *FOXG1* in glioma biology in an elegant study demonstrating interaction with FoxO factors, as mutually antagonistic effectors of TGF-beta and PI3K signalling pathways that compete to respectively downregulate or upregulate Cdkn1a/p21 expression in NS and glioblastoma (Figure 1-10) (48). These pathways represent the targets for a range of novel cancer therapeutics, from receptor tyrosine kinase inhibitors, to agents responsible for directing FOXO3 subcellular localisation through post-translational modifications (99).

1.4.4 Forkhead factors interact with protein cofactors to regulate transcription

FoxO3a and FoxP1 have demonstrated roles in transcriptional repression through partnership with Nuclear Receptor Corepressor (NCoR) complexes, recruiting histone deacetylases (HDACs). FoxM1, FoxP and FoxA factors also achieve DNA methylation and chromatin compaction by direct and indirect recruitment of DNA methyltransferases and HDACs (99). The FoxG1 sequence incorporates a predicted Groucho-binding domain, which may mediate similar interactions with the Groucho/TLE family of transcriptional co-repressors (114).

Category	**Normal Role**	**Key targets**	**Results of Dysregulation**	**Mechanisms of dysregulation**
FOXO	Cycle arrest/exit; apoptosis; oxidative stress response	P27;p21; Cyclin D; p130, BIM, TRAIL, FASL, MNSOD, catalase, ERa, GADD45	Unchecked Proliferation; resistance to apoptosis/ growth factor withdrawal	PI3K-Akt-IKK upregulation
FOXM	G1-S and G2-M progression; spindle integrity	CyclinA/B; CDC25B; p21/p27 degradation; AURKB; PLK1, SKP2, CKS1, CENPA/B/F, NEK2, KIF20A	Unchecked Proliferation; genomic instability;	Mutation in upstream regulators, gene amplification
FOXP	Haematopoietic development	RAG1/2; TCFE2A, EBF1, CD79B, E2A, EBF, ZAP70, BCL019, ITK, NFKB, NFAT	Evasion of tumour immune surveillance	Overexpression through chromosome translocation; gain of function mutation
FOXA	ER cofactor	E cadherin, p27, Cyclin D1	Endocrine independent proliferation/survival	Methylation of promoter
FOXC	Blood vessel maturation	VEGF, NOTCH1, DLL4	Metastasis and invasion	Overexpression

Table 4 Proposed roles and example targets for forkhead TFs in human cancers. Adapted from (103).

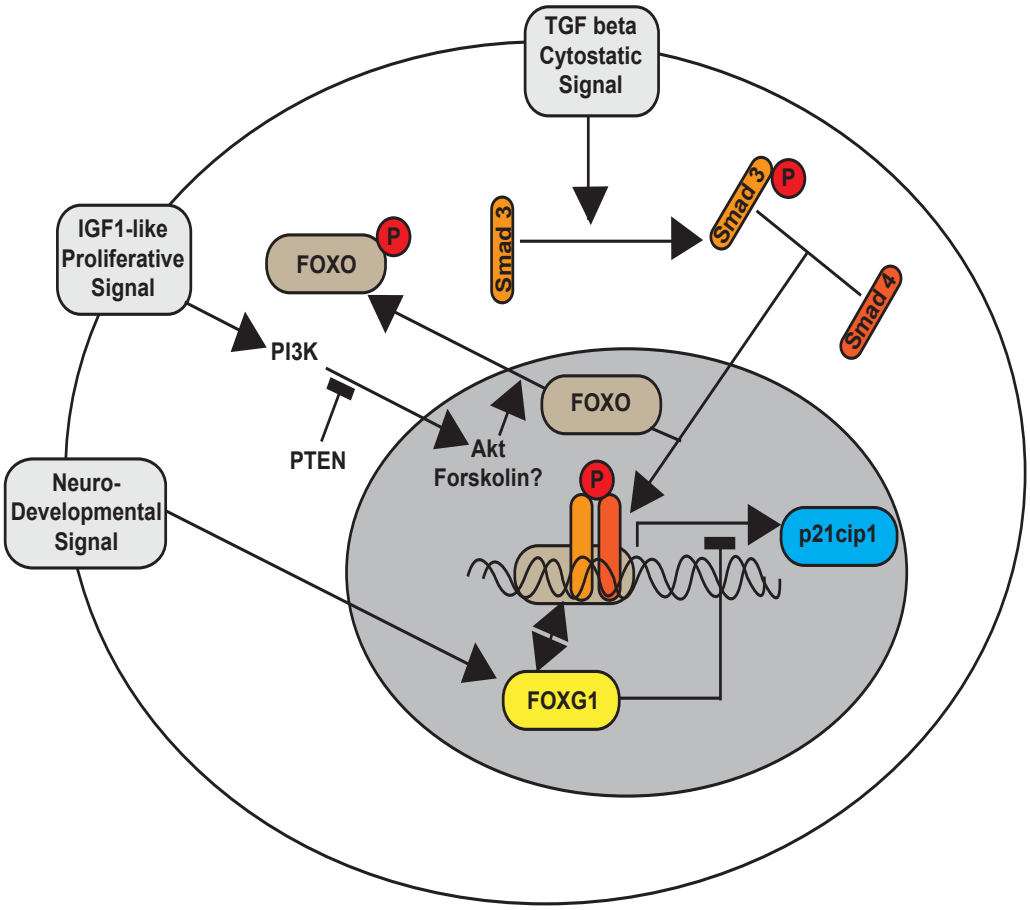


Figure 1-10 - A model of FoxO and FoxG1 activity in GBM

BMP/TGF-beta signalling drives cell cycle exit through activity of a Smad-FOXO3 complex transactivating p21 and p27 cell cycle inhibitors, and inhibiting Cyclin D expression. FOXG1 may antagonise this through sequestration of FOXO3 - after Massague (48).

1.4.5 FOXG1 is critical to brain development and post-natal neurogenesis

Recently, the importance of correct *FOXG1* gene dosage in human development has been clearly demonstrated by human genetic studies that identified heterozygous loss-of-function or gene duplication with variant of Rett syndrome (now termed FoxG1 syndrome), a severe pervasive developmental disorder (115,116).

FOXG1 drives neural stem cell proliferation and self-renewal, at least in part through DNA-binding independent mechanisms, as evidenced by the activity of DNA-binding defective forms (117). During neurogenesis in the embryo, radial glia neural stem cells lacking FoxG1 exit cycle and differentiate into neurons prematurely, resulting in severe, perinatal-lethal telencephalic hypoplasia in $FoxG1^{-/-}$ mice (Figure 1-11) (118). A cell autonomous basis for this effect has been demonstrated using mutant and wild type chimeras (119). Conversely, overexpression in the developing chick neural tube results in hyperplasia of the telencephalon and mesencephalon (120). FOXG1 is also an important part of the apparatus that confers positional identity in the developing telencephalon. It is responsible for coordinating the appropriate transcriptional response to ventral signals, hedgehog from the prechordal plate and Fgf8 from the anterior neural ridge, and opposing dorsal roof plate Wnt signalling (121) (Figure 1-12).

Expression within the dorsal telencephalon is evident at later stages (E15.5), reflecting a functional role beyond patterning, and emphasising the importance of gene dose to function here. These findings are consistent with the *foxg1* knockout phenotype, suggesting that FoxG1 expression preserves self-renewal by driving cell cycle in cortical progenitors (122), but it is also required as part of the timing mechanisms governing the sequence of neuronal subtypes generated throughout development (123).

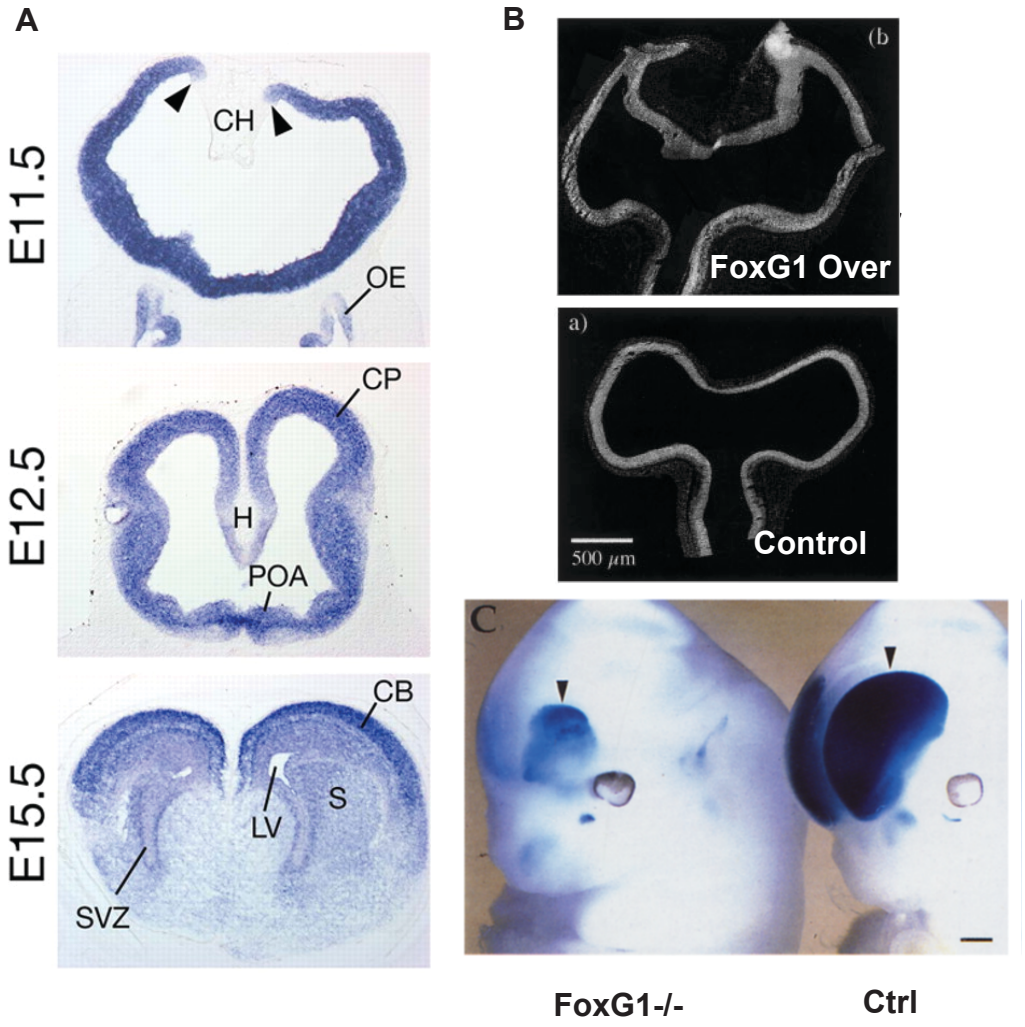


Figure 1-11 - Patterns of FOXG1 expression in development

A FOXG1 is expressed highly in the developing telencephalon, most strongly ventrally and less so in the cortical hem (CH) OE= olfactory epithelium; CP = cortical plate; SVZ= subventricular zone; LV = lateral ventrical; S= striatum; POA = preoptic area; H = hippocampus (124). **B** Overexpression of FOXG1 in the chick neural tube causes overgrowth (120). **C** FOXG1 null embryos die at birth exhibiting severe telencephalic hypoplasia (118).

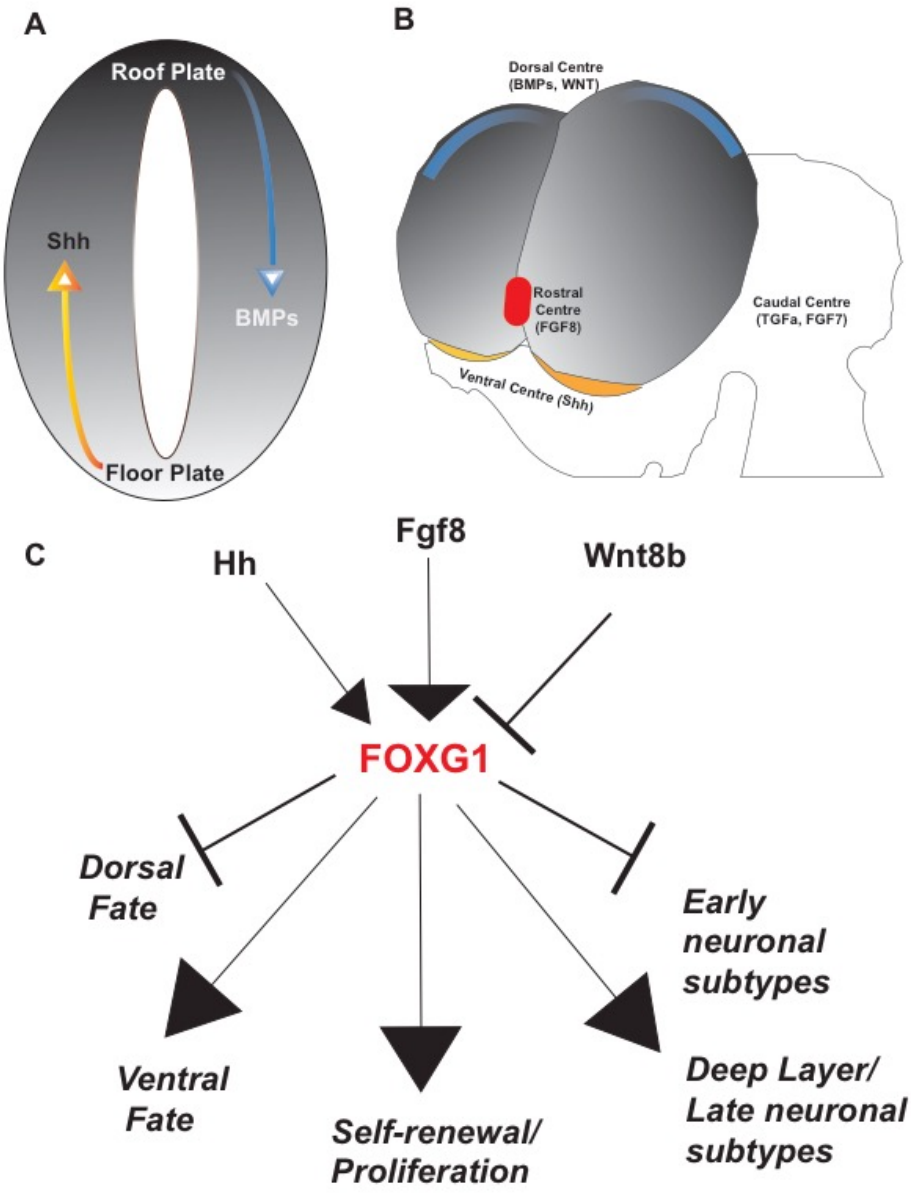


Figure 1-12 - Roles of FoxG1 in cell fate and patterning during development.

A Opposing Shh and BMP/Wnt signalling gradients are established by the floor plate and roof plate of the neural tube respectively. **B** These signalling centres continue to direct patterning into later phases of telencephalon development. **C** FoxG1 is a transcriptional effector of the ventral forebrain patterning axis, and directs self-renewal and fate decisions (125).

Conditional genetic deletion of *foxg1* in cortical precursors leads to an excess production of the Cajal-Retzius neurons (the earliest born neuronal subtype), and failure to generate later deep-layer cortical neurons (126). This element of FoxG1 function, as opposed to its pro-proliferative effects, seems to be dependent on an intact DNA-binding domain (117). FoxG1 has also been shown to be required for the later maturation of pyramidal neurons (127), and expression is retained in the postnatal neurogenic niches of the subventricular zone and dentate gyrus (59,128). A requirement for FoxG1 has also been reported into adult neurogenesis and even to the survival of differentiated adult neurons (129).

The role of FoxG1 in neural stem cell propagation is not determined solely by absolute levels. Rather its phosphorylation on the Serine 19 residue has been shown to regulate nuclear import, whereas phosphorylation in the DNA binding domain in response to FGF signalling drives nuclear export during neuronal differentiation (130).

1.4.6 High FoxG1 Levels may drive glioma stem cell self-renewal

The term ‘master regulator’ has been applied to lineage-specific transcription factors whose expression at a given developmental time-point is necessary and sufficient for correct specification or commitment to a lineage. More recently master regulators have been defined functionally according to their capacity when overexpressed in ‘reprogramming cocktails’ for reprogramming or direct lineage conversion purposes (131). As discussed above, the combination of FoxG1 with Sox2 (39) or with Pax6 (42) has been reported sufficient to induce reprogramming of fibroblasts to precursors with astrocytic and neuronal differentiation potential (Section 1.2.8). Analysis of the motifs associated with regions undergoing epigenetic modification over the course of ES to neural stem/ progenitor transitions also point to FOXG1 and SOX factors as key regulators of these transitions (132).

Reprogramming activity offers obvious parallels with the process of establishing an aberrant NS-like transcriptome and epigenome which is entailed in transformation of distinct

cells of origin (e.g. SVZ stem cells, oligodendrocyte precursors or astrocytes) into glioma stem cells (133) . The polycomb group protein Bmi-1 promotes self-renewal in NS cells and its effects are dependent upon FoxG1 expression, suggesting a possible role in directing the polycomb repressive complex according to the NS cell transcriptional program (59). FoxG1 therefore is a potential key regulator of forebrain neural stem cell self-renewal.

Affymetrix array data from the GeneSapiens database encompassing a range of normal tissues and cancers (134) confirmed *FOXG1* expression restricted to the CNS and testis in healthy tissue. Significant upregulation in a number of cancers was evident, most notably in glioma (Figure 1-13).

Survival data from the Rembrandt database indicates that high expression in primary tumour tissue correlates with reduced survival (Figure 1-14A). Genome-wide analysis using Tag-seq in our lab has previously identified *FOXG1* as amongst the most significantly and consistently upregulated genes when comparing glioma neural stem cells with neural stem cells grown in identical conditions (Figure 1-14B) (43). This difference has been confirmed by the Pollard lab at mRNA level using qPCR, and at protein level using Western blot (Figure 1-14C,D).

Mutation data from the TCGA Research Network: (http://cancergenome.nih.gov/) has identified amplifications or point mutations at the FOXG1 locus in 8 of 556 gliomas profiled. Importantly the point mutations identified were all missense or in frame deletions compatible with preserved protein function.

FoxG1 shRNA knockdown has been reported to reduce proliferation of human GNS cells grown as tumour spheres *in vitro*, and to prolong survival on orthotopic transplant of these cells into mice (45). However, the reported effects were modest and it remains unclear how and why FOXG1 is retained at such high levels across the diversity of GNS cell lines. Exploring these issues is the major goal of this thesis.

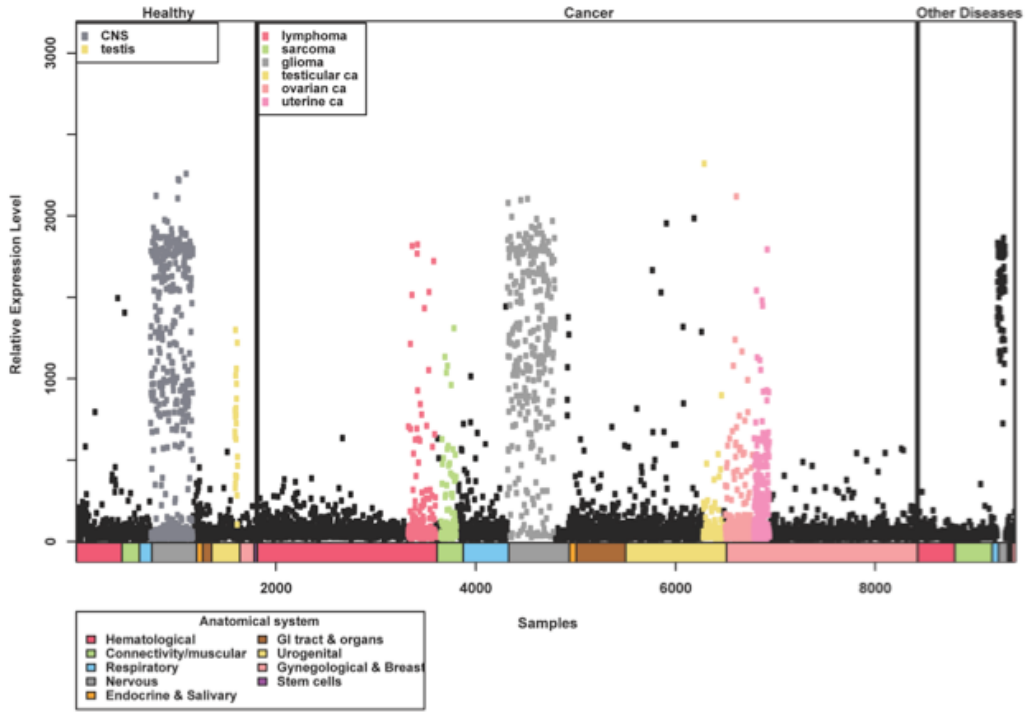


Figure 1-13 - Tissue-specific FOXG1 expression patterns in health and disease

Data from the GeneSapiens database demonstrates high FOXG1 expression in CNS and testis derived normal tissue samples. Expression is also high in many cancer primary tissue samples, especially gliomas.

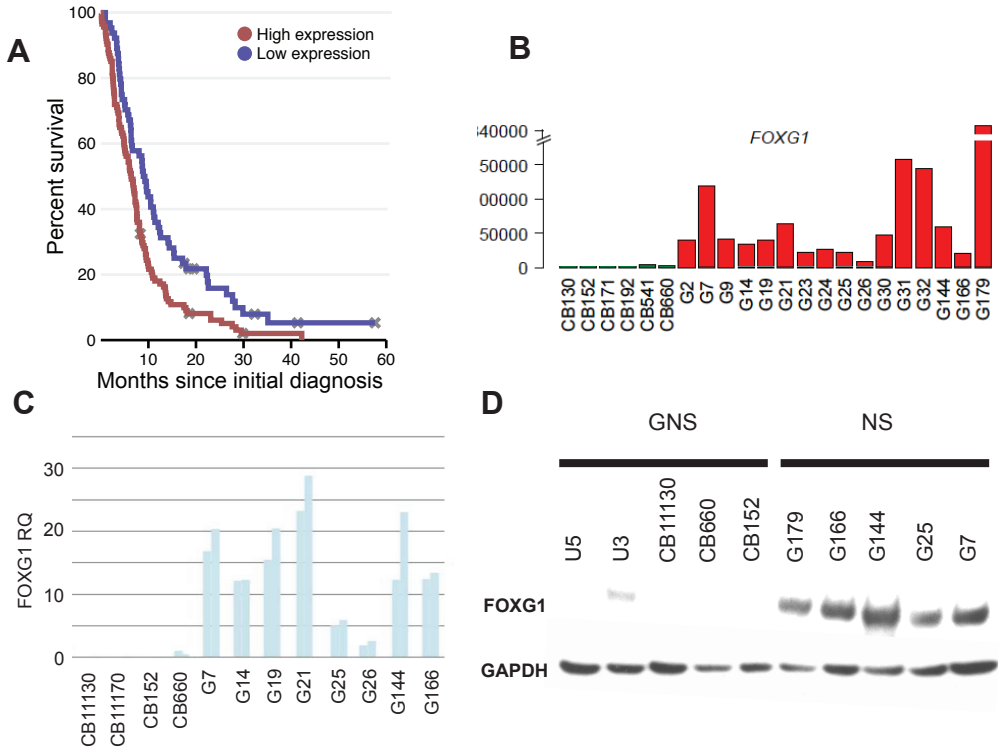


Figure 1-14 - FOXG1 expression in GBM and GNS cells

A In the Rembrandt primary glial tumour dataset, tumours displaying high FOXG1 expression demonstrate significantly reduced survival from diagnosis **B** Tag-Seq data demonstrates consistently higher FOXG1 expression in GNS cell lines compared to NS controls (43). This finding is replicated by qRT-PCR **C** and Western Blot **D**.

1.4.7 Sox2 is a neural stem cell master regulator and is amplified in glioma

The Sox family of proteins comprises around 21 different family members, defined by HMG-box DNA binding domains, and similarities to the prototypical member, SRY (135). The B1 subfamily are transcriptional activators possessing a C-terminus activation domain (136). The B1 family comprises the members *sox1*, *sox2* and *sox3* sharing >95% sequence homology, and each is expressed broadly in neural stem and progenitors during neural development.

Sox2 is expressed in pluripotent embryonic stem cells and neural stem cell populations, from the earliest neuroepithelial cells at gastrulation to adult SVZ astrocytes. While embryos null for *sox1* or *sox3* survive to adulthood with grossly normal CNS development, *sox2* null embryos die around implantantion (137). Conditional *sox2* deletion in the developing brain using Nestin-Cre is perinatal lethal, with elevated Sox3 levels pointing to a degree of compensation and redundancy (138). *In vitro sox2*-null NS cells exit cycle and fail to form self-renewing colonies (139), while conversely overexpression of Sox2 can prevent neuronal differentiation, enforcing a neural stem cell identity (140).

Additional evidence points to Sox2 as perhaps the single most critical regulator of neural stem cell identity: in Xenopus and in mouse, Sox2 expression is sufficient to drive neuroectoderm formation at the expense of other lineages (141,142). In the context of GBM, SOX2 has been shown using shRNA experiments to be necessary to maintain proliferation and tumorgenicity (53) and it may also control the invasive properties of malignant glioma cells (54). SOX2 appears to mediate the pro-tumorigenic of TGF-beta signalling in glioma (46), where FOXG1 has been suggested to interfere with the cytostatic effects of the same signalling cascade mediated through FOXO3 as previously discussed (48). Work in our own lab has failed to demonstrate a direct protein-protein interaction between these two factors, so the links between FOXG1 and SOX2 are likely at the gene regulatory network level rather than a shared protein complex (Pollard lab, unpublished).

SOX2 has attracted much interest recently as it is one of the Yamanaka factors overexpressed for the original demonstration of induced pluripotency in fibroblasts (94), and remains an almost universal component of further reprogramming cocktails, including those used to achieve fibroblast reprogramming to a neural stem cell state (39) (Section 1.2.8).

1.5 Aims and Hypotheses

1.5.1 A Hypothesis for FoxG1 Activity in NS cells and GNS cells

On the basis of established insights into its activity, we hypothesized that FOXG1 is a neural stem cell master regulator that when expressed alone or in combination with other NS master regulators at high levels is sufficient to:

- Maintain the neural stem cell program.
- Impair terminal differentiation and promote re-acquisition of neural stem cell identity.
- Drive the radial glia-like NS cell transcriptional and epigenetic state in committed and terminally differentiated cells.

The aims of this thesis are to directly test these predictions and determine the major downstream effectors of FOXG1 in neural stem cells, astrocytes and especially at the high expression levels encountered in GBM.

2 Materials and Methods

2.1 Cell culture

Unless otherwise stated, all cell lines were cultured at 37°C and 5% CO_2 and grown on uncoated tissue culture plastic in adherent monolayer. Dissociation was performed using Accutase (Sigma). Cells were passaged 1:6 to 1:8, or media changed as appropriate, every 3-4 days.

2.1.1 Self-renewal media

Mouse and human neural stem (NS) cells and glioma-derived neural Stem cells (GNS) were grown under serum-free conditions in DMEM F-12 supplemented with N2 and B27, penicillin-streptomycin, 1 μg/ml Laminin, 10 ng/ml EGF and 10 ng/ml FGF-2 as previously described (143).

2.1.2 NS cell astrocyte differentiation media

To drive astrocyte differentiation cells were exposed to BMP-4. Media composition was identical to self-renewal culture media, except that the growth factors EGF and FGF-2 were replaced with BMP4 10ng/ml (R&D Systems).

2.1.3 Primary astrocyte culture media

Astrocytes were derived using cerebral cortical tissue dissected from P3 mouse pups using established protocols (144), and were plated on plastics precoated with poly-D-lysine 50ug/ml at 37C for 1 hour. Media comprised DMEM F-12 supplemented with N2, 10% fetal bovine serum.

2.1.4 Freezing media

Freezing media was based on DMEM-F12, supplemented with 10% Dimethylsulfoxide. Cells were dissociated using accutase then pelleted in wash media, then resuspended in freezing media and placed in the -80 freezer in a freezing jar.

2.2 Immunocytochemistry

Cells were washed with PBS and fixed using 4% paraformaldehyde for 10min at room temperature. Fixed cells were next washed and permeabilised in PBST (PBS with 0.1% Triton), then blocked for 30min in blocking solution comprising PBST with 0.1% BSA and 3% goat serum. Overnight incubation at 4^{o}C was performed with primary antibodies suspended in blocking solution at the concentrations indicated. Residual primary antibody was removed with 3 x 5min PBST washes, then secondary antibodies suspended in PBST at the concentrations indicated were applied and incubated for one hour. Wash steps were repeated as before, and the cells were incubated in 1:5000 DAPI (Sigma-Aldrich) for nuclear counter-staining. Images were obtained using the Zeiss Observer Z1 microscope and Axiovision software, or the PerkinElmer Operetta high content imaging system and Harmony software.

2.2.1 Quantitation of Ki67 immunoreactive cells

The effect of FoxG1 expression level on cell cycle was established by immunocytochemistry for Ki67 and DAPI at 48 hours (2,83). A custom CellProfiler pipeline was used to identify and segment individual nuclei, then to classify each object as Ki67 positive or negative. Typically six random fields were recorded from 2 independent wells and analysed in this way (~300 nuclei per field; total n= ~3600).

2.2.2 EdU incorporation assays

EdU immunostaining was performed using the Click-iT EdU Alexa Fluor 488 assay kit (Life Technologies) according to manufacturers guidelines.

2.2.3 Primary Antibodies used in this study

Antigen	Host/Clone	Reactivity	Dilution	Supplier
Alpha-tubulin	Rat hybridoma	H,M	WB 1:1000	DSHB
Beta-tubulin	Mouse IgG2a	H,M	IF 1:500	Covance
FoxG1	Rabbit Ab18259	H,M	ChIP 10ul	Abcam
FoxG1	Mouse IgG2a (17B12)	H,M	IF 1:3; WB 1:15	Pollard lab
FoxO3	Rabbit IgG (D19A7)	H,M	IF 1:800	CST
FoxO3	Rabbit IgG (75D8)	H,M	IF 1:200 WB 1:1000	CST
GFAP	Rabbit (IgG)	H,M	IF 1:1000	Sigma
GFAP	Mouse IgG1 (G-A-5)	H,M	IF 1:1000, WB1:1000	Sigma
Ki67	Rabbit IgG (SP6)	H,M	1:500	Labvision
Nestin	IgG1	H	IF 1:500	R & D
Nestin	mIgG1	M	IF 1:10	DSHB
Sox2	mIgG2a	H,M	IF 1:50, WB 1:400	R & D
Nmyc	mIgG1	H,M	IF 1:50	Santa-Cruz
V5 tag	mIgG2b	-	IF 1:1000	eBioscience
V5 tag	Rabbit IgG	-	ChIP	Abcam
Flag tag	mIgG2b	-	IF 1:1000	eBioscience
H3K4me3	Rabbit IgG	H,M	ChIP	Abcam

2.2.4 Secondary Antibodies

Antigen	Host	Conjugation	Dilution	Supplier
Various IgG	Goat	Alexa Dyes	IF 1:1000	Invitrogen
Rabbit IgG	Donkey	HRP	WB 1:5000	GE
Mouse IgG	Sheep	HRP	WB 1:5000	R & D

2.3 Western immunoblotting

Cell pellets were washed with PBS and then lysed in an aqueous buffer comprising: NaCl 150mM; NP-40 0.25%; Tris-HCl 20mM; EDTA 2mM; NaF 1mM. Protease inhibitors were added to the lysis buffer as follows: AEB5F 1:200; Leupeptin 1:1000; Benzamidine 1:1000; DTT 1:2000. Protein separation was undertaken on gels composed as follows:

	10% Resolving Gel	**Stacking gel**
30% Acrylamide	5.0ml	830ul
Tris HCl 1.5M (pH 8.8)	3.8ml	-
Tris HCl 1M (pH 6.8)	-	630ul
10% SDS	150ul	50ul
10% APS	150ul	50ul
TEMED	10ul	5ul
Water	5.9ml	3.4ml
Final Volume	15ml	5ml

2.4 Taqman qRT-PCR and Taqman Low Density Arrays

RNA extraction was performed using the Qiagen RNeasy Plus Mini spin column kit, eluting in 50ul RNAse free water and using a additional DNAse step. RNA concentration was detemrined using the Qubit RNA High Sensitivity kit (Life Tech). Reverse transcription was performed using Invitrogen Superscript III kit according to manufacturers' instructions. Taqman qPCR and Taqman Low Density Array Card assays were performed using Taqman Universal PCR Master Mix (Applied Biosystems) and assays as detailed in Appendix 9.1, according to manufacturers' guidelines.

2.5 Plasmid construction

2.5.1 Gibson Assembly

Gibson assembly entails a single tube isothermal assembly; briefly, digestion of the 5' ends of the linearised DNA by T5 exonuclease, annealing of the resulting complementary backbone and insert DNA, and restoration of double strand continuity by Phusion DNA polymerase/Taq ligase activity. This single isothermal reaction was performed according to published protocols at 50^{o}C for one hour (145).

2.5.2 Cloning of full length V5 tagged FOXG1

Production of FOXG1 expression plasmids originally involved an unverified commercially available FOXG1 expression plasmid, which was found to have a C-terminal deletion of several hundred bases (SP 23; Figure 2-1B) SeqBuilder software was used to design a custom gene incorporating the missing C-terminal sequence, and flanked by sequence arms complementary to the plasmid backbone adjacent to ORF and 3' UTR cut sites (Figure 2-1C). Additionally, I incorporated sequence encoding a V5 epitope tag prior to the stop codon. The custom gene sequence was PCR amplified from the pMK-RQ plasmid supplied by the Life Tech Geneart Custom Gene Service. The insert (at twice equimolar concentration) was incorporated by Gibson assembly into a backbone derived by double digest of the truncated pFOXG1CDel plasmid using Sfi1 and BamH1, The backbone was annealed with the V5C Insert custom gene (the latter at twice equimolar concentration) using the Gibson assembly technique, resulting in a final lentiviral expression vector (plasmid was designated 'SP31'; Figure 2-1D).

2.5.3 Cloning of additional lentiviral FOXG1 constructs

Using the pFoxG1V5 construct as a template, further custom genes were ordered to allow Gibson assembly of modified FOXG1 constructs within the pHIV-dTomato plasmid. Double digestion with BsaB1 and Hpa1 allowed removal of a 612bp fragment comprising a short stretch of 5' UTR and the N-terminus of the FOXG1 ORF. The resulting backbone was

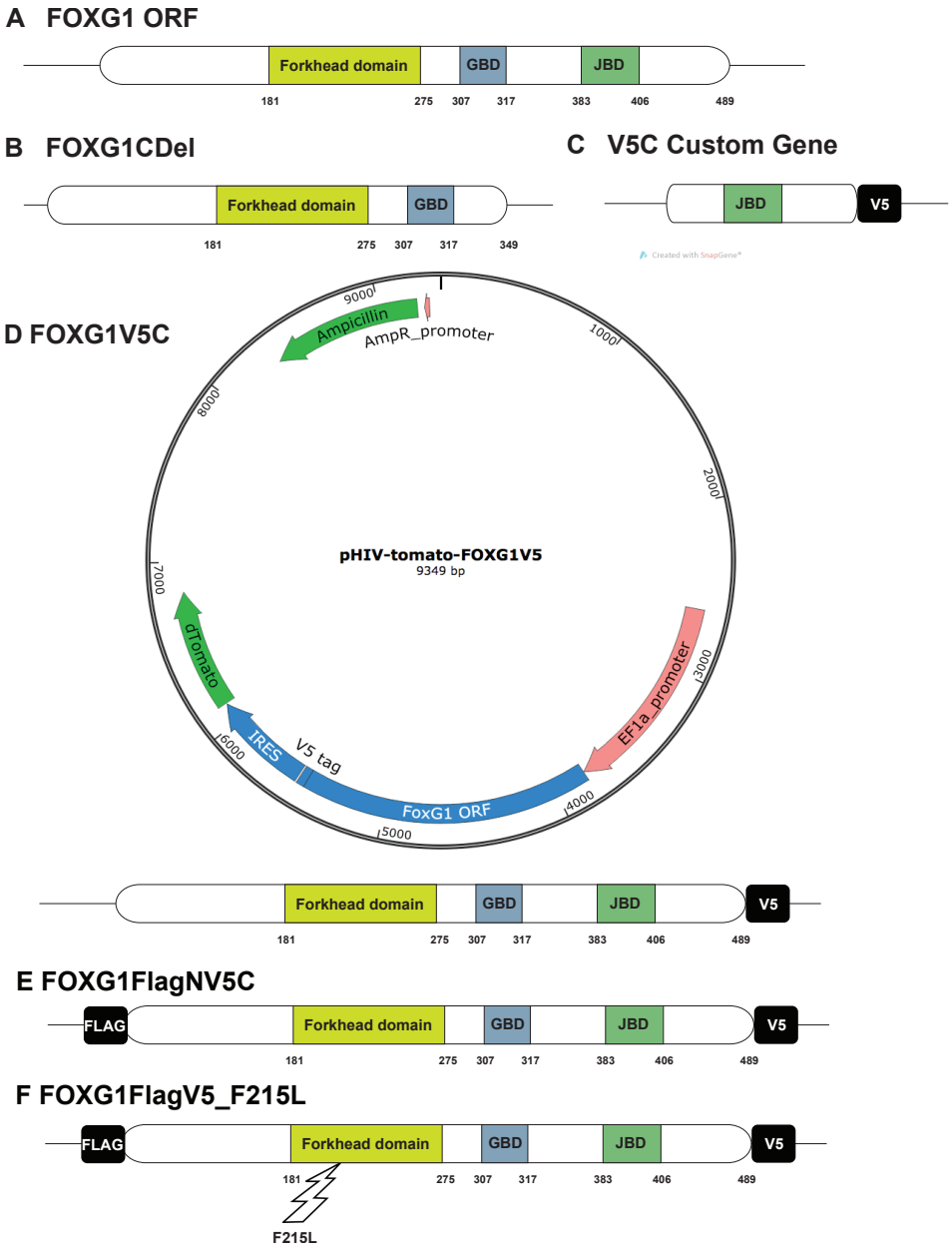
subject to Gibson assembly with oligos or custom genes to produce an N-terminal Flag-tagged construct (SP32; FOXG1FlagNV5C; Figure 2-1E) a variant on this construct incorporating a single base mutation in the forkhead domain previously reported in a case of the human Rett Syndrome (SP33; FOXG1FlagV5_F215L; Figure 2-1F) (115), and truncated epitope-tagged modifications (SP29; FOXG1FlagCNDel. SP30; FoxG1FlagCDel).

2.5.4 Bacterial transformation

OneShot Top10 competent bacteria were transformed with plasmid constructs using a 30 second heat shock in a water bath at 42C, and grown on LB agar plates with appropriate antibiotic selection. Mini-prep, midi-prep and maxi-prep were performed using the appropriate Qiagen kits according to manufacturers' instructions.

Figure 2-1 - FOXG1 lentiviral expression vector cloning

A Schematic representation of the full length FoxG1 open reading frame with DNA-binding Forkhead Domain and predicted Groucho-binding (GBD) and Jarid-binding (JBD) domains **B** Our existing FOXG1 plasmid proved to have a C-terminal deletion at amino acid 349 of 489. **C** The V5C custom gene was designed to rescue a full length epitope-tagged construct by Gibson assembly **D** pFOXG1V5C expression plasmid and ORF schematic **E** pFOXG1FlagNV5C **F** pFoxG1FlagV5_F215L contains a point mutation resulting in phenylalanine to leucine substitution at amino acid 215 in the FoxG1 transcript (point mutation associated with human Rett syndrome) .



(Figure legend overleaf).

(Figure legend

2.5.5 Gateway cloning of FOXG1, FOXG1V5 and SOX2 expression casettes

Primers were designed according to the Life Technologies Gateway Cloning guidelines comprising attB1 and attB2 recombination sites preceding respectively forward and reverse primers specific for the 5' and 3' UTRs of the commercially supplied Origene FOXG1 Refseq plasmid, the previously cloned FOXG1-V5 plasmid, and SOX2 genomic DNA template from the 2A_SOX2 custom gene detailed below. Extensive PCR optimisation was required for FOXG1 amplification, likely a consequence of the 70% GC content of this amplicon. Satisfactory amplification was achieved using Phusion polymerase (NEB) with a GC-Rich buffer, supplemented with DMSO 3% and Betaine 1M, and annealing temperature of 60^{o}C.

After PCR cleanup, the FOXG1attb and FOXG1V5attb amplicons were subject to BP clonase recombination (according to standard Gateway cloning protocols) into the pDONR221attL vector. FOXG1attR (SP 411) and FOXG1V5attR (SP 176) and SOX2attR (SP 177) Entry clones were verified by restriction digest, and then Sanger sequencing across the FOXG1 amplicon using M13 forward/reverse primers and internal primers.

LR clonase was used to recombine the entry clones into the Destination Vector pDEST-TRE-Ires-BSD (SP 170) using the standard Gateway cloning protocol (Life Tech). This incorporates PiggyBac sequences for genomic incorporation by transposase, with a Tet-On 3G Inducible promoter (Clontech) upstream of the Gateway sites for ORF insertion, and a blasticidin selection cassette downstream (gift from Austin Smith's laboratory). These plasmids were again verified using restriction digest and Sanger sequencing. Plasmid IDs and maps are provided in Appendix 9.2.

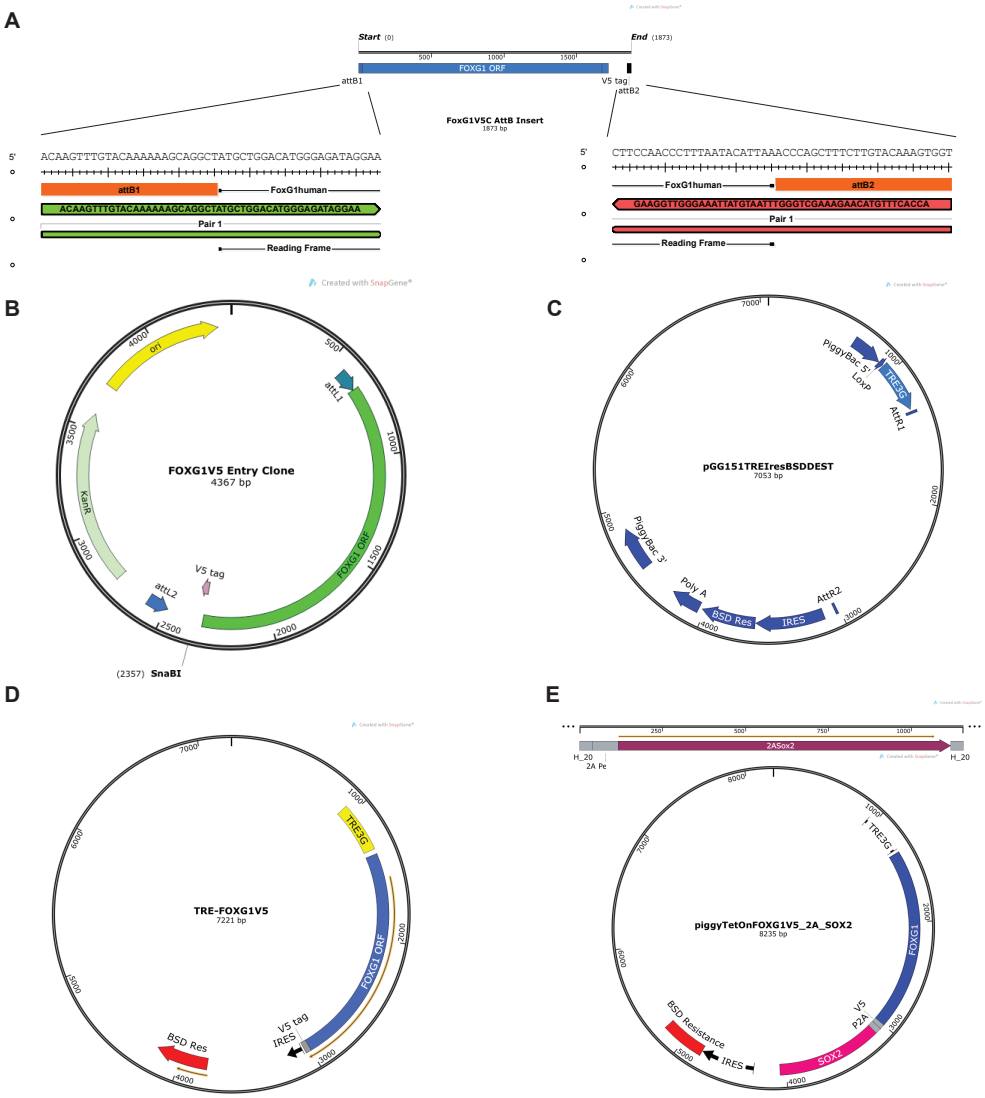


Figure 2-2 - Gateway cloning of FOXG1 inducible constructs

A AttB PCR of the FOXG1 ORF. **B** The entry clone is constructed by BP clonase recombination of the AttB PCR product into the pDONR221 vector. **C** Tet-On 3G Gateway destination vector **D** Gateway LR recombination of (B) and (C) produced the expression vector TRE FOXG1V5. **E** Digestion of TRE FOXG1V5 in the V5 tag using SnaB1 allowed integration of the P2A_SOX2 custom gene sequence by Gibson assembly.

2.5.6 Polycistronic expression cassettes

We used the viral self-cleaving 2A peptide to create polycistronic mRNAs. A modular approach was adopted for cloning of additional transcription factor cassettes into the FOXG1 and SOX2 vectors detailed above. pENT_FOXG1V5_2A_SOX2 (pENT FS; SP178) was generated by SnaB1 digest of the FOXG1V5 Entry Clone followed by introduction using Gibson assembly of custom gene sequence (Life Technologies GeneArt) comprising the SOX2 ORF preceded by a 2A encoding sequence. pENT BRN2_2A_SOX2 (pENT BS; SP409) was constructed likewise. Triple constructs containing P2A-linked FOXG1, SOX2 and OLIG2 or BRN2 ORFs were also produced using this strategy (pENT FSB SP179; pENT FSO SP180), and Gateway cloning allowed for insertion of these transgenes into a number of backbones. A complete list of the transgene entry vectors and resulting inducible and constitutive PiggyBac and AAVS1 targeted expression constructs derived in the course of the project is provided in Appendix 9.2.

2.6 Genome editing using the CRISPR/Cas9 system

Crispr guide RNAs (gRNAs) and targeting vectors were designed and cloned by Raul Bressan, Mantas Matjusaitis and Claudia Diaz (Pollard lab members). I designed and constructed the plasmids for gRNAs for deletion of the FoxO3 intron peak (Cis regulatory region). Oligonucleotide sequences for each gRNA and targeting vector construct are provided in Appendix 9.3. For gRNAs italic sequence indicates the PAM sequence. For targeting vector homology arm oligos, bold sequence indicates bases complementary to the human locus, normal sequence indicates bases complementary to the intermediate targeting vector backbone for Gibson assembly of the targeting vector. Targeting vector arms were around 1kb in length and flanked an EF1a-Puromycin selection cassette to replace the target exon.

2.6.1 Guide RNA Design and Cloning

Guide RNA sequences were selected using the Zifit web-based tool (zifit.partners.org/ZiFiT/Disclaimer.aspx) to bind at instances of the PAM sequence occurring within gene open reading frames, with low predicted off-target binding.

Oligos were denatured and slowly cooled to anneal and produce double stranded guide inserts with 4-base overhangs for ligation into a U6 expression plasmid backbone (gift from Sebastian Gerety, Sanger Institute). The guide inserts were phosphorylated, and the U6 vector (SP 117) digested with Bsa1 to generate matching overhangs, and cleaned up on columns. Backbone and insert were ligated using T4 DNA ligase (Fermentas) according to manufacturers guidelines, and the resulting guide RNA plasmids were checked by restriction digest (Nhe1/EcoR1) to confirm incorporation of an insert, and then sequence verified.

2.6.2 Targeting Vector Design and Cloning

Homology arms comprising ~1000bp of genomic sequence flanking the targeted exon, with overhangs appended to allow for Gibson assembly into the intermediate targeting vector (Bill Skarnes lab), were generated by Phusion PCR from genomic DNA template using custom primers as detailed in the appendix, supplied by IDT. The intermediate targeting vector was produced using a 4-part Gibson assembly comprising these arms and the double-digested intermediate targeting vector backbone. Gateway recombination was then applied to insert the EF1a-PURO cassette and produce the final targeting vector. The primers used are detailed in the appendix, and maps of the locus indicating guide RNA target binding and homology arm locations are included in the relevant Results Chapters.

2.7 Derivation of stable transgenic cell lines

A summary table of the transgene overexpressing mouse and human NS lines generated during this project is provided in the Appendix 9.4. For the mouse lines a series of individual clones were derived and characterised by qPCR and/or ICC to identify clones with low baseline and high inducible expression. For convenience I describe the data relating

to the expression characteristics and functional properties of these cell lines in the relevant Results sections.

2.7.1 shRNA Knockdown

FoxG1 knockdown in human cell lines was achieved using Mission lentiviral shRNA constructs 013949, 013950, 013952, 273934 and 273975 (Sigma Aldrich) according to manufacturer's titres, applied to cells growing at ~50% confluence in 6-well plates at final multiplicity of infection between 1 to 5. Puromycin selection was applied 48 hours after selection for at least 1 week prior to functional analysis or harvesting for Western Blot.

2.7.2 Lentiviral transduction (pHIV-tomato-FOXG1 overexpression constructs)

The pHIV-Tomato-FOXG1 plasmid variants described were tested by transient transfection in ANS4 cells using Lipofectamine LTX according to manufacturers' guidelines. At 48 hours, Tomato expression was confirmed by eye, and the cells were fixed and stained using FOXG1, V5 and Flag antibodies as appropriate. For stable lentiviral transduction, a suspension was then prepared comprising pHIV packaging plasmid (15ug), VSVG envelope plasmid (5ug), pHIVtomatoFOXG1 plasmid (20ug), 2.5M CaCl2 (50uL) and water to a total volume of 450ul. This suspension was admixed 1:1 with HEPES buffer, and this mixture added to 20cm plates containing 293T cells growing at 50% confluence. 4 hours later the cells were washed with PBS and resuspended in NS culture medium. After 24 hours this medium was aspirated and filtered, then the virus was PEG precipitated. Aliquots of this virus were introduced to NS cells growing at 50-70% confluence in culture, and the resulting populations were flow sorted to isolate the highest 5% of cells expressing dTomato.

2.7.3 Lipofection of Mouse NS Cells for PiggyBac Stable Integration

Mouse NS stable inducible lines were generated by Lipofectamine LTX transfection of ~100,000 NS cells per well, growing in a 6-well plate at 50% confluence, with a total of 1ug DNA, comprising pBase (piggybac transposase SP59), pCAG-Tet3G (rtTA SP169) and Tet-On expression vector (derivates of the SP170 destination vector) in a 1:1:2 ratio. 48

hours after transfection, the cells were dissociated using accutase and replated in 10cm dishes in growth medium supplemented with 1ug/ml doxycycline hyclate (Sigma) and 5ug/ml blasticidin hydrochloride (Sigma). Colonies were allowed to emerge over ~2weeks. These were picked, grown up and assayed for baseline and Dox-inducible transgene expression using combinations of ICC, qPCR and Western blotting.

2.7.4 Neon/Amaxa Transfection of Human Cell NS Cells for PiggyBac Stable Integration

Neon (Life Technologies) and Amaxa (Lonza) nucleofection systems were used at the UCL Cancer Institute and MRC Centre for Regenerative medicine, respectively. Neon transfection was undertaken using 2x 1100V pulses of width 20ms. Amaxa transfection employed the X005 pulse protocol (human cells) or the T030 protocol (mouse cells). In each case 1-2 million cells were transfected with a total of 6-12ug DNA comprising pBASE (SP59), pCAG-Tet3G (SP169) and pDEST-TetOn vector as above in 1:1:2 ratios for inducible PiggyBac constructs. For Crispr targeting, guide RNAs (x2), targeting vector (where appropriate) and Cas9 nickase were transfected in a 1:1:1:2 ratio.

The cells were plated in 10cm dishes, with doxycycyline added after 24 hours where appropriate, and selection was commenced 48 hours post-transfection using blasticidin 5ug/ml, puromycin 1ug/ml or hygromycin 100ug/ml. Each of these antibiotics produced uniform cell death within 7 days in untransduced mock controls (both human NS and GNS cells). After 14 days' selection, expression was confirmed by immunocytochemistry and moderate or high levels was observed in a majority of cells. Inducible expression was confirmed by immunocytochemistry, qPCR and Western immunoblotting.

2.8 Next generation sequencing: ChIP-Seq, RNA-Seq, and ATAC-Seq

Chromatin preparation and immunoprecipitation was undertaken based on protocols adapted from those provided by the laboratory of Dr. Suzana Hadjur (UCL Cancer Institute).

2.8.1 Isolation and Preparation of FOXG1 cross-linked Chromatin

Samples of ~100 million cells grown to confluence in standard adherent conditions in 6x T150 flasks were pelleted, then subjected to formaldehyde fixation (1% formaldehyde for 10 minutes; quenched with 0.125M glycine). The cells were washed and pelleted sequentially in wash buffers 1 and 2, then lysed in 200ul lysis buffer supplemented with protease inhibitors. The lysis buffer was supplemented with SDS prior to sonication using a Bioruptor (45 min max power, 30 seconds on, 30 seconds off). Optimal sonication was obtained by addition of 50ul of 3.5% SDS to the lysate to achieve a final 0.7% SDS concentration. Samples of the sonicated lysate were de-crosslinked by heating to 65^{o}C overnight, then analysed on agarose gel and/or using Agilent Bioanalyser technology. Each of the buffers was supplemented with Roche Complete Protease Inhibitors w/ EDTA immediately prior to use:

Wash Buffer 1	**Wash Buffer 2**	**Lysis/Sonication Buffer 3**
10 mM Hepes pH 7.5	10 mM Hepes pH 7.5	150 mM NaCl
10 mM EDTA	200 mM NaCl	25 mM Tris pH 7.5
0.5 mM EGTA	1 mM EDTA	5 mM EDTA
0.75% Triton X-100	0.5 mM EGTA	1% Triton
H2O to 250 ml	H2O to 250 ml	0.5% Deoxycholate
		H20 to 100ml

2.8.2 Chromatin immunoprecipitation

Dynabead protein G sepharose beads (Thermo Scientific) were washed in Wash Buffer A (WBA) supplemented with BSA 1%, then antibody was conjugated at 4^{o}C in suspension overnight on the rocker shaker, followed by a further x2 washes in WBA. Chromatin samples were diluted to a final SDS concentration of 0.1%, and pre-cleared by mixing with blocked Protein G Sepharose beads without antibody conjugated. 1% of the total chromatin was removed and frozen to provide an input control. The beads and chromatin were mixed and IP allowed to proceed overnight on the rocker shaker. The final ChIP mixture comprised (suspended in 250ul WBA) 10ul ChIP grade antibody conjugated to 25ul Dynabeads Protein G and 100ug chromatin.

Chromatin IP was allowed to proceed overnight, and the beads were then separated on a magnetic rack. Subsequent washes were conducted sequentially in Wash Buffers A (x3), B and C then TE buffer at 10 minute intervals on the rocker shaker. Each of these buffers is supplemented with Roche Complete Protease Inhibitors w/ EDTA immediately prior to use:

Wash Buffer A	**Wash Buffer B**	**Wash Buffer C**
50 mM Tris pH8.0	50 mM Tris pH8.0	50 mM Tris pH8.0
150 mM NaCl	500 mM NaCl	250 mM LiCl
0.1% SDS	0.1% SDS	0.5% deoxycholate
0.5% deoxycholate	0.5% deoxycholate	1% NP40
1% NP40	1% NP40	1 mM EDTA
1 mM EDTA	1 mM EDTA	

Finally, the pulldown DNA along with the input sample were eluted in 0.1M $NaHCO_3$ with 1% SDS supplemented with Proteinase K (10mg/ml) and RNAse A (10mg/ml), then de-crosslinked at 37^{o}C for 2hr, then 65^{o}C overnight. The pulldown DNA was then column extracted (Qiagen Minelute) and eluted in water.

Effective chromatin preparation and pulldown using these protocols in our cell lines was confirmed using a validated ChIP grade antibody against the active chromatin marker trimethylated Histone H3K4. ChIP-PCR demonstrated 10 to 100-fold enrichment of sequences corresponding to the bodies and promoters of genes active in these lines when compared to IgG control pulldown at the same loci, or to ChIP sample enrichment of nearby upstream regions or the beta actin control locus (data not shown).

2.8.3 Library preparation for ChIP-Seq

Sequencing libraries were prepared from pulldown and control chromatin samples using NEBNext ChIP-Seq reagents (New England Biolabs E6240) according to the manufacturers' protocols. Specifically, chromatin fragments were end-repaired, dA-tailed and ligated to NEB Multiplex adapters (E7335), with Ampure XP bead cleanup at each stage. The resulting fragments were PCR-amplified and bead-purified once more to create final libraries.

For the successful FOXG1 pulldowns, ChIP-PCR demonstrated enrichment at key candidate loci (*Etv4, Jarid2, Nfia, Nr4a2, Rarb*) in the fragment pool compared to a *MyoD* control region.

2.8.4 ChIP-PCR Primers

Locus	Forward	Reverse
Etv5	AGCACACACGTCCCCATT	AGCTGGATTTGCCTGAAGAC
Rarbp	CTGCCTCTCAGTTGCTACCC	CATGGATCGTCCAATCACAG
Nfia	CCATTTCACGACCTGTGAGG	AACAAGGAAATGGCTGTGC
Nr4a2	GCCAATGTGCCTTTGTTTAT	CGCAGACTTTAGGTGCATGT
Etv4	TCGCTGATCCTTACAAAGACG	CTTCCCTTTGGTCTCCTTCC

2.8.5 RNA Seq Library preparation

RNA sequencing libraries were prepared from 100ng mRNA extracted using Qiagen RNeasy kits. Library prep was conducted using NEBNext mRNA prep reagents (E6100) and multiplex indices for Illumina (E7335).

2.8.6 ATAC Library preparation

ATAC-Seq libraries were prepared using Illumina Nextera reagents as described, with PCR amplification and indexing using published sequencing adapter primer sequences, supplied as oligos (Sigma) (146).

2.8.7 Library Quality Control

Libraries were assessed on the Bioanalyser (DNA ChIP 1000) or Bioanalyser TapeStation (High Sensitivity kit). Library concentration was assessed using the Qubit High Sensitivity kit (Life Technologies).

2.8.8 Library Sequencing

Following denaturation, quantification and library profile assessment, libraries were diluted and loaded into the Illumina MiSeq V2 Reagent Cartridge for sequencing according to Illumina protocols. For deep sequencing of multiple libraries in parallel, libraries prepared as described using NEB Multiplex indices were submitted individually, or pooled at uniform final concentrations as assessed by Qubit, to the Heidelberg Core Facility or to Edinburgh Genomics for sequencing on HiSeq 2000 and 2500 instruments.

2.8.9 Analysis of NGS Data

Filtered read files were imported to the Galaxy web-based analysis portal. Within Galaxy, the files were parsed into Sanger FastQ format, then each read was truncated from 100 base pairs to 55 (base pairs 10-65 of the original read). The read files were each mapped to the mouse genome (mm9 or mm10 assemblies) using Bowtie configured with default parameters. The resulting BAM alignment files were merged into a single file, and peak calling was performed using the MACS 2.0 algorithm. Galaxy was also used to determine motif enrichment (SeqPos Motif tool), and the Stanford Genomic Regions of Enrichment Annotations Tool (GREAT) was used for target gene and ontology analysis.

3 Results 1 – FOXG1 loss-of-function in NS cells and GNS cells

3.1 Introduction

The aim of this chapter is to test the hypothesis that FOXG1 expression is necessary for self-renewal of neural stem cells and glioma neural stem cells. I will describe experiments directed at characterising FOXG1 expression in NS and GNS cell lines, and at interrogating the effects of knockdown and knockout of FOXG1 in mouse and human primary cell lines.

FoxG1 deletion in mice results in severe telencephalic hypoplasia (118) and premature neuronal differentiation (117), while heterozygous loss-of-function in the human results in a pervasive neurodevelopmental disorder, Rett syndrome (115). Using conditional FoxG1 knockouts, an ongoing functional requirement for FoxG1 in adult neurogenesis in the dentate gyrus has also been reported (147). Together these findings point to a possible requirement for FoxG1 in maintenance of the neural stem cell pool *in vivo*.

In the context of human gliomas, a recent study from the Stifani laboratory identified a small but significant reduction in rate of self-renewal of primary GBM stem cultures following FoxG1 knockdown, and a corresponding small increase in survival on xenotransplant into mice *in vivo* (45). Previous work has pointed to a possible underlying mechanism involving direct inhibition by FoxG1 of a FoxO-Smad complex normally responsible for driving p21 transcription and cell cycle arrest in response to TGF-beta signalling (48).

In order to establish a potential requirement for FOXG1, and to reproduce the Stifani laboratry findings, I initially derived and characterised a new mouse NS cell line, obtained from the SVZ of adult conditional *foxg1* knockouts. I also explored lentiviral shRNA constructs against *FOXG1* in GNS cells. Finally, I exploited Cas9-assisted gene targeting to delete *FOXG1* from GNS cells – the first time these technologies have been used for knockout in neural lineage human cells. I have examined the effect of these interventions on

cell cycle and proliferation, both in self-renewal conditions supplemented with the growth factors EGF/FGF, and in the response to BMP-induced differentiation.

3.2 Exploring FoxG1 expression in mouse and human

3.2.1 FoxG1 expression in developing forebrain, brain tumours and NS/GNS cell lines suggests a potential role in glioma

Previous work in the lab had pointed to consistent overexpression of FOXG1 across a range of glioma neural stem cells derived from GBMs (43), including examples exhibiting classical, proneural and mesenchymal signatures(11). Affymetrix microarray data produced by our collaborators (Paul Bertone, EBI, Cambridge) at the start of this project confirmed the clear differential expression between human NS and GNS cells for *FOXG1* mRNA that was previously reported using a smaller set of lines cell lines using Tag-Seq and qRT-PCR datasets (Figure 1-14). In fact, these data identified FOXG1 as the most significantly and consistently differentially upregulated transcript when comparing GNS cells to NS cells (-Figure 3-1A).

Data from the cancer genome atlas (11) accessed via the Memorial Sloan Kettering cBioportal revealed four *FOXG1* mutations and no amplifications across 273 GBM samples. *FOXG1* was amplified in only 4 of 286 low grade glioma samples. These data imply that the consistently high levels of expression are not the result of direct genetic disruptions to *FOXG1*, but may instead reflect an obligate epigenetic configuration converged upon during gliomagenesis, or may be the result of activation of core glioma signalling, including EGF receptor and PI3 kinase pathways. Interestingly, EGFRvIII mutations have very recently been reported to drive increased FOXG1 expression (148).

To further explore FOXG1 function in glioma the Pollard laboratory initially generated a set of new monoclonal antibodies (collaboration with P. Bertone). In order to validate these monoclonal antibodies for further application, I performed immunohistochemistry using fixed E14.5 mouse forebrains and prepared sagittal sections

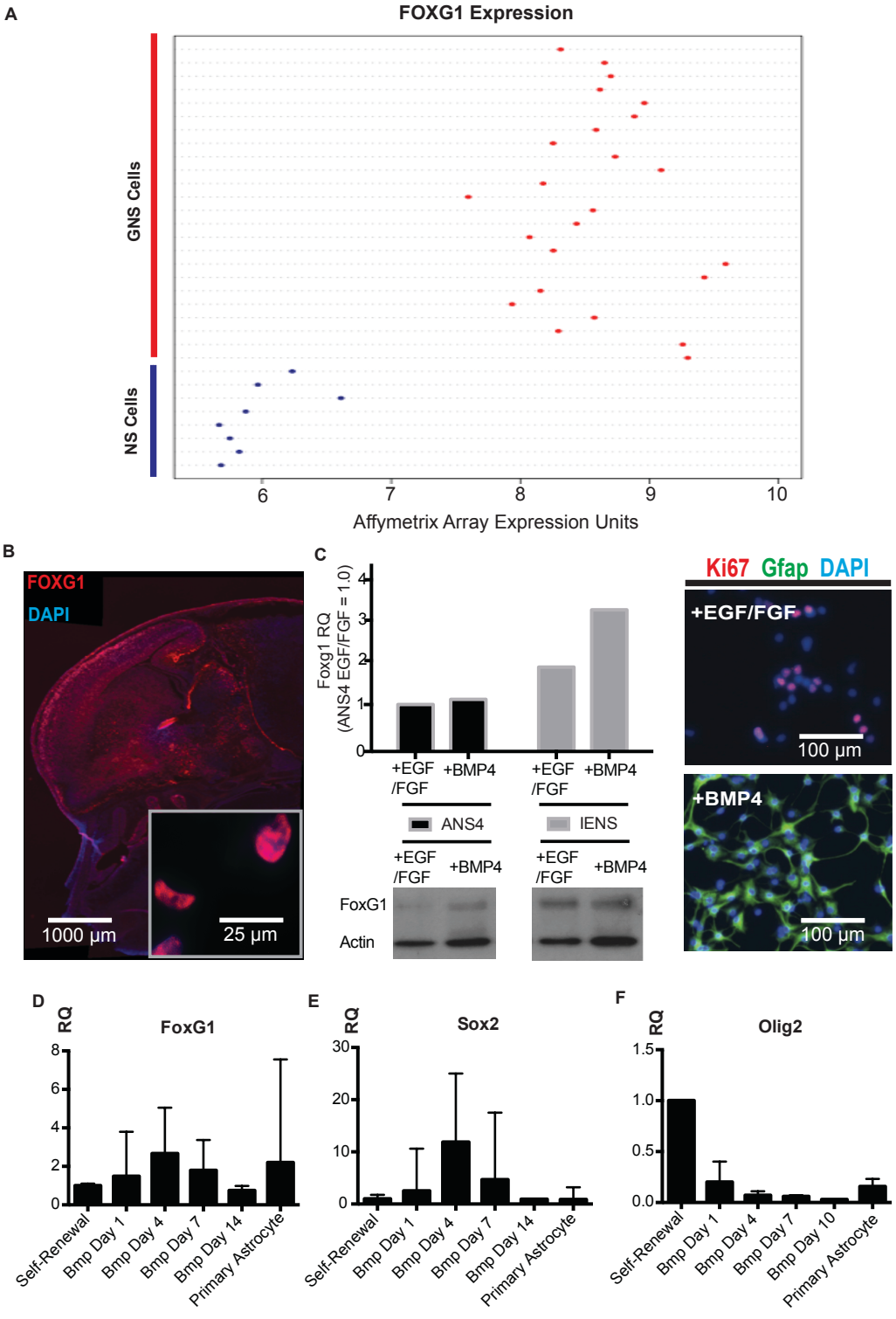
using a Leica cryostat. FoxG1 was observed to be expressed in the forebrain and was nuclear (Figure 3-1B). Western blot and qPCR data confirmed expression of FoxG1 in mouse NS cells. Consistent with the previous findings for human GNS cells and with recent reports implicating EGFRvIII in FOXG1 upregulation, we find that the mouse glioma initiating cell line IENS (Ink4a/ARF; EGFRvIII overexpression) has much greater levels of FOXG1 expression, highlighting the value of this mouse glioma line to model the disease. Western blotting of forebrain midbrain and hindbrain with the new antibodies also confirmed forebrain specific expression (Christine Ender, not shown).

We next tested the consequences of BMP treatment, a known cytostatic and astrocyte differentiation inductive signal. As expected wild-type adult NS cells (ANS4) cells readily exited cycle and upregulated GFAP. However, we found FoxG1 and Sox2 mRNA expression levels are maintained or increased on initial BMP treatment, and retained at least at levels equivalent to those of self-renewing populations up to 14 days (**Figure 3-1**D). Protein expression is also seen to be maintained at the day 4 time-points. Foxg1 can therefore be co-expressed in GFAP positive progeny as well as self-renewing NS cells. We find that overall expression is maintained at comparable levels in serum-derived astrocyte cultures from P3 mouse forebrain, and notably FOXG1 expression also remains high in serum-derived classical glioma cell lines (148). These experiments were performed at near confluent cell densities where astrocytes may be maintained in an immature or quiescent astrocyte-like stem cell state (i.e. as Type B cells). FOXG1 may also be controlled via nuclear export rather than downregulation during early differentiation (130).

These data are consistent with in vivo expression patterns. It appears that some level of Foxg1 expression is not specific for the proliferating radial glia-like neural stem cell state, but is common to a range of progenitors and neurons in the developing forebrain. Thus, extinguishing FOXG1 expression seems unlikely to be the major route by which NS cells differentiate.

Figure 3-1 - FOXG1 expression in NS and GNS cells

A New exon array data from our collaborators confirms consistent overexpression of FOXG1 in GNS cells compared to NS controls; in fact, this is the most upregulated transcript genome-wide compared to NS cells. **B** Validation of FOXG1 a novel monoclonal antibody (17B12) by ICC confirms expression in mouse forebrain and adult mouse NS cell line ANS4. **C** BMP4 treatment of ANS4 cells leads to uniform cell cycle exit and upregulation of GFAP (48hr). FoxG1 expression is retained in these cells on exposure to BMP4, and this is also the case in mouse glioma NS cells (IENS cells) which express higher levels of FoxG1 in self-renewal conditions and on BMP4 treatment./ **D-F** Olig2 expression is rapidly extinguished on exposure of ANS4 cells to BMP4, whereas FoxG1 and Sox2 expression levels are maintained by day 14.



(Figure legend overleaf)

3.2.2 FOXG1 expression correlates to an extent with malignant grade

In order to test whether high level FOXG1 expression extends to lower grade tumours, I analysed expression levels in a set of four independent WHO Grade III primary glioma cultures alongside Grade IV lesions (Figure 3-2A). The lower grade cultures expressed neural (Tuj-1) and astrocytic (GFAP) markers upon exposure to serum for 7 days, confirming their neural origin.

As previously reported, both for our existing GNS cell cultures and published data from the Stifani group (45), the most malignant WHO Grade IV tumours consistently express high FOXG1 levels, even in the case of an atypical lesion exhibiting sarcomatous histopathological features (Gliosarcoma DD1). However, FOXG1 and SOX2 are expressed at lower levels in the cultures from lower grade tumours (Figure 3-2D, E).

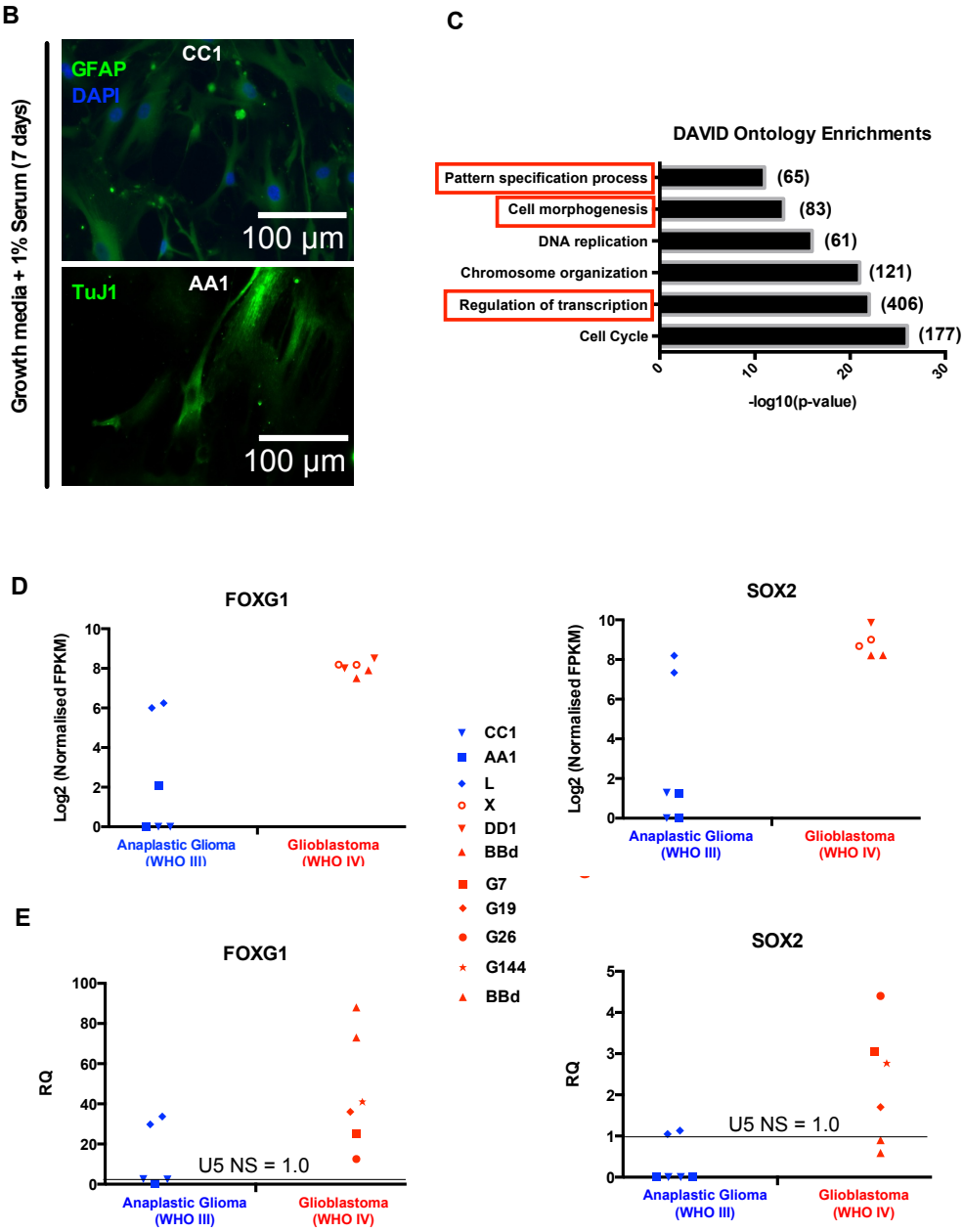
RNA-Seq expression profiling for the Grade III lines CC1 and AA1 was performed to compare gene expression with the Grade IV lines X and BBd. This analysis has revealed 1793 genes significantly differentially expressed between these two groups. *FOXG1* and *SOX2* were among the genes up-regulated as part of the Grade IV signature, and the most significant Gene Ontology enrichments (GOTERM_BP_FAT) for this set included 'Pattern specification process', 'Cell morphogenesis' and 'Regulation of transcription', GO categories in which FOXG1 is represented (Figure 3-2C). High level FOXG1 overexpression, and less marked SOX2 expression were also confirmed independently using Taqman qRT-PCR. These data indicate that FOXG1 and SOX2 may be upregulated late during malignant transformation.

Figure 3-2 - FOXG1 expression in newly-derived WHO Grade III and Grade IV cell lines

A New glioma neural stem cell lines were derived from primary and secondary GBMs, and lower grade gliomas by our collaborator Paul Brennan (University of Edinburgh). **B** Representative immunocytochemistry confirmed GFAP and Tuj-1 expression in these tumours indicating they were tumours of neural origin. **C** Comparison by RNA-Seq of the transcriptomes of Grade III with Grade IV lesions identified 1793 differentially expressed genes, enriched for the gene ontology terms indicated. FOXG1 was highly enriched in Grade IV lesions and is assigned to the Ontology categories highlighted in red. **D** RNA-Seq expression data for *FOXG1* and *SOX2* shows variable expression in Grade III lesions, with consistent overexpression of *FOXG1* especially in Grade IV lesions. **E** This finding is supported by independent Taqman qRT-PCR data, normalised to U5 NS. Differences in cell lines analysed and technical differences between RNA-Seq and qRT-PCR quantification account for the difference in pattern of distribution, but the trends are the same.

A

ID	tumour	grade	Age	gender	Comments
AA1	Diffuse astrocytoma w/ anaplastic foci	II/III	29	F	
BBD	GBM	IV	56	F	
CC1	anaplastic oligodendroglioma	III	39	F	1p/19q deleted
D	gliosarcoma	IV	57	F	
L	Anaplastic astrocytoma	III	25	M	
X	GBM	IV	60	M	



(Figure legend overleaf)

3.3 Acute FoxG1 genetic deletion using a new conditional mouse NS cell line

3.3.1 Generation of *FoxG1*$^{fl/fl}$ mouse NS cell lines

In order to assess the requirement for *foxg1* in wild-type mouse NS cell self-renewal, I derived a new NS cell line from the forebrain subventricular zone of available homozygous adult *foxg1*$^{fl/fl}$ mice (Mice provided V. Fotaki; originally produced by the Fischell lab) (127). These cells exhibited characteristic marker expression, and were expanded for 5 passages before freezing aliquots (Figure 3-3). Excision of *foxg1* can be confirmed indirectly via activation of a GFP reporter from the ROSA26 locus and the resulting cells exhibit complete loss of function.

To achieve Cre-mediated excision of the *foxg1* alleles I delivered a Cre expression plasmid using transient transfection; this plasmid contains an mCherry fluorescent reporter linked via an IRES (CAG-Cre-IRES-Cherry) (139). Visual inspection of the resulting transfected cultures using wide-field ICC microscopy confirmed that the majority of transfected cells had activated GFP, the reporter of FoxG1 excision. Western blot demonstrated reduced FoxG1 expression in the bulk population, and clonally expanded lines were confirmed as lacking FoxG1 expression (Figure 3-3).

3.3.2 *foxg1* null NS cells proliferate normally and retain NS cell marker expression

Proliferation of the *foxg1* null clones harvested for Western Blot suggested that this gene is not necessary to sustain *in vitro* proliferation of mouse NS cells. In order to quantify proliferation rates more accurately and search for any deficit, I determined the proportion of cells in the bulk population positive for the GFP reporter over successive passages, reasoning that any requirement for FoxG1 expression would manifest as a proliferative advantage for the unexcised GFP negative population over time. Following transfection with a Cre-Cherry plasmid, GFP expression was evident in ~70% of cells. The proportion of GFP cells did not decrease over serial passages: 0, 1, 2, 5 (Figure 3-3D), implying that *foxg1* deletion confers

no proliferative defect in normal growth conditions. GFP positive cells demonstrated normal expression of the neural stem cell master regulators Sox2 and Olig2, and induced GFAP expression upon exposure to BMP4 (Figure 3-3F).

3.3.3 FoxG1 null Mouse NS cells exit cycle readily in response to inductive differentiation cues.

The *foxg1*$^{fl/fl}$ and derivative Cre-excised *foxg1*$^{-/-}$ clonal cell lines were plated at 50,000 cells per well in 4-well plates in self-renewal media with the growth factors EGF/FGF (self-renewal conditions), BMP4 (astrocyte differentiation condition), or combinations of the two (Figure 3-3G). After 48 hr the cells were fixed and stained for Ki67. Delivering both differentiation and self-renewal signals together poses a suboptimal differentiation condition. A significant decrease in the proportion of cells positive for Ki67 was observed between the foxg1 null cell lines and parental unexcised controls when treated using the sub-optimal differentiation conditions: EGF (2ng/ml), FGF (2ng/ml) and BMP4 (8ng/ml).

When plated at higher densities in BMP alone the resulting astrocytes remain able to re-enter cell cycle, probably as a result of autocrine/paracrine FGF and other signalling interactions antagonising the BMP-driven differentiation cascade. I therefore examined the influence of *foxg1* deletion on this process by plating *foxg1*$^{-/-}$ NS cells alongside parental *foxg1*$^{fl/fl}$ control cells in culture media supplemented with 10ng/ml BMP4 at high density (500 cells/mm2). After 7 days, BMP4 was removed and the cells returned to normal growth media. After a further 10 days, the cells were dissociated and plated at low density (5 cells/mm2) for clonal growth (4 plates each condition). Colony counts after a further 7 days demonstrated significantly higher numbers of colonies in the *foxg1*$^{fl/fl}$ parental controls compared to the *foxg1*$^{-/-}$ population (Figure 3-3H). Altogether this suggests *foxg1* loss results

in sensitisation of mouse NS cells to BMP4 inductive signals, and is consistent with past studies implicating FoxG1 as a negative regulator of cytostatic TGF-beta signalling (48).

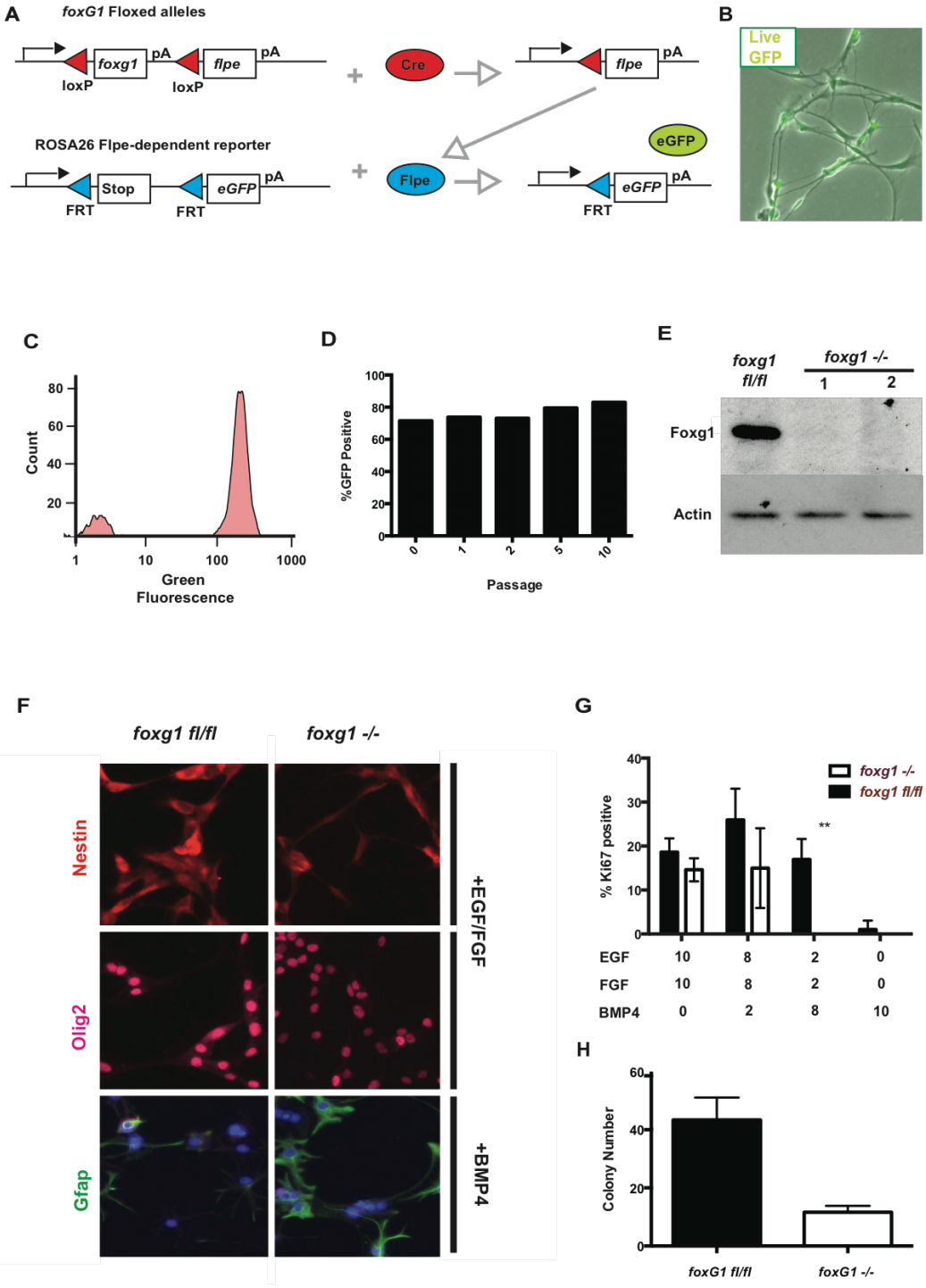
3.3.4 Summary 1

Higher levels of FoxG1 in both human GNS cells and mouse glioma NS cell lines (IENS) suggest a gain of function phenotype may be relevant to glioma. Here, we explored whether loss of FoxG1 would have consequences for NS cell proliferation. We find that FoxG1 is dispensable for maintenance of neural stem cell self-renewal and proliferation *in vitro* in optimal conditions – consistent with observations of FoxG1 negative midbrain and hindbrain NS cell lines are still highly proliferative. Nevertheless, we found that FoxG1 null mouse NS cells are sensitised to BMP differentiation, and demonstrate reduced capacity to return to cycle and form colonies after BMP4 treatment.

Figure 3-3 - FoxG1 knockout in a newly generated *foxg1*$^{fl/fl}$ mouse NS cell line.

A In the floxed *foxg1* mouse NS cell line (termed FF), the *foxg1* coding exons are flanked by *loxP* elements. Cre excision removes all FoxG1 activity and results in expression of the Flpe recombinase, which in turn removes a stop cassette to trigger eGFP expression from the ROSA26 locus. **B** Excision of *foxg1* results in activation of the GFP reporter. **C** 48 hr after Cre-mediated excision of *foxg1* ~70% of the gated cells indicated are GFP-positive and this proportion remains constant over time **D**. **E** FoxG1 expression is absent in *foxg1* null clonal derivatives. **F** Compared to parental controls, expression of neural stem cell markers Nestin and Olig2 is retained in *foxg1* null cells, and GFAP is appropriately upregulated in response to BMP4 treatment. **G** Parental controls tend to retain Ki67 expression in response to exposure to mixtures of growth factors and BMP4, while the *foxg1* null progeny readily exit cycle in these conditions. **H** Parental controls form colonies with higher efficiency than *foxg1* null progeny when replated after BMP4 treatment at high density.

(Figure legend overleaf)



3.4 *FOXG1* knockdown in human GNS cells using shRNA

3.4.1 GNS cells remain proliferative following *FOXG1* knockdown

Previous studies have suggested knockdown of FOXG1 can reduce the proliferation of GBM stem cells(45). To independently verify this using a different GNS cell line we infected G7 cells with the Sigma Mission lentiviral shRNAs against FOXG1 (sh949, sh934, sh950 or sh952 individually or as pools), with pools of constructs at multiplicity of infection (MOI) of 1 and 5. The resulting cell cultures were selected using puromycin resistance, and knockdown was quantified using Western immunoblotting, and by qRT-PCR. Optimal knockdown was achieved by transfection with the pooled guide RNAs at MOI 5 , and further assays were conducted using this population (Figure 3-4 A and B).

I transfected these G7 shPool GNS cells with a PiggyBac inducible FOXG1V5 construct together with a PiggyBac constitutive rtTA, and a PiggyBac recombinase (Figure 3-4 C and Methods). After 48 hours, doxycycline and blasticidin were introduced, and selection continued over 14 days. The resulting G7 shTRE-FOXG1 cell line expresses FOXG1 at levels well below the parental line in the absence of doxycycline, at approximately wild type levels in the presence of low doxycycline concentrations and at levels well in excess of the parental line on exposure to higher doxycycline concentrations (Figure 3-4 D).

Using the G7shPool cell line (without inducible FOXG1 construct), comparison with parental controls under self-renewal conditions (EGF/FGF), failed to demonstrate any significant effect of *FOXG1* knockdown on the proportion of cycling cells as determined using ICC for Ki67. I next tested whether the G7 cells displayed increased sensitivitiy to BMP differentiation cues by adding EGF/FGF plus BMP4 in knockdown cells. Again no change in the proportion of Ki67 nuclei was evident (Figure 3-4 E).

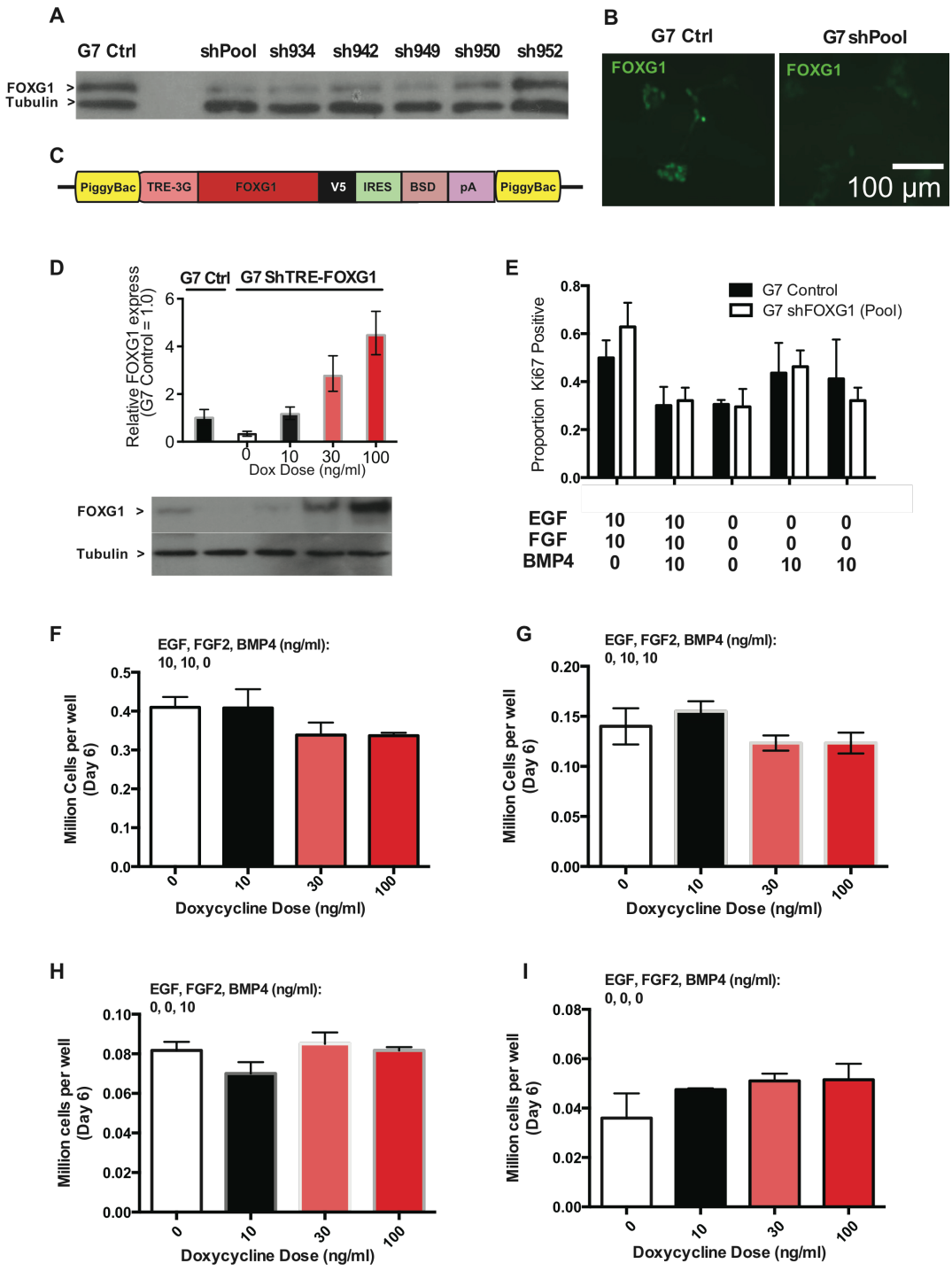
The introduction of the FOXG1 inducible cassette allowed for precise titration of gene expression levels and assessment of induced transgene function in experimental wells

plated from a single starting cell population. Once again there was no evidence of FOXG1 dose-dependence in the proliferation of this line (Vicount cell counts in technical triplicate and biological replicate) and we observed no consistent differences in response to introduction of low doses of BMP4 (Figure 3-4 F-I).

We conclude that for human GNS cells (G7) there is no criticial role for FOXG1 in control of cell proliferation of differentiation responses in these in vitro culture conditions. However, shRNA provides only knockdown and not complete genetic ablation. Either the residual FOXG1 protein, or line-to-line variations in FOXG1 dependencies might explain the discrepancy with published results.

Figure 3-4 - FOXG1 shRNA knockdown in G7 GNS cells

A Infection with single shRNA constructs including sh949, or with a combination of constructs, followed by antibiotic selection, results in significant knockdown of protein expression, also evident using ICC **B**. **C** A Tet-On FOXG1 expression construct and rtTA were incorporated into G7 shPool cells by PiggyBac recombination resulting in doxycycline controllable levels as confirmed by Western and qPCR **D**. **E** Various combinations of growth factor and BMP4 supplementation fail to elicit FOXG1 dose-dependent differences in the proportion of cells in cycle. **F-I** This finding is confirmed by cell counts (day 6) in a range of conditions (50,000 cells plated on day 0).



(Figure legend overleaf)

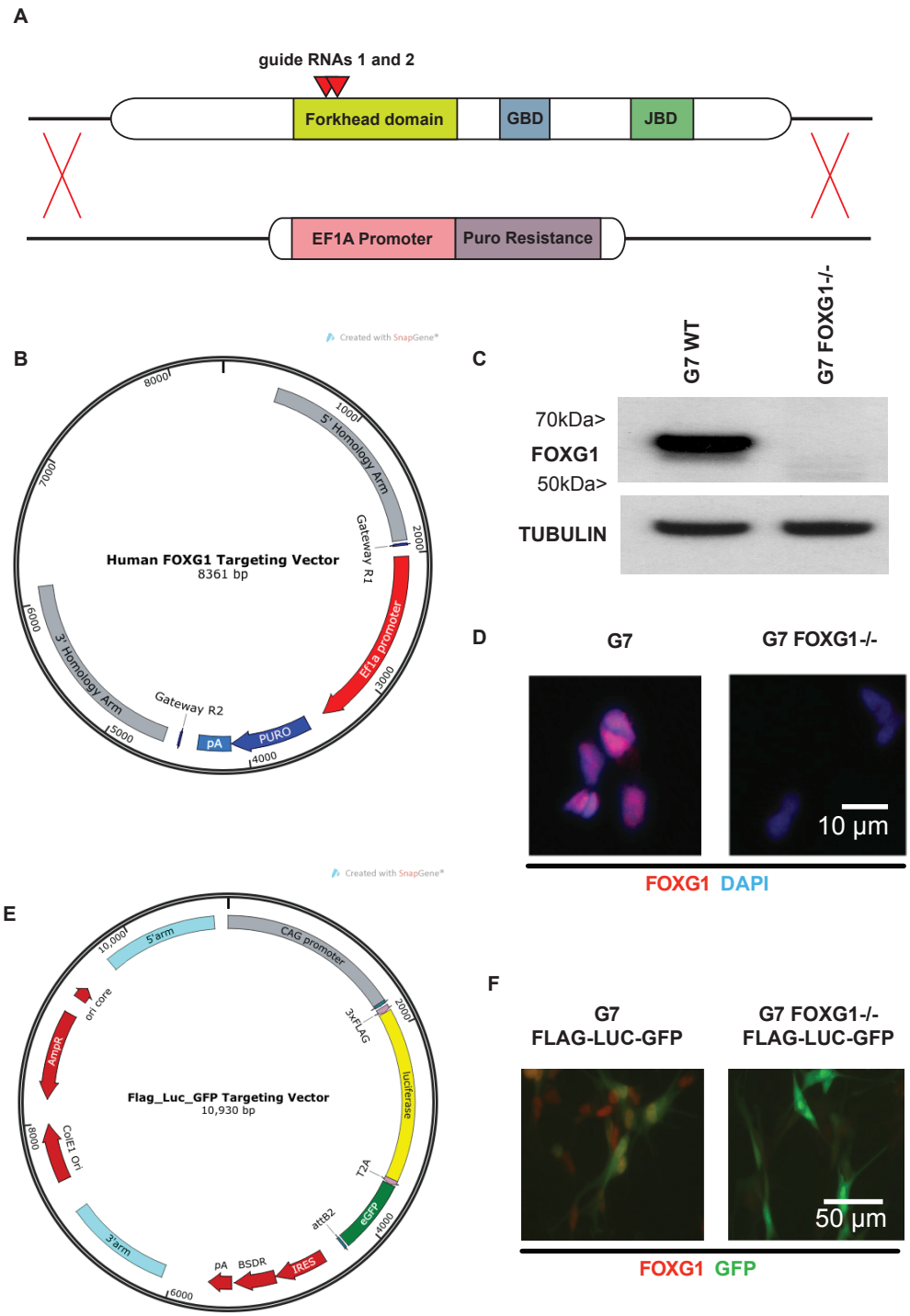
3.5 FOXG1 knockout in human GNS using CRISPR/Cas-assisted gene targeting

3.5.1 Generation of FOXG1 null clonal GNS cells using CRISPR/Cas gene targetting

Given that our shRNA knockdown results differed from other reports (45,148), I next sought to define the role of FOXG1 under normal self-renewal culture conditions through genetic knockout. This has recently become feasible with advances in genome editing, and the Pollard lab has successfully demonstrated in collaboration with Bill Skarnes (Sanger Institute) that gene targeting is possible in human GNS cells. Cas9-assisted homologous recombination can lead to biallelic mutations in target genes (manuscript in preparation). Guide RNAs were designed and produced within the FOXG1 exon (Figure 3-5 A) and a targeting vector was produced carrying an EF1a-PURO cassette between homology arms as indicated (Figure 3-5 B; gift from Bill Skarnes lab; cloning work performed by Raul Bressan). I performed transfections of these targeting plasmids into G7 cells and clonal cell lines were subsequqently expanded and screened by western blot to identify six heterozygous and one homozygous deleted clone (clone A1; Figure 3-5C; C. Blin and V. Grant assisted in these experiments).

Figure 3-5 - FOXG1 Crispr Targeting Strategy

A guide RNAs complementary to sequence in the forkhead binding domain were designed, together with a targeting vector incorporating homology arms as indicated. **B** The final targeting vector replaces the FOXG1 exon with an EF1a-PURO cassette. **C-D** Protein expression is abolished in the A1 clone by Western and by ICC. **E** For transplant purposes these cells were targeted to the AAVS1 safe harbour locus with a Flag-Luciferase-GFP construct. Residual cells were replated, fixed and stained after transplant to confirm FOXG1 and GFP expression. **F** Residual cells were replated following the xenotransplants, confirming viability and FOXG1 expression/ knockout in the respective populations.



(Figure legend overleaf).

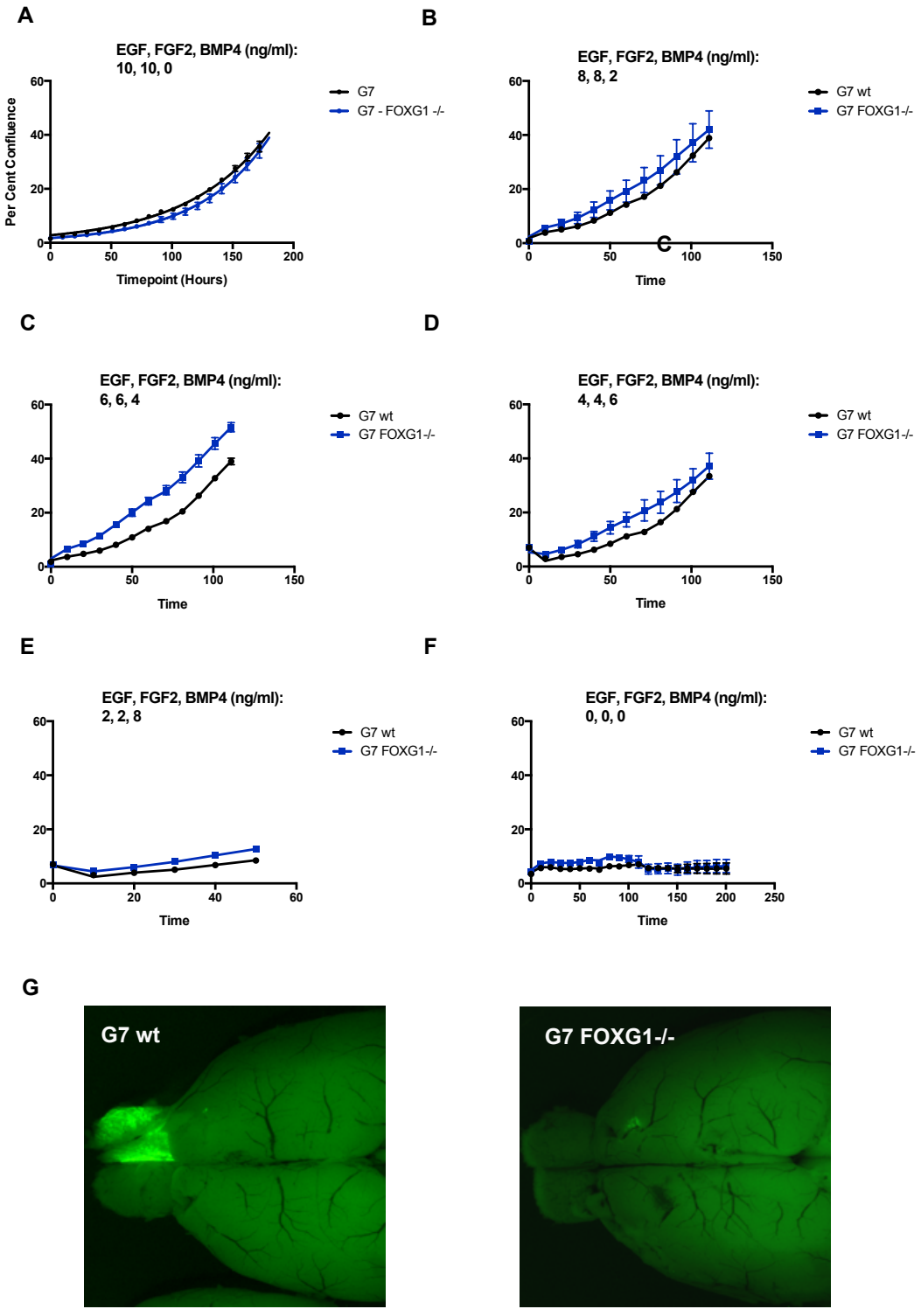
3.5.2 *FOXG1* deletion in GNS line G7 has no discernible impact on proliferation in vitro

G7 FOXG1$^{-/-}$ clonal line A1 was plated alongside G7 parental controls in media supplemented with combinations of EGF, FGF and BMP4 (Figure 3-6 A-F). Under no conditions was a significant difference in proliferation rate evident between these two lines. Thus, at least under these in vitro conditions we could not identify human GNS cells as having a specific addiction or dependency on FOXG1 for sustained in vitro proliferation.

3.5.3 Preliminary results suggest that FOXG1 deletion impairs tumour formation

We next transplanted the mutant cells orthotopically into immunocompromised mice to assess if FOXG1 deletion affected tumorigenicity. In order to aid tracking of cells in vivo I used a CAG-Luciferase-GFP reporter construct with AAVS1 homology arms (Figure 3-6 E), and transfected this into both G7 and G7 *FOXG1*-null lines. The resulting GFP-expressing cells were transplanted into the forebrains of NOD-SCID mice (n=5 for each condition) (experiments performed by S. Pollard). I confirmed viability and GFP expression as well as FOXG1 expression in the residual cells post-transplant (Figure 3-6 F).

Two mice from each transplant group (4 total) were sacrificed 6 months post-transplantion to monitor tumour formation. In mice which had received control G7 cells, the expected diffuse infiltration of the olfactory bulb by GFP-positive tumour cells was evident (Figure 3-6 G), reflecting migration/invasion along the rostral migratory stream. No tumour formation was evident in the mice implanted with FOXG1-deleted G7 cells although it was clear that a subset of cells had survived the transplant and were stably engrafted. Further investigation of the remaining transplanted mice will be undertaken by other investigators in the lab in the near future.



(Figure legend overleaf)

3.6 Conclusions

Altogether the data presented in this chapter have confirmed that FOXG1 is expressed across a diverse set of GNS cell lines at very high levels compared to forebrain foetal NS cells. FOXG1 is expressed at variable levels in WHO Grade III tumour derived cell lines, but uniformly to high levels in 12/12 WHO Grade IV derived GNS cell lines studied to date. High levels of expression are not however essential to drive proliferation of NS and GNS cell lines under *in vitro* self-renewal conditions. However, our preliminary data supports the published finding that FOXG1 expression is important for sustaining growth of tumours *in vivo* and we have performed gene knockouts using gene targeting successfully for the first time in primary human cancer cells. Thus, while FOXG1 appears dispensable for sustaining proliferation of GNS cells in vitro, we considered that uniform high expression in GBM might impede exit from self-renewal and drive ongoing rapid cell cycle. In other words, FOXG1 may act as a master regulator by interfering with induced differentiation or quiescence, and may be key to initiation rather than maintenance of NS cell identity. In the next chapter we present a series of experiments addressing the FOXG1 gain of function phenotype to test directly whether FOXG1 can drive dedifferentiation of astrocytes. This might explain the consistently high levels of expression in GBMs.

Figure 3-6 – Functional consequences of *FOXG1* knockout in G7 GNS cells

A G7 *FOXG1*-/- clone A1 demonstrates absent expression of the protein **B-F** A range of combinations of EGF/FGF and BMP supplementation fail to elicit differences in proliferation between wild type and *FOXG1*-/- derivatives in vitro. **G** GFP-positive G7 are seen to proliferate and invade over 6 months following xenotransplant, where *FOXG1*-null derivatives fail to do so.

4 Results 2 – Overexpression of FOXG1 and SOX2 in NS cells and astrocytes

4.1 Introduction

We next explored the working hypothesis that high levels of FOXG1 expression might be involved in the initiation of the glioma NS cell state, and subsequent resistance to BMP-induced differentiation. We also explore whether high levels could drive dedifferentiation of postmitotic astrocytes, explaining the block in differentiation commitment that is a feature of GNS cells (Caren et al., Stem Cell Reports, *in press*).

Rodent astrogenesis occurs predominantly in the first two weeks of postnatal life, and these early postnatal astrocyte populations can be expanded in serum-free culture conditions *in vitro*. Astrocytes can also be derived *in vitro* by exposing NS cells to inductive cues, here BMP4 (Figure 4-1 A). Astrocytes in culture typically display a flattened and stellate morphologies reminiscent of fibrous astrocytes *in vivo*: this contrasts with the typical bipolar phase-bright appearance of neural stem cells in culture (Figure 4-1 A and C). Compared to NS cell populations, astrocytes express low nestin levels and high GFAP levels. As discussed in the main Introduction, no single marker offers sensitive and specific identification of differentiated astrocytes. Importantly, although adult cortical astrocytes are generally postmitotic, astrocyte injury can stimulate mature astrocytes to reactivate by upregulating nestin and proliferating, *in vivo* or *in vitro* (86). In this respect, astrocytes are somewhat reminiscent of differentiated hepatocytes, which are effective terminally differentiated, but can still re-engage in cell cycle following injury or damage. Therefore they harbour a latent capacity for cell cycle re-entry. Given the lack of clear cut markers to distinguish quiescent stem cell like astrocytes (i.e. type B cells) from terminally differentiated astrocytes, I have employed a working definition of an *in vitro* 'differentiated' astrocyte: differentiated astrocytes are NS-derived cells with stellate or flattened morphology,

low Nestin and high GFAP expression, which remain postmitotic despite exposure to growth factors EGF and FGF-2 (NS cell proliferation conditions).

In this Chapter I present the results from assessment of *FOXG1* constitutive lentiviral overexpression and then inducible expression of *FOXG1* in NS cells and in postmitotic differentiated astrocytes. Given the reported successful reprogramming of fibroblasts to NS-like cells using a combination of *FOXG1* and *SOX2* transgenes, I also explored a possible synergistic reprogramming of these factors. Combinatorial overexpression of *FOXG1* and *SOX2* was able to overcome BMP induced cell cycle exit. Moreover, this combination was able to drive the postmitotic differentiated astrocytes to re-enter cycle and dedifferentiate. I also investigated the effect on this process of overexpressing additional NS lineage master regulators, BRN2 or OLIG2, in combination with FOXG1 and SOX2 as part of triple constructs (39,51) (51) and also established the dedifferentiation potential of single transgene expressing lines. Finally, I show that when overexpressed at very high levels FOXG1 alone is sufficient to drive efficient astrocyte cell cycle re-entry and dedifferentiation.

4.2 BMP4 treatment of mouse NS cells plated at low density drives stable cell cycle exit and astrocyte differentiation commitment.

Differentiation of mouse NS cells to astrocytes can be triggered *in vitro* by supplementing media with BMP4 or other factors in place of the mitogens EGF and FGF-2. Previous work in the lab suggested that cells plated at high density and exposed to BMP4 treatment failed to undergo terminal differentiation, so that restoration of EGF/FGF-2, even after weeks of BMP4 treatment, was sufficient to drive re-entry into cell cycle and colony formation. This state may correspond to the condition of reversible cell cycle exit known as quiescence, either because the astrocytes are immature, or driven into a quiescent stem cell

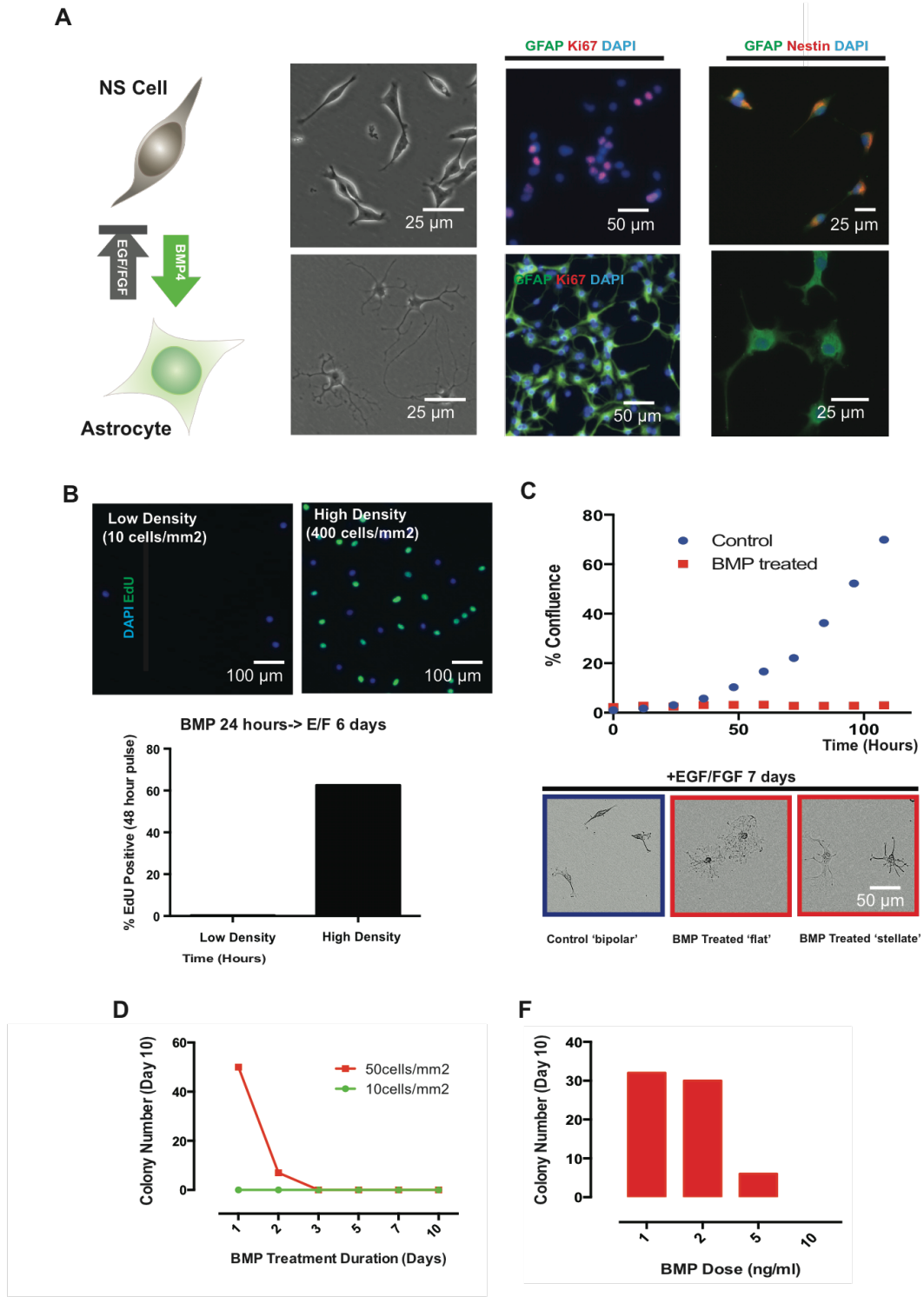
like state (83). However, our goal was focussed on testing the activity of FOXG1 when delivered to postmitotic differentiated astrocytes as this might inform its role in glioma.

In order to establish a reliable quantitative assay of de-differentiation I first established conditions that could drive astrocyte terminal differentiation. At clonal cell densities cell-cell contact and paracrine signalling is avoided and this may help drive terminal differentiation. A clear demonstration of the importance of density is provided by EdU labelling experiments performed here at low density (10cells/mm2) and high density (400cells/mm2). ANS4 cells were plated at the given density in media supplemented with BMP4 at 10ng/ml for 24 hours, before changing to media with EGF/FGF. After 96 hours in these conditions, EdU was added for a 48 hour pulse, then the cells were fixed and stained. Whereas >60% of the cells in the high density condition were EdU positive, compatible with a cell cycle time of 24-48 hours typical for NS cells, at low density only 0.3% of the cells were EdU positive, implying almost universal cell cycle exit after BMP4 treatment, refractory to restoration of growth factors (Figure 4-1 B).

Preliminary experiments testing different densities allowed me to establish that for the three different NS cell lines tested (ANS4, NS FoxG1$^{fl/fl}$, and FS3), plated at densities up to 50 cells/mm2, 72 hours of treatment with BMP4 at 10ng/ml was sufficient to establish cell cycle exit which persisted despite reintroduction of the mitogens EGF and FGF. Lower concentrations of BMP4 (1-5ng/ml) failed to achieve uniform commitment at this intermediate plating density over 72 hours. For accurate colony formation assays, lower plating densities are desirable, and further experiments confirmed that the ANS4 cell line derivatives studied here exit cycle and enter a dormant or terminally differentiated astrocyte state after 24 hours' BMP4 treatment at a plating density of 10 cells/mm2 (Figure 4-1 A). This is demonstrated by upregulation of the astrocyte marker GFAP, and refractory cell cycle exit with loss of colony formation capacity on return to growth conditions (Figure 4-1 C).

Thus, we can drive NS cells to postmitotic and differentiation committed state by plating at low densities in the presence of BMP. This enables us to test the ability of FOXG1, SOX2, other TFs or pharmacological manipulation to drive dedifferentiation, quantified according to the emergence of colonies upon re-exposure to growth factors. Regardless of the maturity of astrocyte differentiation after 24 hours in BMP, this assay provides a reliable cellular model system for interrogating the key functional transition of interest, namely re-entry into cell cycle and reacquisition of NS cell identity.

Figure 4-1 - Assays of astrocyte commitment by NS cells in response to BMP treatment. **A** Mouse neural stem cells growing in media supplemented with EGF and FGF proliferate and self-renew. Replacement of these growth factors with BMP4 drives prompt and uniform astrocyte specification comprising morphological alterations, exit from cell cycle and upregulation of GFAP. Our working hypothesis is that high FoxG1 levels can compromise this process, and even reverse established astrocyte commitment on return to EGF/FGF conditions. **B** ANS4 cells treated with BMP4 at low density (10cells/mm2) fail to incorporate EdU in the window 96-144 hours following restoration of EGF/FGF. Cells plated at high density (400cells/mm2) re-enter cycle and incorporate EdU extensively. **C** ANS4 Neural stem cells plated at 10 cells/mm2 demonstrate exponential growth to confluence in EGF/FGF conditions. ANS4 cells growing in identical conditions but pre-treated with BMP4 for 24 hours prior to plotting growth curves remain cycle exited, and retain characteristic ‘stellate’ and ‘fried egg’ morphologies. **D** Colony forming assays demonstrate that colony formation capacity is completely abolished in ANS4 cells after BMP treatment (10ng/ml) for 24 hours (10cells/mm2) or 72 hours (50cells/mm2). **E** BMP4 concentrations <10ng/ml fail to completely abolish colony formation after 72 hours in ANS4 cells plated at 50cells/mm2.



(Figure legend overleaf)

4.3 Effects of FOXG1 overexpression on mouse NS cell proliferation and differentiation

4.3.1 Constitutive FOXG1-V5 expression in mouse NS cells does not influence cell proliferation, but attenuates BMP4-induced cell cycle exit

In order to achieve stable FOXG1 overexpression we transduced adult wild-type NS cells (ANS4) with lentivirus FOXG1-V5 (see Methods), and sorted for high tomato expression after 48 hours. We demonstrated FOXG1 overexpression in this line (termed A4FGO) by Western immunoblotting using the lab's newly generated mouse hybridoma anti-FoxG1 clone 17B12, which can detect both mouse and human FOXG1 (Figure 4-2A). Transgene expression was also confirmed by V5 immunostaining (Figure 4-2B).

I next assessed whether FOXG1 constitutive overexpression would alter the responsiveness of NS cells to BMP4, which triggers cell cycle exit and astrocyte differentiation. Parental ANS4 cells and A4-FGO cells were plated at a density of 50,000 per well in 4-well plates in complete media with the growth factors EGF/FGF or with BMP; self-renewal or differentiation conditions, respectively. After 48 hours, the cells were fixed and stained for Ki67. No significant difference was observed between the proportions of ANS4 and A4FGO cells expressing Ki67 in either self-renewal conditions (each 35-40% positive) or differentiation conditions (each 0% positive).

We next challenged the cells with suboptimal differentiation conditions wherein cells were exposed to 1ng/ml or 10ng/ml BMP4 combined with normal EGF/FGF supplementation. Here we observed that significantly more A4FGO cells remained in cycle, 41.5% vs 30.7% of controls in BMP 1ng/ml, and 15.8% vs 8.4% of controls in BMP 10ng/ml (Figure 4-2C). This suggested that FOXG1 overexpression may attenuate the response to differentiation cues. In keeping with this, upregulation of the astrocyte marker GFAP after BMP treatment is seen to be impaired in A4FGO compared to ANS4 controls (Figure 4-2D). Overall these data indicate that FOXG1 limits differentiation commitment.

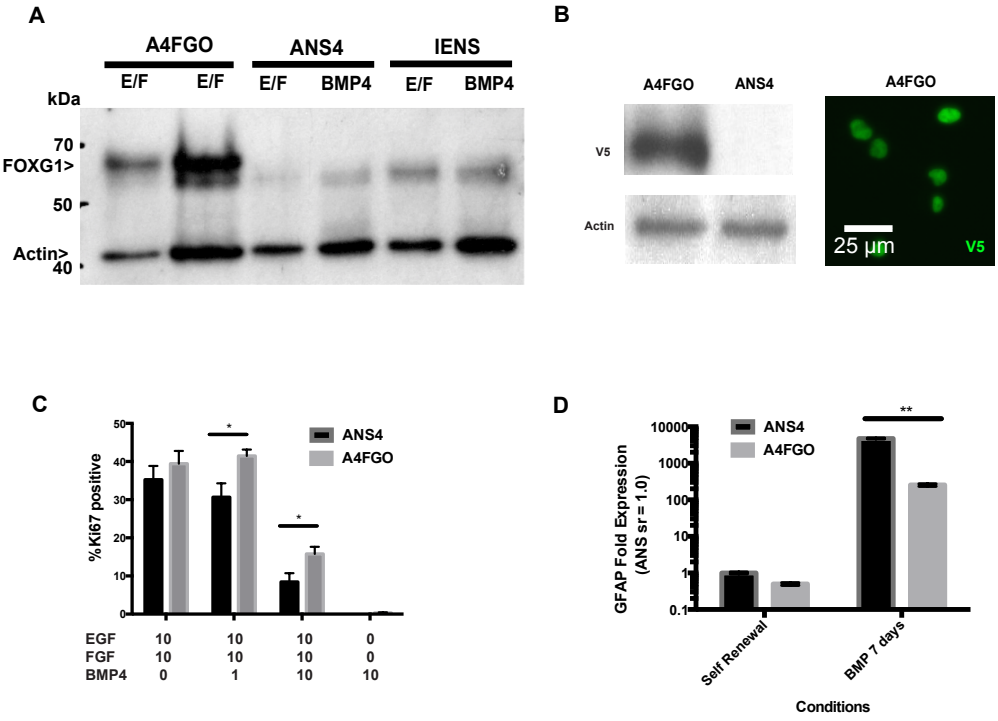


Figure 4-2 - Functional effects of FOXG1 overexpression

A ANS4 cells expressing the lentiviral FOXG1V5 construct (A4FGO) demonstrate high level FOXG1 overexpression compared to parental controls and IENS glioma model lines **B** ICC and Western blot confirm expression of the V5 epitope tag. **C** A4FGO cells demonstrate reduced tendency to exit cycle on exposure to combinations of BMP4, EGF and FGF compared to parental controls **D** A4FGO cells demonstrate reduced upregulation of GFAP in response to BMP treatment.

4.3.2 FOXG1 and SOX2 were overexpressed in isolation or in combination using PiggyBac Doxycycline-inducible Transgenes

The above data suggested that higher levels of FOXG1 might restrict BMP induced astrocyte differentiation. However, this effect was rather modest and the majority of cells activate GFAP expression and exited cell cycle. One possibility is that some other limiting factor is missing that could co-operate. We considered SOX2 a likely candidate cofactor, based on existing evidence for its role in the processes of interest. Firstly, the combination of FOXG1 and SOX2 is sufficient to drive fibroblast reprogramming to an NS cell state (39). Secondly, SOX2 is highly expressed consistently across glioma subtypes and is sometimes genetically amplified. Thirdly, SOX2 and FOXG1 are reported to be involved in distinct parallel TGF-beta response pathways, raising the possibility of functional synergy between the two (46) (48).

In order to establish any potential synergistic effect, ANS4 mouse NS cells were transfected with a newly generated contruct, PiggyBac vectors with doxycycline-inducible FOXG1, SOX2, or FOXG1_2A_SOX2 self-cleaving fusion transgenes, as well as the PiggyBac constitutive rtTA expression plasmid, and the PiggyBac recombinase (see Methods). The transformants were plated at low density and allowed to form colonies under antibiotic selection over 2 weeks. Clonal lines were derived (Figure 4-3; n = 24 clones were picked for each transgene). Initial selection of these clones was undertaken on the basis of the Dox responses of replica plates following fixation and immunocytochemistry for FOXG1 and SOX2. This identified clonal lines F6 (FOXG1V5), TS15 (SOX2) and FS3 (FOXG1V5_2A_SOX2), exhibiting low background (i.e not leaky) but significant high level induction upon Dox treatment, and this was confirmed by qRT-PCR and Western (Figure 4-3). These inducible FOXG1, SOX2 or FOXG1 + SOX2 NS cell lines were used to explore gain of function effects on differentiation.

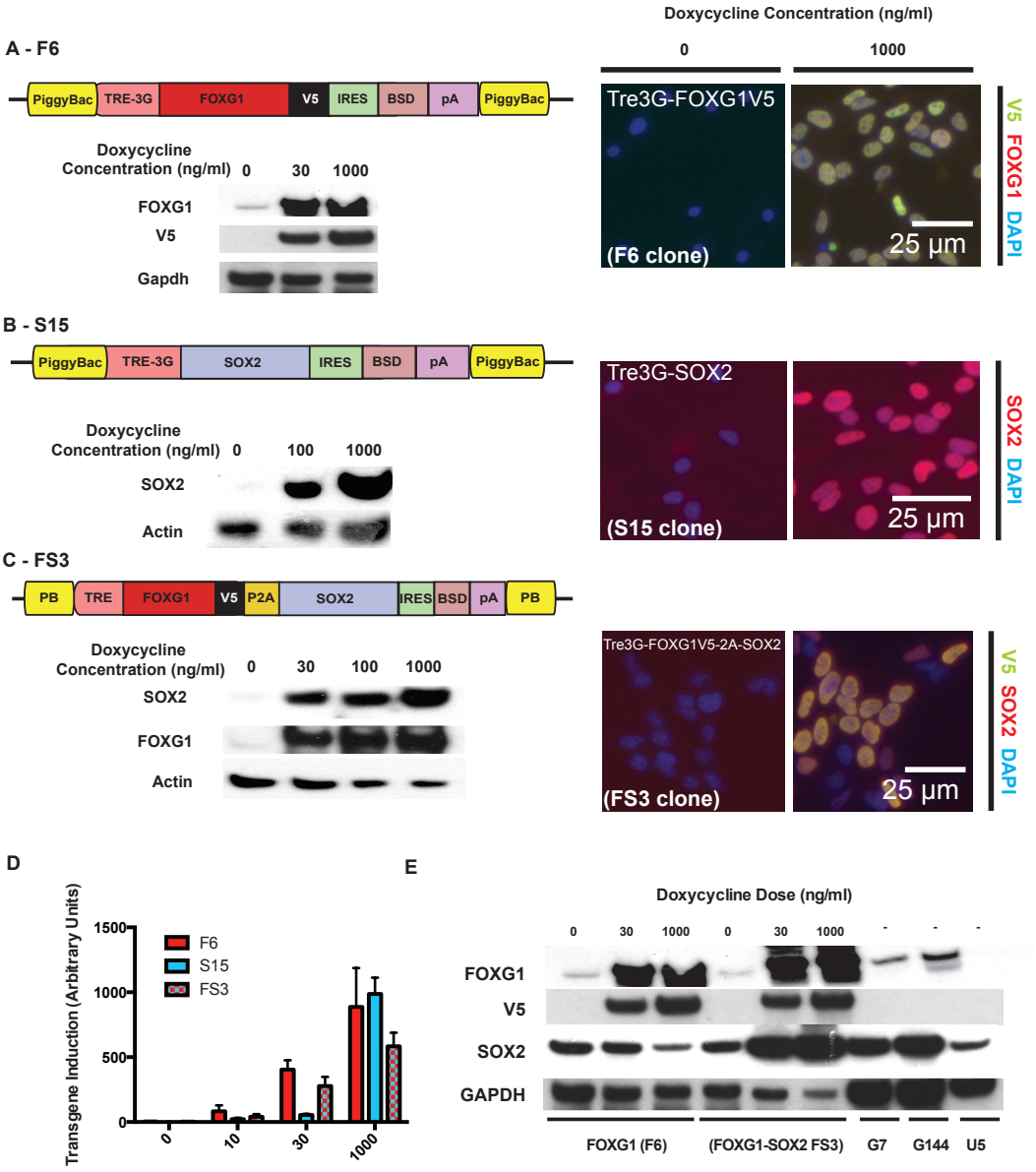


Figure 4-3 - Clonal NS cell lines with doxycycline-inducible expression cassettes.

Clonal cell lines express high levels of inducible transgene constructs FOXG1-V5 **A**, SOX2 **B**, and FOXG1-V5_2A_SOX2 **C** as assessed by Western and ICC. **D** Clones F6, S15 and FS3 demonstrate comparable transgene induction properties, as assessed by qRT-PCR for a shared amplicon **E** FOXG1 protein expression in clonal cell lines F6 and FS3 is seen to be lower at baseline and higher in the presence of doxycycline than is the case in human GNS lines G7 and G144.

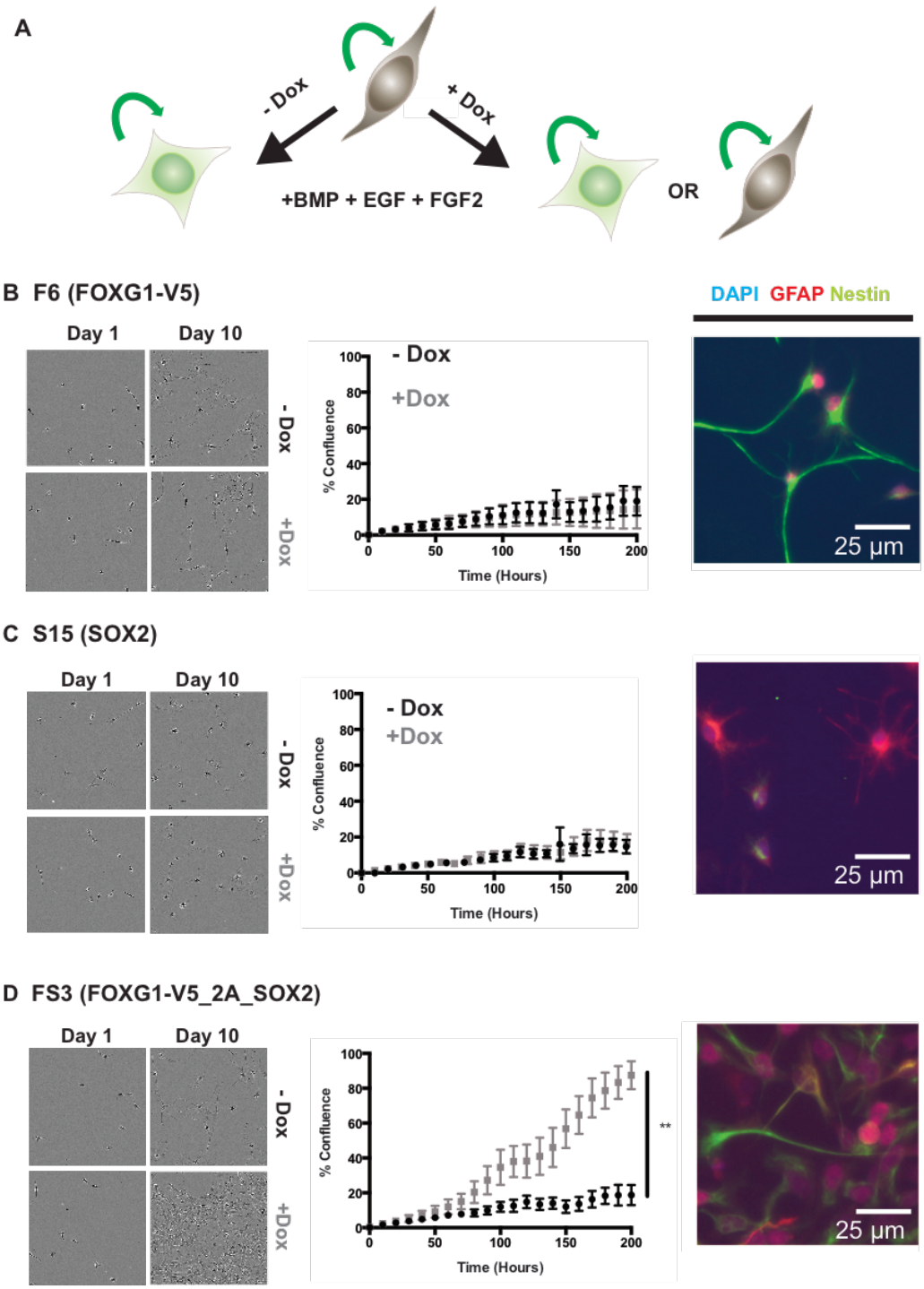
4.3.3 Forced expression of FOXG1 and SOX2 prevents cell cycle exit in response to differentiation cues.

The propensity of ANS4 clonal derivatives to persist in self-renewal was assayed by plating these cell lines in sub-optimal growth conditions (EGF 8ng/ml; FGF2 8ng/ml; BMP4 2ng/ml) at 5000 cells per well in triplicate wells in 6-well plates, in the presence or absence of doxycycline (Figure 4-4). Confluence plots from clonal lines overexpressing FOXG1 (F8), SOX2 (S6) and FOXG1_2A_SOX2 (FS3) transgenes are displayed in the figure, along with controls plated simultaneously without doxycycline. Dox-treated F8 and FS3 cells retained stronger nestin expression than was the case for S6. However only cell line FS3, treated with doxcycline to induce overexpression of FOXG1 and SOX2, demonstrated rapid proliferation to confluence under these mixed growth/ differentiation conditions, and this finding was repeated in more stringent conditions (EGF 2ng/ml; FGF 2ng/ml; BMP4 8ng/ml; not shown).

We next considered the possibility that these transgenes, alone or in combination, might be capable of driving committed astrocytes to re-enter cycle and perhaps to dedifferentiate.

Figure 4-4 - Effects of transgene overexpression on proliferation

A Exposure of ANS4 cells to a mixture of the growth factors EGF/FGF and the inductive driver of astrocyte differentiation BMP4 results in slow division of a GFAP positive population. We hypothesised that transgene induction might drive a more rapid-cycling NS-like phenotype **B** and **C** Induction of the single FOXG1 and SOX2 transgenes by doxycycline supplementation has no discernible impact on proliferation rate, although high FOXG1 expression is accompanied by stronger nestin expression compared to the SOX2-induced population. **D** Induction of the dual FOXG1_2A_SOX2 transgene drives rapid NS-like proliferation in a population expressing Nestin and GFAP.



(Figure legend overleaf).

4.4 Astrocyte de-differentiation is triggered in response to FOXG1 and SOX2 overexpression

4.4.1 Combined overexpression of FOXG1 and SOX2 drives differentiated astrocytes to re-enter cell cycle and acquire an NS cell-like morphology

The Dox-inducible NS line FS3 (CAG-FOXG1V5-SOX2) was plated at an intermediate density (50,000 cells per well of a 6 well plate; ~50 cells/mm2) in media supplemented with BMP4 (Figure 4-5). This promotes astrocyte differentiation commitment in all the cells. After 3 days, the media was changed for growth media supplemented with EGF and FGF-2, with or without Dox. In the absence of Dox no NS -like colonies emerge, consistent with a starting population of committed postmitotic astrocytes. However, in the presence of Dox rapidly cycling NS-like cells emerged in proliferating foci. These cells were highly motile, bipolar, and expressed nestin. The number of foci that emerged was doxycycline/transgene dose dependent. These data demonstrate a clear function for the FOXG1/SOX2 transgene in driving astrocyte de-differentiation.

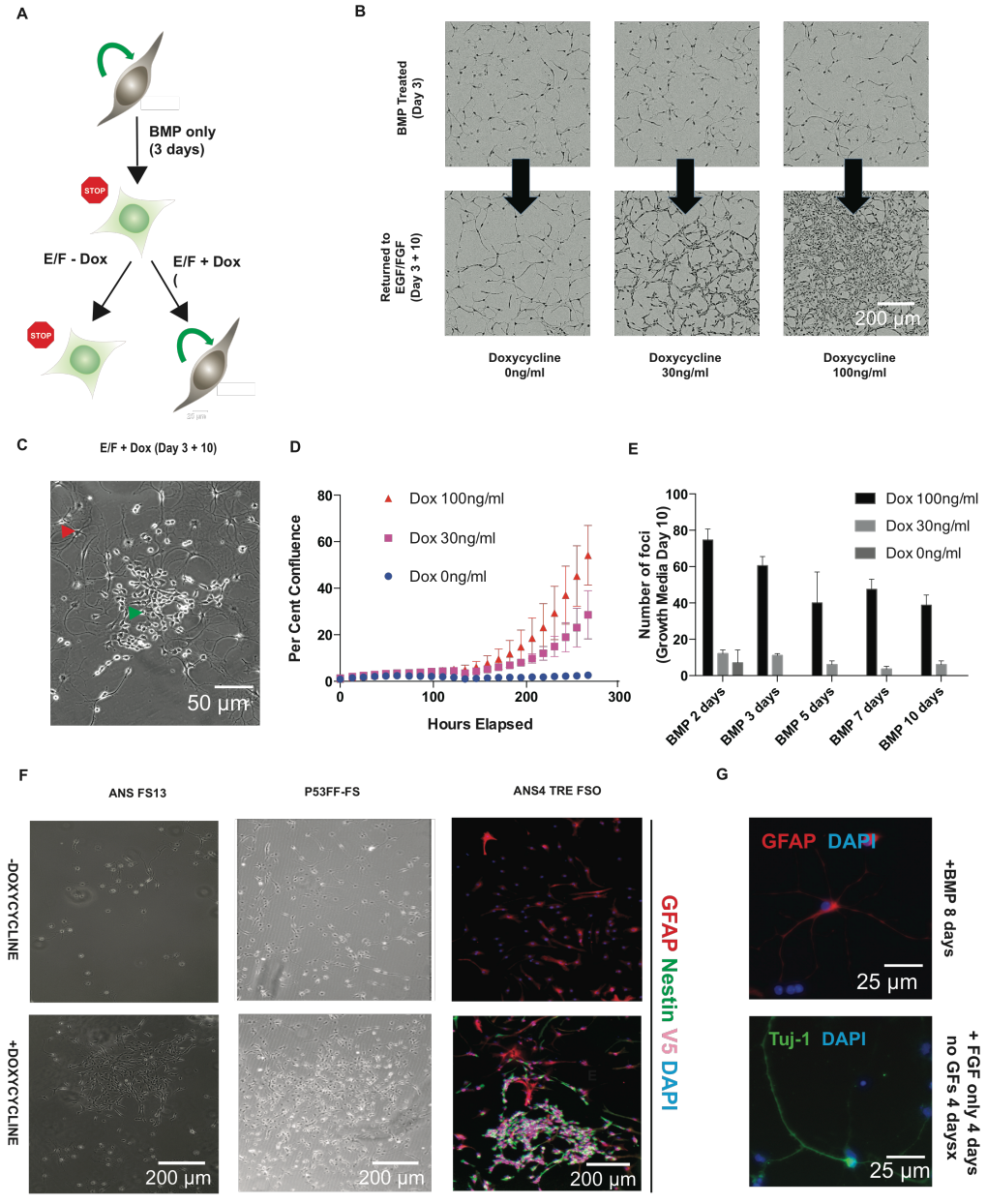
Longer periods of BMP treatment prior to Dox exposure (up to 10 days) had minimal effects on the observed efficiency of cell cycle re-entry in response to EGF/FGF and growth factors, suggesting the dedifferentiation was not limited to early immature astrocytes. Dox was required continuously to generate maximal colony numbers, compatible with a stochastic process underlying the putatitive cell cycle re-entry and dedifferentiation, explored further in low density colony formation assays discussed below.

To confirm that the response to Dox was not limited to the FS3 cell line, we assessed a second clonal line from the same bulk population (ANS FS13), as well as a completely independent mouse NS cell line generated from p53 floxed adult mouse SVZ (p53floxed TRE FS) that had been transfected stably with the same inducible transgene. In both instances induction of the transgene triggered astrocytes to re-enter cell cycle and form NS cell-like colonies when exposed to growth factors EGF and FGF. The same phenotype was

also evident in response to doxycycline administered to a cell line overexpressing a FOXG1V5_2A_SOX2_2A_OLIG2 triple transgene construct (Figure 4-5E).

Figure 4-5 – Driving astrocyte cell cycle re-entry by FOXG1-SOX2 forced expression

A Astrocytes were derived by plating a single parental NS cell batch at 50 cells/mm^2 in experimental and control wells, in BMP media. After 72 hours differentiation, the media was removed and replaced with growth media, with or without doxycycline respectively. **B** FS3 cells remain out of cycle on restoration of growth media, but addition of doxycycline induces the same cells to re-enter cycle and proliferate rapidly over 10 days, with efficiency reflecting doxycycline dose. **C** On doxycycline treatment, proliferating clusters of cells with NS-like morphology (green arrow) are evident against a background of refractory cell cycle exited astrocytes (red arrow). **D** The doxycycline dose, and therefore the level of FOXG1 and SOX2 forced expression determines rate of proliferation on return to EGF/FGF. **E** FOXG1/SOX2 retain the capacity to drive return to cycle after extended BMP4 treatment up to at least 10 days. **F** Cell cycle re-entry is replicated across ANS4 clonal lines overexpressing the FOXG1_2A_SOX2 transgene (e.g ANS FS13), derivatives of another mouse NS cell line expressing the same construct (P53FF-FGO), and an ANS4 derivative expressing the FOXG1_2A_SOX2_2A_OLIG2 triple construct (ANS4 TRE FSO). **G** After return to cycle, FS3 cells demonstrate the ability to differentiate into astrocytic and neuronal phenotypes in appropriate conditions.



(Figure legend overleaf).

4.4.2 Establishment of a colony-forming assay to explore astrocyte cell cycle re-entry and de-differentiation

To further explore the effects of FOXG1 and SOX2 when overexpressed in astrocytes we next performed similar experiments using lower densities to test clonal responses and rule out any potential paracrine influences on the dedifferentiation. Cells were plated at 50,000 per 10 cm dish (~10cells/mm2) in BMP media to trigger astrocyte differentiation. After 24 hours in these conditions, wild type mouse NS cells (ANS4 or FS3 cells) are postmitotic, express the astrocyte marker GFAP, and lack nestin expression, suggesting adoption of a postmitotic astrocyte identity (Figure 4-1). After 24hrs we challenged these astrocytes to determine if differentiation commitment had occurred. BMP was withdrawn and replaced with EGF and FGF-2 (NS cell self-renewal conditions). In FS3 (no Dox) controls, we failed to find any colony formation and astrocytes remained post-mitotic (Figure 4-6A). In contrast, the transformed NS cell line (IENS; EGFRvIII overexpression; INK4ARF deletion), which is glioma initiating when transplanted, did form small numbers of proliferative colonies (60). This suggests this assay is useful to explore failure of differentiation commitment in glioma

4.4.3 Combined overexpression of FOXG1 and SOX2 is sufficient to drive re-entry into cell cycle by postmitotic astrocytes

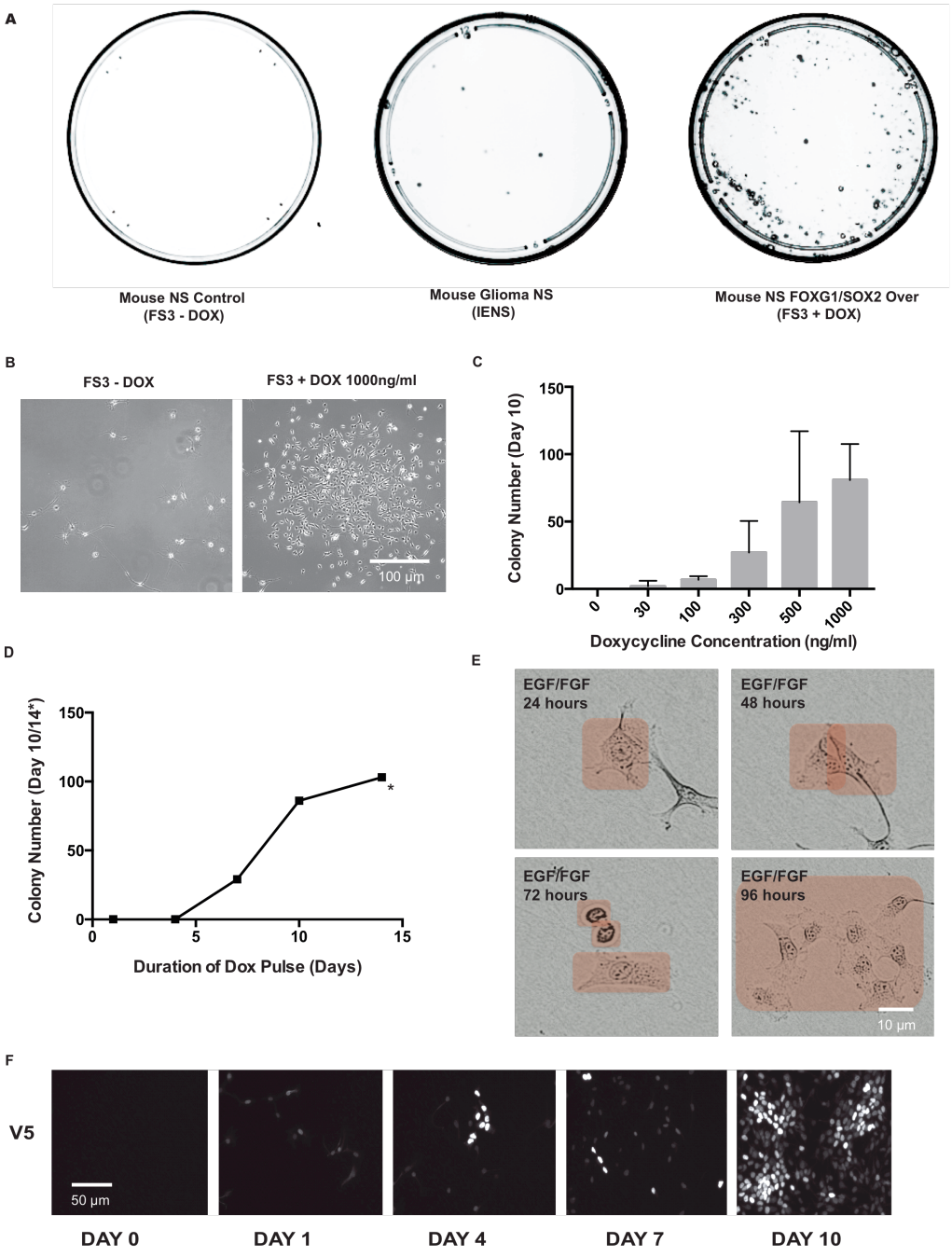
Using this colony formation assay we next explored whether FS3 cells derived astrocytes would re-enter cell on administration of Dox. We found a clear ability of the Dox induced cultures to generate NS cell-like colonies, and this was transgene dose-dependent (Figure 4-6C). V5 ICC staining of these cultures at serial timepoints demonstrates induction of the FOXG1_SOX2 transgene at day 1 post media change, and by day 4 high level transgene accumulation is evident in nascent colonies. For maximal colony formation, Dox was required continuously (rather than a 1 or 2 days pulse) suggesting that both early and late targets of the transgene might drive colony formation (Figure 4-6D).

Time-lapse videos generated using the Incucyte live cell imaging system allowed visualisation and tracking of cell cycle re-entry by individual cells, and confirmed cells with

astrocytic morphology can undergo division within 24-48 hours of exposure to growth factors and doxycycline. Tracking of single cells indicated that further cell division occurred every ~24hrs, the doubling time of proliferating NS cells. A mitotic figure is evident at 72 hours, and by 96 hours some cells begin to exhibit bipolar morphology reminiscent of NS cells (Figure 4-6E). Altogether, these observations suggest that induction of FOXG1 and SOX2 can rapidly drive astrocyte cell cycle re-entry and morphological changes indicative of a de-differentiation to an NS cell-like state.

Figure 4-6 - Induction of cell cycle re-entry by astrocytes at low plating density

A Example colony formation in the indicated cell lines/conditions at low plating density. Example images shown here were obtained after a further 7 days in growth media to allow expansion of colonies for clear visualisation. 50,000 cells plated in a 10cm dish (5 cells/mm2) in DMEM/F12 supplemented with BMP4 10ng/ml, replaced with growth media after 24 hours. **B** At low density, combined overexpression of FOXG1 and SOX2 drives colony formation. **C** Colony formation is dependent on doxycycline dose/ transgene expression level and **D** on prolonged transgene induction. **E** Re-entry into cell cycle by individual astrocytes is observed within 24-48 hours after addition of growth factors and doxycycline. The resulting clones exhibit the same cell cycle time of ~24 hours observed in the parent NS cell lines in these conditions. **F** High level induction of the V5 transgene in a subpopulation by Day 4 results in generation of V5-positive colonies by Day 10.


A
Mouse NS Control
(FS3 - DOX)
Mouse Glioma NS
(IENS)
Mouse NS FOXG1/SOX2 Over
(FS3 + DOX)
B
FS3 - DOX
FS3 + DOX 1000ng/ml
100 µm
C
Colony Number (Day 10)
150
100
50
0
0
30
100
300
500
1000
Doxycycline Concentration (ng/ml)
D
Colony Number (Day 10/14*)
150
100
50
0
0
5
10
15
*
Duration of Dox Pulse (Days)
E
EGF/FGF
24 hours
EGF/FGF
48 hours
EGF/FGF
72 hours
EGF/FGF
96 hours
10 µm
F
V5
50 µm
DAY 0
DAY 1
DAY 4
DAY 7
DAY 10

4.4.4 Primary cortical astrocytes are driven to a proliferative NS cell-like state upon overexpression of FOXG1 and SOX2

Astrocytes generated *in vitro* via NS cell differentiation may be immature or more vulnerable to de-differentiation than astrocytes isolated directly from the mouse CNS. We therefore next tested whether FOXG1 and SOX2 could drive dedifferentiation of primary postnatal astrocytes.

Primary postnatal astrocyte cultures were prepared according to established protocols (Methods; Figure 4-7A). These were transfected using lipofection with the plasmids (pBase, pTet3G, pDEST; 2:1:1 ratio) leading to stable Piggybac-mediated integration of the transgene (Figure 4-7B). Serum-containing astrocyte culture media was also supplemented with 100ng/ml Dox (except in negative control wells). After 24 hours (Day 1), the astrocyte media was replaced with NS growth media, again supplemented with Dox where appropriate. After a further 48 hours (Day 3), example wells were fixed for staining to confirm transgene expression, while cells in the remaining wells were dissociated and replated at clonal density in 10cm dishes, in NS media plus or minus Dox (100ng/ml) and scored any proliferative colonies at Day 14 (4 independent plates; 2 independent experiments). We observed a substantial increase in colony formation (4-fold) in the presence of Dox. Background colony formation in the absence of Dox, likely represents the presence of contaminating precursor cells in the serum-derived astrocyte cultures. Thus, we observed a similar effect of FOXG1 and SOX2 in driving cell cycle and colony formation in primary astrocytes as those astrocytes produced by NS cell differentiation in vitro.

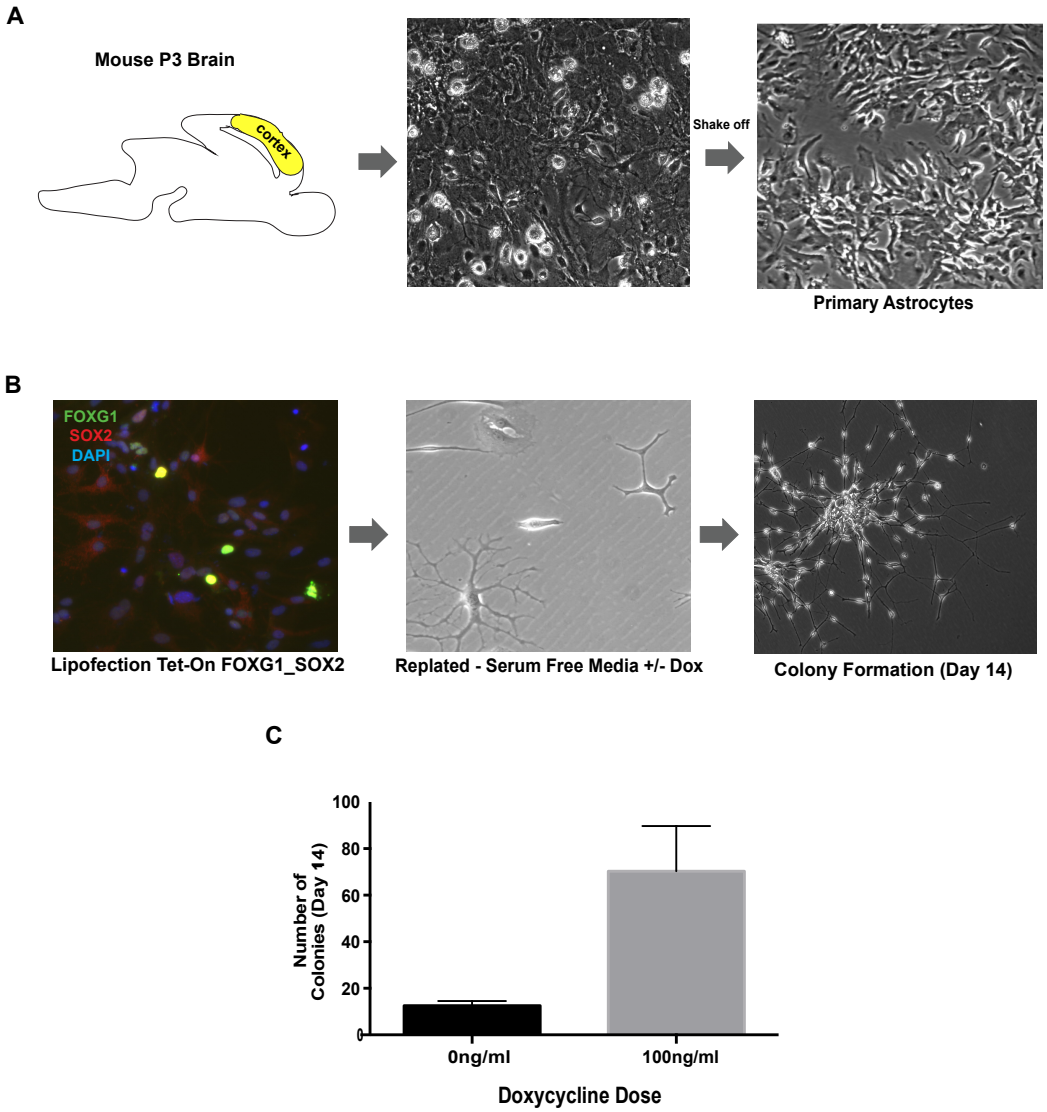


Figure 4-7 - Induction of cell cycle re-entry by primary astrocytes

A Mouse primary astrocytes are isolated by dissection and dissociation of P3 mouse pup cortices, followed by growth on poly-D-lysine coated plates in 1% FCS. The resulting mixed populations are depleted for OPCs and other contaminating populations by shake-off **B** Inducible overexpression of the FOXG1_2A_SOX2 transgene is achieved by lipofection, and these populations are plated at low density in serum free media with or without doxycycline supplementation. **C** Significant increases in colony formation efficiency are associated with doxycycyline supplementation.

4.5 FOXG1/SOX2 derived cell cycle re-entry is accompanied by reacquisition of the radial glia-like NS cell state

4.5.1 Cycling cells re-express NS cell markers

The morphological changes associated with re-entry prompted us to explore the possibility that these cells have de-differentiated and re-acquired the molecular markers and differentiation potential of the radial glia-like NS cells. To this end we assessed a range of molecular markers (Figure 4-8).

Immunocytochemistry was first performed to explore levels of Nestin and its correlation to the V5 transgene. This is one of the best markers for distinguishing NS cells from astrocytes. Scoring of cells was achieved in an objective manner using 'image cytometry' from large numbers of images acquired systematically using the Operetta imaging system (PerkinElmer). Cells within the V5-expressing colonies expressed high levels of Nestin (scored across 60 fields; n =3) and we noted a strong correlation between transgene expression and Nestin expression. This is consistent with dedifferentiation and acquisition of the NS cell state.

Using higher magnifications we were able to segment images and bin cells into distinct V5 'high' and V5 'low' expressing populations. We noted that V5 nuclear intensity is significantly higher in cells comprising part of a cluster (t-test $p<0.001$). This likely reflects higher transgene expression in association with general upregulation of the transcription/translation machinery in association with re-entry to cycle (20 fields per well).

Dox-treated wells demonstrate a shift in the population towards a Nestin-high, GFAP-low expression profile. Staining of the dedifferentiated colonies showed expression of NS cell expressed TFs Nkx2-2 and Olig2. The expression of Olig2, Nkx2.2, nestin and low or negative GFAP staining is similar to the original proliferative NS cells. We surmise that induction of FOXG1 and SOX2 drives astrocytes to dedifferentiate and reacquire the radial glia-like NS cell identity.

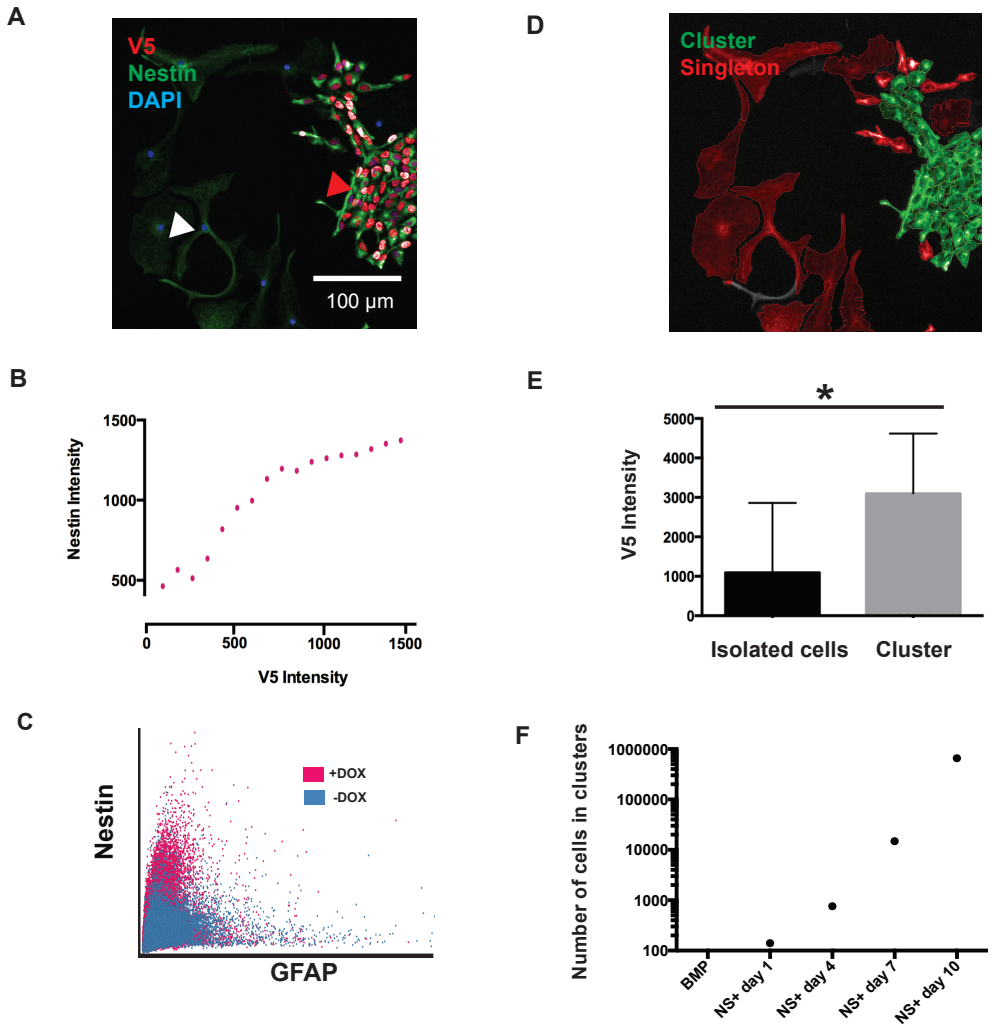


Figure 4-8 – Operetta-based image cytometry analysis of the dedifferentiation process

A High FOXG1-SOX2 transgene expression (V5 - red) drives re-entry into cell cycle with expression of nestin (Green). **B** Transgene expression is correlated with nestin expression in treated wells. **C** Image cytometry demonstrates a transgene-induced shift in distribution with an increase in the Nestin-high GFAP-low fraction at day 10 in EGF/FGF **D** Operetta images from panel A are computationally segregated into dedifferentiating colonies (>10 blue DAPI nuclei <10 pixels apart; DAPI - blue) and background astrocytes, and these regions are displayed in green and red respectively. **E** Cells in clusters express higher transgene (V5) levels **F** The number of cells in clusters increases exponentially over 10 days' dedifferentiation.

4.5.2 High levels of FOXG1 overexpression are sufficient to drive astrocyte dedifferentiation with high efficiency

Investigation of the effects of FOXG1 or SOX2 expression alone on dedifferentiation had indicated that neither transgene was sufficient in isolation to drive this phenotype. However, the levels of transgene induction in the clones studied were not as high as for FS3. Therefore I derived and characterised further clonal lines, including the final lines described here, F6 and S15. Each line demonstrated transgene induction to the same or greater copy number than FS3, as measured by qPCR for a region common to all 3 transcripts (Figure 4-3D).

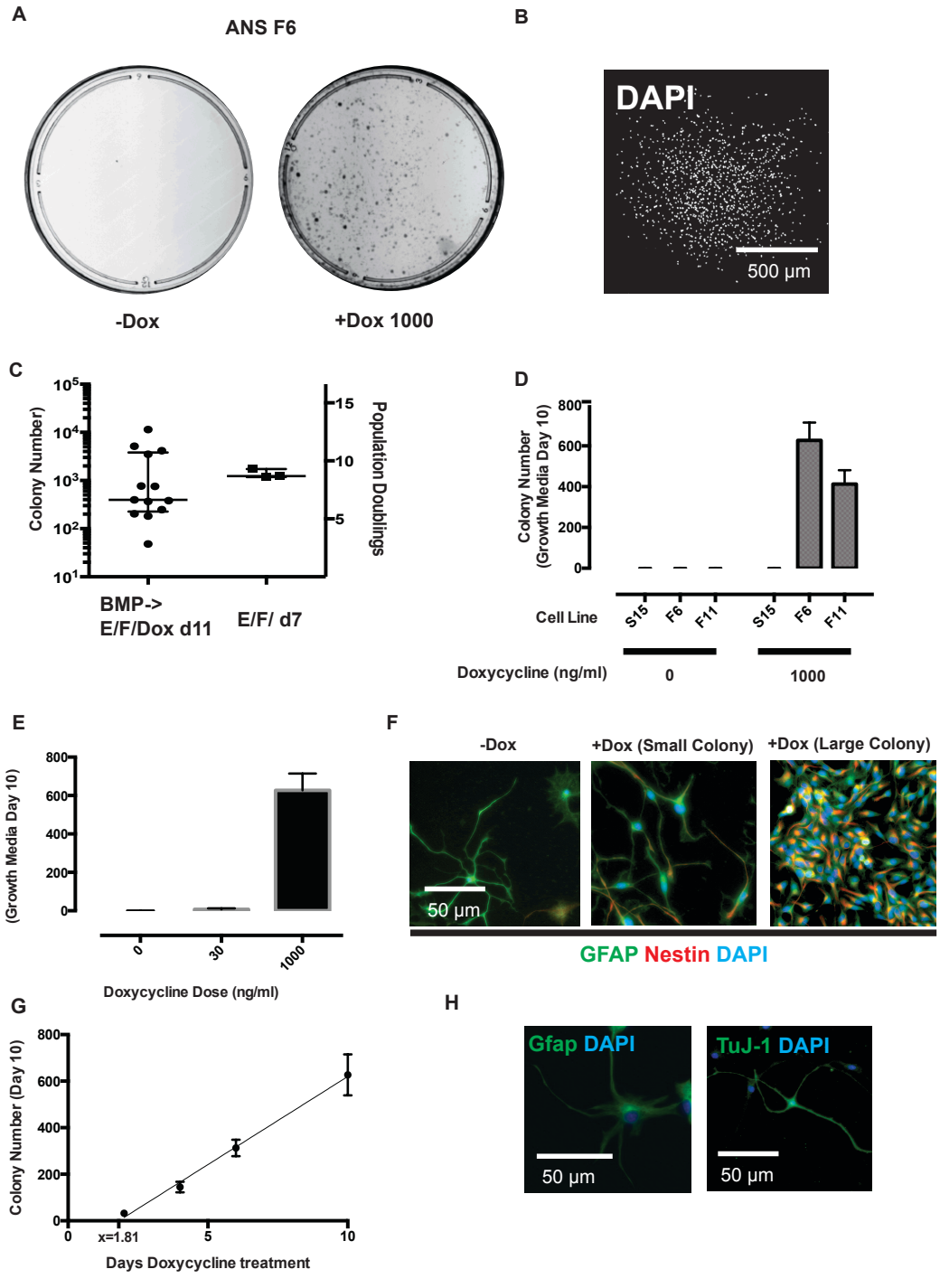
As for FS3 cells, S15, F6 and F11 cells were each plated in 6 dishes at 50,000 cells per dish in 10cm dishes, in media supplemented with 10ng/ml BMP4. After 24 hours, the media was changed for growth media supplemented with EGF/FGF, triplicate wells with and without doxycycline supplementation. Colony counts were conducted at 10 days. S15 cells overexpressing the SOX2 transgene alone demonstrated no colony formation. However, the FOXG1-overexpressing clones each demonstrated efficient colony formation (Figure 4-9D). Without Dox no colonies were observed. With doxycycline 1000ng/ml colony counts for F6 cells were 543, 620 and 718 (mean 627) . For F11 cells the counts were 418, 472 and 342 (mean 413). Therefore F6 cells in this assay were calculated to have a colony formation efficiency of 1.25+/-0.1%. For comparison, FS3 cells gave a mean of only 88 colonies.

F6 NS cells were plated at a density of 1000 cells per 10 cm dish and colony counts performed on day 7. The median number of cells per colony was 1234, which is compatible with a single cell doubling every 17.3 hours. After BMP treatment, the number of cells per colony was counted for 14 representative colonies formed at very low plating density (1 cell /mm2) to ensure strict clonal origin, and fixed on dedifferentiation day 11 (Figure 4-9C). These colonies contained a median of 396 cells (range 48-11429). This is compatible with a stochastic process of return to cell cycle from day 1 to day 7, followed by divisions with the same ~18 hour cycle time observed for NS cells. A stochastic process of FOXG1-driven re-

entry into cell cycle followed by consistent NS-like rapid division data is also compatible with data presented for colony formation in response to pulsed doxycycline treatment for 48, 96 or 144 hours (Figure 4-9G). The observed data is compatible with a model in which sustained FOXG1 expression for a minimum 24-48 hours (x-intercept 43 hours) drives stochastic re-entry into cycle and acquisition of clonogenic capacity with an efficiency ~0.15% per 24 hours transgene expression. Review of timelapse video of the colony formation process supports this model: colonies are seen to arise with varying latencies, but in every case to grow rapidly once established. The colony size data in isolation could also be explained by a mixture of colony types, some comprising slow cycling populations. However this is not in keeping with the uniform cell morphology and colony expansion observed on timelapse video.

F6 cells also demonstrated the ability to form colonies with lower efficiency after BMP treatment, at doxycycline doses as low as 30ng/ml. Transgene expression in these conditions is ~50% of maximal levels, and the threshold level of expression seems to correspond closely to that required for colony formation in the FS3 line, suggesting that FOXG1 transgene expression alone is key to this phenotype.

To test whether the dedifferentiated cells retained an ability to differentiate into neurons and astrocytes we exposed them to differentiation conditions (FGF but no EGF for 4 day, then –GFs for 4 days; or BMP4, respectively). In parallel the same cells were treated with BMP4. Neurons and astrocytes formed in these respective conditions, fixed and stained for Tuj-1 and GFAP respectively are shown (Figure 4-9H).



(Figure legend overleaf.)

Figure 4-9 - Dedifferentiation in response to FOXG1 induction alone

A F6 cells are plated in BMP media at 10cells/mm2 then changed to growth media with or without doxycycyline. **B** An example colony visualised by DAPI staining. **C** Distribution of cell number per colony in dedifferentiating astrocytes (E/F/Dox Day 11) and parental NS cell colonies (Day 7). **D** Two clonal ANS4 derivatives demonstrate colony formation with no background in response to FOXG1 transgene induction. No colony formation is observed in response to SOX2 induction. **E** A dose response effect is evident with mean 7 colonies per well on exposure to Dox 30ng/ml, mean 627 per well with Dox 1000ng/ml. **F** Dox 0ng/ml controls remain GFAP-high nestin-low after 10 days in EGF/FGF. In Dox 1000ng/ml plates, cells re-enter cycle and then upregulate nestin to produce Nestin-high GFAP-low colonies. **G** A linear relationship is observed between duration of doxycycline treatment and colony number at day 10, compatible with a stochastic process of cell cycle re-entry over at least the first 7 days of E/F/Dox treatment. **H** Dedifferentiated F6 cells differentiate into astrocytes and neurons in appropriate culture conditions.

4.5.3 Conclusions

In this chapter I have presented a new colony formation assay which offers reproducible and quantitative assessment of astrocyte dedifferentiation. In these low density conditions paracrine FGF signalling and cell-cell Notch and Ephrin signalling are not activated, with the apparent result that BMP is able to drive differentiation to a postmitotic astrocyte state unresponsive to growth factors.

Using this assay and my newly generated inducible FOXG1 and SOX2 transgenic NS cell lines we conclude that high levels of FOXG1 are sufficient to enable growth factor responsiveness and drive a process of dedifferentiation comprising cell cycle re-entry and upregulation of NS markers. Combined induced overexpression of FOXG1 and SOX2 also supports maintenance of NS cell proliferation in media supplemented with a range of combinations of BMP4, EGF and FGF which elicit uniform cell cycle exit in the same cells in the absence of transgene induction.

Based on these findings, we suggest that FOXG1 is an important factor in restricting the ability of GBM stem cells to undergo differentiation commitment. This may explain the consistently high levels observed in GNS cells, which are required to limit GBM stem cell terminal differentiation.

5 Results 3 – Targets of FOXG1 and SOX2 in mouse.

5.1 Introduction

In the previous chapter I uncovered a clear function for FOXG1 overexpression in driving astrocytes to dedifferentiate into proliferating neural stem cells. An obvious next step was to determine how FOXG1 might be doing this; what are the critical FOXG1 transcriptional targets? The FS3 and F6 inducible cell lines provide a tractable cellular model to explore this. Thus, I next used chromatin immmunoprecipitation (ChIP)-Seq to define genome-wide binding sites for the epitope-tagged FOXG1-V5 in mouse NS cells. In order to establish potential shared targets of FoxG1 and Sox2, I intersected my newly generated FOXG1-V5 datasets with published Sox2 binding data (149). Furthermore, to define which of the target genes is regulated by FOXG1, we used RNA-Seq to define transcriptional changes following induction of FOXG1 and SOX2 during astrocyte dedifferentiation. Chromatin accessibility mapping using ATAC-Seq was also performed to determine whether FOXG1 target genes might be persistently 'open' in GNS compared to NS cells.

My data reveal that FOXG1 binds directly at many core cell cycle regulators, lineage-associated transcription factors and chromatin regulators (DNA and histone methylation). We focus on a clear functional role for FOXG1-mediated repression of *FoxO3* as well as induction of *MycN* (using Crispr/Cas genetic ablation and pharmacological strategies, respectively). Several other notable targets emerged, including *FoxO6, Plk1, Hes1* and the DNA and histone demethylation apparatus (*Dnmt1, Chd3 and Tet3*). Altogether these data are consistent with an important role for FOXG1 in key aspects of the GBM program including cell cycle re-entry, rapid proliferation and epigenetic resetting to the neural stem cell state.

5.2 Defining FoxG1 transcriptional targets in mouse NS cells

5.2.1 Exploring the feasibility of FoxG1 Native ChIP in mouse NS cells

FoxG1 ChIP was undertaken initially using our newly generated monoclonal antibodies against FoxG1 (clones 17B12 and 13A6; see Results 1). After conjugation of these antibodies to magnetic beads, pulldown of chromatin samples derived from ANS (mouse NS) and IENS (mouse glioma NS) cell lines was performed as described in the Methods. Previously reported FoxG1 binding sites were assessed by ChIP-PCR of forkhead motif containing sequences in promoter regions of putative target (wnt8b(121), Sox2, p21 (48)) and control (MyoD, Actin) loci. Unfortunately, no convincing enrichment at these loci was demonstrated over repeat FoxG1 ChIP experiments.

We considered the most likely reason for this failure is that the monoclonals are not suitable for ChIP. Both 17B12 and 13A6 hybridoma antibodies target the forkhead binding domain of the FoxG1 protein, which may be inaccessible or altered in conformation when DNA-bound. It may also be that refinement of the hybridoma supernatant is required for effective antibody-bead conjugation.

5.2.2 Defining binding sites of FOXG1-V5 in mouse NS cells using ChIP-Seq

Forced overexpression of a TF is often not desirable for defining the specific functions due to the risk of artefacts arising from the non-physiological levels. However, our primary goal was to understand whether the aberrantly high levels of FOXG1 expression in human GBM are functionally important; therefore, defining the bound targets of FOXG1 in the context of artificially high levels of the human protein could be justified. We therefore considered that overexpression of the epitope tagged overexpressed FOXG1V5 construct – for which we had confirmed clear activity in our functional assay of dedifferentiation – could provide new insights into the mechanisms of driving dedifferentiation.

We performed ChIP using two independent adult NS cell lines (A4FGO and P53FF-FGO; described in Chapter 1). ChIP PCR confirmed enrichment over control at a series of

candidate binding targets, and so sequencing libraries were prepared and sequenced using the Illumina MiSeq benchtop instrument. 22.9 million of 25 million reads passed quality control filters and were exported from the Illumina Basespace environment into the Galaxy web-based NGS analysis software, where subsequent analysis tools were applied. I aligned the reads to the genome (Bowtie tool) and called peaks using the MACS algorithm. Convincing enrichment of the Forkhead motifs was observed (SeqPos Motif tool) and binding peaks included many stem cell relevant targets (Stanford Genomic Regions of Enrichment Annotation tool). Therefore we proceeded to deep sequencing (Illumina HiSeq instrument) and bioinformatics analysis. This was led by our collaborators Ewan Johnston and Paul Bertone (EBI/EMBL).

5.2.3 FOXG1 binds to multiple key NS cell regulators

10545 peak regions were called by MACS independently in both the biological replicate libraries, so represent high confidence targets for the FOXG1V5 expression construct in neural stem cells. These peaks enrich most strongly for the canonical forkhead box motif, but nuclear factor I, bHLH and HMG box motifs are also highly enriched (Figure 5-1A). These latter motifs are recognised by key lineage specific transcription factors involved in neural fate specification, including *Sox2, Nfia, Nfix, Olig2, Ascl1* and *Hes1*, raising the possibility of cooperative or competitive binding with FoxG1 at shared regulatory elements.

Annotation of peaks to individual genes and analysis of ontology was performed using GREAT (Bejerano lab, Stanford). The strongest enrichment was for ‘Genes involved in Transcription’ (binomial FDR Q-value 1.5e-23). Biological processes including ‘stem cell maintenance’ and ‘negative regulation of gliogenesis’, and the disease ontology category ‘Glioma’ (FDR Q-value 1.2e-10) were enriched, and examples of FOXG1-bound gene loci comprising these categories are presented (Figure 5-1).

5.2.4 FOXG1 and Sox2 bind together to regions enriched for the respective canonical motifs, at loci encoding cell cycle and epigenetic regulators.

Given we had observed functional collaboration in dedifferentiation with FOXG1 and SOX2 co-expressed, we next searched for common targets. By intersecting my consensus mouse NS ChIP-Seq dataset with published mouse NS Sox2 ChIP-Seq datasets (149), I was able to identify 3731 peaks exhibiting overlapping FoxG1 and Sox2 binding. These peaks enriched for HMG box and forkhead motifs. The GREAT tool was used to assign these peaks to individual genes, and the resulting GO enrichments included categories associated with cell cycle, DNA methylation and histone modification, and stem cell maintenance.

5.3 Expression profiling to establish regulated targets of FOXG1 and SOX2.

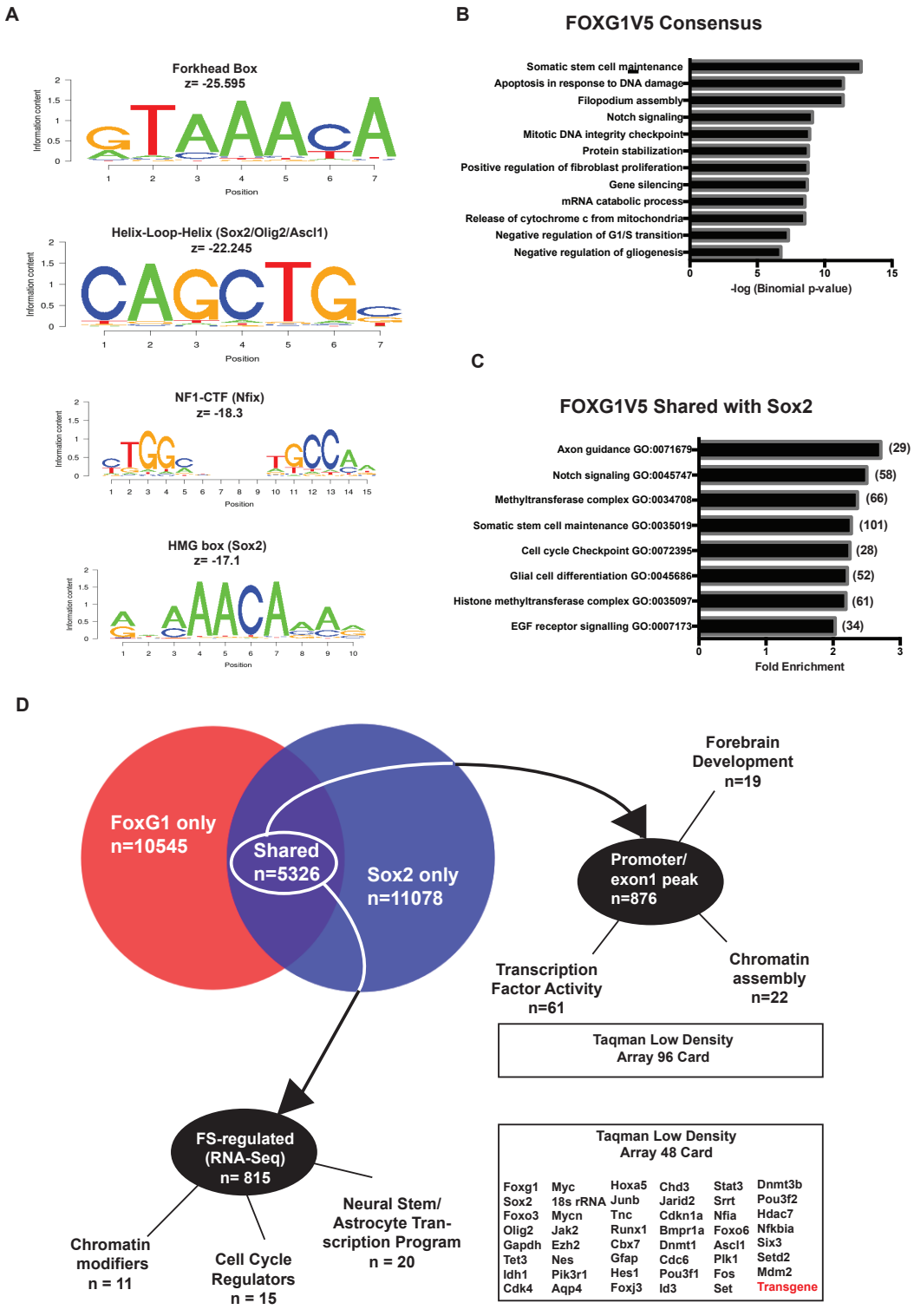
5.3.1 ChIP-Seq alone fails to reliably identify regulated targets

Of the shared FOXG1 and Sox2 bound sites identified using ChIP-Seq as described above, 876 were located in gene promoters (up to 2 kb upstream of the TSS), or in the first exon. Gene ontology analysis demonstrated enrichment for GO terms 'Transcription Factor Activity' (61 genes), 'Chromatin Assembly/Disassembly' (22 genes) and 'Forebrain Development' (19 genes) (Figure 5-1C). Given the many clearly relevant candidate genes identified we decided to quickly determine if many of these were altered when FOXG1 and SOX2 were induced (Figure 5-1D). We generated a custom 96-gene Taqman Low Density Array Card designed to allow assessment of expression levels in response to manipulation of FOXG1 and SOX2 levels, and during differentiation and reprogramming. We assessed the relative expression of these targets in control and Dox-treated cells, in biological triplicate 24 hours after restoration of growth media (Figure 5-2). However, no convincing early regulated targets were identified on the basis of these data, or subsequent parallel datasets produced using the F6 cell line (not shown). Therefore, FOXG1 binds to many more sites

than are actually regulated; this has been a clear theme emerging from ChIP-Seq and ChIP-on-chip studies over the years.

Figure 5-1 - FOXG1V5 ChIP-Seq in mouse and intersection with Sox2 ChIP-Seq

A ChIP-Seq for epitope tagged FOXG1 in mouse ANS4 and P53FF NS cell lines demonstrates consistent profiles with 10545 shared peaks enriching highly for forkhead and related NS-relevant motifs. **B** The most enriched ontology categories for genes assigned to FOXG1 binding peaks include 'stem cell maintenance/Notch signalling' and 'negative regulation of gliogenesis'. **C** The FOXG1V5 targets identified here overlap extensively with published SOX2 targets in neural stem cells, with ontology enrichments including stem cell maintenance and neural/glial development. **D** Of 5326 shared FOXG1-SOX2 binding peaks, 876 were located in the promoter or first exon of a candidate gene target. Of these, 93 gene targets assigned to the ontology categories shown, along with 3 housekeeping genes, were selected for inclusion in a TLDA 96 card. A TLDA 48 array was later designed with the benefit of preliminary RNA-Seq expression analysis.



(Figure legend overleaf.)

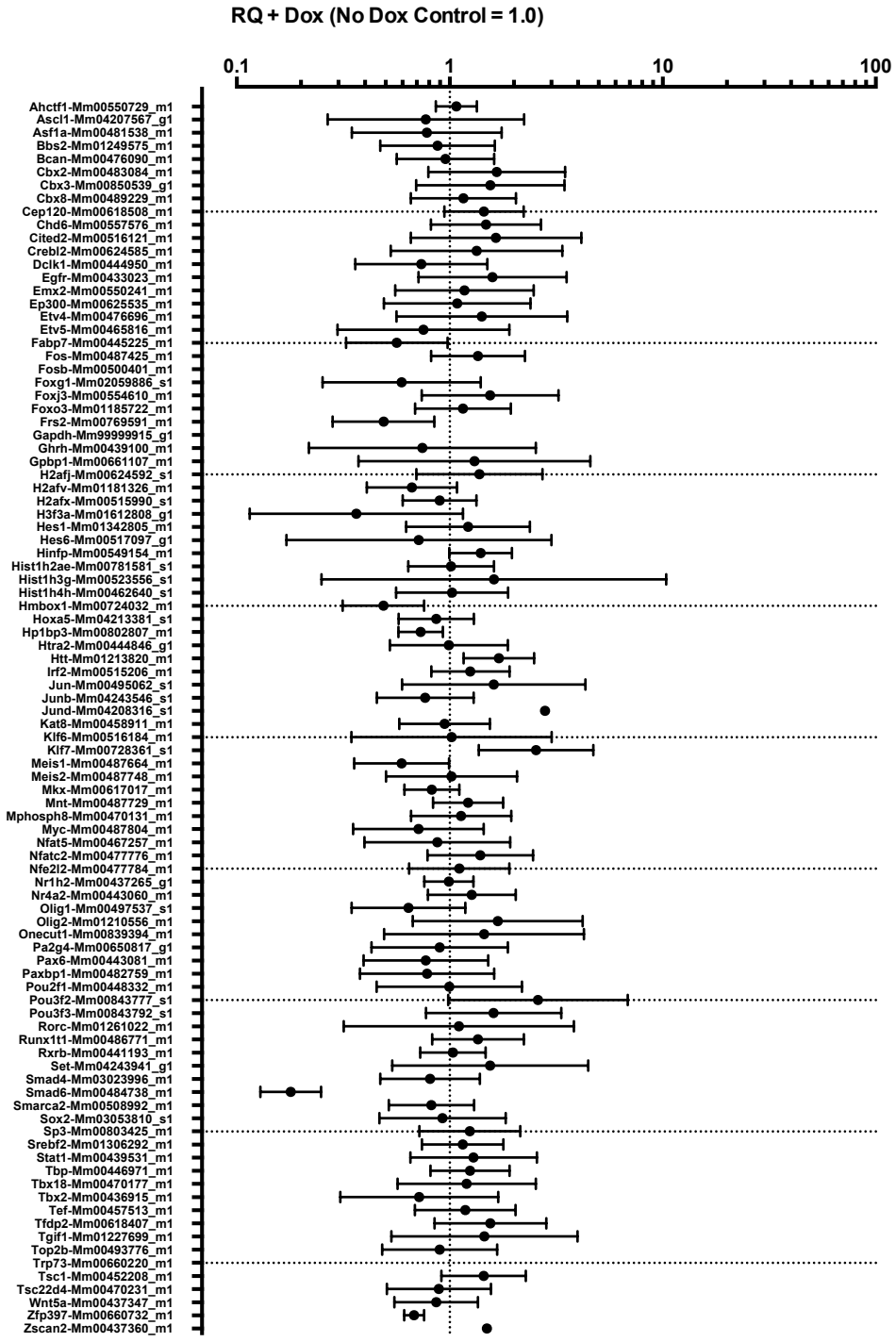


Figure 5-2 – Dedifferentiation Day 1 TLDA Card data for FS3 lines (TLDA 96 card)

Relative expression of candidate targets included on the TLDA96 array card. BMP treatment for 24 hours was followed by 24 hours in growth media with doxycycline, compared to controls plated and harvested in parallel without doxycycline treatment.

5.3.2 RNA-Seq identifies transcriptional correlates of dedifferentiation

RNA-Seq libraries were prepared from FS3 NS cells, in self-renewal conditions, and at time-points following BMP treatment and return to growth conditions, with or without doxycycline supplementation. The heatmap displays the 100 most variable genes across the RNA-Seq datasets derived. The group which are upregulated early during dedifferentiation, are predominantly (90-95% of genes) regulators and effectors of cell cycle, together with chromatin modifiers and neural stem cell markers including *Nestin*. The genes downregulated later during dedifferentiation, include astrocyte markers *Gfap* and *Aqp4*, as well as cell adhesion molecules including *Ncan* and *Nfasc*. The timing of these expression trends leads us to postulate that cell cycle re-entry precedes loss of astrocyte identity in the dedifferentiation process.

These heatmaps once again illustrate considerable variation between biological replicates at early dedifferentiation timepoints. This variability in replicates likely represents capture of intermediate states and mixed populations in a dynamic process subject to stochastic variability. Replicates in the steady state conditions (NS self-renewal, day 4 without doxycycline and day 14 with doxycycline/ dedifferentiated) display close transcriptome identity.

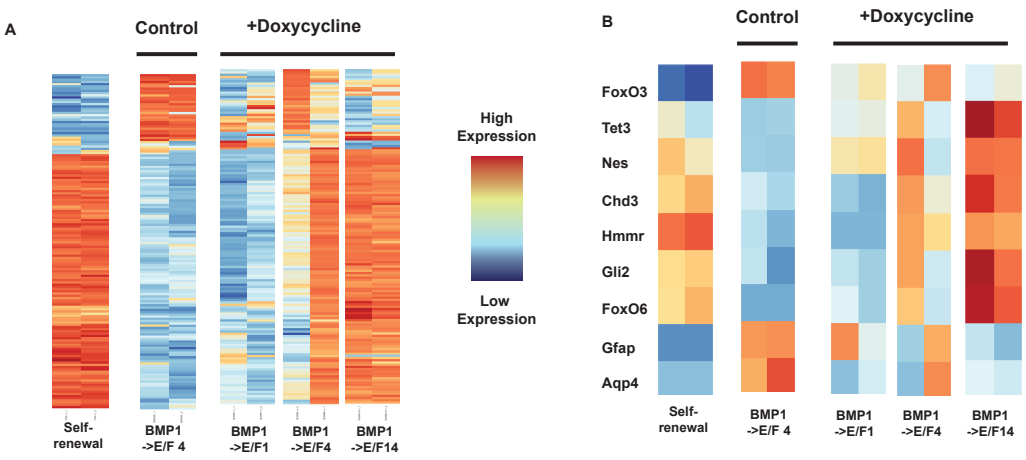


Figure 5-3 - RNA-Seq in FS3 cells on differentiation and dedifferentiation

RNA-Seq libraries were prepared from FS3 cells in self-renewal conditions, and the same cells plated in media with BMP4, then changed to media with EGF/FGF + doxycycline for 1,4 or 14 days, or media without doxycycline for 4 days (controls). **A** NS expression patterns are progressively restored in the dedifferentiating doxycycline-treated populations, a trend evident in a panel of the 100 most differentially expressed genes across these RNA-Seq libraries. The genes downregulated on BMP treatment have a predominantly cell cycle ontology. The genes upregulated are mostly astrocyte markers and cell adhesion molecules. **B** Key candidate targets bound by FOXG1 and SOX2 are upregulated (*FoxO3, Gfap, Aqp4*) or downregulated (*Tet3, Nes, Chd3, FoxO6* etc.) in control BMP treated cells compared to parental NS. NS expression patterns are progressively restored in the dedifferentiating doxycycline-treated populations.

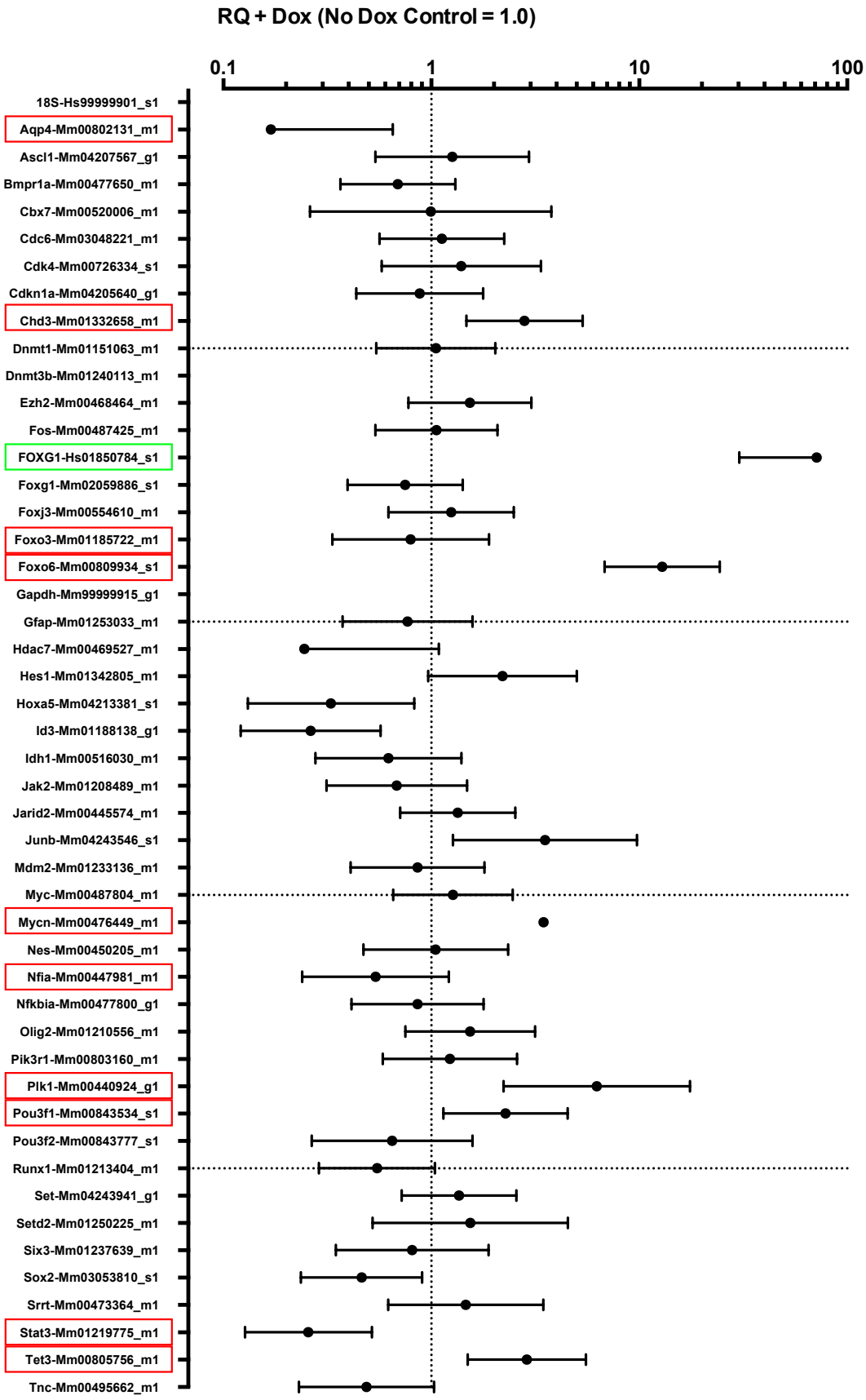
5.3.3 Direct targets identified using ChIP-Seq and RNA-Seq

A new set of candidate regulated target genes was defined by selecting genes with a ChIP-Seq peak assigned using GREAT in both SOX2 and FOXG1 datasets, which were also significantly differentially expressed in the RNA-seq datasets between the astrocyte and NS/dedifferentiated. 816 genes met these criteria, and these were highly enriched for chromatin modifiers, cell cycle regulators and neural stem cell gene ontology categories., Representative gene sets were selected from these categories for validation by TLDA analysis (Taqman Low Density Array 48 Card). Candidate early targets identified in this manner and included on the RNA-Seq heatmap include *FoxO3, FoxO6, Chd3* and *Tet3* (Figure 5-3B).

To simplify our search for FOXG1 target genes, we performed TLDAs on both FS3 and F6. Combined overexpression of FOXG1 and SOX2 in the FS3 results in regulation of some of the same set of targets, but this was less marked (data not shown), in keeping with the lower efficiency of the dedifferentiation process in this cell line. Data is presented for biological and technical duplicate TLDA qRT-PCR datasets investigating the expression of candidate targets in F6. Astrocyte markers *Aqp4* and *Nfia*, as well as *Stat3*, part of the BMP signalling cascade, appear highly downregulated. Meanwhile the proto-oncogene cell cycle regulators *Plk1* and *MycN* are upregulated, along with epigenetic modifiers *Chd3* and *Tet3*. Forkhead factor *FoxO6*, a brain specific forkhead factor, is also highly upregulated at this early timepoint (150). These data are consistent with the observed phenotype of FOXG1 overexpression and suggest that these genes represent important direct transcriptional targets that allow rapid and efficient cell cycle re-entry and epigenetic resetting.

Figure 5-4 – TLDA 48 Card data for the F6 line- day 1 dedifferentiation

Relative expression of the transgene (green box) and candidate targets included on the TLDA48 array card. BMP treatment for 24 hours was followed by 24 hours in growth media with doxycycline, compared to controls plated and harvested in parallel without doxycycline treatment. Regulated targets discussed in the text are highlighted in red.



(Figure legend overleaf).

5.4 MycN is an early direct target of FOXG1/SOX2

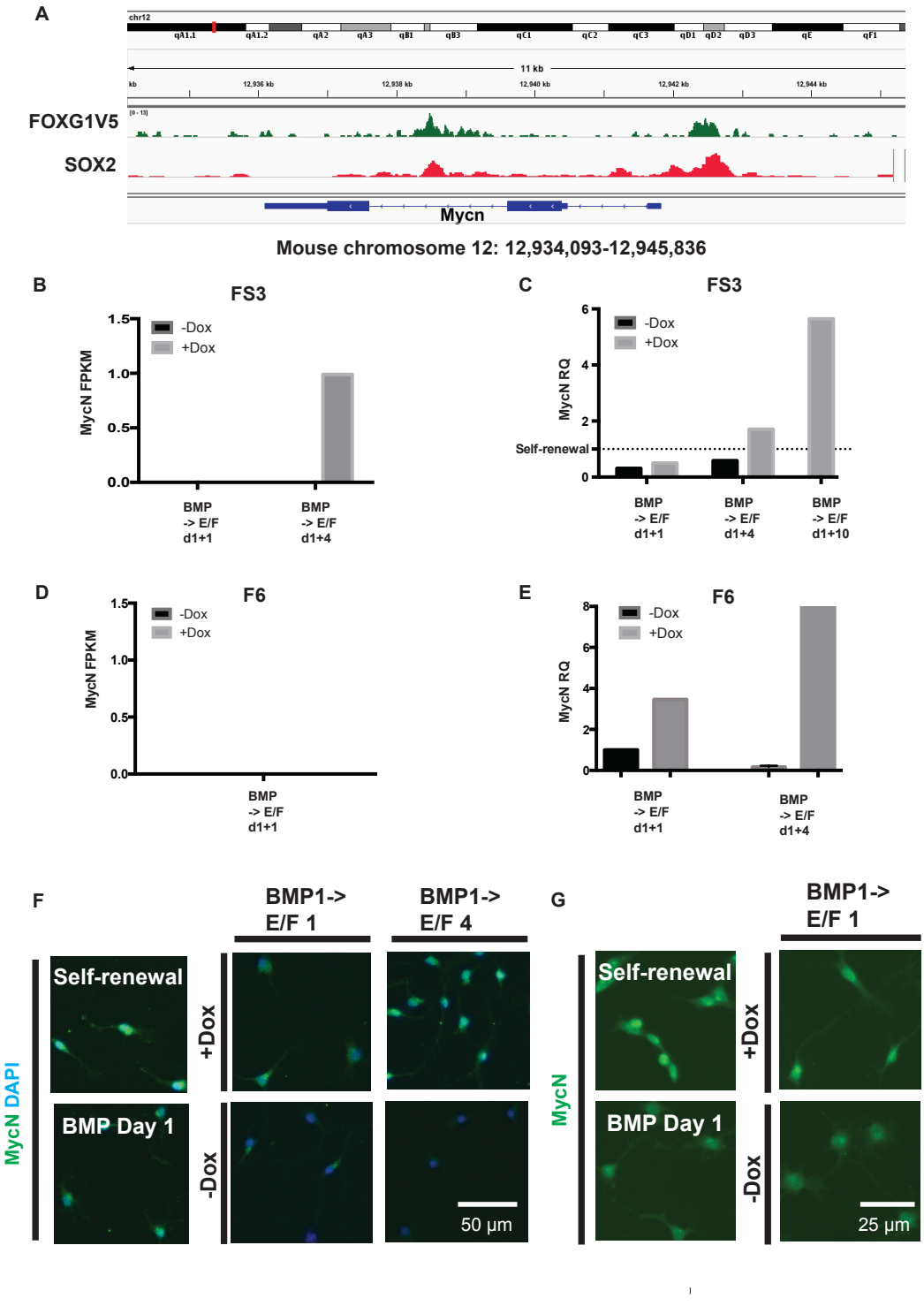
5.4.1 MycN protein is rapidly induced following induction of FOXG1/SOX2

MycN is a Myc class cell cycle regulator and proto-oncogene. It is overexpressed in malignant glioma and other brain tumours, and forced expression of a stabilised mutant drives medulloblastoma formation in the cerebellum, or diffuse glioma formation in the forebrain (151), and has been implicated in the pathogenesis of histone H3 mutant paediatric GBM. It is directly bound by FOXG1 and SOX2 in the proximal promoter and first intron (Figure 5-5A).

In FS3 cells, *MycN* is markedly downregulated following BMP treatment, and in EGF/FGF alone levels continue to fall so that mRNA was undetectable by RNA-Seq and qPCR after 4-10 days (Figure 5-5B,C). Self-renewal media supplemented with doxycycline to induce FOXG1/SOX2 resulted in *MycN* levels higher from day 1, and 5-6 fold upregulated over self-renewal by day 10. In F6 cells, TLDA card data again points to strong early upregulation of *MycN* in response to Dox treatment. Increased expression in Dox treated FS3 cells at all timepoints, and F6 cells on day 1, was confirmed by ICC (Figure 5-5F,G).

Figure 5-5 - MycN is a regulated direct target of FoxG1 both with and without Sox2

A The MycN locus is bound by FOXG1 and Sox2 in proximal promoter and intron regions. **B** RNA-Seq data from FS3 cells indicates upregulation of MycN in response to FOXG1_SOX2 transgene induction **C** Upregulation is confirmed by Taqman qRT-PCR at early and especially at later timepoints. F6 cells demonstrate FOXG1-driven upregulation **D** on RNA-Seq and **E** on Taqman qRT-PCR. Transgene induced upregulation of MycN following BMP treatment is confirmed at protein level by ICC in FS3 cells **F** and F6 cells **G**.



(Figure legend overleaf)

5.4.2 Pharmacological inhibition points to a key role for Myc in cell cycle re-entry

In order to investigate the functional importance of MycN, I tested two small molecule Myc inhibitors, 10074-G5 and 10058-F4 (152), to see if they could compromise dedifferentiation. These compounds are structurally unrelated, but both are believed to bind to the bHLHZip domain of Myc family proteins, interfering with Max heterodimerization. Importantly these inhibitors are not specific to MycN: in fact c-*MYC* is also a recently reported FOXG1 target (148).

I first established that the maximal tolerated doses at which these compounds have no discernible effect on proliferation of NS cells were 5uM and 10uM respectively (Figure 5-6A,B). I then tested these doses to establish that standard NS cell colony formation was unaffected: F6 cells were plated at clonal density in self-renewal conditions in the presence of these inhibitors, and colony counts were performed after 7 days. No difference in colony-formation was evident between control and inhibitor treated plates Figure 5-6C). These doses would therefore not interfere with NS cell self-renewal, enabling us to probe a role in the dedifferentiation process and use of the colony forming assay.

F6 and FS3 cells were plated in BMP media, and this was changed to media supplemented with EGF/FGF and doxycycline after 24 hours, with or without the Myc inhibitors. For each cell line a significant reduction in colony formation in the inhibitor treated plates by comparison with positive control (+Dox, no inhibitors) was observed. I conclude that there is a selective requirement for Myc activity for re-entry to cell cycle and colony formation by BMP-treated NS cells.

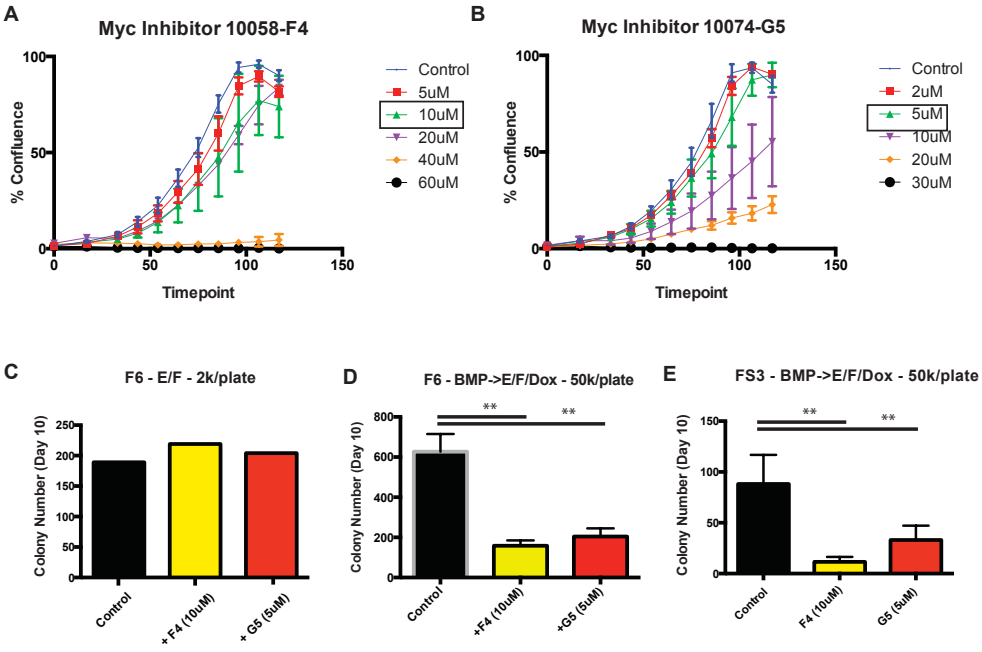


Figure 5-6 - Myc inhibition impairs dedifferentiation, but not NS cell proliferation

A Incucyte growth curves are provided for cell line FS3 in the presence of varying concentrations of the MycN inhibitor 10058-F4. No significant impairment in proliferation is evident at concentrations of 10uM and below. **B** Growth curves for FS3 cells in the presence of MycN inhibitor 10074-G5. No significant impairment in proliferation is evident at concentrations of 5uM and below. **C** F6 cells were plated at 2000 cells per 10 cm dish in EGF/FGF media, with or without inhibitors, and colonies were counted on day 7. No difference is evident between control and inhibitor treated plates. **D** Administration of MycN inhibitors at the indicated concentrations together with E/F/Dox at day 1 and at subsequent media changes produces a significant reduction in colony formation by BMP-treated F6 cells as shown **E** Significant reductions in colony formation in the presence of MycN inhibitors is also evident in BMP-treated FS3 cells.

5.5 *foxo3* and *foxo6* are transcriptional targets of FOXG1

5.5.1 *foxo3* is a direct target downregulated in response to FOXG1/SOX2

FOXO factors are believed to play a central role in maintaining the neural stem cell pool. In particular FOXO3 can negatively regulate both proliferation and neuronal commitment to prevent depletion of the endogenous adult neural stem cell pool through senescence or differentiation respectively (99,110). FOXO factors are also central to longevity and tumour suppression, through control of cell cycle and pro-apoptotic activity (98).

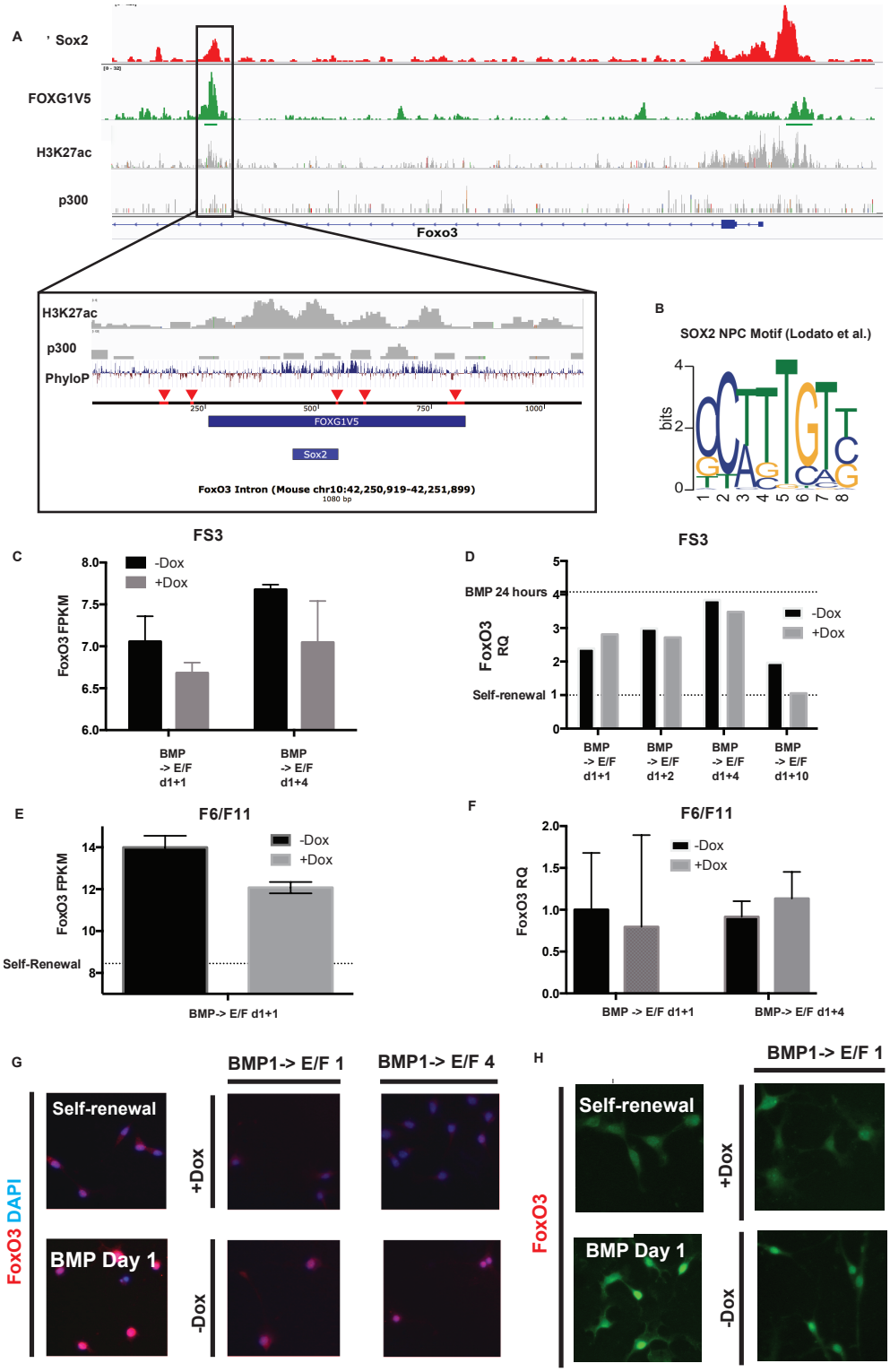
FOXO3 expression is sufficient to eliminate glioma cells in some contexts (105,106), and protein-protein interactions between FOXO3 and FOXG1 have been implicated in the dysregulation of cytostatic responses to TGF-beta signalling encountered in glioblastoma: FOXG1 is proposed to sequester FOXO3 away from its tumour suppressor target p21 (48). ChIP peaks shared between my FOXG1V5 ChIP-Seq dataset and the published Sox2 data included binding sites in the promoter and first intron of *foxo3*. This suggested the possibility of direct transcriptional regulation of *foxo3* by FOXG1 (Figure 5-7).

The FOXG1/SOX2 ChIP-Seq peak within *foxo3* is a cis-regulatory region (CRR) that is highly conserved across mammalian species (PhyloP conservation score) and contains several AAACA repeat regions (red triangles). This sequence comprises part of the canonical forkhead box motif (GTAAACA, see Figure 5-1A) as well as the antisense strand of a SOX2 NPC motif identified by the Boyer group (Figure 5-7 B) (149). The RNA-Seq data (biological replicates day 1 and day 4 after return to growth factors with and without Dox), and Taqman qPCR array sets (biological replicate conditions of self-renewal, BMP treatment, and reintroduction of growth factors following BMP treatment, with or without Dox, over 1 to 10 days) suggest transcriptional downregulation of *foxo3* in response to forced FOXG1 and SOX2 expression in FS3 cells. The protein is also altered accordingly when inspected by ICC (Figure 5-7 G,H). The degree of transcript regulation is not as

marked as for FoxO6, and is not clearly evident in the F6 cell line. Post-translational modification and consequent changes in subcellular localisation are known to be important components of FoxO3 activity in NS cell self-renewal (48), and this, alongside regulation at the transcript level, may also be important in dedifferentiation.

Figure 5-7 – *foxo3* is a regulated target of FoxG1 and Sox2

A The *foxo3* locus is bound by FoxG1 and Sox2, at the promoter and at a cis-regulatory region in the first intron. The latter demonstrates p300 and h3k27ac enrichment consistent with enhancer activity (proliferating mouse NS cell ChIP-Seq libraries from the Guillemot laboratory (83)). The cis regulatory region peak is highly conserved (PhyloP score), includes multiple stretches of AAACA repeats (red triangles). **B** AAACA comprises part of the canonical forkhead box motif and this sequence is complementary to the reported Sox2 motif in NS cells. **C** and **D** FoxO3 is upregulated in FS3 cells in response to BMP treatment on TLDA qPCR, and doxycycline-induced transgene expression downregulates expression on qPCR and RNA-Seq. **E** and **F** Although transcript levels are not significantly altered by transgene induction at the earlier timepoints in BMP-treated F6 and F11 cells, protein expression changes are evident in FS3 cells (**G)** and F6 cells (**H**).



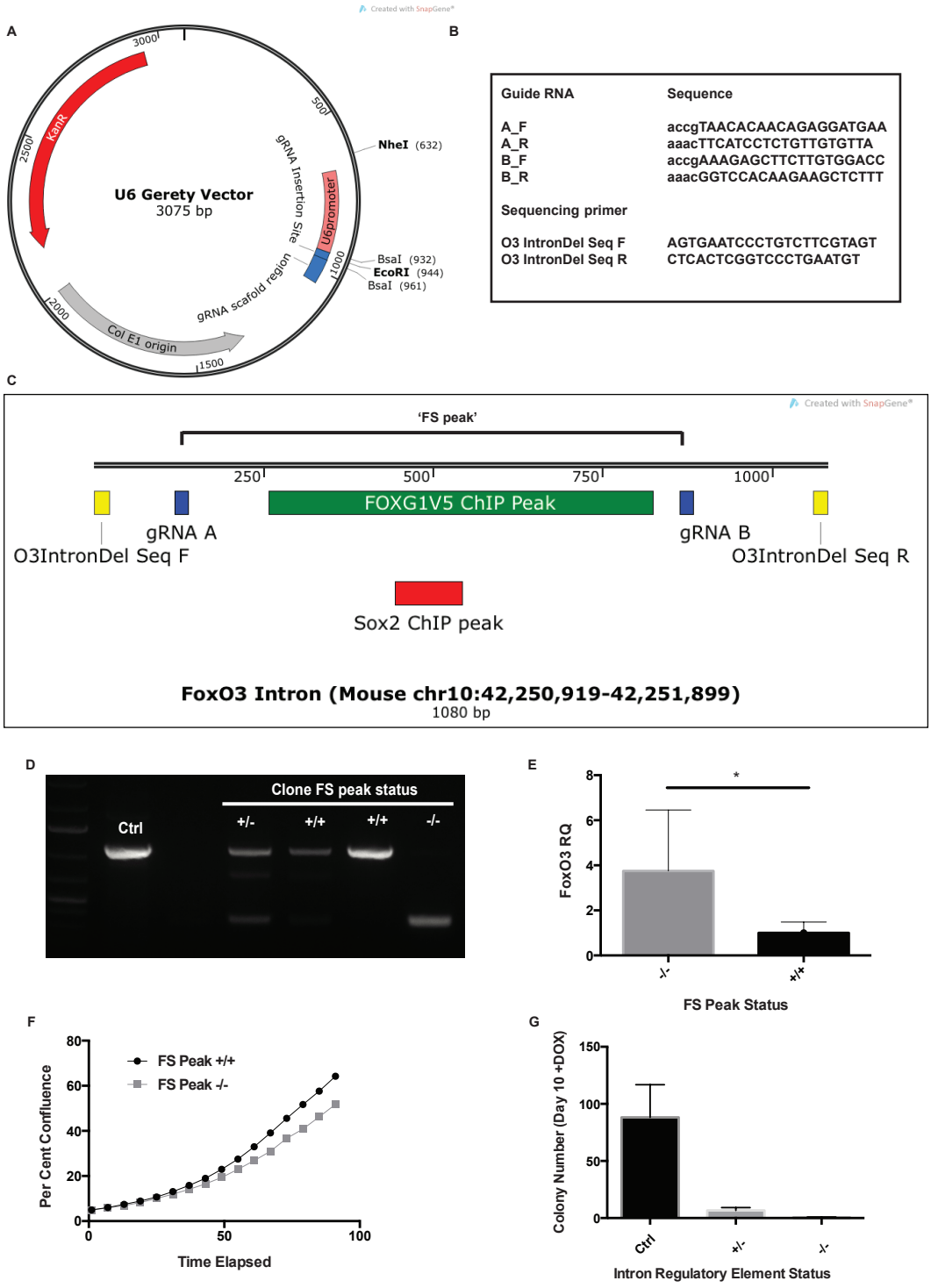
(Figure legend overleaf).

5.5.2 Genetic ablation of the FOXG1/SOX2 bound *foxo3* cis-regulatory element was achieved using Crispr/Cas.

We explored the function of the candidate binding peak using CRISPR/Cas to ablate it. I selected CRISPR gRNAs flanking this region using ChopChop software. Oligos A_F and B_F were annealed with A_R and B_R (Figure 5-8) the products were phosphorylated and ligated into the Bsa1-digested U6 Gerety backbone (Figure 5-8A). The gRNAs were transfected into FS3 cells along with the Cas9 expression plasmid, and a GFP plasmid; the positive population was flow sorted after 48 hours and plated at clonal density. Colonies were picked and genotyped after 2 weeks. From the initial batch of 12 clones screened, PCR across the FS-bound intron peak revealed homozygous deletion in one clone (FS3 FOXO3 Intron Deleted Clone 11; FID11) and heterozygous deletion in a further four clones. Genotyping for clones FID6 (+/-) and FID11 (-/-) is shown (Figure 5-8D). The region concerned was not sequenced, so it is possible that the non-deleted allele in the FID 6 clone has damage as a result of the Cas9 activity.

5.5.3 Deletion of the FOXG1/SOX2 cis-regulatory region derepresses FOXO3, and abolishes NS cell colony forming ability.

FID11 cells expressed higher FOXO3 levels than parental controls, compatible with derepression of FOXO3 on deletion of the FS peak (Figure 5-8). These cells demonstrated a minimal proliferative deficit in normal self-renewal conditions compared to wild type parental controls. However, when plated alongside FS3 parental controls, FID11 cells were unable to form colonies in the presence of doxycycline after BMP treatment as previously described. Colony formation by clone FID6 was also significantly impaired (Figure 5-8G). Thus, FOXO3 repression is required to enable dedifferentiation.



(Figure legend overleaf)

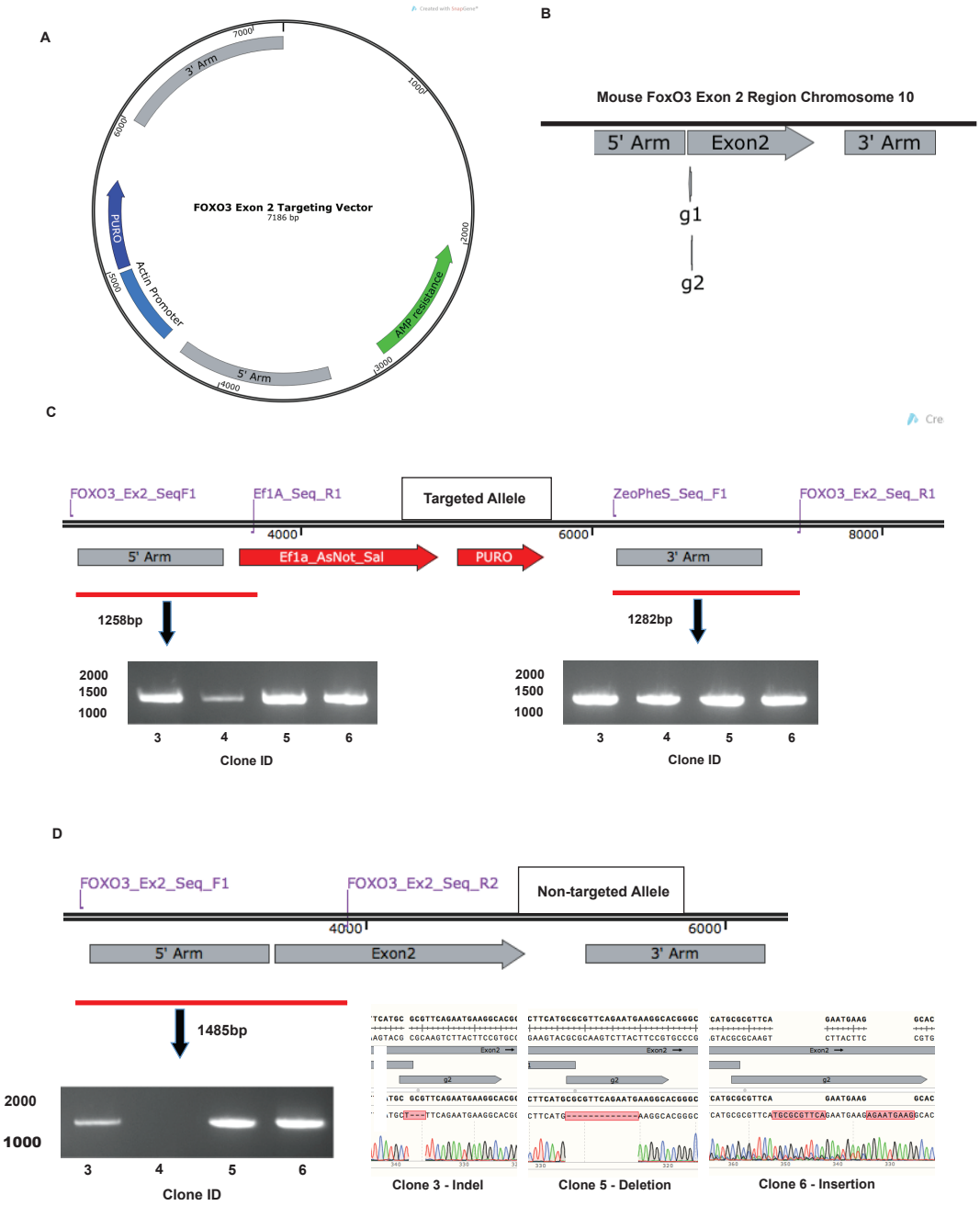
Figure 5-8 - Crispr deletion of the FoxO3 intron cis-regulatory region

A The U6 Gerety vector expresses a tracrRNA/crRNA hybrid guide RNA from a strong mammalian promoter. The backbone includes a tracrRNA scaffold region and a restriction site for insertion of target-specific crRNA sequence to form the final guide RNA. Bsa1 digest of this backbone leaves 4-base overhangs complementary to the overhangs presented by the annealed insert oligos, here shown in lower case **B** Crispr deletion of the FS peak **C** using the resulting guide RNAs cotransfected with the Cas9-GFP nuclease results in FS peak +/- (FID6) and -/- (FID11) clones **D**. FID11 cells demonstrate elevated FoxO3 expression **E** and a slight proliferative deficit **F**. Unlike parental FS3 controls, these cells are unable to form colonies on exposure to EGF/FGF with doxycycline after BMP treatment **G**.

5.5.4 *foxo3* genetic deletion using CRISPR/Cas assisted gene targeting

foxo3 gene targeting was achieved in the FS3 cell line by cotransfection with a pair of guide RNAs, an EF1a-Puro targeting vector (1kb homology arms, to enable homologous recombination) and the Cas9 nickase (Figure 5-9; see Methods). Around 100 colonies were generated in the presence of puromycin selection. Correct gene targeting on one allele was confirmed in these clones by PCR using one primer upstream/downstream of the homology arm and another within the EF1a-Puro cassette (FOXO3_Ex2_Seq_F1 and Ef1a_Seq_R1 for the 5' arm; ZeoPheS_Seq_F1 and FOXO3_Ex2_Seq_R1 for the 3' arm). PCR for 4 correctly targeted clones is shown.

For the correctly targeted clones, the sequence of the non-targeted allele was assayed by PCR using a primer upstream of the homology arm, and another within the *foxo3* exon. Clone 4 likely had a large deletion that removed PCR genotyping primer sites. For the other clones, the PCR product was gel extracted and sent for Sanger sequencing. As anticipated these clones exhibit a mixture of frame-shift mutations on the non-targeted allele attributable to non-homologous end joining. These include an indel (clone 3), a deletion (clone 5), and an insertion (clone 6).



(Figure legend overleaf)

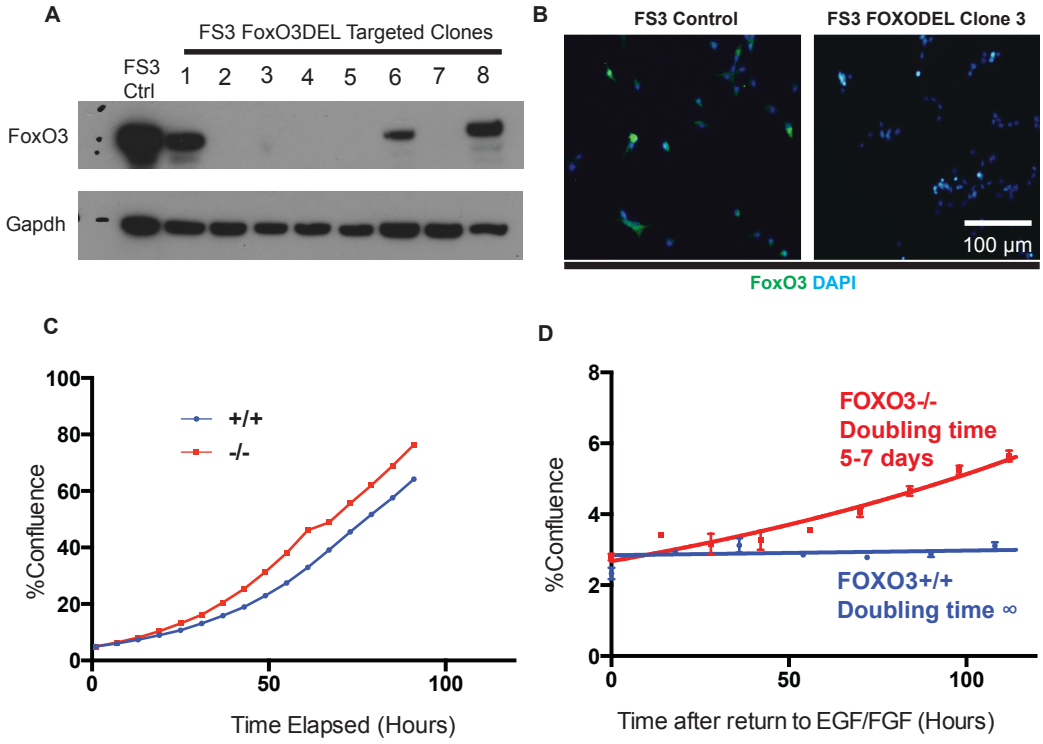
Figure 5-9 - Crispr targeting of *foxo3* exon 1

A The FoxO3 targeting vector comprises an EF1a-PURO antibiotic resistance cassette flanked by homology arms, constructed by Gibson assembly as described in the Methods. **B** The homology arms of the targeting vector correspond to 1kb regions flanking the *foxo3* second exon. The gRNAs direct the Cas9 nickase to the 5' portion of this exon. **C** Following Crispr targeting genomic DNA is extracted from puromycin-resistant clones and PCR performed across the TV/flanking sequence to confirm correct integration of the construct. Clones 3,4,5 and 6 have incorporated the resistance cassette in place of the *foxo3* exon 2 locus in at least one allele. **D** Given the established targeting of one allele, a third PCR amplicon incorporating exon 2 can only be amplified from the remaining non-targeted allele. Clone 4 likely contains an extensive deletion on the non-targeted allele. For clones 3, 5 and 6, the PCR product amplified from the second, non-targeted allele was sequenced. Clone 5 demonstrates a 13bp frameshift deletion at the site of guide RNA 2, resulting in termination and accounting for the absent protein expression. Clone 6 demonstrated insertions totalling 19bp, while clone 3 demonstrated an indel comprising 3bp deletion with 1bp insertion. In each case these mutations resulted in frameshift.

5.5.5 *foxo3* deleted populations re-enter cell cycle spontaneously after BMP treatment

Complete ablation of FoxO3 protein expression was confirmed across multiple clones (IDs 2,3,4,5,7) using Western blot (performed by Carla Blin) and ICC. I proceeded to characterise clone 3 (FOD3). These cells demonstrate a small proliferative advantage over parental controls in self-renewal conditions (Figure 5-10C). After exposure to BMP and return to growth factors, they re-enter cell cycle without Dox administration, in contrast to FS3 parental controls (Figure 5-10D). However, the observed initial doubling time is 5-7 days, rather than the ~24 hours associated with neural stem cells and FOXG1/SOX2 dedifferentiated astrocytes, so that no colony formation is evident after 10 days. Moreover these populations initially continue to express low Nestin and high GFAP levels (Figure 5-10E). For these reasons, it seems likely that these cells represent cycling astrocytes rather than neural stem cells.

Loss of FoxO3 therefore removes a barrier to cell cycle re-entry and astrocytes are now growth factor responsive, but this is not sufficient to trigger immediate dedifferentiation, so additional targets must be involved. These data also indicate that we can effectively uncouple cell cycle re-entry from the dedifferentiation process, and these are controlled separately by FOXG1/SOX2 (Figure 5-10F).



(Figure legend overleaf)

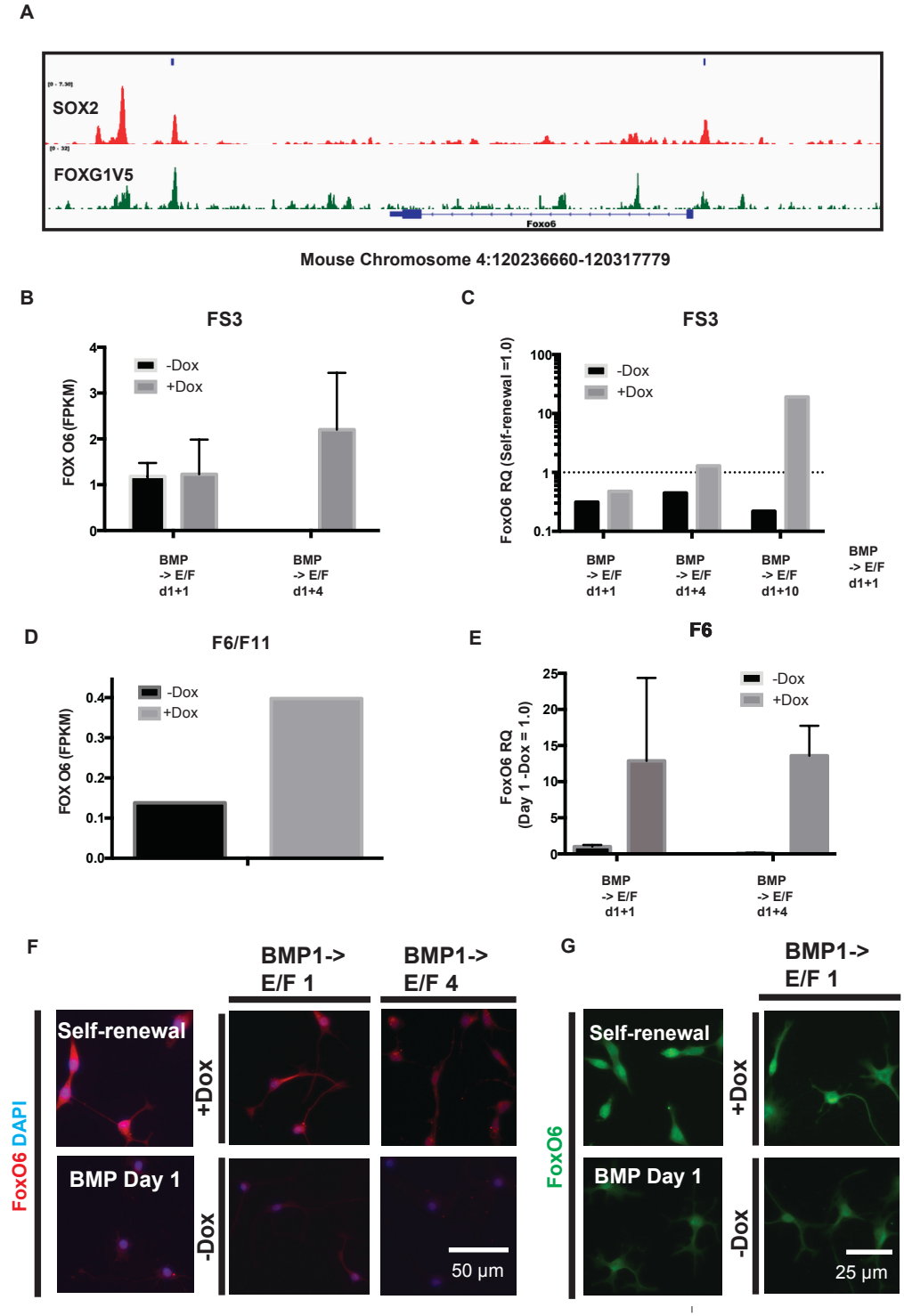
Figure 5-10 – *foxo3* genetic deletion prevents stable BMP-induced cell cycle exit

A Clonal lines derived from FS3 cells Crispr-targeted for FoxO3 demonstrate reduced or absent FoxO3 expression. The *foxo3* null clone FOD3 was chosen for further characterisation. **B** FOD3 cells demonstrate absence of FoxO3 expression on ICC **C** FOD3 cells demonstrate a minor proliferative advantage over wild type parental controls. **D** FOD3 cells plated at low density proliferate slowly after BMP treatment, with a calculated doubling time of 5-7 days, in contrast to BMP-treated FS3 parental controls which do not proliferate, and to untreated FS3 cells, which display a doubling time <24 hours **E** BMP-treated FOD3 cells proliferating slowly in EGF/FGF conditions after 7 days are GFAP-high and Nestin-low, suggesting that these cells have re-entered cycle while retaining astrocyte identity. **F** A working model of FOXO3 function in the dedifferentiation process, incorporating dissociated mechanisms for induction of cell cycle re-entry and reacquisition of NS cell epigenetic identity.

5.5.6 *foxo6* is a strongly upregulated in response to FOXG1

FOXO6 is specifically and highly expressed in the developing brain, but is also overexpressed in gastric cancers, where levels control proliferation through induction of Myc (Qinyu et al. 2013). The *foxo6* locus in mouse demonstrates clear ChIP binding by both FOXG1 and SOX2, with overlapping MACS peaks called for these factors in both the *foxo6* proximal promoter and downstream of the coding sequence (Figure 5-11A).

Expression of *foxo6* on return to growth factors after BMP treatment is strongly induced in FS3 and F6 cells in response to transgene induction by addition of Dox. In FS3 cells transcript levels are increased in doxycycline treated cells compared to controls by 50% on day 1, threefold on day 4 and nearly 100-fold by day 10 (Figure 5-11C). The induction in Dox-treated F6 cells is even more dramatic, ~20-fold on day 1 and >100-fold on day 4 (Figure 5-11E). This upregulation is also evident in F6 cells at protein level by ICC (Figure 5-11F,G). The high level induction in F6 cells indicates that FOXG1 overexpression alone is sufficient to drive this target's upregulation. FOXO6 is therefore is a candidate pro-tumorigenic downstream effector; it is expressed highly in proliferating NS cells, is rapidly extinguished in posmitotic astrocytes, and then is reactivated early in response to FOXG1 induced dedifferentiation.



(Figure Legend overleaf)

Figure 5-11 – FoxO6 is a regulated direct target of FoxG1 +/- Sox2

A The *foxo6* locus on mouse chromosome 4 comprises 2 exons. ChIP-Seq demonstrates overlapping binding by FOXG1 and Sox2 at the proximal promoter and distal regulatory elements. FS3 cells demonstrate upregulation of *foxo6* in response to doxcycycline following BMP treatment at early to intermediate timepoints **B** on RNA-Seq and **C** on Taqman qRT-PCR. Stronger upregulation at early timepoints in response to transgene induction is evident in F6 cells by **D** RNA-Seq and **E** qRT-PCR. Upregulation of FoxO6 at protein level in response to transgene induction is evident from day 1+1 onwards in dedifferentiating FS3 cells (**F)** and F6 cells (**G**).

5.6 Epigenetic remodelling factors are candidate FOXG1/SOX2 direct targets

Our previous data suggests cell cycle re-entry is not sufficient to trigger dedifferentiation, and that additional targets might be involved. Epigenetic regulators are promising candidates for this role. 11 genes annotated as 'Chromatin modifiers' were among the 48 candidate direct targets identified using ChIP-Seq and RNA-Seq for inclusion in Taqman Low Density Array cards (Figure 5-1). Among these a majority demonstrate a progressive upregulation in response to transgene induction after BMP treatment, in FS3 and F6 cells, including: *Dnmt1, Dnmt3a, Chd3, Tet3, Ezh2* (Figure 5-12A,B). Several of these genes were upregulated at day 10, rather than earlier timepoints, suggesting they are not early targets.

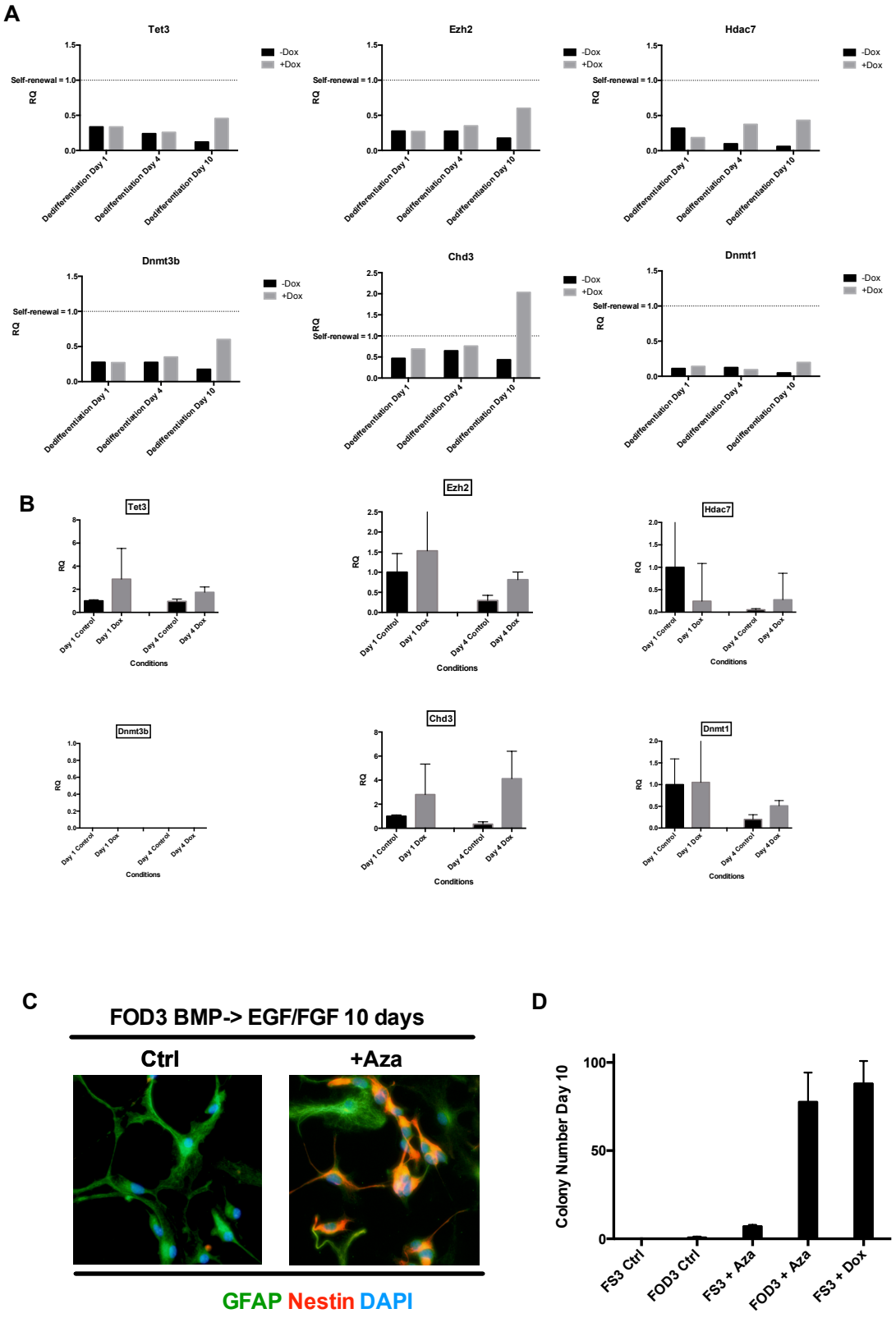
5.6.1 Induction of DNA methylation remodelling combines with *foxo3* deletion to drive dedifferentiation.

The genes activated included core components regulating both DNA and histone methylation. The small molecules 5-azacytidine (5-Aza) and ascorbic acid (Vit C) can alter the stability of DNA and histone methylation, and have previously been shown in direct reprogramming studies to aid epigenetic resetting (163). To test directly the role of epigenetic modifier targets in the dedifferentiation process, we assayed the effects of 5-Aza and Vit C in astrocyte dedifferentiation. FOD3 and FS3 cells were plated in BMP media for 24 hours, then returned to growth conditions with or without a 24-hour pulse of 5-azacytidine (5-Aza) at 3uM, an inhibitor of DNA methyltransferase activity. BMP-treated FS3 cells exposed to growth media with or without Dox comprised positive and negative controls for dedifferentiation respectively. FS3 cells treated with 5-Aza remained cycle arrested with little or no colony formation as for the negative controls (Figure 5-12D). Aza-treated FOD3 cells however demonstrated colony formation with an efficiency similar to the FS3 + Dox positive controls. Thus, in the context of *foxo3* deletion, 5-Aza is able to replace the requirement for Dox. Efficient colony formation was also observed on supplementation

with Vitamin C (L-ascorbic acid 2-phosphate, Sigma 100ug/ml; replaced q. 48 hours). Cells within the Aza-induced colonies were seen to be rapid cycling and nestin-high on ICC, compatible with dedifferentiation to an NS state (Figure 5-12C). These data suggest that suppression of *foxo3* combined with suppression of DNA methylation is sufficient to recapitulate the effects of FOXG1/SOX2 overexpression.

Figure 5-12 - Epigenetic modifier direct targets drive reacquisition of NS cell identity

A number of transcripts with established epigenetic regulatory activity are upregulated at early to intermediate time-points in response to transgene induction in **A** FS3 cells and **B** F6 cells. **C** and **D** FOD3 cells (FoxO3-/-) re-enter cycle spontaneously after BMP treatment, but fail to upregulate nestin or form NS-like colonies. Treatment with the DNA methyltransferase inhibitor 5-Azacytidine during dedifferentiation restores nestin-positive colony formation to a degree similar to that observed in dox-treated FS3 cells.



(Figure legend overleaf)

6 Results 4 – FOXG1 Targets in Human NS and GNS

6.1 Introduction

On the basis of the findings from the mouse NS cell lines overexpressing FOXG1, we hypothesised that high FOXG1 expression in human glioma drives acquisition and maintenance of GNS identity in human cells. With this in mind I examined patterns of FOXG1 binding in human NS and GNS cells using native ChIP-Seq, and then investigated using TLDAs the effect on candidate FOXG1-bound targets of overexpressing FOXG1 in U5 NS cells, which demonstrate very low baseline expression.

In order to better understand the role of FOXG1 in the maintenance of GNS cell self-renewal, I performed RNA-Seq and ATAC-Seq human NS and GNS cell lines, while also making use of expression datasets generated for these lines using Affymetrix arrays by previous investigators in the lab.

6.2 ChIP-Seq to define FOXG1 binding in human GNS cells

6.2.1 Chromatin preparation and immunoprecipitation

Procedures for harvesting, formaldehyde fixation, lysis, and IP were optimised using G7 chromatin. The commercial Abcam Ab18259 antibody provided the best pulldown as assessed by ChIP-PCR, and was selected over hybridoma antibodies 13A6 and 17B12 for ChIP. These were performed in NS cell lines U3 and U5, and GNS cell lines G14, G25, G26, G144, G166.

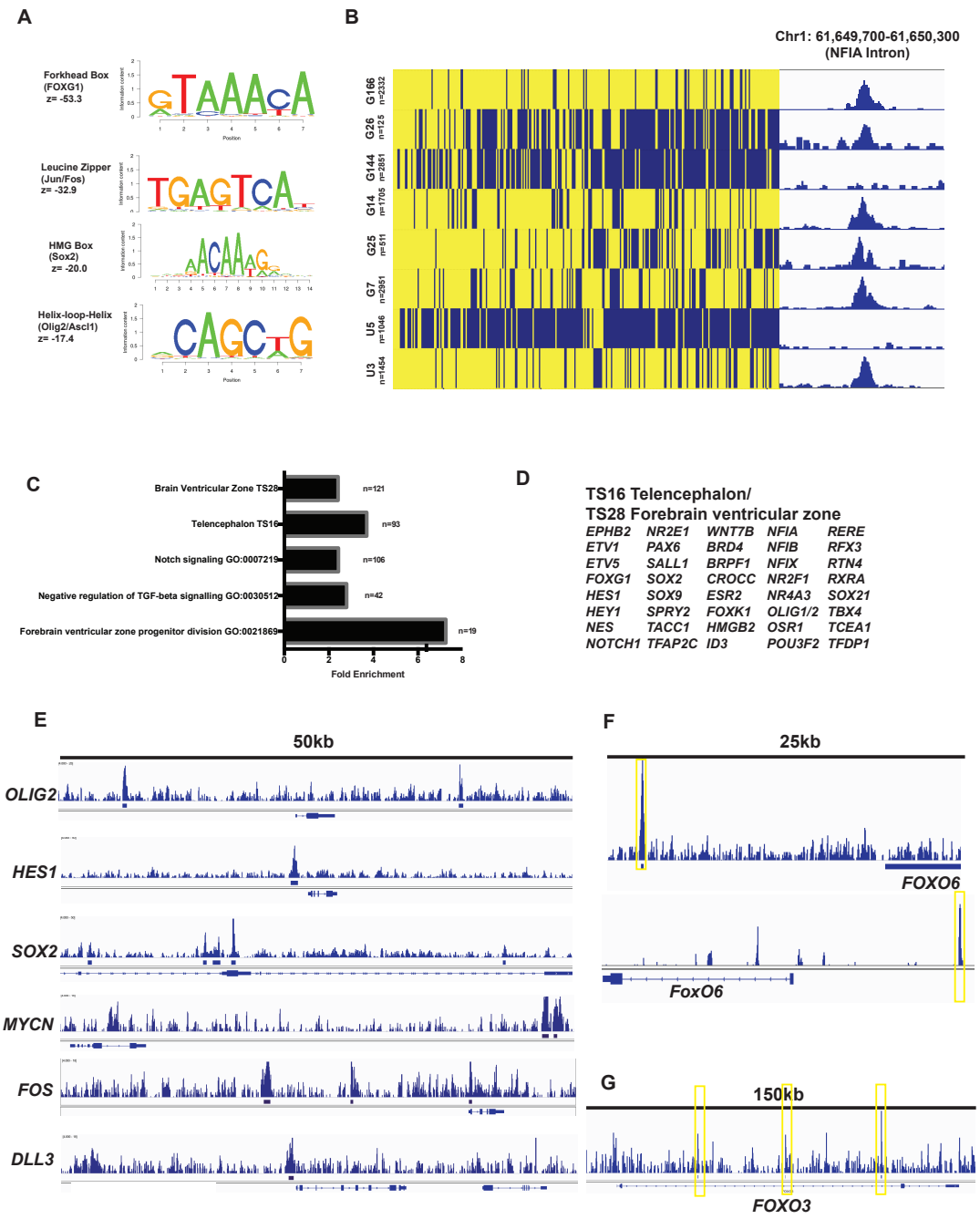
6.2.2 ChIP-Seq for native FOXG1 in human NS and GNS cells identifies binding at key NS regulatory targets

As expected for native antibody ChIP, weaker pulldown was achieved compared with the V5 pulldown reported in mouse. MACS peaksets were called for each ChIP library. Across the libraries a total 16520 peaks were derived at a MACS threshold of 50, and 3268 at a MACS threshold of 100. These regions enriched strongly for the forkhead box motif,

with 3201 instances in the 3268 strongly FOXG1-bound regions. Other motifs enriched, as in mouse, include the leucine zipper common to Jun-Fos oncogenes and T-box transcription factors, and HLH and HMG motifs common to key lineage-specific neural development factors including the examples shown (Figure 6-1A).

A heatmap shows the intersection of the most consistently called peaks across the libraries, and example traces from each library at a positive control binding peak in the *NFIA* intron (Chr1: 61,649,700-61,650,300), predicted by synteny from the mouse datasets (Figure 6-1B). On this basis ChIP libraries for U5 and G144 were considered to represent failed pulldowns, and I proceeded to further analysis the set of 2955 peaks represented in multiple ChIP libraries. Our goal was to identify FOXG1 targets that are generic across GNS cell lines (sacrificing line or subtype specific information, which would require increased biological replicates).

The 2955 peaks were annotated to 1658 distinct gene loci using the Stanford Genomic Regions of Enrichment Annotations tool, and these enriched for GO Biological Process terms including 'Notch signaling', 'Forebrain ventricular progenitor proliferation' and 'negative regulation of TGFβ signalling'. MGI_Expression terms 'Forebrain ventricular zone' and 'telencephalon' were also identified (Figure 6-1C). Assignment of these regions to gene targets using the Genomics Region of Enrichment Annotations tool followed by ontology assignment using DAVID revealed enrichment for transcription factor activity including: *SOX2, NKX2-2, POU3F2, ASCL1, HES1, NFIA, NFIX, OLIG1, OLIG2, PAX6, cMYC* and *MYCN*. This gene set additionally enriched for the KEGG pathway 'Glioma', including peaks assigned to: *CAMK2D, CALML6, CCND1, CDK6, IGF1, IGF1R, PIK3CA, PIK3CB, PDGFA, PDGFB, TGFA, KRAS* and *AKT3*. Noteworthy, in light of the results in mouse NS cells, *FOXO6* was strongly bound in these native ChIP-Seq datasets at a region orthologous to the mouse binding peak (Figure 6-1F).



(Figure legend overleaf)

Figure 6-1 - Human Native antibody FOXG1 ChIP-Seq

A The forkhead box motif is most strongly enriched, along with other neural developmental lineage-specific TF motifs. **B** The heatmap shows occurrence in individual libraries of peaks present in the majority of libraries (yellow). Most of these peaks are represented in libraries U3, G7, G14, G25, and G166, suggesting that these libraries display the best pulldown. **C** Binding loci are annotated to genes which enrich for relevant tissue-specific and functional motifs. **D** The set of genes bound annotated as representing telencephalon and forebrain ventricular zone includes key NS regulators. **E** Example ChIP-Seq tracks are presented for loci of interest, including orthologs of the mouse target *MYCN*. In each case a combined ChIP-Seq track for all libraries is shown across a 50kb region surrounding the locus. Peaks called by MACS in at least two libraries are indicated by marks under the track. **F** A strong proximal enhancer peak is present upstream of *FOXO6* exon 1 (upper panel yellow box), in a region corresponding to the same upstream enhancer binding established in the mouse FOXG1V5 datasets (lower panel yellow box). **G** Three MACS peaks are called within the large *FOXO3* intron, including one syntenic to the CRR which demonstrated a functional phenotype on deletion in mouse.

6.3 Expression of FOXG1 bound genes in GNS cells was assessed in NS cell lines overexpression of FOXG1

TLDA cards were designed to assess expression of 192 genes including candidate FOXG1 targets identified on preliminary analysis of ChIP-Seq data. These were generated prior to availability of more recently generated RNA-Seq datasets. To select these targets, I used the UCSC Liftover utility to successfully map 91% of the consensus mouse FOXG1V5 ChIP-Seq peaks (mm10) onto corresponding human genome coordinates (hg19). I then intersected these peaks with my preliminary human G7 ChIP-seq data resulting in a limited set of 477 high confidence mouse/human FOXG1 binding sites. These peaks were assigned to genes using the Nebula 'Genomic Annotation of ChIP-Seq peaks' tool (nebula.curie.fr) and the DAVID gene ontology tool was used to interrogate these candidate targets, resulting in enriched gene categories including: transcription regulation (GO-0030528; 87 genes), neuron differentiation (GO-0030182; 28 genes), apoptosis (GO-0007346; 22 genes), chromatin Modification (GO-0016568; 14 genes) and mitotic Cell Cycle (GO-0007346; 12 genes).

Assays for these gene targets were incorporated in a custom Taqman Low Density Array Card (list of assays provided in the Appendix). Biological replicate experiments generated expression data for control U5 human NS cells, and U5 TF derivatives expressing the Dox-inducible FOXG1V5 transgene, to low levels as a result of background leak (Dox 0) or to high levels (Dox 30).

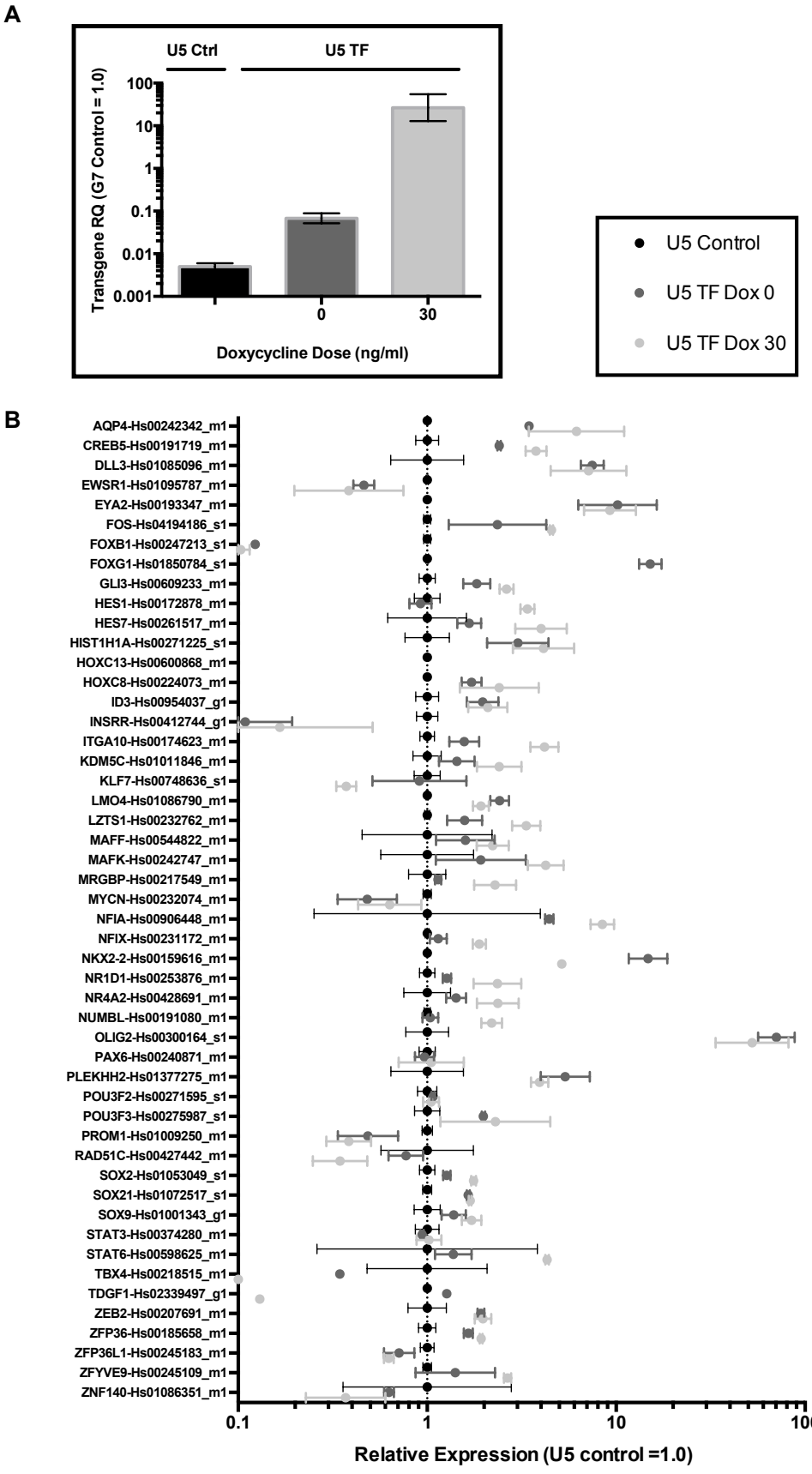
FOXG1 expression in these latter conditions reaches levels seen in G7 GNS cells, and is therefore a relevant model of the high levels observed in GBMs (Figure 6-3A). Expression values are plotted in these conditions for genes of interest in the context of the mouse data presented previously, and genes demonstrating significant regulation in response to FOXG1 overexpression. Of particular note, *OLIG2* is significantly upregulated in response to FOXG1 overexpression. *OLIG2* is one of four factors reported by the Bernstein laboratory as capable of driving glioma stem cell identity (51). *NFIA* is upregulated in

response to *FOXG1* forced expression, and this factor has been reported to drive GBM growth and invasion through repression of p21 and p53 among others (154) (58).

Other targets upregulated targets include NS cell master regulators *HES1* and *SOX2*, the proto-oncogene *FOS*, neural developmental TFs *EYA2* and *NR4A2*, Notch ligand *DLL3* and the Sonic hedgehog target *GLI3*. However, *MYCN* is not validated as a regulated target of FOXG1 overexpression, at least in these optimal growth conditions. Future work will be needed to explore the more recently identified candidates from the mouse studies.

Figure 6-2 – Transcription responses to FOXG1 overexpression - Human U5

A FOXG1 expression levels are plotted in U5 human NS cells and FOXG1-inducible derivatives, with reference to the levels expressed in G7 GNS cells. The inducible expression conditions presented here in U5 NS cells bracket the expression levels encountered in GNS line G7. **B** Transcript levels across biological replicate samples, for selected targets from a panel of 192 assessed by Taqman Low Density Array card assay are presented.



(Figure legend overleaf).

6.4 ATAC Seq reveals that differentially open chromatin regions in GNS cells versus NS cells are enriched for the forkhead box factor binding

ATAC-Seq is a recently described technique for genome-wide mapping of chromatin accessibility. A hyperactive derivative of the bacterial transposase Tn5 can be used to simultaneously fragment double strand DNA and insert sequencing adapters/ PCR primers. This process, Assay of Transposase Accessible Chromatin with Sequencing (ATAC-Seq), results in libraries enriched for fragments of transposase-accessible open chromatin, while heterochromatin wrapped around nucleosomes is protected (Figure 6-3A)(146). ATAC-Seq libraries were prepared in biological duplicate from GNS (G7, G25, G26, G144, G166, G179) and NS (U3, U4, U5, U7) cell lines. The tracks shown here represent GNS and NS pooled datasets. Example average transposase cut site density profiles around forkhead motifs in open chromatin are shown, demonstrating footprinting (steric protection of the motif region from transposase cutting by a bound TF, here FOXG1). The NS and GNS cell ATAC-Seq libraries demonstrate comparable profiles to a control human fibroblast dataset at a housekeeping control locus, *GAPDH* (Figure 6-3C). The *FOXG1* locus comprises inaccessible heterochromatin in fibroblasts as expected, but is accessible in NS cells and is more pronounced in GNS cells consistent with the higher expression levels encountered in the latter. This technique can also be used as an indirect method for monitoring local genomic amplifications, for example the previously reported amplification surrounding CDK4 in G144.

No well validated peak calling algorithms are available for the biases specific to the Tn5 transposase derived library. However, my collaborator Ewan Johnstone (EBI, Cambridge) used the flexible peak-calling software package F-seq to identify sequence tag enriched loci compared to the background using local density estimates for 600bp and 2000bp windows, and to compare across different libraries for the same sites. The peak sets obtained were subjected to a principal components analysis (Figure 6-3D). Of note NS cell line U3, an atypical cell line with a neuroepithelial rather than radial glial identity and high

FOXG1 expression, clusters significantly closer to FOXG1-high GNS peak sets. The most differentially accessible regions between NS and GNS datasets are illustrated in **Figure 6-3**E. Relatively higher variability is evident in GNS lines compared to NS.

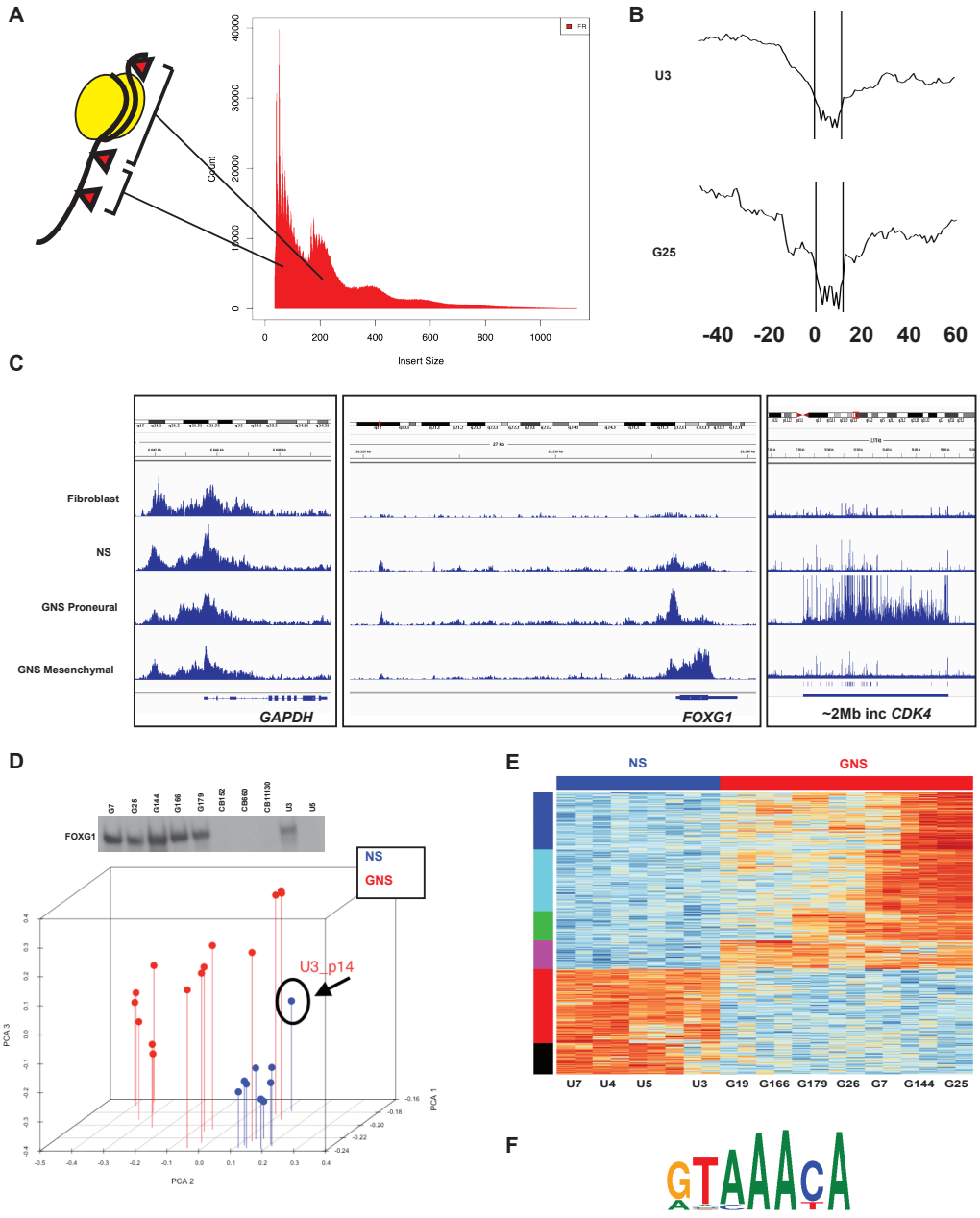
459 peak regions appeared in one or more FOXG1 ChIP-Seq datasets, and demonstrated significantly greater transposase accessibility in GNS cell ATAC datasets compared to NS ATAC sets. These included peaks annotated to *EGFR, GLI3, HES1, NKX2-2* and *OLIG2*; these are genes demonstrated to be upregulated in response to FOXG1 overexpression in the TLDA datasets.

Comparison of differentially enriched motifs identifies 1003 motifs enriched in the regions more accessible in GNS, whereas only 11 are enriched in regions more accessible in NS. Forkhead motifs, including the FOXG1 motif, were most enriched in GNS open chromatin, and in fact variants on these motifs comprised 13 of the top 20 identified (Figure 6-3F) (155). Open chromatin enrichment for forkhead motifs was common to GNS cell lines with proneural and mesenchymal expression profiles. A wide range of neural developmental TF families was also enriched in GNS open chromatin, including CEBP, E2F, ELF, ELK, ETS, FOX, GATA, HMGA, HOX, MEF, NKX, PAX, POU and SOX families.

Comparisons of pooled NS cell and GNS cell ATAC-Seq library traces, together with regions of significant differential accessibility called as described above, as well as FOXG1 ChIP-Seq peaks, are supplied (Figure 6-4). Traces B, D and E illustrate accessibility at some of the candidate FoxG1 binding regions identified in the mouse datasets. A preliminary finding of note was that the region homologous to the mouse cis-regulatory region in the *FoxO3* intron (see above) is FOXG1-bound in these human lines. ATAC-Seq libraries suggest preserved accessibility in this region on BMP treatment in FOXG1-high GNS cells, but not in FOXG1-low NS cells.

A consistent finding across other example traces provided here is significantly increased chromatin accessibility in GNS lines across the gene bodies of neural lineage specific developmental transcription factors with reported activity in GBM, and across the

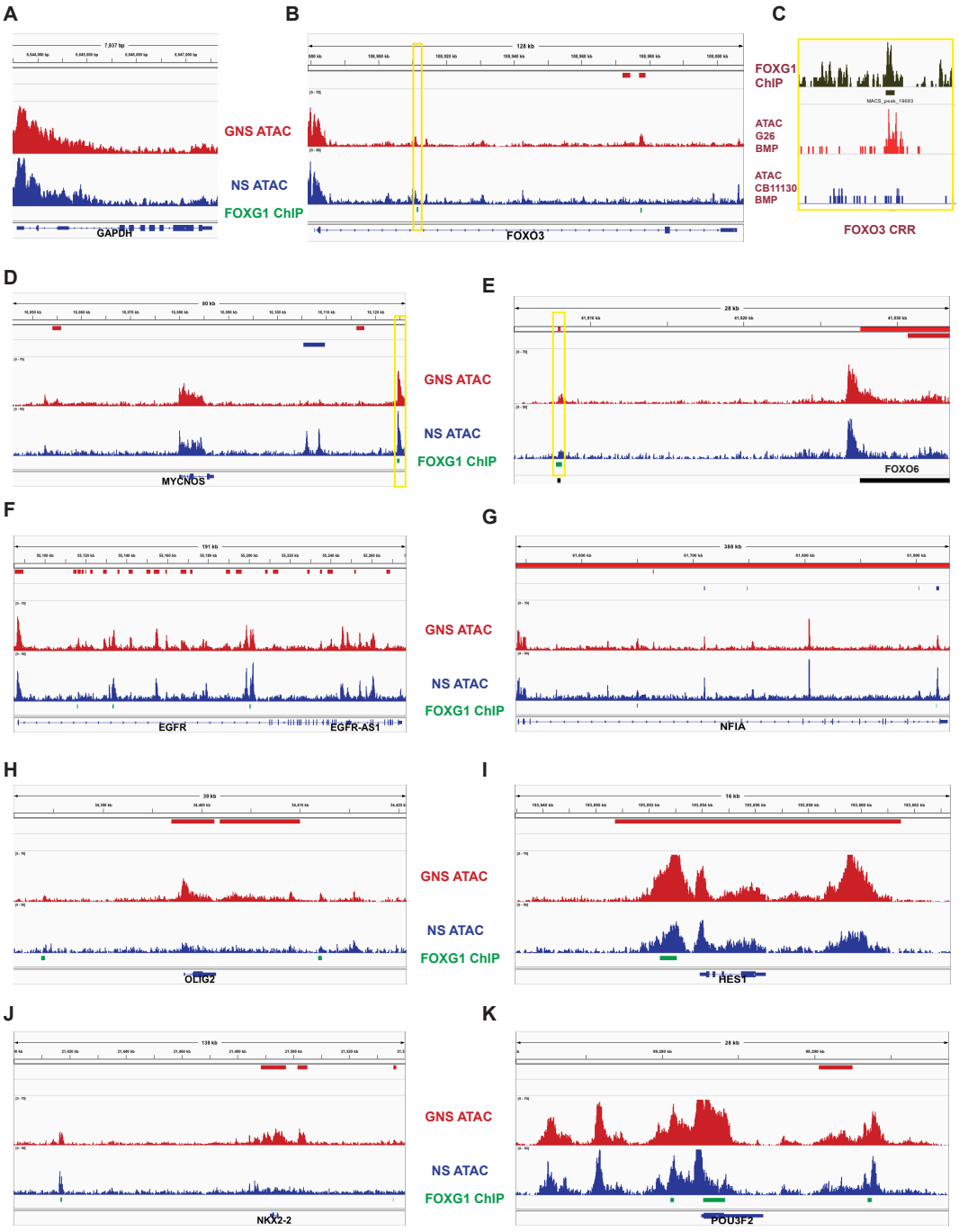
EGFR locus. These traces represent an important resource for future analysis seeking to identify accessible regulatory regions, perhaps in some cases tumour-specific, on which to base genome editing approaches. Altogether these data support our working model that high FOXG1 levels maintain GBM stem cell self-renewal through direct control of the core transcriptional circuit and cell cycle machinery.



(Figure legend overleaf).

Figure 6-3 - ATAC-Seq profiles chromatin accessibility in NS and GNS cell lines

A The Tn5 transposase cuts accessible chromatin and appends adapter sequences allowing for subsequent PCR amplification and sequencing of libraries enriched in 'open' fragments. The histogram demonstrates a typical library fragment size profile for ATAC Seq- the observed ~200bp periodicity reflects fragments incorporating zero, one or two nucleosomes. **B** The plots indicate the average probability of a Tn5 cut site at each position in the 100bp surrounding all forkhead motif instances in the sequenced open chromatin. Reduced accessiblity due to 'footprinting' by FOXG1 binding is evident. **C** Example ATAC traces are provided for fibroblasts, NS cells and GNS (proneural and mesenchymal lines) at a housekeeping gene locus (GAPDH), at the FOXG1 locus, and at the CDK4 locus amplified in the proneural cell line G144. **D** Principal components analysis differentiates the open chromatin profiles of NS and GNS lines. U3 cells, an atypical neuroepithelial cell type with high FOXG1 expression, cluster more closely with GNS lines in this analysis. **E** A chromatin accessibility heatmap for the highest fold change differentially accessible regions between GNS and NS cell lines demonstrates high variability in GNS cells. **F** The forkhead motif is the most highly enriched in the differentially accessible loci between GNS and NS.



(Figure legend overleaf)

Figure 6-4 - Example chromatin accessibility profiles for loci of interest in NS and GNS

Example ATAC-Seq tracks in GNS (red) and NS (blue) cells with FOXG1 ChIP Seq peaks also indicated (lowermost track). Significantly increased accessibility in GNS cells is indicated by a red mark, whereas increased accessibility in NS cells is indicated by a blue mark (uppermost tracks). **A** *GAPDH* is included as a housekeeping gene demonstrating similar chromatin accessibility in GNS and NS **B** *FOXO3* demonstrates a similar accessibility profile in NS and GNS **C** The cis regulatory element whose deletion abolished colony formation in response to FOXG1/SOX2 overexpression (Chapter 2) has a homologous FOXG1-bound counterpart in human cells. ATAC-Seq suggests that this region is maintained in an open configuration in FOXG1-high GNS cells on BMP treatment, but not in FOXG1-low NS cells. **D** and **E** ATAC Seq tracks are shown for human homologs of mouse FOXG1 targets, *MYCN* and *FOXO6*. Each demonstrates regions of significant differential accessibility in GNS compared to NS, not obviously related to FOXG1 binding. **F** to **K** Further example tracks are provided for a number of targets of interest in the neural stem cell context. Neural lineage developmental TFs *OLIG2, HES1, NKX2-2* and *POU3F2* all show increased accessibility in and around the gene locus in GNS cells. This technique offers potential for identifying regulatory elements and even potentially differential usage of these elements in normal and cancer cells.

7 Discussion

7.1 Function and Targets of FOXG1 in GBM

FOXG1 is the most strongly upregulated transcript in glioblastoma-derived GNS cells compared to their normal NS counterparts. This thesis has been concerned with determining any functional impact on GBM stem cell malignancy. We tested the hypotheses that FoxG1 is required to maintain the neural stem cell program, to impair terminal differentiation and promote re-acquisition of neural stem cell identity through induction of the neural stem cell identity and associated gene regulatory network in astrocytes. Our findings suggest that FOXG1 directly drives cell cycle and transcriptional/epigenetic resetting in astrocytes explaining why the high levels are maintained in GBM; high levels of FOXG1 restricts exit from self-renewal and limits differentiation commitment.

7.1.1 FoxG1 is dispensable for NS cell and GNS cell proliferation *in vitro*

FoxG1 is a known regulator of forebrain development in mouse and human (156). I confirmed that FoxG1 is constitutively expressed at low levels in genetically normal NS cells *in vitro*. Genetic loss of function in mouse NS cell using conditional Cre mediated excision, or in human using CRISPR/Cas demonstrates convincingly that the low level of expression is dispensable for NS cell self-renewal *in vitro*. This is consistent with the observation that NS cells can be expanded in culture from midbrain and hindbrain regions, which lack FoxG1 expression. Therefore, the consistent expression of FOXG1 in glioma is not simply a reflection of a critical role in sustaining proliferation in existing GBM stem cells. This directed us to consider whether the high levels rather restrict exit from self-renewal or transition of quiescent or postmitotic cells back into cycle.

Expression levels in GBM stem cell cultures, mouse and human, are consistently higher than in NS cells. Recently published work from the Stifani lab, using FoxG1 shRNA knockdown in primary glioma lines, reports a reduction in sphere-forming efficiency to 60-80% of normal, and reduced tumour formation on xenotransplant (45). Heterogeneity of

cells in spheres due to exposure of individual cells to a gradient of growth factor and autocrine signalling influences, depending on their location within a growing sphere, is inherent to this culture system. Spheres therefore encounter harsher and more differentiation-prone culture conditions. By contrast adherent conditions present uniform exposure of all cells to optimal growth conditions. In these conditions, we find no consistent proliferative deficit *in vitro* associated with FOXG1 knockdown in GNS cells, and this finding extends to genetic knockout of FOXG1 in the G7 GNS line using CRISPR/Cas. Crucially, however, our preliminary *in vivo* results are in keeping with the Stifani group findings, suggesting that FOXG1 is key to tumour formation. In seeking to reconcile these seemingly discrepant findings, we postulated an influence of FoxG1 expression levels on the fate choice of cells exposed to a combination of proliferative and pro-differentiation cues, as might be the case *in vivo* or in the centre of a growing sphere.

7.1.2 FoxG1 deletion predisposes to cell cycle exit and differentiation, whereas FOXG1 and SOX2 overexpression prevent these responses

Constitutive and especially inducible overexpression of FOXG1 allowed us to assay the effects on genetically normal NS cells of the high level FOXG1 expression encountered in primary glioma lines and in mouse model glioma lines.

By contrast with my observations in optimal growth conditions, a range of assays incorporating ambiguous growth and arrest cues reveal a consistent increased tendency to exit cycle and differentiate in response to suboptimal BMP4 treatment in the context of FoxG1 depletion.

Strikingly, combinatorial overexpression of FOXG1 together with SOX2 in mouse NS cells permitted these populations to continue to proliferate rapidly even in the face of high concentrations of BMP4. Overexpression of FOXG1 or SOX2 alone was demonstrated to be insufficient to achieve this effect.

I conclude that FoxG1 activity is dose-dependent. Its expression is not essential to NS or GNS self-renewal *in vitro* in the presence of saturating mitogen doses. On the other hand the response to combinations of mitogens and BMP4, a situation more reflective of the mixture of signals encountered *in vivo,* was clearly predisposed towards cell cycle exit or towards proliferation by knockout or overexpression of FOXG1 respectively. This finding was replicated across the human GNS and mouse NS cell populations.

7.1.3 FOXG1 overexpression drives astrocyte dedifferentiation.

Existing reports suggest that dedifferentiaton of astrocytes to a neural stem cell like state can be achieved by injury, oncogenic transformation, and perhaps by expression of pluripotency factors. I have attempted to apply a strictly defined model system to investigate the ability of a specific neural lineage specific transcription factor, FOXG1, as well as potential partners, to drive dedifferentiation. Plating NS cells at low density in medium supplemented with BMP4 results in universal cell cycle exit and upregulation of astrocyte markers, with no colony formation by these populations on return to growth conditions (EGF/FGF) after 24 hours. The results presented here demonstrate that overexpression of FOXG1 alone, or in combination with SOX2, is sufficient to drive BMP-derived astrocytes to re-enter cell cycle and dedifferentiate to a multipotent NS-like state with high efficiency.

Given the synergistic effects of FOXG1 and SOX2 in maintaining NS proliferation despite BMP cues, I investigated the joint regulatory activity of these factors on candidate shared targets of the two factors, as well as targets of FOXG1 alone.

7.1.4 FOXG1 drives dedifferentiation through key pathways and candidate drug targets

The regulated targets of FOXG1 in mouse identified in this study can be categorised into key functional categories. Firstly, regulators of cell cycle and self-renewal include the tumour suppressor FoxO3 (downregulated) and the proto-oncogenes Plk1, FoxO6 and MycN (upregulated).

Secondly, epigenetic modifiers include regulators of DNA methylation from the Dnmt and Tet3, families, and the histone modifier Chd3 (upregulated). Thirdly neural stem cell regulators such as Ascl1, Hes1 and Brn4 are upregulated, while astrocyte markers including Id3 and Aqp4 are correspondingly downregulated.

Together these targets are convincing candidate components of a coordinated program driving cell cycle and neural stem cell identity. Further investigation is required to establish the true directly regulated targets of FOXG1 in human glioma lines, a set of genes which are likely to enrich strongly for potential drug targets.

7.2 Further application of BMP-treated NS colony forming assays

7.2.1 BMP Assay Development

The BMP-treated colony forming assay presented offers a simple and reproducible quantitative gauge of astrocyte commitment, requiring no dedicated equipment. In our hands it seems to be applicable to NS cell and astrocyte identity, as well as glioma biology, in a range of adult mouse NS cell lines.

The assay offers potential as the basis for small molecule screens which we are in the process of developing, and which have already provided exciting insights into the biological processes driving escape from BMP-driven commitment. Ultimately variations on this assay might also offer drug screening potential. In particular, it would be valuable to investigate the possible correlation between the results of the BMP-treated NS colony formation assay presented here and tumour-forming capacity of transplanted cells *in vivo*, a correlation suggested by the ability of mouse glioma lines with defined mutations including INK4Arf-/-;EGFRvIII (IENS) and p53 deleted (223) to generate colonies in this assay. If this correlation holds on further investigation, colony formation after BMP treatment could prove to be a valuable *in vitro* index of tumorgenicity with widespread applications, especially for screening.

7.2.2 Assay Application to Human NS cells

Modifications to this assay will be necessary for its application to human NS cell lines. Firstly these lines do not generate the convincing astrocyte phenotype associated with mouse cells in response to BMP treatment, and it may be that other differentiation cues are required to achieve astrocyte commitment and especially the refractory cell cycle exit which is the basis for this assay. Differentiation protocols incorporating additional or alternative inductive cues, perhaps including CNTF, LIF or serum, and potentially also blockade of FGF receptor or other signalling cascades, may be of value here. Likewise, variants on this assay based on primary astrocyte dedifferentiation may be of value in exploring particular biological questions. Secondly the slower cycle time of human NS cells means that colony formation is prohibitively slow: an EdU incorporation assay or similar is likely to be more useful in this context.

7.2.3 Investigation of Density Effects

The influence of plating density on the response to BMP treatment is key to the assays presented here. At high plating densities (>50/mm2) we observed that brief BMP4 treatment resulted in a quiescent phenotype, reversible on restoration of growth factors. At very high densities, the results of even prolonged BMP treatment are rapidly and fully reversible, as previously reported for combinations of BMP and FGF (83). In contrast, at low plating densities, BMP4 treatment for just 24 hours is sufficient to drive universal terminal astrocyte differentiation as assessed by inability to re-express NS markers or to form colonies on restoration of growth factors.

The fundamental importance of density in this context has escaped thorough study to date, probably because the sphere assays which dominate the literature present individual cells with varying levels of density-dependent cues depending on the position of each cell within the sphere, so do not lend themselves to controlled study.

Future work could seek to clarify the parameters governing density-dependent fate determination in NS cells and their derivatives. In the first place, the relative importance of density during BMP treatment and during subsequent growth factor exposure could be assayed by replating cells at the time of media change. This would help determine whether density-dependent cues determine a choice between quiescence and differentiation during BMP treatent, or whether a uniform BMP differentiation response, irrespective of density, is reversible in response to density-dependent autocrine/paracrine cues, on subsequent growth factor exposure.

Secondly, conditioned media experiments could be used to establish whether density effects depend on paracrine signalling by diffusible messengers, or whether physical cell-cell interactions, mediating Notch signalling for instance, are necessary. These studies might be expected to direct biological characterisation of the density-dependent mechanisms involved, and even perhaps to demonstrate upstream regulators of FOXG1.

7.3 Implications for our understanding of NS and GNS cell identity

7.3.1 Roles of FOXG1

The expression data, human and mouse, presented here indicates that the most malignant gliomas converge on an identity incorporating high level FOXG1 expression. High FOXG1 expression in GNS cells is compatible with several underlying mechanisms. For instance, FoxG1 expression could be a feature of the glioma cell-of-origin, preserved through gliomagenesis. Alternatively, high FoxG1 expression could be a consistent and conserved byproduct of activation of the core glioma pathways established during gliomagenesis, or the result of epigenetic drift and clonal selection in developing malignant populations which have ceased to maintain epigenetic stability.

The expression profiling presented here for GNS lines derived from lower grade tumours indicates some of these lines have lower FoxG1 levels, suggesting contrary to the first mechanism proposed that high FoxG1 levels are not an obligate feature of the cell-of-origin

for all gliomas. This is also corroborated by expression data from the Rembrandt database which suggests that FOXG1 expression varies across gliomas, and strongly predicts survival. These findings raise the interesting possibility that lower grade glial tumours may express variable FOXG1 levels according to the cell of origin and driver mutations, but that high level expression reliably accompanies the transition to the fully malignant state (Grade IV, GBM). The functional results of driving FOXG1 expression in these WHO Grade III cultures to levels typical for WHO Grade IV lines is an important area for future investigation.

Each of the mechanisms presented is consistent with a requirement for FoxG1 in establishing or maintaining the glioblastoma malignant program. Alternatively the preserved self-renewal capacity of FOXG1-null GNS cells in optimal conditions *in vitro* raises the possibility that FOXG1 expression in gliomas could be an incidental and functionally inconsequential result of the activation of a set of glioma core pathways.

Our *in vitro* data, established in mouse FoxG1-conditional and FOXG1/SOX2 overexpressing cells, as well as certain human GNS lines, confirms the functional role of FOXG1 in preserving self-renewal in the sub-optimal conditions which pertain *in vivo*. This is confirmed by our demonstration, in keeping with previous evidence from the Vescovi group, that FOXG1 is necessary for tumour formation *in vivo*. This role of FOXG1, equipping GNS cells to escape differentiation cues and persist in proliferation, parallels its developmental role in preventing premature differentiation and depletion of the NS pool(117). Furthermore we demonstrate that FOXG1, through distinct and complementary downstream targets, drives terminally differentiated astrocytes to re-enter cell cycle and to reacquire an NS cell identity, a process with important parallels to gliomagenesis.

7.3.2 A model for FOXG1 function in GBM

An overview schema for the potential genetic and epigenetic transitions involved in gliomagenesis by a postmitotic astrocyte cell of origin is set out below (Figure 7-1). Early

driver mutations affecting tumour suppressors like *TP53* and *RB1* enable astrocytes to begin proliferating slowly. A process of clonal evolution gradually converges on a FOXG1-high state, through chance derepression of the *FOXG1* locus in single cells or through the activity of upstream regulators still to be defined, followed by selective pressure. FOXG1-high cells dominate this process since they are locked into a GNS program and will proliferate rapidly irrespective of prevailing differentiation cues.

In this model, the pattern of mutations should to some extent predict the time to acquisition of the FOXG1-high state and malignant transformation. Primary glioblastoma (arising *de* novo) would be expected to occur on a background of early mutations directly driving FOXG1 expression, especially EGFR mutations. On the other hand, low grade glioma progressing to secondary GBM might represent early disruption of DNA repair and cell cycle checkpoints, enabling slow proliferation with retained astrocyte identity (low grade glioma), with genetic instability promoting eventual transformation. These predictions are in keeping with the relatively high incidence of EGFR mutations in primary GBM, and of *TP53* mutations in low grade glioma (7). The data presented here using the IENS genetically defined glioma cell line suggests that even a minimal mutation set comprising EGFRvIII and p16INK4Arf mutations is sufficient to drive FoxG1 expression as part of a tumorigenic program.

In light of this, an important line of further inquiry relates to establishing the contribution of EGF and other RTK signalling as upstream drivers of FOXG1 expression. Another candidate upstream pathway is sonic hedgehog: evidence from previous studies of astrocyte dedifferentiation in response to injury demonstrate a key role for sonic hedgehog signalling, and this also lies upstream of FoxG1 in the context of dorsal/ventral patterning as discussed in the introduction (157,158)

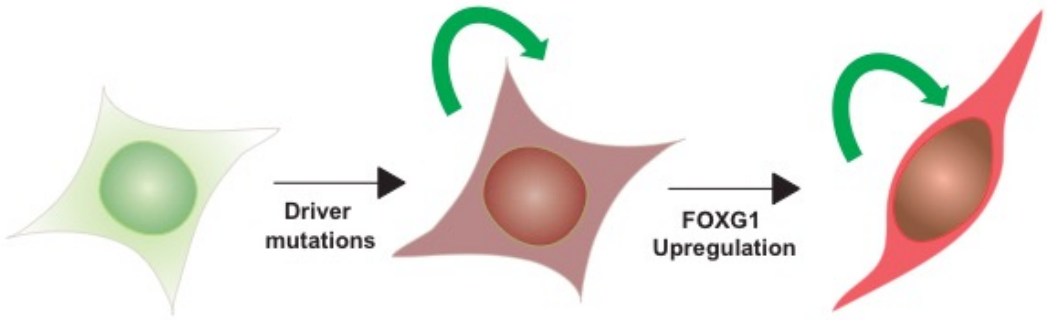


Figure 7-1- A model for gliomagenesis and high grade transformation

A combination of driver mutations usually including p53 knockout results in development of a low grade glioma, comprising slow-dividing astrocyte-like cells, which continue to accumulate mutations. Within this epigenetically diverse population, FOXG1 high clones preferentially resist differentiation cues and are at a selective advantage. Very high FOXG1 levels drive acquisition of GNS cell identity, resulting in the rapid division which characterises transformed malignant gliomas including GBM.

7.3.3 Validating the role of FOXG1 in gliomagenesis *in vivo*

A number of *in vivo* assays based on existing cell lines and targeting/expression constructs would complement the insights into FOXG1's role in the GNS program presented here and help to validate or refute the gliomagenesis model presented above.

In particular, I would like to adapt the model used by the Bernstein laboratory to investigate the ability of FOXG1 to drive acquisition of glioma neural stem cell properties in serum-treated differentiated glioma cells (DGCs) (51). Is FOXG1 alone sufficient to drive this process in GNS, as in the mouse NS model presented here?

I would like to investigate the effects of induced FOXG1 expression on the tumorgenicity of low grade glioma lines AA1 and CC1, and of Crispr-targeted human and mouse NS cells and astrocytes on xenotransplant. Will FOXG1 forced expression constitute an epigenetic 'hit' resulting in high grade tumour formation in the presence of founder mutations to targets such as *TP53* or *CDKN2A* ?

In a similar vein it would be intriguing to investigate whether FOXG1 lentivirus injection in mice is sufficient to generate tumours, perhaps in the context of adult inducible astrocyte-specific mutations (159). If so, is this specific to the forebrain, in keeping with the finding that FOXG1-high paediatric GBM, in the context of Histone H3 G34R mutation, is restricted to the cerebral hemispheres (160)? This pertains to the more general question of why glioma arises predominantly in the forebrain. Does this simply reflect the distribution of cycling populations most vulnerable to transformation, or is it in part a product of high FOXG1 expression in these regions?

7.3.4 A unifying model for FOXG1 function in health and disease

The effects of *FoxG1* knockout presented here complement existing data pointing to a requirement for FoxG1 in preventing premature differentiation of NS cells (117). Equally, the overexpression data points to a role for high FOXG1 levels in resisting and reversing the differentiation process. One intriguing possibility is that FoxG1 may represent a key

regulator of the program which restricts neuroepithelial cells, radial glia and ultimately subventricular zone astrocytes (or adult neural stem cells) from undergoing terminal differentiation to a postmitotic astrocyte state. A unifying model of FoxG1 as a driver of neural stem cell identity and a block to differentiation would then pertain to both normal neural stem cells and glioma neural stem cells. Upstream pathways contributing to maintenance of FOXG1 expression in subventricular zone astrocytes, where it is extinguished in postmitotic cortical astrocytes, could depend on cell-cell interactions established within the pinwheel architecture of the subventricular zone, mediated by paracrine and direct contact-based interactions.

7.3.5 Translational implications

The work presented here suggests that high level FOXG1 expression is necessary and sufficient to enforce an ongoing process of astrocyte reprogramming critical to tumour development and recurrence. Therefore FOXG1, along with its upstream regulators and its downstream targets, represent important potential therapeutic targets. With the exception of nuclear receptors, TFs have represented a challenging therapeutic target, because small molecule inhibitors are generally not able to target TF activity specifically. Over the last few years novel approaches, for example stapled peptides (161), have emerged promising direct and highly specific TF targeting using membrane-permeable drugs designed according to rational principles. cMyc, here identified as a FOXG1 target, is widely dysregulated across a spectrum of cancers, and its importance as a drug target (162) has been recognised as one of Cancer Research UK's seven Grand Challenges. Cell type specific pathways, governed by cell type specific TFs, would seem to present a lower risk of off-target effects. In any case, downstream targets of the FOXG1 program are likely to offer important therapeutic potential.

Upstream regulators of FOXG1 activity offer more immediate promise, since many are likely subject to modulation by established FDA-approved compounds. EGFR signalling

is a published example (148), but other RTKs and related signalling cascades are likely to be involved. I have trialled the Operetta system for medium-throughput screening of a small molecule library, using nuclear counts and colony formation as a readout for functional effects on dedifferentiation. A similar approach could also be applied in primary human NS or GNS cells to screen drug libraries for regulatory effect on FOXG1 expression. Given the specific importance of high level FOXG1 expression for GNS cell escape from differentiation (as opposed to more generic survival and proliferation functions), pharmacological suppression of this axis might be expected to offer an excellent therapeutic index. Further, since GBM occurs and recurs almost exclusively within the CNS, impregnated wafers or Ommaya reservoir delivery systems offer the potential to achieve high local drug concentrations in the tumour bed with minimal systemic side effects.

8 References

1. Singh SK, Clarke ID, Terasaki M, Bonn VE, Hawkins C, Squire J, et al. Identification of a cancer stem cell in human brain tumors. 2003 Sep 15;63(18):5821–8.

2. Pollard SM, Yoshikawa K, Clarke ID, Danovi D, Stricker S, Russell R, et al. Glioma Stem Cell Lines Expanded in Adherent Culture Have Tumor-Specific Phenotypes and Are Suitable for Chemical and Genetic Screens. Cell Stem Cell. 2009 Jun;4(6):568–80.

3. Larjavaara S, Mäntylä R, Salminen T, Haapasalo H, Raitanen J, Jääskeläinen J, et al. Incidence of gliomas by anatomic location. Neuro-oncology. 2007 Jul;9(3):319–25.

4. Ostrom QT, Bauchet L, Davis FG, Deltour I, Fisher JL, Langer CE, et al. The epidemiology of glioma in adults: a "state of the science" review. Neuro-oncology. 2014 Jun 13;16(7):896–913.

5. Louis D, Ohgaki H, Wiestler O, Cavenee W, Burger P, Jouvet A, et al. The 2007 WHO classification of tumours of the central nervous system. Acta Neuropathol. 2007 Aug 1;114(2):97–109.

6. Ichimura K, Pearson DM, Kocialkowski S, Backlund LM, Chan R, Jones DTW, et al. IDH1 mutations are present in the majority of common adult gliomas but rare in primary glioblastomas. Neuro-oncology. 2009 Aug 6;11(4):341–7.

7. Ohgaki H, Kleihues P. Genetic pathways to primary and secondary glioblastoma. Am J Pathol. 2007 May;170(5):1445–53.

8. Stupp R, Mason WP, van den Bent MJ, Weller M, Fisher B, Taphoorn MJB, et al. Radiotherapy plus Concomitant and Adjuvant Temozolomide for Glioblastoma. N Engl J Med. 2005 Mar 10;352(10):987–96.

9. Hegi ME, Diserens A-C, Gorlia T, Hamou M-F, de Tribolet N, Weller M, et al. MGMT gene silencing and benefit from temozolomide in glioblastoma. N Engl J Med. 2005 Mar 10;352(10):997–1003.

10. Westphal M, Ram Z, Riddle V, Hilt D, Bortey E, Executive Committee of the Gliadel Study Group. Gliadel wafer in initial surgery for malignant glioma: long-term follow-up of a multicenter controlled trial. Acta neurochirurgica. 2006 Mar;148(3):269–75–discussion275.

11. Verhaak RGW, Hoadley KA, Purdom E, Wang V, Qi Y, Wilkerson MD, et al. Integrated Genomic Analysis Identifies Clinically Relevant Subtypes of Glioblastoma Characterized by Abnormalities in PDGFRA, IDH1, EGFR, and NF1. Cancer Cell. 2010 Jan 1;17(1):98–110.

12. Kim J, Lee I-H, Cho HJ, Park C-K, Jung Y-S, Kim Y, et al. Spatiotemporal Evolution of the Primary Glioblastoma Genome. Cancer Cell. Elsevier Inc; 2015 Sep 14;28(3):318–28.

13. Phillips HS, Kharbanda S, Chen R, Forrest WF, Soriano RH, Wu TD, et al. Molecular subclasses of high-grade glioma predict prognosis, delineate a pattern of disease progression, and resemble stages in neurogenesis. Cancer Cell. 2006 Mar;9(3):157–73.

14. Snuderl M, Fazlollahi L, Le LP, Nitta M, Zhelyazkova BH, Davidson CJ, et al. Mosaic amplification of multiple receptor tyrosine kinase genes in glioblastoma. Cancer Cell. 2011 Dec 13;20(6):810–7.

15. Parsons DW, Jones S, Zhang X, Lin JC-H, Leary RJ, Angenendt P, et al. An integrated genomic analysis of human glioblastoma multiforme. Science. 2008 Sep

26;321(5897):1807–12.

16. Schwartzentruber J, Korshunov A, Liu X-Y, Jones DTW, Pfaff E, Jacob K, et al. Driver mutations in histone H3.3 and chromatin remodelling genes in paediatric glioblastoma. Nature. 2012;482(7384):226–31.

17. Carén H, Pollard SM, Beck S. Molecular Aspects of Medicine. Molecular Aspects of Medicine. Elsevier Ltd; 2013 Aug 1;34(4):849–62.

18. Kotliarova S, Fine HA. SnapShot: glioblastoma multiforme. Cancer Cell. 2012 May 15;21(5):710–1.

19. Furnari FB, Fenton T, Bachoo RM, Mukasa A, Stommel JM, Stegh A, et al. Malignant astrocytic glioma: genetics, biology, and paths to treatment. Genes Dev. 2007 Nov 1;21(21):2683–710.

20. Lee J, Kotliarova S, Kotliarov Y, Li A, Su Q, Donin NM, et al. Tumor stem cells derived from glioblastomas cultured in bFGF and EGF more closely mirror the phenotype and genotype of primary tumors than do serum-cultured cell lines. Cancer Cell. 2006 May;9(5):391–403.

21. Patel AP, Tirosh I, Trombetta JJ, Shalek AK, Gillespie SM, Wakimoto H, et al. Single-cell RNA-seq highlights intratumoral heterogeneity in primary glioblastoma. Science. 2014 Jun 19;344(6190):1396–401.

22. Pierce GB, Speers WC. Tumors as caricatures of the process of tissue renewal: prospects for therapy by directing differentiation. Cancer Res. 1988 Apr 15;48(8):1996–2004.

23. Sun Y, Pollard S, Conti L, Toselli M, Biella G, Parkin G, et al. Long-term tripotent differentiation capacity of human neural stem (NS) cells in adherent culture. Molecular and Cellular Neuroscience. 2008 Jun;38(2):245–58.

24. Conti L, Pollard SM, Gorba T, Reitano E, Toselli M, Biella G, et al. Niche-independent symmetrical self-renewal of a mammalian tissue stem cell. PLoS Biol. 2005 Sep 1;3(9):e283.

25. Son MJ, Woolard K, Nam D-H, Lee J, Fine HA. SSEA-1 is an enrichment marker for tumor-initiating cells in human glioblastoma. Cell Stem Cell. 2009 May 8;4(5):440–52.

26. Galli R, Binda E, Orfanelli U, Cipelletti B, Gritti A, De Vitis S, et al. Isolation and characterization of tumorigenic, stem-like neural precursors from human glioblastoma. Cancer Res. 2004 Oct 1;64(19):7011–21.

27. Singh SK, Hawkins C, Clarke ID, Squire JA, Bayani J, Hide T, et al. Identification of human brain tumour initiating cells. Nature. 2004 Nov 18;432(7015):396–401.

28. Beier D, Hau P, Proescholdt M, Lohmeier A, Wischhusen J, Oefner PJ, et al. CD133(+) and CD133(-) glioblastoma-derived cancer stem cells show differential growth characteristics and molecular profiles. Cancer Res. 2007 May 1;67(9):4010–5.

29. Stiles CD, Rowitch DH. Glioma Stem Cells: A Midterm Exam. Neuron. 2008 Jun 1;58(6):832–46.

30. Bao S, Wu Q, McLendon RE, Hao Y, Shi Q, Hjelmeland AB, et al. Glioma stem cells promote radioresistance by preferential activation of the DNA damage response. Nature. 2006 Oct 18;444(7120):756–60.

31. Chen J, Li Y, Yu T-S, McKay RM, Burns DK, Kernie SG, et al. A restricted cell population propagates glioblastoma growth after chemotherapy. Nature. 2012 Aug 1;488(7412):522–6.

32. Reya T, Morrison SJ, Clarke MF, Weissman IL. Stem cells, cancer, and cancer stem cells. Nature. Nature Publishing Group; 2001 Nov 1;414(6859):105–11.

33. Spitz F, Furlong EEM. Transcription factors: from enhancer binding to developmental control. Nature Publishing Group. Nature Publishing Group; 2012 Aug 7;13(9):613–26.

34. Kim J, Efe JA, Zhu S, Talantova M, Yuan X, Wang S, et al. Direct reprogramming of mouse fibroblasts to neural progenitors. Proc Natl Acad Sci USA. 2011 May 10;108(19):7838–43.

35. Thier M, Wörsdörfer P, Lakes YB, Gorris R, Herms S, Opitz T, et al. Direct conversion of fibroblasts into stably expandable neural stem cells. Cell Stem Cell. 2012 Apr 6;10(4):473–9.

36. Han DW, Tapia N, Hermann A, Hemmer K, Höing S, Araúzo-Bravo MJ, et al. Direct reprogramming of fibroblasts into neural stem cells by defined factors. Cell Stem Cell. 2012 Apr 6;10(4):465–72.

37. Sheng C, Zheng Q, Wu J, Xu Z, Wang L, Li W, et al. Direct reprogramming of Sertoli cells into multipotent neural stem cells by defined factors. Cell Res. 2012 Jan;22(1):208–18.

38. Abad M, Mosteiro L, Pantoja C, Cañamero M, Rayon T, Ors I, et al. Reprogramming in vivo produces teratomas and iPS cells with totipotency features. Nature. Nature Publishing Group; 2013 Nov 28;502(7471):340–5.

39. Lujan E, Chanda S, Ahlenius H, Südhof TC, Wernig M. Direct conversion of mouse fibroblasts to self-renewing, tripotent neural precursor cells. Proc Natl Acad Sci USA. National Acad Sciences; 2012;109(7):2527–32.

40. Ring KL, Tong LM, Balestra ME, Javier R, Andrews-Zwilling Y, Li G, et al. Short Article. Stem Cell. Elsevier Inc; 2012 Jul 6;11(1):100–9.

41. Niu W, Zang T, Smith DK, Vue TY, Zou Y, Bachoo R, et al. Stem Cell Reports. Stem Cell Reports. The Authors; 2015 Apr 21;:1–15.

42. Raciti M, Granzotto M, Do Duc M, Fimiani C, Cellot G, Cherubini E, et al. Reprogramming fibroblasts to neural-precursor-like cells by structured overexpression of pallial patterning genes. Molecular and Cellular Neuroscience. Elsevier Inc. 2013;57:1–12.

43. Engström PG, Tommei D, Stricker SH, Ender C, Pollard SM, Bertone P. Digital transcriptome profiling of normal and glioblastoma-derived neural stem cells identifies genes associated with patient survival. Genome Med. 2012;4(10):76.

44. Ligon KL, Huillard E, Mehta S, Kesari S, Liu H, Alberta JA, et al. Olig2-Regulated Lineage-Restricted Pathway Controls Replication Competence in Neural Stem Cells and Malignant Glioma. Neuron. 2007 Feb;53(4):503–17.

45. Verginelli F, Perin A, Dali R, Fung KH, Lo R, Longatti P, et al. Transcription factors FOXG1 and Groucho/TLE promote glioblastoma growth. Nature Communications. 2013 Dec;4:2956.

46. Ikushima H, Todo T, Ino Y, Takahashi M, Miyazawa K, Miyazono K. Autocrine TGF-b Signaling Maintains Tumorigenicity of Glioma-Initiating Cells through Sry-Related HMG-Box Factors. Stem Cell. Elsevier Ltd; 2009 Nov 6;5(5):504–14.

47. Rheinbay E, Suvà ML, Gillespie SM, Wakimoto H, Patel AP, Shahid M, et al. An Aberrant Transcription FactorNetwork Essential for Wnt Signalingand Stem Cell Maintenance in Glioblastoma. CellReports. The Authors; 2013 May 30;3(5):1567–79.

48. Seoane J, Le H-V, Shen L, Anderson SA, Massagué J. Integration of Smad and forkhead pathways in the control of neuroepithelial and glioblastoma cell proliferation. Cell. 2004 Apr 16;117(2):211–23.

49. Gong A, Huang S. FoxM1 and Wnt/β-catenin signaling in glioma stem cells. Cancer Res. 2012 Nov 15;72(22):5658–62.

50. Kamnasaran D, Qian B, Hawkins C, Stanford WL, Guha A. GATA6 is an astrocytoma tumor suppressor gene identified by gene trapping of mouse glioma model. Proc Natl Acad Sci USA. 2007 May 8;104(19):8053–8.

51. Suvà ML, Rheinbay E, Gillespie SM, Patel AP, Wakimoto H, Rabkin SD, et al. Reconstructing and Reprogramming the Tumor-Propagating Potentialof Glioblastoma Stem-like Cells. Cell. Elsevier Inc; 2014 Apr 9;:1–15.

52. Soroceanu L, Murase R, Limbad C, Singer E, Allison J, Adrados I, et al. Id-1 is a key transcriptional regulator of glioblastoma aggressiveness and a novel therapeutic target. Cancer Res. 2013 Mar 1;73(5):1559–69.

53. Gangemi RMR, Griffero F, Marubbi D, Perera M, Capra MC, Malatesta P, et al. SOX2 silencing in glioblastoma tumor-initiating cells causes stop of proliferation and loss of tumorigenicity. Stem Cells. 2009 Jan;27(1):40–8.

54. Alonso MM, Diez-Valle R, Manterola L, Rubio A, Liu D, Cortes-Santiago N, et al. Genetic and epigenetic modifications of Sox2 contribute to the invasive phenotype of malignant gliomas. PLoS ONE. 2011;6(11):e26740.

55. Suvà ML, Rheinbay E, Gillespie SM, Patel AP, Wakimoto H, Rabkin SD, et al. Reconstructing and Reprogramming the Tumor-Propagating Potentialof Glioblastoma Stem-like Cells. Cell. Elsevier Inc; 2014 Apr 9;:1–15.

56. Muraguchi T, Tanaka S, Yamada D, Tamase A, Nakada M, Nakamura H, et al. NKX2.2 suppresses self-renewal of glioma-initiating cells. Cancer Res. 2011 Feb 1;71(3):1135–45.

57. Gallo M, Ho J, Coutinho FJ, Vanner R, Lee L, Head R, et al. A Tumorigenic MLL-Homeobox Network in Human Glioblastoma Stem Cells. Cancer Res. 2013 Jan 2;73(1):417–27.

58. Lee JS, Xiao J, Patel P, Schade J, Wang J, Deneen B, et al. A novel tumor-promoting role for nuclear factor IA in glioblastomas is mediated through negative regulation of p53, p21, and PAI1. Neuro-oncology. 2014 Jan 18;16(2):191–203.

59. Fasano CA, Phoenix TN, Kokovay E, Lowry N, Elkabetz Y, Dimos JT, et al. Bmi-1 cooperates with Foxg1 to maintain neural stem cell self-renewal in the forebrain. Genes Dev. 2009 Mar 1;23(5):561–74.

60. Bruggeman SWM, Hulsman D, Tanger E, Buckle T, Blom M, Zevenhoven J, et al. Bmi1 controls tumor development in an Ink4a/Arf-independent manner in a mouse model for glioma. Cancer Cell. 2007 Oct 1;12(4):328–41.

61. Carro MS, Lim WK, Alvarez MJ, Bollo RJ, Zhao X, Snyder EY, et al. The transcriptional network for mesenchymal transformation of brain tumours. Nature. Nature Publishing Group; 2010 Jan 11;463(7279):318–25.

62. Alvarez-Buylla A, García-Verdugo JM, Tramontin AD. A unified hypothesis on the lineage of neural stem cells. Nat Rev Neurosci. 2001 Apr;2(4):287–93.

63. Doetsch F, Caillé I, Lim DA, García-Verdugo JM, Alvarez-Buylla A. Subventricular zone astrocytes are neural stem cells in the adult mammalian brain. Cell. 1999 Jun 11;97(6):703–16.

64. Liu C, Sage JC, Miller MR, Verhaak RGW, Hippenmeyer S, Vogel H, et al. Mosaic analysis with double markers reveals tumor cell of origin in glioma. Cell. 2011 Jul 22;146(2):209–21.

65. Herculano-Houzel S, Lent R. Isotropic fractionator: a simple, rapid method for the quantification of total cell and neuron numbers in the brain. Journal of Neuroscience. 2005 Mar 9;25(10):2518–21.

66. Bachoo RM, Maher EA, Ligon KL, Sharpless NE, Chan SS, You MJ, et al. Epidermal growth factor receptor andInk4a/Arf:Convergent mechanisms governing terminal differentiation and transformation along the neural stem cell to astrocyte axis. Cancer Cell. 2002 Jan 1;1(3):269–77.

67. Friedmann-Morvinski D, Bushong EA, Ke E, Soda Y, Marumoto T, Singer O, et al. Dedifferentiation of Neurons and Astrocytes by Oncogenes Can Induce Gliomas in Mice. Science. 2012 Nov 22;338(6110):1080–4.

68. Chow LML, Endersby R, Zhu X, Rankin S, Qu C, Zhang J, et al. Cooperativity within and among Pten, p53, and Rb pathways induces high-grade astrocytoma in adult brain. Cancer Cell. 2011 Mar 8;19(3):305–16.

69. Rowitch DH, Kriegstein AR. Developmental genetics of vertebrate glial–cell specification. Nature. 2010 Nov 11;468(7321):214–22.

70. Deneen B, Ho R, Lukaszewicz A, Hochstim CJ, Gronostajski RM, Anderson DJ. The transcription factor NFIA controls the onset of gliogenesis in the developing spinal cord. Neuron. 2006 Dec 21;52(6):953–68.

71. Bignami A, Eng LF, Dahl D, Uyeda CT. Localization of the glial fibrillary acidic protein in astrocytes by ICC. Brain research. 1972 Aug 25;43(2):429–35.

72. Walz W, Lang MK. Immunocytochemical evidence for a distinct GFAP-negative subpopulation of astrocytes in the adult rat hippocampus. Neurosci Lett. 1998 Dec 4;257(3):127–30.

73. Hydén H, McEwen B. A glial protein specific for the nervous system. Proc Natl Acad Sci USA. 1966 Feb;55(2):354–8.

74. Chaudhry FA, Lehre KP, van Lookeren Campagne M, Ottersen OP, Danbolt NC, Storm-Mathisen J. Glutamate transporters in glial plasma membranes: highly differentiated localizations revealed by quantitative ultrastructural immunocytochemistry. Neuron. 1995 Sep;15(3):711–20.

75. Nielsen S, Nagelhus EA, Amiry-Moghaddam M, Bourque C, Agre P, Ottersen OP. Specialized membrane domains for water transport in glial cells: high-resolution immunogold cytochemistry of aquaporin-4 in rat brain. J Neurosci. 1997 Jan 1;17(1):171–80.

76. Barry D, McDermott K. Differentiation of radial glia from radial precursor cells and transformation into astrocytes in the developing rat spinal cord. Glia. 2005 May;50(3):187–

97.

77. Pringle NP, Yu W-P, Howell M, Colvin JS, Ornitz DM, Richardson WD. Fgfr3 expression by astrocytes and their precursors: evidence that astrocytes and oligodendrocytes originate in distinct neuroepithelial domains. Development. 2003 Jan;130(1):93–102.

78. Molofsky AV, Krenick R, Ullian E, Tsai HH, Deneen B, Richardson WD, et al. Astrocytes and disease: a neurodevelopmental perspective. Genes Dev. 2012 May 1;26(9):891–907.

79. Rajan P, McKay RD. Multiple routes to astrocytic differentiation in the CNS. J Neurosci. 1998 May 15;18(10):3620–9.

80. Kretzschmar M, Massagué J. SMADs: mediators and regulators of TGF-beta signaling. Current Opinion in Genetics & Development. 1998 Feb;8(1):103–11.

81. Bonaguidi MA, McGuire T, Hu M, Kan L, Samanta J, Kessler JA. LIF and BMP signaling generate separate and discrete types of GFAP-expressing cells. Development. 2005 Dec;132(24):5503–14.

82. Samanta J. Interactions between ID and OLIG proteins mediate the inhibitory effects of BMP4 on oligodendroglial differentiation. Development. 2004 Sep 1;131(17):4131–42.

83. Ben Martynoga, Mateo JL, Zhou B, Andersen J, Achimastou A, Urbán N, et al. Epigenomic enhancer annotation reveals a key role for NFIX in neural stem cell quiescence. Genes Dev. 2013 Aug 15;27(16):1769–86.

84. Sun Y, Hu J, Zhou L, Pollard SM, Smith A. Interplay between FGF2 and BMP controls the self-renewal, dormancy and differentiation of rat neural stem cells. J Cell Sci. 2011 Jun 1;124(Pt 11):1867–77.

85. Llorens-Bobadilla E, Zhao S, Baser A, Saiz-Castro G, Zwadlo K, Martin-Villalba A. Single-Cell Transcriptomics Reveals a Population of Dormant Neural Stem Cells that Become Activated upon Brain Injury. Stem Cell. Elsevier Inc; 2015 Sep 3;17(3):329–40.

86. Buffo A, Rite I, Tripathi P, Lepier A, Colak D, Horn A-P, et al. Origin and progeny of reactive gliosis: A source of multipotent cells in the injured brain. Proc Natl Acad Sci USA. 2008 Mar 4;105(9):3581–6.

87. Shimada IS, LeComte MD, Granger JC, Quinlan NJ, Spees JL. Self-Renewal and Differentiation of Reactive Astrocyte-Derived Neural Stem/Progenitor Cells Isolated from the Cortical Peri-Infarct Area after Stroke. Journal of Neuroscience. 2012 Jun 6;32(23):7926–40.

88. Lang B, Liu HL, Liu R, Feng GD, Jiao XY, Ju G. Astrocytes in injured adult rat spinal cord may acquire the potential of neural stem cells. Neuroscience. 2004 Jan;128(4):775–83.

89. Feng G-D, He B-R, Lu F, Liu L-H, Zhang L, Chen B, et al. Fibroblast Growth Factor 4 Is Required but not Sufficient for the Astrocyte Dedifferentiation. Mol Neurobiol. 2014 Feb 9;50(3):997–1012.

90. Berninger B, Costa MR, Koch U, Schroeder T, Sutor B, Grothe B, et al. Functional Properties of Neurons Derived from In Vitro Reprogrammed Postnatal Astroglia. Journal of Neuroscience. 2007 Aug 8;27(32):8654–64.

91. Heinrich C, Blum R, Gascón S, Masserdotti G, Tripathi P, Sánchez R, et al. Directing Astroglia from the Cerebral Cortex into Subtype Specific Functional Neurons. McKay RDG, editor. PLoS Biol. 2010 May 18;8(5):e1000373.

92. Heinrich C, n SGO, Masserdotti G, Lepier A, Sánchez R, Simon-Ebert T, et al. Generation of subtype-specific neurons from postnatal astroglia of the mouse cerebral cortex. Nat Protoc. Nature Publishing Group; 2011 Feb 3;6(2):214–28.

93. Corti S, Nizzardo M, Simone C, Falcone M, Donadoni C, Salani S, et al. Direct reprogramming of human astrocytes into neural stem cells and neurons. Experimental Cell Research. Elsevier Inc; 2012 Aug 1;318(13):1528–41.

94. Takahashi K, Yamanaka S. Induction of Pluripotent Stem Cells from Mouse Embryonic and Adult Fibroblast Cultures by Defined Factors. Cell. 2006 Aug 1;126(4):663–76.

95. Linnarsson S. Sequencing Single Cells Reveals Sequential Stem Cell States. Stem Cell. Elsevier Inc; 2015 Sep 3;17(3):251–2.

96. Bredenkamp N, Seoighe C, Illing N. Comparative evolutionary analysis of the FoxG1 transcription factor from diverse vertebrates identifies conserved recognition sites for microRNA regulation. Dev Genes Evol. 2007 Jan 27;217(3):227–33.

97. Weigel D, Jürgens G, Küttner F, Seifert E, Jäckle H. The homeotic gene fork head encodes a nuclear protein and is expressed in the terminal regions of the Drosophila embryo. Cell. 1989 May 19;57(4):645–58.

98. Calnan DR, Brunet A. The FoxO code. Oncogene. 2008 Apr 7;27(16):2276–88.

99. Lam EWF, Brosens JJ, Gomes AR, Koo C-Y. Forkhead box proteins: tuning forks for transcriptional harmony. Nature Reviews Cancer. 2013 Jul;13(7):482–95.

100. Zaret KS, Carroll JS. Pioneer transcription factors: establishing competence for gene expression. Genes Dev. 2011 Nov 1;25(21):2227–41.

101. Roth M, Bonev B, Lindsay J, Lea R, Panagiotaki N, Houart C, et al. FoxG1 and TLE2 act cooperatively to regulate ventral telencephalon formation. Development. 2010 May 1;137(9):1553–62.

102. Soufi A, Donahue G, Zaret KS. Facilitators and Impediments of the Pluripotency Reprogramming Factors' Initial Engagement with the Genome. Cell. Elsevier Inc; 2012 Nov 12;:1–11.

103. Myatt SS, Lam EWF. The emerging roles of forkhead box (Fox) proteins in cancer. Nature Reviews Cancer. 2007 Nov;7(11):847–59.

104. Sunayama J, Sato A, Matsuda K-I, Tachibana K, Watanabe E, Seino S, et al. FoxO3a functions as a key integrator of cellular signals that control glioblastoma stem-like cell differentiation and tumorigenicity. Stem Cells. 2011 Sep 1;29(9):1327–37.

105. Wilk A, Urbanska K, Grabacka M, Mullinax J, Marcinkiewicz C, Impastato D, et al. Fenofibrate-induced nuclear translocation of FoxO3A triggers Bim-mediated apoptosis in glioblastoma cells in vitro. Cell Cycle. 2012 Jul 15;11(14):2660–71.

106. Sato A, Sunayama J, Okada M, Watanabe E, Seino S, Shibuya K, et al. Glioma-Initiating Cell Elimination by Metformin Activation of FOXO3 via AMPK. Stem Cells Transl Med. 2012 Nov 16;1(11):811–24.

107. Lau CJ, Koty Z, Nalbantoglu J. Differential response of glioma cells to FOXO1-directed therapy. Cancer Res. 2009 Jul 1;69(13):5433–40.

108. Koo C-Y, Muir KW, Lam EWF. FOXM1: From cancer initiation to progression and

treatment. Biochim Biophys Acta. 2012 Jan 1;1819(1):28–37.

109. Karadedou CT, Gomes AR, Chen J, Petkovic M, Ho K-K, Zwolinska AK, et al. FOXO3a represses VEGF expression through FOXM1-dependent and -independent mechanisms in breast cancer. Oncogene. 2012 Apr 5;31(14):1845–58.

110. Webb AE, Pollina EA, Vierbuchen T, Urbán N, Ucar D, Leeman DS, et al. FOXO3 Shares Common Targets with ASCL1 Genome-wide and Inhibits ASCL1-Dependent Neurogenesis. CellReports. 2013 Aug 15;4(3):477–91.

111. Wang L, Zhang B, Xu X, Zhang S, Yan X, Kong F, et al. Clinical significance of FOXP3 expression in human gliomas. Clin Transl Oncol. 2013 Apr 12.

112. Wang L, Qin H, Li L, Feng F, Ji P, Zhang J, et al. Forkhead-box A1 transcription factor is a novel adverse prognosis marker in human glioma. Journal of Clinical Neuroscience. Elsevier; 2013 May;20(5):654–8.

113. Li Z, Tuteja G, Schug J, Kaestner KH. Foxa1 and Foxa2 are essential for sexual dimorphism in liver cancer. Cell. 2012 Jan 20;148(1-2):72–83.

114. Yao J, Lai E, Stifani S. The winged-helix protein brain factor 1 interacts with groucho and hes proteins to repress transcription. Mol Cell Biol. 2001 Mar 1;21(6):1962–72.

115. Mencarelli MA, Spanhol-Rosseto A, Artuso R, Rondinella D, De Filippis R, Bahi-Buisson N, et al. Novel FOXG1 mutations associated with the congenital variant of Rett syndrome. Journal of Medical Genetics. 2010 Jan 11;47(1):49–53.

116. Florian C, Bahi-Buisson N, Bienvenu T. FOXG1-Related Disorders: From Clinical Description to Molecular Genetics. Mol Syndromol. 2011.

117. Hanashima C, Shen L, Li SC, Lai E. Brain factor-1 controls the proliferation and differentiation of neocortical progenitor cells through independent mechanisms. Journal of Neuroscience. 2002 Aug 1;22(15):6526–36.

118. Xuan S, Baptista CA, Balas G, Tao W, Soares VC, Lai E. Winged helix transcription factor BF-1 is essential for the development of the cerebral hemispheres. Neuron. 1995 Jun;14(6):1141–52.

119. Manuel MN, Martynoga B, Molinek MD, Quinn JC, Kroemmer C, Mason JO, et al. The transcription factor Foxg1 regulates telencephalic progenitor proliferation cell autonomously, in part by controlling Pax6 expression levels. Neural Dev. 2011;6(1):9.

120. Ahlgren S, Vogt P, Bronner-Fraser M. ExcessFoxG1 causes overgrowth of the neural tube. J Neurobiol. 2003 Nov 3;57(3):337–49.

121. Danesin C, Peres JN, Johansson M, Snowden V, Cording A, Papalopulu N, et al. Integration of Telencephalic Wnt and Hedgehog Signaling Center Activities by Foxg1. Dev Cell. 2009 Apr;16(4):576–87.

122. Martynoga B, Morrison H, Price DJ, Mason JO. Foxg1 is required for specification of ventral telencephalon and region-specific regulation of dorsal telencephalic precursor proliferation and apoptosis. Dev Biol. 2005 Jul;283(1):113–27.

123. Hanashima C, Li SC, Shen L, Lai E, Fishell G. Foxg1 suppresses early cortical cell fate. Science. 2004 Jan 2;303(5654):56–9.

124. Kawauchi S, Kim J, Santos R, Wu HH, Lander AD, Calof AL. Foxg1 promotes olfactory

neurogenesis by antagonizing Gdf11. Development. 2009 Apr 10;136(9):1453–64.

125. Kumamoto T, Toma K-I, Gunadi, McKenna WL, Kasukawa T, Katzman S, et al. Foxg1 Coordinates the Switch from Nonradially to Radially Migrating Glutamatergic Subtypes in the Neocortex through Spatiotemporal Repression. CellReports. The Authors; 2013 Mar 28;3(3):931–45.

126. Shen Q, Wang Y, Dimos JT, Fasano CA, Phoenix TN, Lemischka IR, et al. The timing of cortical neurogenesis is encoded within lineages of individual progenitor cells. Nat Neurosci. Nature Publishing Group; 2006 May 7;9(6):743–51.

127. Miyoshi G, Fishell G. Dynamic FoxG1 Expression Coordinates the Integration of Multipolar Pyramidal Neuron Precursors into the Cortical Plate. Neuron. Elsevier. 2012 Jun 21;74(6):1045–58.

128. Ghosh-Dastidar S, Narayanan S, Stifani S, D'Mello SR. Transducin-like enhancer of Split-1 (TLE1) combines with Forkhead box protein G1 (FoxG1) to promote neuronal survival. J Biol Chem. 2012 Apr 27;287(18):14749–59.

129. Dastidar SG, Landrieu PMZ, D'Mello SR. FoxG1 Promotes the Survival of Postmitotic Neurons. Journal of Neuroscience. 2011 Jan 12;31(2):402–13.

130. Regad T, Roth M, Bredenkamp N, Illing N, Papalopulu N. The neural progenitor-specifying activity of FoxG1 is antagonistically regulated by CKI and FGF. Nature Cell Biology. 2007 Apr 15;9(5):531–40.

131. Chan SS-K, Kyba M. What is a Master Regulator? J Stem Cell Res Ther. 2013;03(02).

132. Ziller MJ, Edri R, Yaffe Y, Donaghey J, Pop R, Mallard W, et al. Dissecting neural differentiation regulatory networks through epigenetic footprinting. Nature. Nature Publishing Group; 2014 Dec 24;:1–16.

133. Suvà ML, Riggi N, Bernstein BE. Epigenetic reprogramming in cancer. Science. 2013 Mar 29;339(6127):1567–70.

134. Kilpinen S, Autio R, Ojala K, Iljin K, Bucher E, Sara H, et al. Systematic bioinformatic analysis of expression levels of 17,330 human genes across 9,783 samples from 175 types of healthy and pathological tissues. Genome Biol. 2008;9(9):R139.

135. Arnold K, Sarkar A, Yram MA, Polo JM, Bronson R, Sengupta S, et al. Sox2(+) adult stem and progenitor cells are important for tissue regeneration and survival of mice. Cell Stem Cell. 2011 Oct 4;9(4):317–29.

136. Uchikawa M, Kamachi Y, Kondoh H. Two distinct subgroups of Group B Sox genes for transcriptional activators and repressors: their expression during embryonic organogenesis of the chicken. Mech Dev. 1999 Jun;84(1-2):103–20.

137. Avilion AA, Nicolis SK, Pevny LH, Perez L, Vivian N, Lovell-Badge R. Multipotent cell lineages in early mouse development depend on SOX2 function. Genes Dev. 2003 Jan 1;17(1):126–40.

138. Miyagi S, Masui S, Niwa H, Saito T, Shimazaki T, Okano H, et al. Consequence of the loss of Sox2 in the developing brain of the mouse. FEBS Letters. 2008 Aug 6;582(18):2811–5.

139. Gómez-López S, Wiskow O, Favaro R, Nicolis SK, Price DJ, Pollard SM, et al. Sox2 and Pax6 maintain the proliferative and developmental potential of gliogenic neural stem cells In vitro. Glia. 2011 Jul 15;59(11):1588–99.

140. Bylund M, Andersson E, Novitch BG, Muhr J. Vertebrate neurogenesis is counteracted by Sox1-3 activity. Nat Neurosci. 2003 Nov;6(11):1162–8.

141. Kishi M, Mizuseki K, Sasai N, Yamazaki H, Shiota K, Nakanishi S, et al. Requirement of Sox2-mediated signaling for differentiation of early Xenopus neuroectoderm. Development. 2000 Feb;127(4):791–800.

142. Zhao S, Nichols J, Smith AG, Li M. SoxB transcription factors specify neuroectodermal lineage choice in ES cells. Mol Cell Neurosci. 2004 Nov;27(3):332–42.

143. Pollard SM. In vitro expansion of fetal neural progenitors as adherent cell lines. Methods Mol Biol. 2013;1059:13–24.

144. Schildge S, Bohrer C, Beck K, Schachtrup C. Isolation and Culture of Mouse Cortical Astrocytes. JoVE. 2013;(71).

145. Gibson DG, Young L, Chuang R-Y, Venter JC, Hutchison CA, Smith HO. Enzymatic assembly of DNA molecules up to several hundred kilobases. Nat Methods. 2009 Apr 12;6(5):343–5.

146. Buenrostro JD, Giresi PG, Zaba LC, Chang HY, Greenleaf WJ. Transposition of native chromatin for fast and sensitive epigenomic profiling of open chromatin, DNA-binding proteins and nucleosome position. Nat Methods. 2013 Oct 6;10(12):1213–8.

147. Tian C, Gong Y, Yang Y, Shen W, Wang K, Liu J, et al. Foxg1 has an essential role in postnatal development of the dentate gyrus. Journal of Neuroscience. 2012 Feb 29;32(9):2931–49.

148. Liu F, Hon GC, Villa GR, Turner KM, Ikegami S, Yang H, et al. EGFR Mutation Promotes Glioblastoma through Epigenome and Transcription Factor Network Remodeling. Molecular Cell. Elsevier Inc; 2015 Oct 15;60(2):307–18.

149. Lodato MA, Ng CW, Wamstad JA, Cheng AW, Thai KK, Fraenkel E, et al. SOX2 co-occupies distal enhancer elements with distinct POU factors in ESCs and NPCs to specify cell state. PLoS Genet. 2013;9(2):e1003288.

150. Jacobs FMJ, van der Heide LP, Wijchers PJEC, Burbach JPH, Hoekman MFM, Smidt MP. FoxO6, a Novel Member of the FoxO Class of Transcription Factors with Distinct Shuttling Dynamics. Journal of Biological Chemistry. 2003 Sep 19;278(38):35959–67.

151. Swartling FJ, Savov V, Persson AI, Chen J, Hackett CS, Northcott PA, et al. Distinct Neural Stem Cell Populations Give Rise to Disparate Brain Tumors in Response to N-MYC. Cancer Cell. 2012 May;21(5):601–13.

152. Müller I, Larsson K, Frenzel A, Oliynyk G, Zirath H, Prochownik EV, et al. Targeting of the MYCN Protein with Small Molecule c-MYC Inhibitors. Nordheim A, editor. PLoS ONE. 2014 May 23;9(5):e97285.

153. Qinyu L, Long C, Zhen-dong Du, Min-min S, Wei-ze W, Wei-ping Y, et al. FOXO6 promotes gastric cancer cell tumorigenicity via upregulation of C-myc. FEBS Letters. Federation of European Biochemical Societies; 2013 Jul 11;587(14):2105–11.

154. Glasgow SM, Laug D, Brawley VS, Zhang Z, Corder A, Yin Z, et al. The miR-223/nuclear factor I-A axis regulates glial precursor proliferation and tumorigenesis in the CNS. Journal of Neuroscience. 2013 Aug 14;33(33):13560–8.

155. Jolma A, Yan J, Whitington T, Toivonen J, Nitta KR, Rastas P, et al. DNA-binding

specificities of human transcription factors. Cell. 2013 Jan 17;152(1-2):327–39.

156. Danesin C, Houart C. A Fox stops the Wnt: implications for forebrain development and diseases. Current Opinion in Genetics & Development. 2012 Aug 1;22(4):323–30.

157. Bjerke L, Mackay A, Nandhabalan M, Burford A, Jury A, Popov S, et al. Histone H3.3 Mutations Drive Pediatric Glioblastoma through Upregulation of MYCN. Cancer Discovery. 2013 May 8;3(5):512–9.

158. Sirko S, Behrendt G, Johansson PA, Tripathi P, Costa M, Bek S, et al. Reactive glia in the injured brain acquire stem cell properties in response to sonic hedgehog. [corrected]. Cell Stem Cell. 2013 Apr 4;12(4):426–39.

159. Song Y, Zhang Q, Kutlu B, Difilippantonio S, Bash R, Gilbert D, et al. Evolutionary etiology of high-grade astrocytomas. Proc Natl Acad Sci USA. 2013 Oct 29;110(44):17933–8.

160. Sturm D, Witt H, Hovestadt V, Khuong-Quang D-A, Jones DTW, Konermann C, et al. Hotspot Mutations in H3F3Aand IDH1 Define Distinct Epigeneticand Biological Subgroups of Glioblastoma. Cancer Cell. Elsevier Inc; 2012 Oct 16;22(4):425–37.

161. Kritzer JA. Stapled peptides: Magic bullets in nature's arsenal. Nat Chem Biol. 2010 Aug 1;6(8):566–7.

162. Soucek L, Whitfield J, Martins CP, Finch AJ, Murphy DJ, Sodir NM, et al. Modelling Myc inhibition as a cancer therapy. Nature. 2008 Oct 2;455(7213):679–83.

163. Blaschke K, Ebata K, Karimi M, Zepeda J, Goyal P et al. Vitamin C induces Tet-dependent DNA demethylation and a blastocyst-like state in ES cells. Nature. 2013 500(7461): 222-226

9 Appendices

9.1 Taqman assays (qRT-PCR and Taqman Low Density Array Cards)

9.1.1 Taqman Assays – Mouse

Target	Assay	Target	Assay	Target	Assay
18s rRNA	Hs99999901_s1	H2afv	Mm01181326_m1	Onecut1	Mm00839394_m1
Actb	Mm00607939_s1	H2afx	Mm00515990_s1	Pa2g4	Mm00650817_g1
Ahctf1	Mm00550729_m1	H3f3a	Mm01612808_g1	Pax6	Mm00443081_m1
Aqp4	Mm00802131_m1	Hdac7	Mm00469527_m1	Paxbp1	Mm00482759_m1
Ascl1	Mm04207567_g1	Hes1	Mm01342805_m1	Pik3r1	Mm00803160_m1
Asf1a	Mm00481538_m1	Hes6	Mm00517097_g1	Plk1	Mm00440924_g1
Bbs2	Mm01249575_m1	Hinfp	Mm00549154_m1	Pou2f1	Mm00448332_m1
Bcan	Mm00476090_m1	Hist1h2ae	Mm00781581_s1	Pou3f1	Mm00843534_s1
Bmpr1a	Mm00477650_m1	Hist1h3g	Mm00523556_s1	Pou3f2	Mm00843777_s1
Cbx2	Mm00483084_m1	Hist1h4h	Mm00462640_s1	Pou3f3	Mm00843792_s1
Cbx3	Mm00850539_g1	Hmbox1	Mm00724032_m1	Rorc	Mm01261022_m1
Cbx7	Mm00520006_m1	Hoxa5	Mm04213381_s1	Runx1	Mm01213404_m1
Cbx8	Mm00489229_m1	Hp1bp3	Mm00802807_m1	Runx1t1	Mm00486771_m1
Cdc6	Mm03048221_m1	Htra2	Mm00444846_g1	Rxrb	Mm00441193_m1
Cdk4	Mm00726334_s1	Htt	Mm01213820_m1	Set	Mm04243941_g1
Cdkn1a	Mm04205640_g1	Id3	Mm01188138_g1	Setd2	Mm01250225_m1
Cep120	Mm00618508_m1	Idh1	Mm00516030_m1	Six3	Mm01237639_m1
Chd3	Mm01332658_m1	Irf2	Mm00515206_m1	Smad4	Mm03023996_m1
Chd6	Mm00557576_m1	Jak2	Mm01208489_m1	Smad6	Mm00484738_m1
Cited2	Mm00516121_m1	Jarid2	Mm00445574_m1	Smarca2	Mm00508992_m1
Crebl2	Mm00624585_m1	Jun	Mm00495062_s1	Sox2	Mm03053810_s1
Dclk1	Mm00444950_m1	Junb	Mm04243546_s1	Sp3	Mm00803425_m1
Dnmt1	Mm01151063_m1	Jund	Mm04208316_s1	Srebf2	Mm01306292_m1
Dnmt3b	Mm01240113_m1	Kat8	Mm00458911_m1	Srrt	Mm00473364_m1
Egfr	Mm00433023_m1	Klf6	Mm00516184_m1	Stat1	Mm00439531_m1
Emx2	Mm00550241_m1	Klf7	Mm00728361_s1	Stat3	Mm01219775_m1
Ep300	Mm00625535_m1	Mdm2	Mm01233136_m1	Tbp	Mm00446971_m1
Etv4	Mm00476696_m1	Meis1	Mm00487664_m1	Tbx18	Mm00470177_m1
Etv5	Mm00465816_m1	Meis2	Mm00487748_m1	Tbx2	Mm00436915_m1
Ezh2	Mm00468464_m1	Mkx	Mm00617017_m1	Tef	Mm00457513_m1
Fabp7	Mm00445225_m1	Mnt	Mm00487729_m1	Tet3	Mm00805756_m1
Fos	Mm00487425_m1	Mphosph8	Mm00470131_m1	Tfdp2	Mm00618407_m1
Fosb	Mm00500401_m1	Myc	Mm00487804_m1	Tgif1	Mm01227699_m1
FOXG1V5	Hs01850784_s1	Mycn	Mm00476449_m1	Tnc	Mm00495662_m1
Foxg1	Mm02059886_s1	Nes	Mm00450205_m1	Top2b	Mm00493776_m1
Foxj3	Mm00554610_m1	Nfat5	Mm00467257_m1	Trp73	Mm00660220_m1
Foxo3	Mm01185722_m1	Nfatc2	Mm00477776_m1	Tsc1	Mm00452208_m1
Foxo6	Mm00809934_s1	Nfe2l2	Mm00477784_m1	Tsc22d4	Mm00470231_m1
Frs2	Mm00769591_m1	Nfia	Mm00447981_m1	Wnt5a	Mm00437347_m1
Gapdh	Mm99999915_g1	Nfkbia	Mm00477800_g1	Zfp397	Mm00660732_m1
Gfap	Mm01253033_m1	Nr1h2	Mm00437265_g1	Zscan2	Mm00437360_m1
Ghrh	Mm00439100_m1	Nr4a2	Mm00443060_m1		
Gpbp1	Mm00661107_m1	Olig1	Mm00497537_s1		
H2afj	Mm00624592_s1	Olig2	Mm01210556_m1		

9.1.2 Taqman Assays - Human

18s rRNA	Hs99999901_s1	ELF2	Hs00745556_s1	HIST1H3A	Hs00543854_s1
ACD	Hs00368526_g1	EN2	Hs00171321_m1	HIST1H3B	Hs00605810_s1
ACIN1	Hs00960114_m1	EP400	Hs00367471_m1	HIST1H3C	Hs00747483_s1
AKAP8	Hs00178674_m1	EPAS1	Hs01026149_m1	HIST1H4A	Hs00747492_s1
ANKRD35	Hs00331975_m1	ERLEC1	Hs00249026_m1	HIST1H4B	Hs00374342_s1
APAF1	Hs00559441_m1	ESRRG	Hs00976243_m1	HMGB2	Hs01127828_g1
AQP4	Hs00242342_m1	ETV1	Hs00951951_m1	HMX3	Hs01392772_m1
AR	Hs00171172_m1	ETV4	Hs00383361_g1	HOXA1	Hs00939046_m1
ARID1A	Hs00195664_m1	ETV5	Hs00927557_m1	HOXA13	Hs00426284_m1
ARNT2	Hs00208298_m1	EWSR1	Hs01095787_m1	HOXA2	Hs00534579_m1
ARNTL	Hs00154147_m1	EYA2	Hs00193347_m1	HOXA3	Hs00601076_m1
ASCL1	Hs00269932_m1	FABP7	Hs00361426_m1	HOXA4	Hs01573270_m1
BAALC	Hs00227249_m1	FBXO32	Hs01041408_m1	HOXA5	Hs00430330_m1
BACH2	Hs00222364_m1	FOS	Hs04194186_s1	HOXA6	Hs00430615_m1
BATF2	Hs00912737_m1	FOXB1	Hs00247213_s1	HOXA7	Hs00600844_m1
BCOR	Hs00372378_m1	FOXC1	Hs00559473_s1	HOXC10	Hs00213579_m1
BHLHE41	Hs00229146_m1	FOXD2	Hs01059445_s1	HOXC11	Hs00204415_m1
BMI1	Hs00180411_m1	FOXG1	Hs01850784_s1	HOXC12	Hs00545229_m1
CBFA2T2	Hs00192687_m1	FOXI1	Hs00738254_m1	HOXC13	Hs00600868_m1
CCRN4L	Hs00232597_m1	FOXJ1	Hs00230964_m1	HOXC4	Hs00538088_m1
CERS4	Hs00226114_m1	FOXK1	Hs01595620_m1	HOXC5	Hs00232747_m1
CHD2	Hs00172280_m1	FOXP1	Hs00908900_m1	HOXC6	Hs00171690_m1
CITED1	Hs00918445_g1	GABARAPL1	Hs00740588_mH	HOXC8	Hs00224073_m1
CLDN25	Hs00893310_s1	GAPDH	Hs99999905_m1	HOXC9	Hs00396786_m1
CREB5	Hs00191719_m1	GFAP	Hs00909233_m1	HOXD1	Hs00707081_s1
CSRNP1	Hs01042624_m1	GLI3	Hs00609233_m1	ID3	Hs00954037_g1
CSRP3	Hs00185787_m1	GRHL1	Hs01119372_m1	INSRR	Hs00412744_g1
CTCF	Hs00902008_m1	GRIK3	Hs00168182_m1	IRF6	Hs01062178_m1
CTSD	Hs00157205_m1	GSX2	Hs00370195_m1	IRX5	Hs04334749_m1
DBP	Hs00609747_m1	GTF2H4	Hs00231008_m1	ISL2	Hs00377575_m1
DCLK1	Hs00178027_m1	H3F3A	Hs02598544_g1	ITGA10	Hs00174623_m1
DLL3	Hs01085096_m1	HBP1	Hs00202110_m1	JARID2	Hs01004460_m1
DLX1	Hs00698288_m1	HDAC5	Hs00608366_m1	JUN	Hs01103582_s1
DLX2	Hs00269993_m1	HES1	Hs00172878_m1	JUNB	Hs00357891_s1
DMRTA2	Hs00294890_m1	HES4	Hs00368353_g1	KAT2B	Hs00187332_m1
DSCC1	Hs00225430_m1	HES6	Hs00936587_g1	KDM3B	Hs00213240_m1
DUSP10	Hs00200527_m1	HES7	Hs00261517_m1	KDM5A	Hs00231908_m1
DUSP6	Hs04329643_s1	HEY1	Hs01114113_m1	KDM5C	Hs01011846_m1
E2F2	Hs00231667_m1	HEY2	Hs00232622_m1	KIAA0430	Hs00430320_m1
EBF4	Hs00325662_m1	HIBADH	Hs00381934_m1	KLF1	Hs00610592_m1
EEF1A1	Hs00265885_g1	HIC1	Hs00359611_s1	KLF15	Hs00362736_m1
EGFR	Hs01076078_m1	HIST1H1A	Hs00271225_s1	KLF3	Hs00974383_g1
EGR2	Hs00166165_m1	HIST1H1C	Hs00271185_s1	KLF4	Hs00358836_m1
EGR3	Hs00231780_m1	HIST1H2BB	Hs00606684_s1	KLF6	Hs00810569_m1
EHF	Hs00171917_m1			KLF7	Hs00748636_s1

LHX2	Hs00180351_m1	OSR2	Hs00369588_m1	SOX9	Hs01001343_g1
LMO4	Hs01086790_m1	OTX1	Hs00951099_m1	STAT3	Hs00374280_m1
LZTS1	Hs00232762_m1	PAF1	Hs00219496_m1	STAT6	Hs00598625_m1
MAFF	Hs00544822_m1	PAX6	Hs00240871_m1	SUPT5H	Hs00231391_m1
MAFK	Hs00242747_m1	PAXBP1	Hs00332699_m1	SUV420H2	Hs00261961_m1
MCM2	Hs01091564_m1	PBX4	Hs00257935_m1	TACC2	Hs00610617_m1
MEIS1	Hs01017441_m1	PDGFRA	Hs00998018_m1	TAF10	Hs00359540_g1
MEIS3	Hs00379502_m1	PFDN1	Hs00961134_g1	TAF13	Hs00232173_m1
MITF	Hs01117294_m1	PHF15	Hs00959516_m1	TAF6L	Hs00366759_m1
MRGBP	Hs00217549_m1	PHF3	Hs00209480_m1	TBX2	Hs00911929_m1
MSX1	Hs00427183_m1	PITX1	Hs00267528_m1	TBX4	Hs00218515_m1
MT2A	Hs02379661_g1	PLCL1	Hs00196518_m1	TDGF1	Hs02339497_g1
MTMR14	Hs00560430_m1	PLEKHH2	Hs01377275_m1	TEAD1	Hs00173359_m1
MXI1	Hs00365651_m1	PLK1	Hs00153444_m1	TFAP2A	Hs01029413_m1
MYB	Hs00920556_m1	POU2F1	Hs00231250_m1	TFAP4	Hs01558245_m1
MYCL	Hs00420495_m1	POU3F2	Hs00271595_s1	TFDP1	Hs00955488_g1
MYCN	Hs00232074_m1	POU3F3	Hs00275987_s1	TFDP2	Hs00963605_m1
MYT1	Hs01027966_m1	PROM1	Hs01009250_m1	THRA	Hs00268470_m1
NCAPD3	Hs00293608_m1	PROX1	Hs00896294_m1	TP73	Hs01056230_m1
NDE1	Hs00214339_m1	RAD51C	Hs00427442_m1	TUB	Hs00163231_m1
NDUFB10	Hs00605903_m1	RANBP3L	Hs00332591_m1	TUBB	Hs00742828_s1
NFATC1	Hs00542678_m1	RARB	Hs00977140_m1	TXNIP	Hs01006900_g1
NFIA	Hs00906448_m1	RFX4	Hs00934212_m1	TXNRD1	Hs00917067_m1
NFIB	Hs01029175_m1	RHOXF2	Hs00261259_m1	UBE2E1	Hs00268678_m1
NFIX	Hs00231172_m1	RRS1	Hs00534971_s1	USP21	Hs00247369_m1
NKX2-2	Hs00159616_m1	RUNX1T1	Hs00231702_m1	VAX2	Hs00232632_m1
NKX2-3	Hs00414553_g1	SALL2	Hs00413788_m1	XPO7	Hs00209262_m1
NKX3-2	Hs00154168_m1	SALL3	Hs00601116_m1	ZEB2	Hs00207691_m1
NOTCH1	Hs01062014_m1	SCML2	Hs00232330_m1	ZFHX4	Hs00257312_s1
NPAS2	Hs00231212_m1	SCML4	Hs00401860_m1	ZFP36	Hs00185658_m1
NPTX2	Hs00383983_m1	SETBP1	Hs01098447_m1	ZFP36L1	Hs00245183_m1
NR1D1	Hs00253876_m1	SHOX2	Hs00243203_m1	ZFYVE9	Hs00245109_m1
NR1D2	Hs00233309_m1	SIM2	Hs00894178_m1	ZIC4	Hs00600885_m1
NR3C1	Hs00353740_m1	SIX1	Hs00195590_m1	ZNF140	Hs01086351_m1
NR4A2	Hs00428691_m1	SIX2	Hs00232731_m1	ZNF219	Hs00387874_g1
NR4A3	Hs00545009_g1	SLC26A3	Hs00995363_m1	ZNF268	Hs00612325_s1
NR5A2	Hs00187067_m1	SMAD6	Hs00178579_m1	ZNF395	Hs00608626_m1
NR6A1	Hs00265966_m1	SMAD7	Hs00998193_m1	ZNF467	Hs00737097_m1
NUMBL	Hs00191080_m1	SMARCB1	Hs00268260_m1	ZNF700	Hs00869252_s1
NUPL2	Hs01032727_m1	SMG6	Hs00214019_m1	ZNF704	Hs01367662_m1
OLIG1	Hs00744293_s1	SOX1	Hs01057642_s1	ZNF708	Hs02339727_m1
OLIG2	Hs00300164_s1	SOX2	Hs01053049_s1	ZNF709	Hs01059799_m1
ONECUT2	Hs00191477_m1	SOX21	Hs01072517_s1	ZW10	Hs00190911_m1
OPRM1	Hs01053957_m1	SOX5	Hs00753050_s1		
OSR1	Hs01586544_m1	SOX8	Hs00232723_m1		

9.2 Plasmids

The summary tables detail the Gateway plasmids derived in the course of this project. The three Gateway destination plasmids used (SP170, SP65, SP188) are listed in the upper panel. The entry vectors and the final expression plasmids resulting from their recombination into destination vectors are listed in the lower panel. All plasmids in italics were derived and sequence verified by me over the course of the project, except SP188, derived by Ester Rodriguez under my direction. Plasmid maps for the destination and entry vectors are provided in appendix 9.2.3.

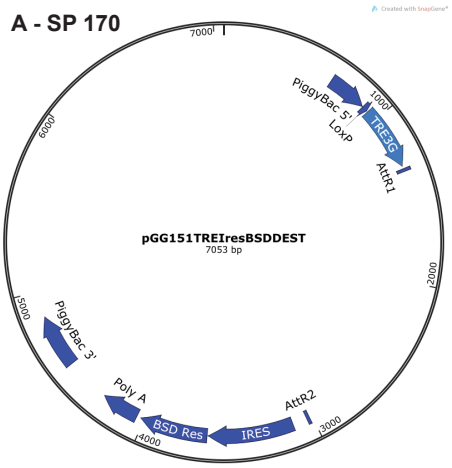
9.2.1 Destination Vectors

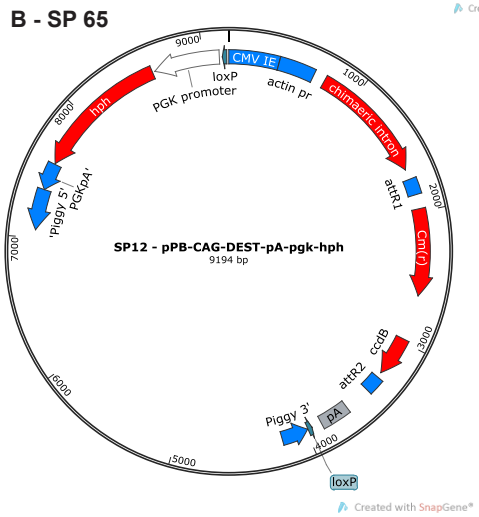
ID	Name	Integration	Promoter	Resistance
SP170	PB-TRE-DEST-IRES-BSD	PiggyBac	Tet-On 3G	Blasticidin
SP65	PB-CAG-DEST-PGK-HPH	PiggyBac	CAG	Hygromycin
SP188	AAVS1-CAG-DEST-BSD	AAVS1 targeting	CAG	Blasticidin

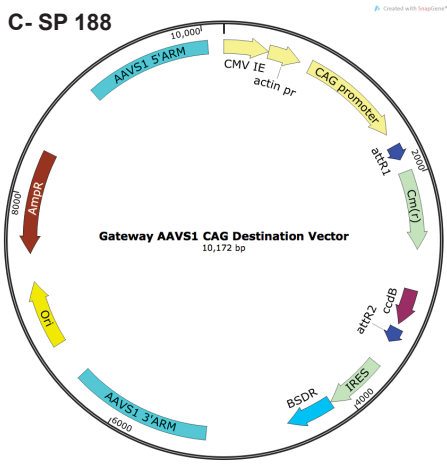
9.2.2 Entry Vectors and Expression Vectors

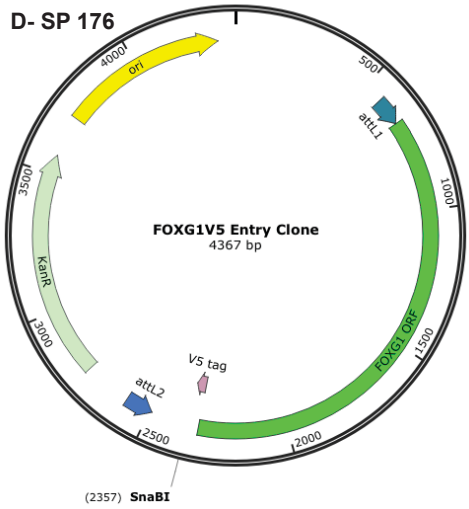
ID	Transgenes	SP170 Dest	SP65 Dest	SP188 Dest
SP411	FOXG1	*SP410*		
SP176	FOXG1_V5	*SP171*	*SP181*	
SP177	SOX2	*SP172*	*SP182*	
SP178	FOXG1_V5, SOX2	*SP173*	*SP183*	*SP416*
SP409	BRN2_MYC, SOX2	*SP415*		
SP179	FOXG1_V5, SOX2, BRN2_MYC	*SP174*	*SP184*	
SP180	FOXG1_V5, SOX2, OLIG2	*SP180*	*SP185*	
SP186	Tet3G rtTA		SP169	*SP187*

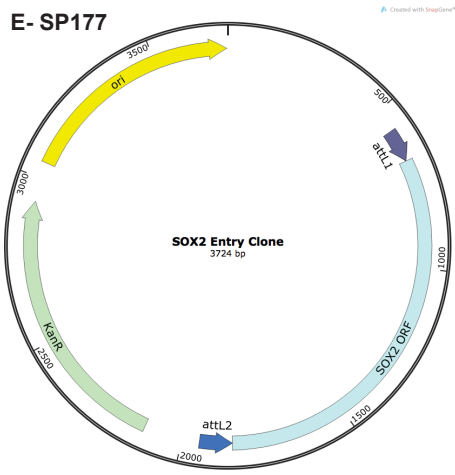
9.2.3 Plasmid Maps

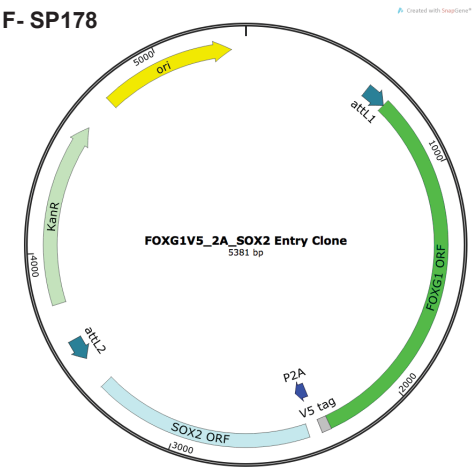




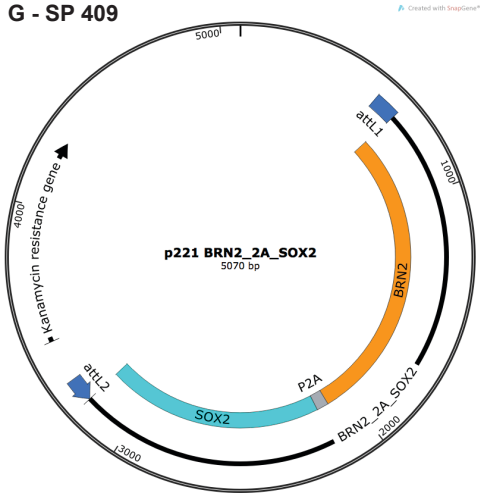




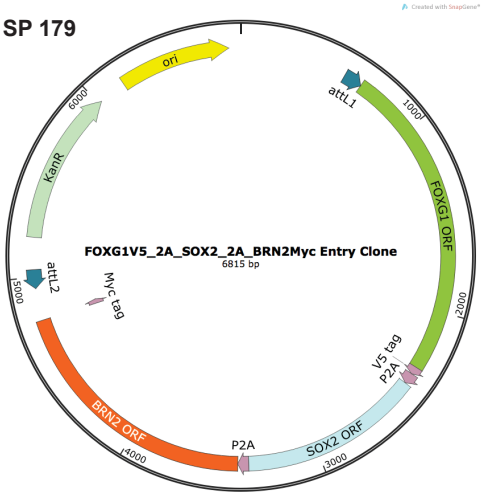




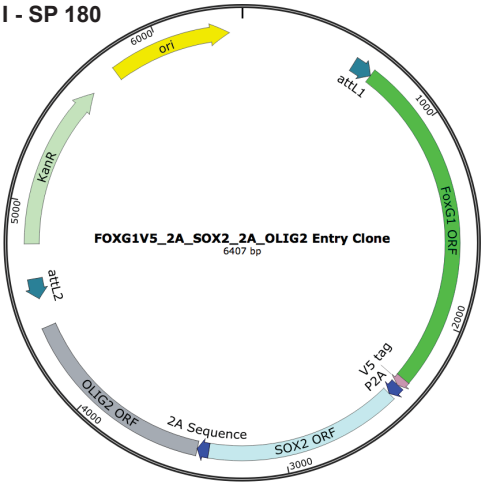
G - SP 409



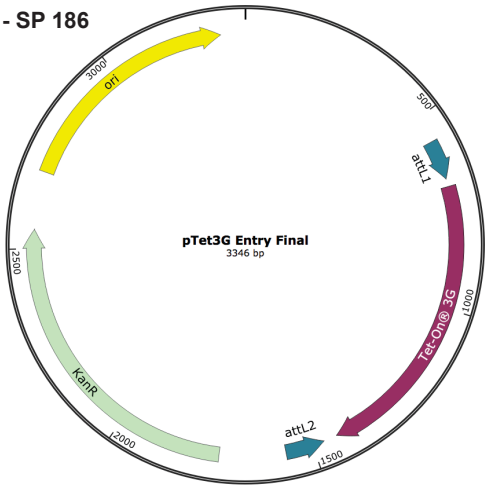
H - SP 179



I - SP 180



J - SP 186



9.3 Guide RNA and Targeting Vector Homology Arm oligos

9.3.1 AAVS1 Targeting

AAVS1 5' Fwd	aacgacggccagtgaattcgat**ttaccatccctccctcgact**
AAVS1 5' Rev	tatcgttatgcgccttgat**ataaggtggtcccagctcgg**
AAVS1 3' Fwd	ctgagctagccatcagtgat**tccttaggcctcctccttcc**
AAVS1 3' Rev	ccatgattacgccaagcttgat**aggactgagggtttcagcgc**
AAVS1 gRNA 1	*cca*ctagggacaggattggtgac
AAVS1 gRNA 8	ggggccactagggacaggat*tgg*

9.3.2 FOXG1 Targeting

FOXG1 5' Arm Forward	aacgacggccagtgaattcgat**aacgaaaatatttccagggt**
FOXG1 5' Arm Reverse	tatcgttatgcgccttgat**cactgagcgctccggcagca**
FOXG1 3' Arm Forward	ctgagctagccatcagtgat**gaagaagaacggcaagtacg**
FOXG1 3' Arm Forward	ccatgattacgccaagcttgat**ccaagtgcattttctagaac**
Guide RNA 1	*ccg*ccctggacggggctaa
Guide RNA 2	gcaagggcgagccggg*cgg*

9.3.3 FoxO3 Targeting

FoxO3 5' Fwd	aacgacggccagtgaattcgat**actctgtggaaggaagttgc**
FoxO3 5' Rev	tatcgttatgcgccttgat**aggaaggtccagttcaaaca**
FoxO3 3' Fwd	ctgagctagccatcagtgat**actctttatgtcctctgttg**
FoxO3 3' Rev	ccatgattacgccaagcttgat**cccttggtacgtccgacctg**
FoxO3 gRNA 1	cgcgttcagaatgaaggcac*ggg*
FoxO3 gRNA 2	cgcatgaagcggctgtgca*ggg*

9.3.4 FoxO3 Cis Regulatory Region Deletion

FoxO3 ID gRNA A	gtaacacaacagaggatgaa*agg*
FoxO3 ID gRNA B	gaaagagcttcttgtggacc*agg*

9.4 Mouse NS Cells Derivatives

9.4.1 Constitutive/inducible transgene overexpressing lines

Parent line / Transgene	mNS (ANS4)	mNS (p53 fl/fl)	mNS (p53CDK4)	Mouse Astrocytes	HuNS (U5)	Human Astrocytes
Lenti F	A4FGO	X				
Lenti F (Rett)	X					
Tet-On F	F6, F8	P53FGO	X	X	X	
Tet-On S	S6, S15	X	X	X	X	
Tet-On FS	F3, FS13	P53FGO	X	X	X	X
Tet-On BS	X					
Tet-On FSB	FSB13					
Tet-On FSO	FSOF				X	
CAG FS						X

9.4.2 Conditional and knockout lines

Parent Line	Name	Modifications/Notes	Clonal
FF NS	FF	FoxG1fl/fl + GFP reporter of excision	
FF NS	FF Cre3	FoxG1-/- GFP+	X
FS3 (ANS4)	FOD3	TRE FS; FoxO3-/-	X
FS3 (ANS4)	FID11	TRE FS; FoxO3 FS peak -/-	X

9.5 Human GNS Derivatives

Parent Line	Name	Modifications/Notes	Clonal
G7	G7 TFLG	AAVS1-CAG-FLAG-LUC-GFP	
G7	G7-A1	FOXG1-/-	X
G7-A1	G7-A1TFLG	FOXG1-/- CAG-FLAG-LUC-GFP	
G7	G7shTRE	shFOXG1 + PB TRE-FOXG1V5	
G7	G7sh	shFOXG1	